Sterically Crowded Copolymers Based on Functionalized Stilbenes

Yi Li

Dissertation submitted to the Faculty of the Virginia Polytechnic Institute and State University in partial fulfillment of the requirements for the degree of

Doctor of Philosophy
in
Chemistry

S. Richard Turner, Chair

Harry W. Gibson

Judy S. Riffle

Herve Marand

Richey M. Davis

Feburary 17, 2012
Blacksburg, Virginia

Keywords: stilbene, alternating copolymers, radical copolymerization, polyelectrolytes, persistence lengths, solution properties

Sterically Crowded Copolymers Based on Functionalized Stilbenes

Yi Li

Abstract

The research in this dissertation is focused on the synthesis and characterization of sterically crowded, precisely charged polyelectrolytes based on substituted stilbene comonomers.

New sterically crowded polyelectrolytes based on functionalized stilbenes with maleic anhydride or functionalized *N*-phenylmaleimides were prepared via a "protected" precursor polymer strategy. The polyelectrolyte precursors readily dissolved in organic solvents and were characterized by ^{1}H NMR, SEC, TGA, and DSC. The polyelectrolytes were obtained via simple deprotection chemistries. The use of different combinations of the donor-acceptor comonomer pairs and the alternating copolymerization of these comonomers lead to precise control over charge density and placement of charged groups along the polymer backbone. Analogous styrenic copolymers, for direct comparison to the stilbene structures, were also prepared.

Broad peaks in ^{1}H NMR spectra were observed. There were no thermal transitions measured by DSC below the degradation temperature. A strong polyelectrolyte effect, for both stilbene and styrene copolymers, occurred in deionized water and was suppressed by adding NaCl to the polymer solution. These results are not consistent with "rigid" rod polyelectrolytes in which chain collapse in the presence of added salt and chain expansion on dilution should not be observed. In response to these observations persistence length measurements were conducted on the stilbene and styrene copolymers

to assess directly the steric crowding effect of added phenyl groups in stilbene copolymers. Both SEC and SAXS measurements were used to obtain persistence lengths. The results from three different approaches, Bohdanecký, graphical and Sharp and Bloomfield Global, were in good agreement. The persistence lengths of stilbene containing copolymers range from 3 to 6 nm and the added phenyl groups increase the rigidity of the polymer chain by about 30-50%. This puts these polymers into a broadly defined "semi-rigid" category of polymers and is consistent with the solution polyelectrolyte effect observed.

In dilute solution characterization of stilbene containing polyanions, a 2-step dissociation behavior was observed for the two adjacent carboxylic acids in maleic acid containing polyanions. Stilbene polyanion solutions showed high R_h values in deionized water as shown by DLS measurements and a decrease of R_h values followed by aggregation upon gradual addition of salt. Bimodal peaks were observed in SEC measurements with the copolymer of 4-methylstilbene and maleic anhydride. DLS measurements indicated interchain aggregation as the origin of the apparent high molecular weight fraction.

The antiviral activity of the polyanion based on sodium 4-styrenesulfonate and *N*-(4-sodium sulfophenyl)maleimide was found to be ~50 times higher than the microbicide, sodium poly(styrene sulfonate). The early study of antiviral activities of carboxylated stilbene and styrene polyanions also showed promising results. The synthesis of methyl sulfonate ester-functionalized polyanion precursors was attempted because they can be characterized without the complications caused by directly using charged sulfonate groups.

Acknowledgements

I would like to thank my advisor, Dr. S. Richard Turner, for his guidance and encouragement throughout my five and half years of graduate school. Without his constant support, encouragement and passion for science, the stilbene research would not have progressed as much as it has. I would like to show my sincere appreciation to Dr. Harry Gibson, Dr. Judy Riffle, Dr. Herve Marand and Dr. Richey Davis for serving on my research committee. I would like to acknowledge Dr. Robert Moore, Dr. Thomas Mourey and Dr. Richard Gandour for sharing their knowledge and guidance in the areas that were totally unknown to me. I would like to thank Dr. Raymond Dessy and Mrs. Dessy who encouraged me to see my academic goals to fruition. I would like to thank Dr. Alan Esker for giving his valuable research advice and Dr. Paul Deck for his help on keeping me in track of the graduate program. Many thanks to Ms. Angie Miller for her administrative support.

I would like to thank the Turner group members for their patience, support and helpful discussions. I especially thank Xu Zhou and Dr. LaShonda Cureton Williams for endless help, support and lifelong friendship: I will never forget those precious memories and moments we shared and grew together. I would like to thank Alice Savage, Jenny Bay England, Lindsay Matolyak, Kevin Barr, Zhengmian Chang, Dr. Bin Zhang and Yanchun Liu for working with me side-by-side through those boiling days in old Davidson lab 124. I would like to thank Dr. Min Mao and Dr. Keiichi Osano for serving as my lab mentors at an early stage of my PhD career. I would like to acknowledge Dr. Hugo Azurmendi and Mr. Geno Iannaccone for their support and discussions on routine NMR

measurements. Many thanks to Mr. Thomas Bell, Ms. Mary Jane Smith, Ms. Tammy Jo Hiner and Ms. Teresa Dickerson for their technical assistance in many areas during my time at Virginia Tech.

I would like to thank the Long group as a whole for their support on a daily basis. I especially would like to thank Dr. Shijing Cheng for being a good friend, a patient listener and a faithful lunch partner of mine. I would like to thank Dr. Matthew Hunley, Dr. Matt Green, Renlong Gao, Tianyu Wu, Mana Tamami, Michael Allen, and Sean Hemp for running my samples and teaching me to use new instruments.

I would like to thank the Moore group as a whole for their support on a daily basis. I especially would like to thank Mingqiang Zhang and Gilles Divoux for their time and effort dedicated to solution SAXS measurements. I would like to thank Scott Forbey and Ninad Dixit for always letting me use SEM and TGA instruments.

There are several professors that, though our interaction may have been brief, have left lasting impressions and enriched my life in one way or another, thank you: Dr. James McGrath, Dr. Sungsool Wi, Dr. Webster Santos, and Dr. Timothy Long.

I would like to acknowledge Dr. Ming Gao, Dr. Justin Spano, Dr. Xingguo Cheng, Dr. Jianfei Zhang, Dr. Yanpeng Hou, Dr. Yu Chen, Jianyuan Zhang, Akiko Nakamura, Daniel Schoonover, Dr. Sangamitra Sen, Dr. Jessica Price Evans for delightful discussions on my research and daily help. Many thanks to Department of Chemistry, MII, Petroleum Research Fund of the American Chemical Society and the National Science Foundation for financially supporting my research.

I would like to thank my entire family for the constant care and support throughout my twenty two years of school. I would like to show my sincere gratitude to my dearest parents: thank you for giving me permissions to fly far away from you to pursue my dreams and thank you for educating me since a very early stage of my life to be a person with a brave heart and a determined mind that help me through all the rough times. I'm so proud of being your daughter!

A very special thanks saved in the last to Dong Dong: thank you for always being there, listening to me, sharing laughter and sadness with me. You are my role model, lighting up my life!

I am sure I have missed my appreciation to many other people. To you all, thank you so much!

Table of Contents

List of Figures

List of Tables

List of Schemes

Chapter 1. Review of Polyelectrolyte Synthesis, Chain Stiffness Measurements and Polyelectrolyte Complexes

1.1. Introduction

Polyelectrolytes are polymers with a high level of charged functional groups attached along the polymer chain.[1] In polar solvents, like water, these charged functional groups dissociate into either positively charged ionic groups to form polycations or negatively charged ionic groups to form polyanions. Polyelectrolytes have high charge densities, which differs from ionomers. Ionomers are defined as polymers with a low level of ionizable groups (usually no more than 15 percent). In general, there are two types of polyelectrolytes-natural polyelectrolytes and synthetic polyelectrolytes. The most common examples are ion containing polypeptides and proteins, ionic polysaccharides, as natural polyelectrolytes, and sodium polyacrylate and sodium poly(styrene sulfonate) as synthetic polyelectrolytes.

Compared to non-ionic polymers, a key feature of polyelectrolytes is the interaction between fixed charged groups along the polymer chain in solution, such that the charges expand or contract chain dimensions to dominate the structure-property relationships of polyelectrolytes. For example, polyelectrolytes with flexible chains usually adopt more extended conformations at low ionic strength than their corresponding non-ionic forms of polymers. This extension is due to strong electrostatic repulsions of charges along the less shielded polymer chain at low ionic strength. The electrostatic repulsions not only can

yield conformational changes, but also can lead to solution property changes, like changes in hydrodynamic volume and in non-Newtonian rheological behavior.[1] Besides ionic strength, many factors can impact electrostatic interactions, such as the nature of functionalities on the polymer backbone, charge densities along the polymer chain, molecular weight, solution pH, temperature, counterions, solvents, chain stiffness, etc.

Polyelectrolytes with electrostatic interactions find many applications in industrial processes and daily life, such as drug delivery,[2-4] waste water purification,[5] surface modification for improved adhesion,[6] and ion conducting materials.[7] For example, natural polyelectrolytes from seeds of plant species have been used in water purification for many centuries, like cationic proteins from Strychnos potatorum, Moringa oleifera's seeds.[8-11] The key building blocks of life, proteins, DNA and RNA, are polyelectrolytes. These natural polyelectrolytes play an important role in maintaining and propagating life in a complex biological system. Research in synthesizing these naturally occurring macromolecules and mimicking their roles in biological systems is of great importance for a deeper understanding of the mechanisms of biological systems and their impacts on human beings' health and life.

Synthetic polyelectrolytes provide a variety of polymer structures for different applications and thus have been an attractive area for scientific research and commercial usage. For example, an emerging area in polyelectrolyte applications is the self-assembly of thin films in new material fabrication. In other words, layer by layer self assembly of oppositely charged polyelectrolytes, or with macroions, or charged colloidal particles lead to new nanocomposite materials with tailored properties for specific applications.[12] Polyelectrolytes can also be used in ionic polymeric sensors, actuators, and artificial

muscles;[13-31] polyelectrolyte solutions, gels and complexes are used for biomedical applications, including dental adhesives, controlled release devices, polymeric drugs, and biocompatible materials.[32-39] Polyelectrolyte multilayer membranes are used for materials separation,[40-42] nanostructures of polyelectrolytes-surfactant complexes as microphase separated materials,[43-47] coacervation formation in colloidal systems used in the development of drug delivery and controlled-released systems, medical devices, and artificial organs, including cell attachment and scaffolding in biological tissues.[48-51]

This chapter presents the motivations and objectives for this work. It describes the state of the art of electric power systems, advances in dc distribution/transmission systems and smart grids, and the roles and challenges of power electronics in this field. A review of the power converter system in utility applications is provided, with special attention paid to low-voltage distribution systems. Challenges in the field and a literature review are also provided, followed by the dissertation outline and the scope of research.

1.2. GENERAL CONSIDERATIONS

1.2.1. Polyelectrolyte synthesis

There are many difficulties in the synthesis and characterization of polyelectrolytes because of the ionic functional groups, such as in determination of molecular weights, molecular weight distributions, molecular structures, etc. To minimize these difficult problems, one may introduce ionic functionalities in a final post-polymerization step. With protection of the ionic groups, polyelectrolyte precursors are soluble in common organic solvents. The synthesis of poly(*p*-phenylene) (PPP) polyelectrolytes is an example. The Suzuki coupling reaction usually has good tolerance of functional groups in the monomers.[52] Two synthetic routes can be applied to synthesize PPP polyelectrolytes:

direct routes (Routes A) and precursor strategies (Routes B), shown in scheme 1.1[52] However, the direct routes A, i.e., the ionic functionalities are already available on the monomers, have been shown to be problematic in characterization of ionic polymers. Instead the precursor strategies, routes B, are selected because the non-ionic polymers prepared from polycondensation process (B1) can be fully characterized by the conventional techniques of polymer analysis. As a result, the molecular information of the backbone of the ionic polymers can be determined without complication due to the ionic groups. As shown in Scheme 1.1, the polycondensation process (B1) and the macromolecular substitution step (B2) lead to the desired PPP polyelectrolytes.[52] Meanwhile, there is a continuous effort in improving direct pathways to polyelectrolytes, avoiding the post-polymerization process because this has the advantage of eliminating the protection and deprotection reaction steps.[53]

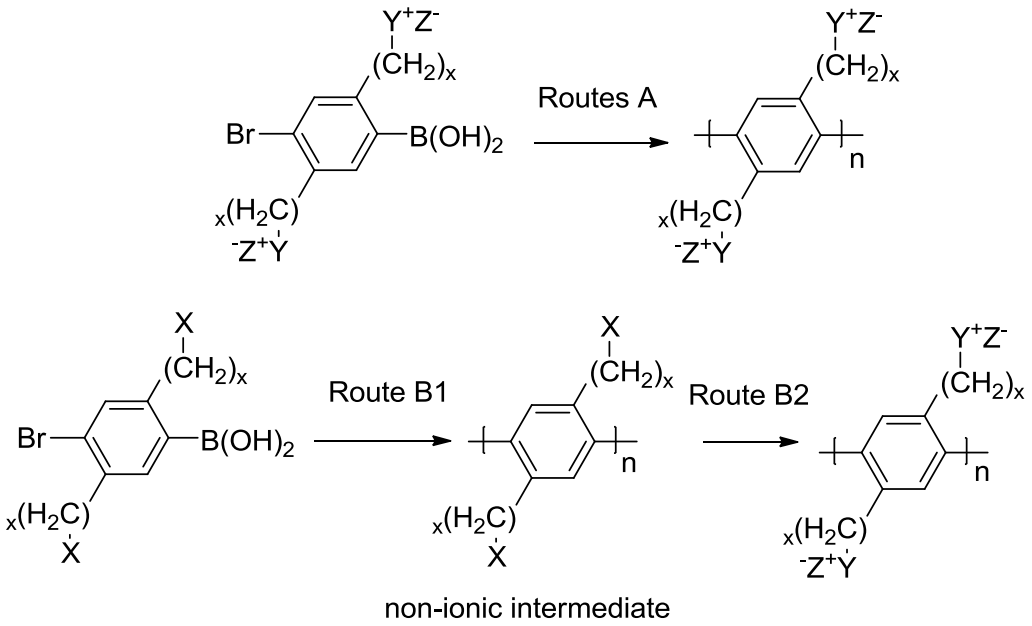

Scheme 1.1 General presentation of direct routes and precursor strategies leading to PPP polyelectrolytes.[52]

In general, synthetic methods used to prepare polyelectrolytes are step-growth polymerizations to yield ionic polyesters, polyurethanes, polyamides, synthetic polypeptides, polynucleotides, and polysaccharides[1] or chain-growth polymerizations of functionalized vinyl, carbonyl monomers, and ring-strained cyclic compounds, as illustrated in Figure 1.1.[1] These monomers may be initiated by using radical, cationic, anionic or coordinated cationic initiators. In industry, emulsion polymerization and suspension polymerization are more likely to be used as low-cost and facile synthetic methods in polyelectrolyte production.[1]

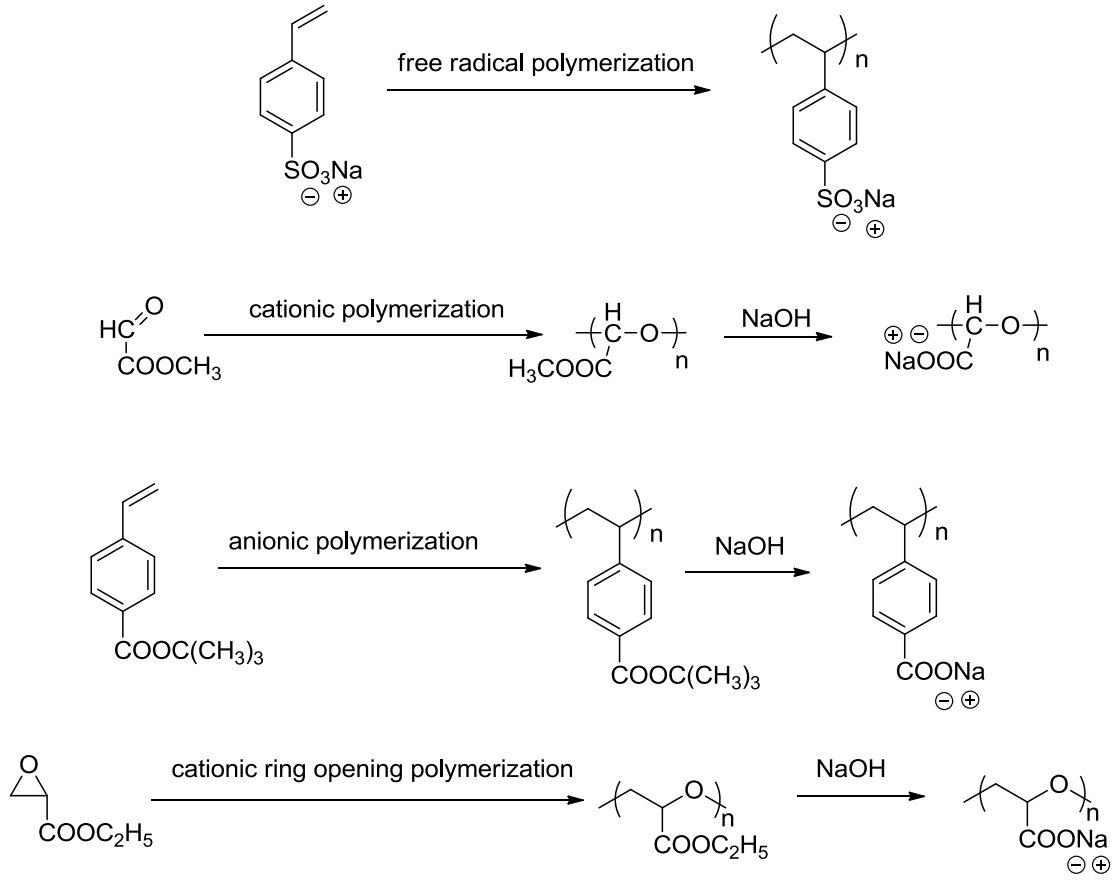

Figure 1.1 Examples of chain growth polymerization.[54-56]

Among various chain growth polymerization methods, classical free radical polymerization is the one most frequently used to prepare polyelectrolytes, because free

radical polymerization processes are known for being tolerant to functional groups. The polymerization can be conducted in water and control of the molecular parameters of free radical polymers such as molecular weight distribution and architecture is readily possible.[57] As new polyelectrolyte structures are continuously evolving, high demands for preparation of polyelectrolytes with precise control of complex architectures and multiple functional groups are growing.[58] Controlled polymerization (CP), in particular the controlled radical polymerization (CRP) synthetic methods, such as nitroxide mediated polymerization (NMP),[59,60] atom transfer radical polymerization (ATRP),[61-63] reversible addition-fragmentation chain transfer (RAFT) polymerization,[64-66] tellurium-mediated radical polymerization (TERP),[67-69] cobalt-mediated chain transfer polymerization (CMTP),[70,71] and living ring-opening metathesis polymerization (ROMP),[72-74] have been considered as major methods for preparing new polyelectrolytes conveniently and in good yields. For example, NMP has been extensively used in the preparation of water soluble poly(acrylic acid),[75-79] sodium poly(styrene sulfonate) based block copolymers,[80-84] and poly(*N,N*-dimethylacrylamide) based block copolymers,[84-88] as shown in Figure 1.2. Homopolymers and block copolymers of a wide variety of nonionic, anionic, cationic, and zwitterionic monomers, like sodium 4-styrenecarboxylate,[89,90] sodium 2-acrylamido-2-methylpropanesulfonate,[89,90] sodium 3-acrylamido-3-methylbutanoate,[89,90] and *N,N*-dimethylacrylamide[91,92] can be prepared by RAFT, in Figure 1.3. As shown in Figure 1.4, ATRP can be used to prepare water-soluble styrenic and acrylate monomers;[93,94] ROMP is an efficient method for polymerization of functionalized 7-oxanorbornene derivatives and norbornene derivatives.[72,95,96] CMTP can be applied in (co)polymerizations of acidic, hydroxy, and zwitterionic functional monomers.[97,98] Besides CRP methods, “click

chemistry" as a simple and facile method has also been applied for precise control of multiple functionalities along the polymer backbone. The thiol-ene addition reaction was developed for making polyelectrolytes, as shown in Figure 1.5.[53,99-101] The CRP techniques have many similarities to conventional free radical polymerizations: they all are highly tolerant to a variety of functional groups and a radical initiation step is involved for all. Simultaneously, CRP methods bear many of the characteristics associated with living polymerizations. They can be applied to prepare complex polyelectrolyte architectures with precise control, such as blocks, brushes, or stars. Molecular weights of synthetic polyelectrolytes can be easily tuned via the monomer/initiator ratio with narrow molecular weight distributions; additionally, polymerization may be conducted under a wide range of conditions, such as bulk, solution, dispersion, emulsion, etc.

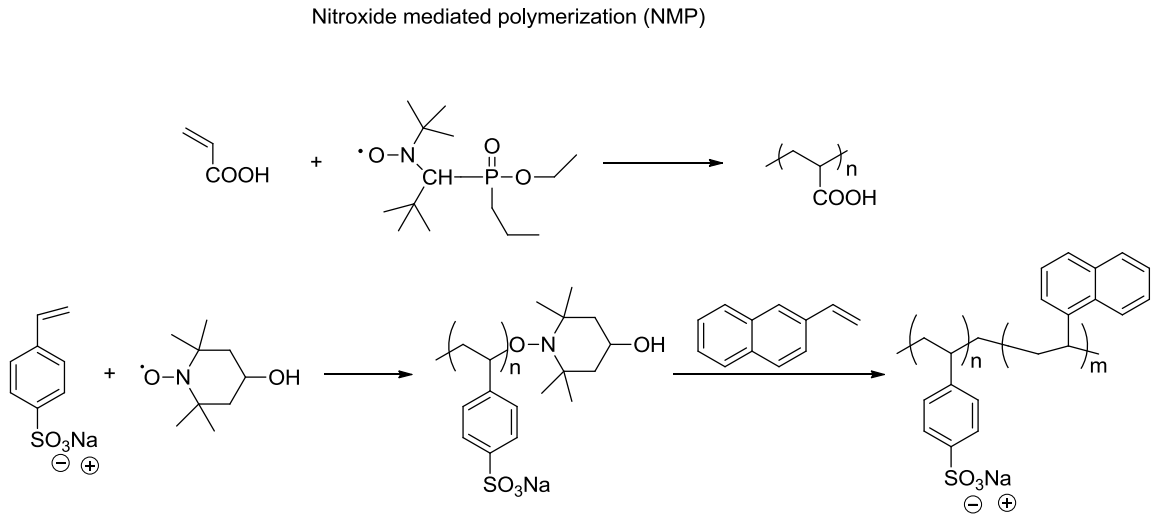

Figure 1.2 Examples of NMP method for the synthesis of polyelectrolytes.[75,80]

Reversible addition-fragmentation chain transfer (RAFT)

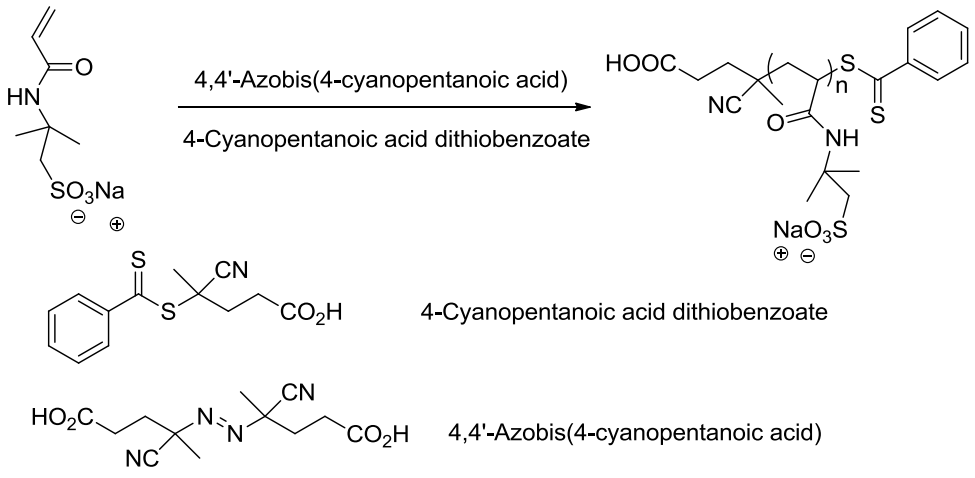

RAFT mechanism

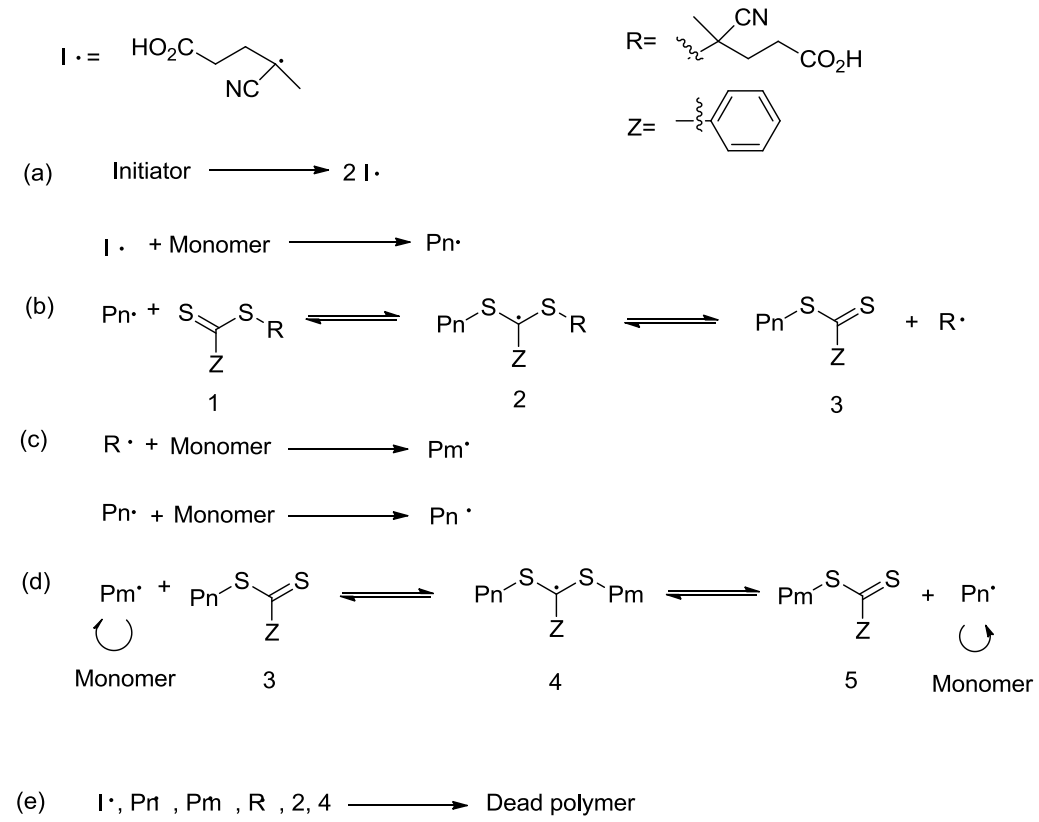

Figure 1.3 RAFT method for the synthesis of polyelectrolytes and mechanism.[89,90]

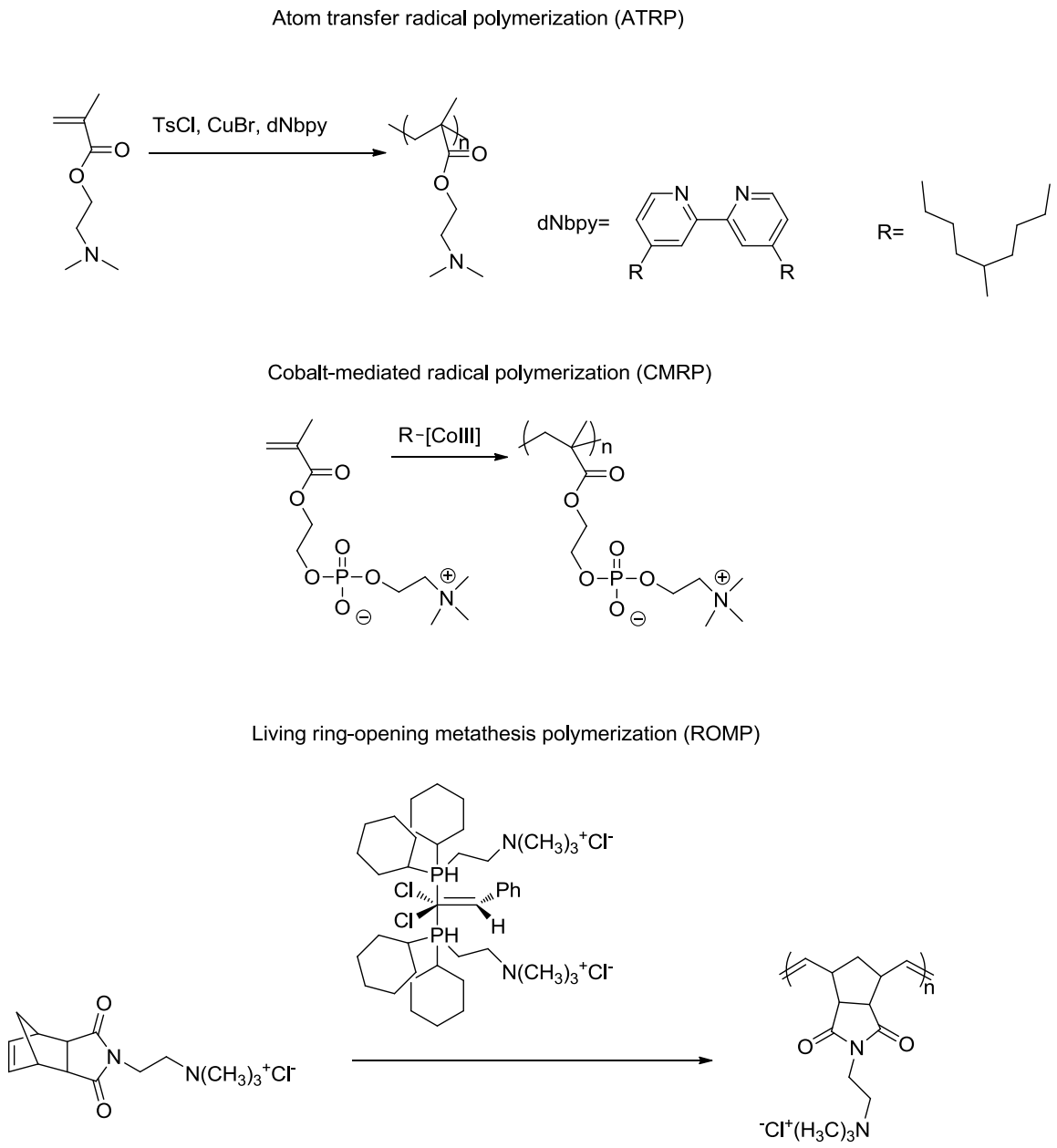

Figure 1.4 Examples of ATRP,[93] CMRP,[97] ROMP[95] methods for the synthesis of polyelectrolytes and polyelectrolyte precursors.

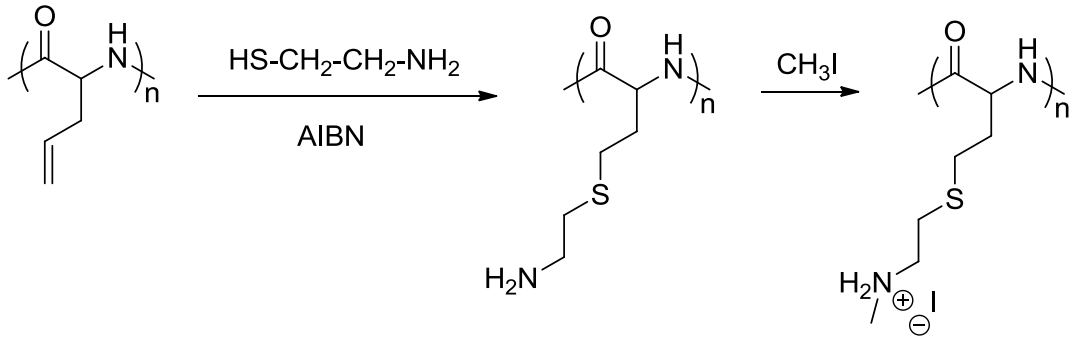

Figure 1.5 Example of thiol-ene "click" reactions.[53,102]

So far most of the living polymerization methods have been applied for the synthesis of new polyelectrolytes, with much of the research conducted in academic research laboratories.[1] Among these techniques, ATRP and RAFT are the more widely investigated. In terms of tolerance of different types of monomers, RAFT is the most versatile method. For example, controlled polymerization of acrylamido based monomers can so far only be accomplished by RAFT because techniques such as NMP or ATRP are problematic, often requiring special conditions.[103] Maleic anhydride is a monomer often used in the synthesis of polyanions. Maleic anhydride does not homopolymerize. Controlled copolymerization of maleic anhydride with electron rich monomers by NMP or ATRP can be problematic because of the electron rich monomer resulting in a non-alternating structure at the high temperature required in NMP techniques or the formation of metal carboxlate complexes in ATRP that inhibit polymerization.[93,104] Addition-fragmentation chain transfer agents (CTA), appropriate thiocarbonylthio compounds [S=C(Z)S-R], are key to control in RAFT polymerizations. Typical CTA includes dithiobenzoates, trithiocarbonates, dithioalkanoates, dithiocarbonates (xanthates), and dithiocarbamates,[105] as shown in Figure 1.6. To conduct the polymerizations directly in

water requires the use of appropriate water-soluble CTA, such as RAFT reagents (a)-(f) in Figure 1.6.

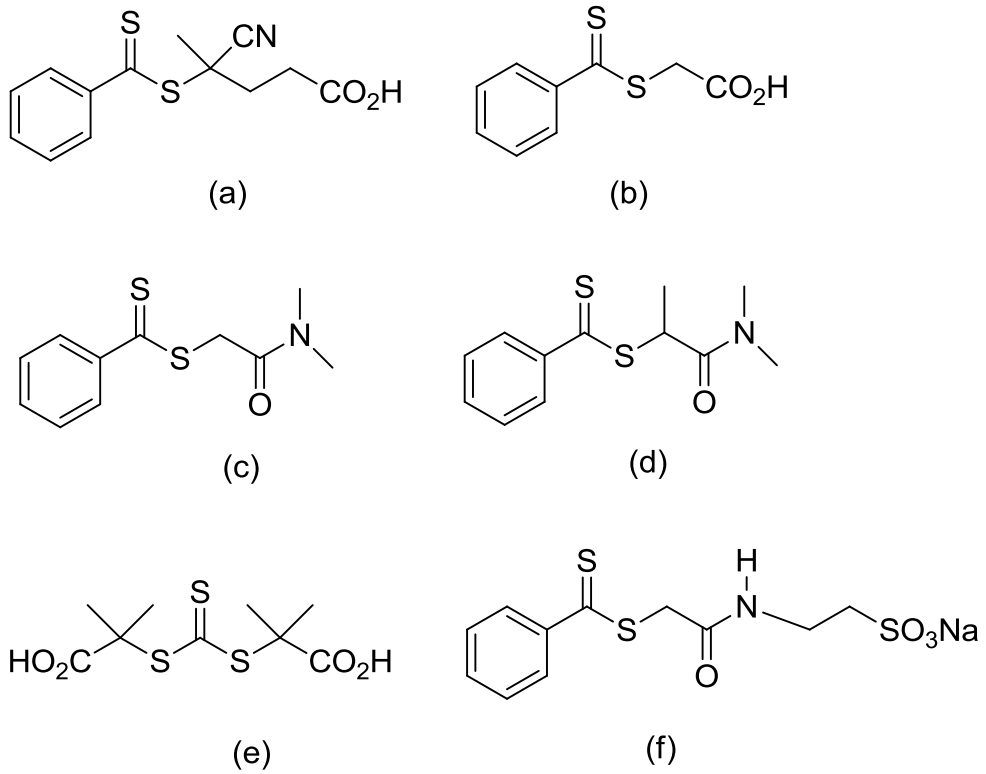

Figure 1.6 Example of typical RAFT agents.

Step-growth condensation reactions have been also widely examined in the preparation of polyelectrolytes. They can be carried out in solution or in bulk, interfacially or microheterogeneously, or on a solid support to prepare synthetic polypeptides, polynucleotides, and polysaccharides. For example, polyelectrolytes with a rigid backbone, such as PPP polyelectrolytes, are often prepared by Suzuki coupling condensation reactions, followed by a post-polymerization to yield charged functional groups along the polymer chain, shown in Figure 1.7.[52] Charged polyesters or polyamides are often made by solution condensation methods at relatively low temperatures.[1] Both anionic charged and cationic charged polyfluorene have been synthesized via step-growth

condensation reactions, as shown in Figure 1.8.[106,107] Fully sulfonated poly(aramide)s were successfully prepared by application of the Yamazaki-Hifashi polycondensation technique from 2,5-diaminobenzenesulfonic acid and sulfoterephthalic acid in the presence of triphenyl phosphate, pyridine, and lithium chloride in *N*-methylpyrrolidone as the solvent, shown in Figure 1.9.[108]

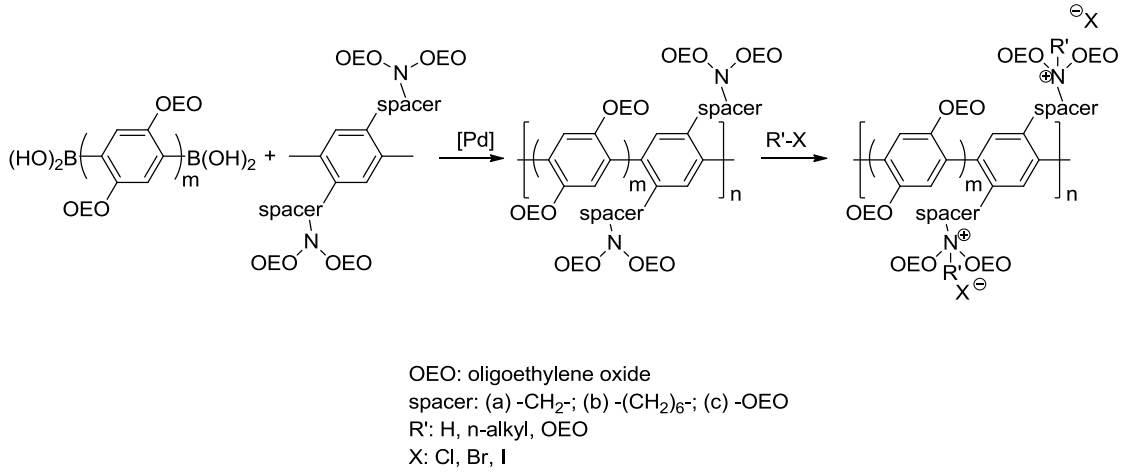

Figure 1.7 Synthesis of cationic PPP polyelectrolytes via water-soluble amino-functionalized precursors.[52]

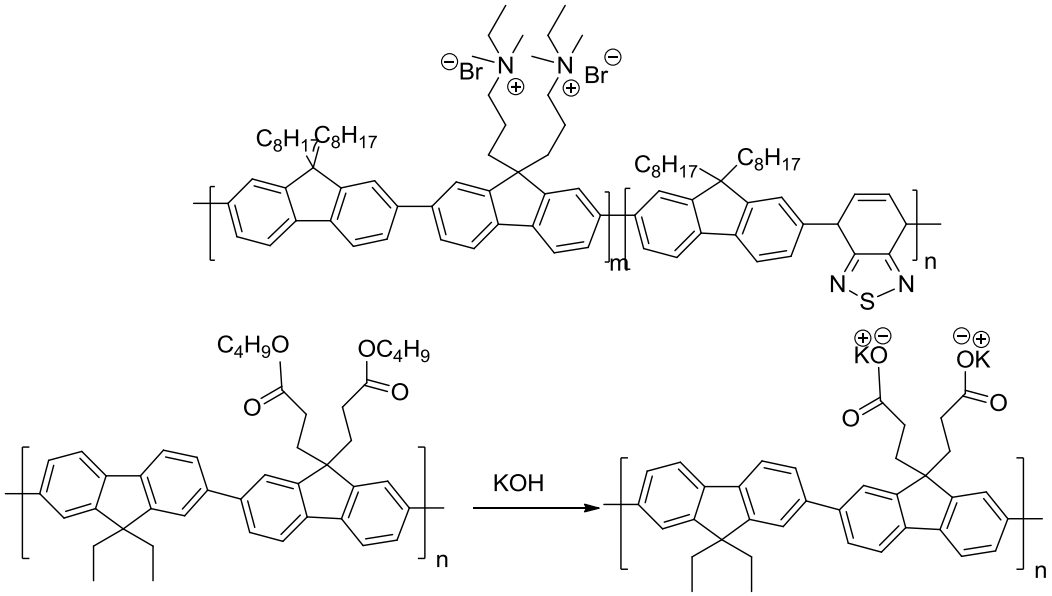

Figure 1.8 Examples of anionic charged and cationic charged polyfluorene prepared via step-growth condensation reactions.[106,107]

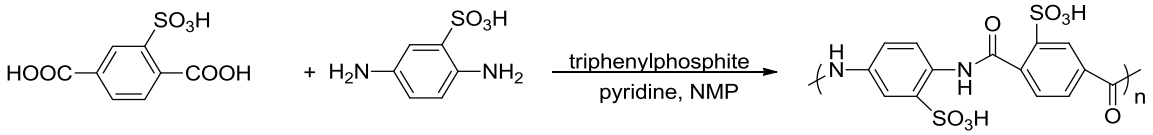

Figure 1.9 Example of fully sulfonated poly(aramides) synthesized via step growth polymerization.[109,110]

Polyelectrolytes can be divided into two categories with respect to charge types. Positively charged polyelectrolytes are so-called polycations and negatively charged polyelectrolytes are polyanions. A great number of functional groups can dissociate into positive charges or negative charges to impart water solubility in polymers. As shown in Figure 1.10, most of the reported polycations are amines or quaternary ammonium ions based on their relative stability, basicity, and versatility. Sulfonium ions, phosphonium ions and metal organic moieties are positively charged functionalities as well.[53] Classical polyanions equivalent to amines or quaternary ammonium ions based polycations are usually oxygen centered anionic sites, such as carboxylates, sulfates, sulfonates, phosphates and phosphonates. The degree of solubility of polyelectrolytes is impacted by many factors, including different types, the number, position, and frequency of charged functionalities along the polymer backbone.

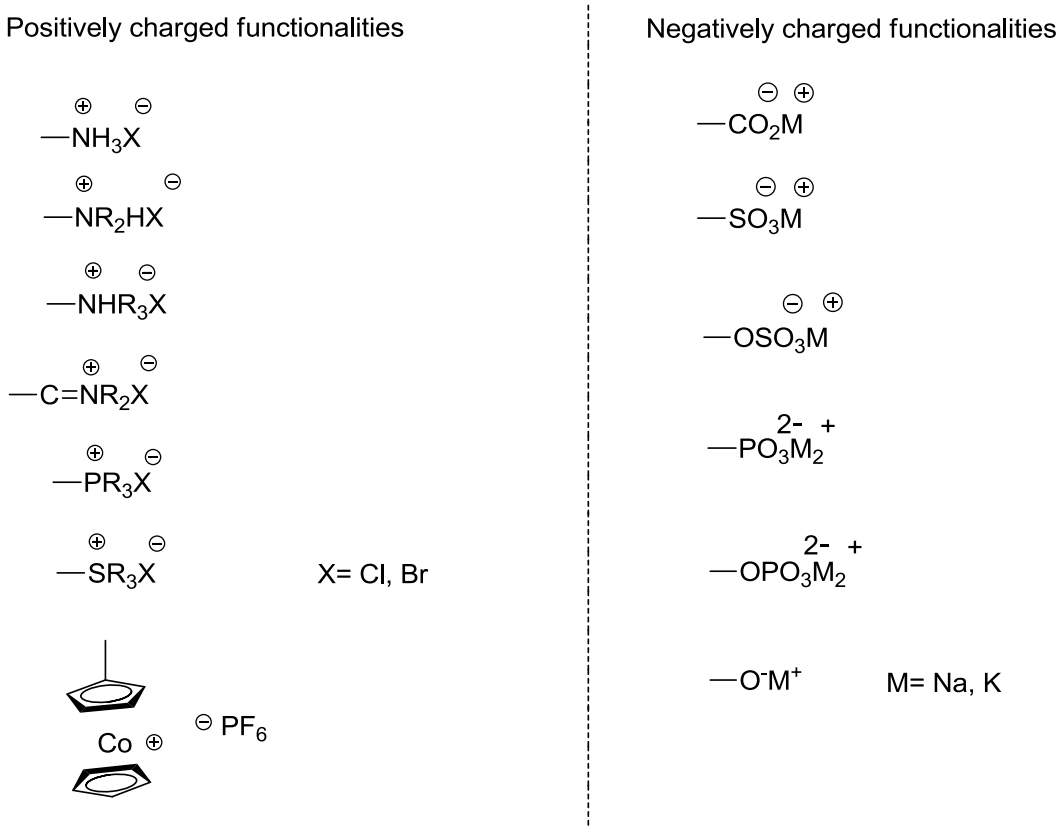

Figure 1.10 Examples of positively charged and negatively charged functionalities.[1,53]

Physical properties of polyelectrolytes, like solution properties and mechanical properties, are dependent on specific structural characteristics of polymer backbones. Primary structure is determined directly by the nature of the repeating units (bond lengths, steric crowding, charge densities, space between charges, polymer chain's hydrophobicity, hydrophilicity, stiffness, etc.). The secondary structure of polyelectrolytes is related to configuration and conformation that are impacted by intramolecular interactions, such as hydrogen bonding and electrostatic interactions. Tertiary structure is related to intermolecular and solvent-polyelectrolyte interactions. Lastly, quaternary structure involves chain aggregation.[1] The polymer structure may derive from repeating of a single monomer unit to form linear homo-polyelectrolytes like sodium polyacrylate and sodium poly(styrene sulfonate) or form multiple monomers to

yield random, alternating, block, graft star-shaped polyelectrolytes or dendrimers,[111] or hyperbranched polymers,[112-114] as shown in Figure 1.11.

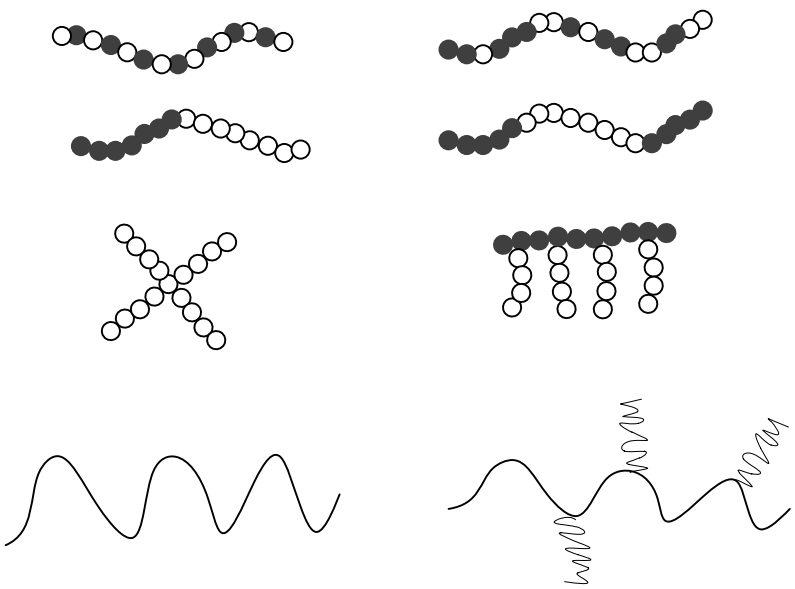

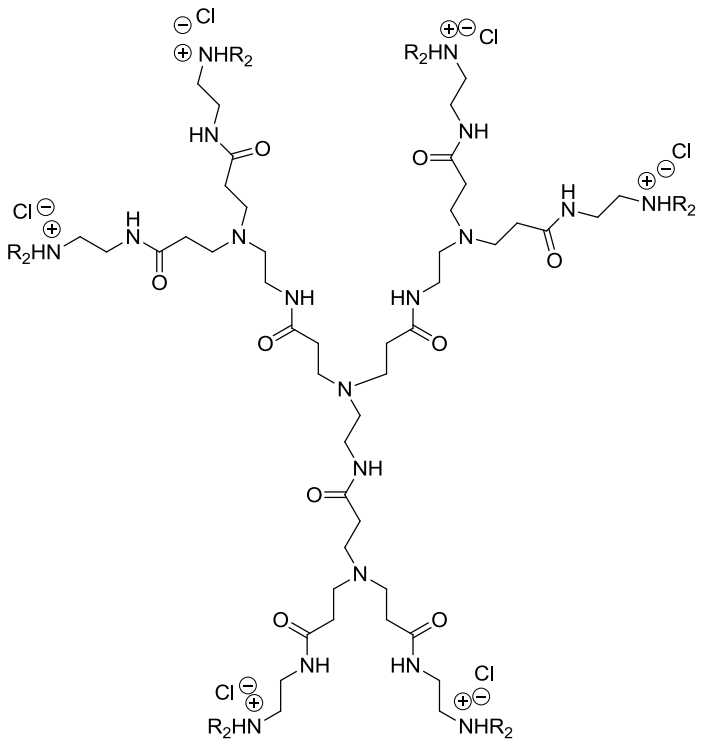

Dendrimer

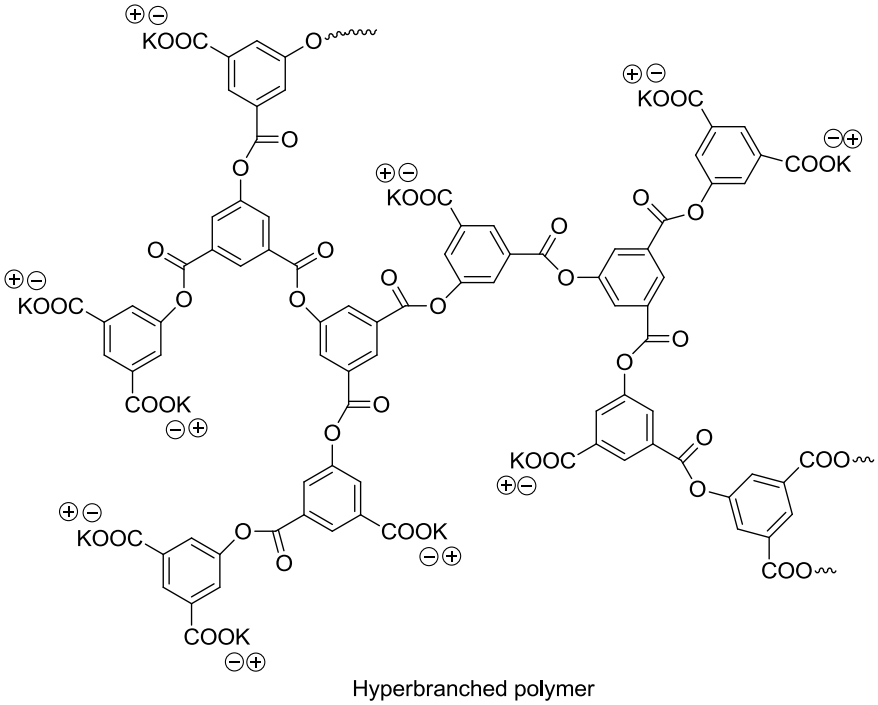

Figure 1.11 Possible polyelectrolyte topologies.[1,111,113]

In nature, materials make use of self-assembly to achieve a variety of functional behaviors which is often impossible to replicate in today's synthetic materials. This self-assembly behavior of biological molecules has attracted considerable scientific attention and understanding. Therefore, much research has been focused on the self-assembly of polyelectrolytes, such as making polyelectrolyte microcapsules by self-assembly techniques.[115-118] The key in this area is to control polyelectrolyte morphology in solution by tuning the polymer architectures and understanding external stimuli's impact on morphology, like ionic strength. Polyelectrolytes dissolved in water can have structures ranging from random coils and extended rods, to polymeric micelles, and polymeric vesicles, as shown in Figure 1.12.[1] Different types of morphology will impart polymers with different physical properties for various applications. For example, random coils and

extended rods are often used for rheology control in industrial applications, such as mineral separation, paints, coatings and food industries.[119-125]

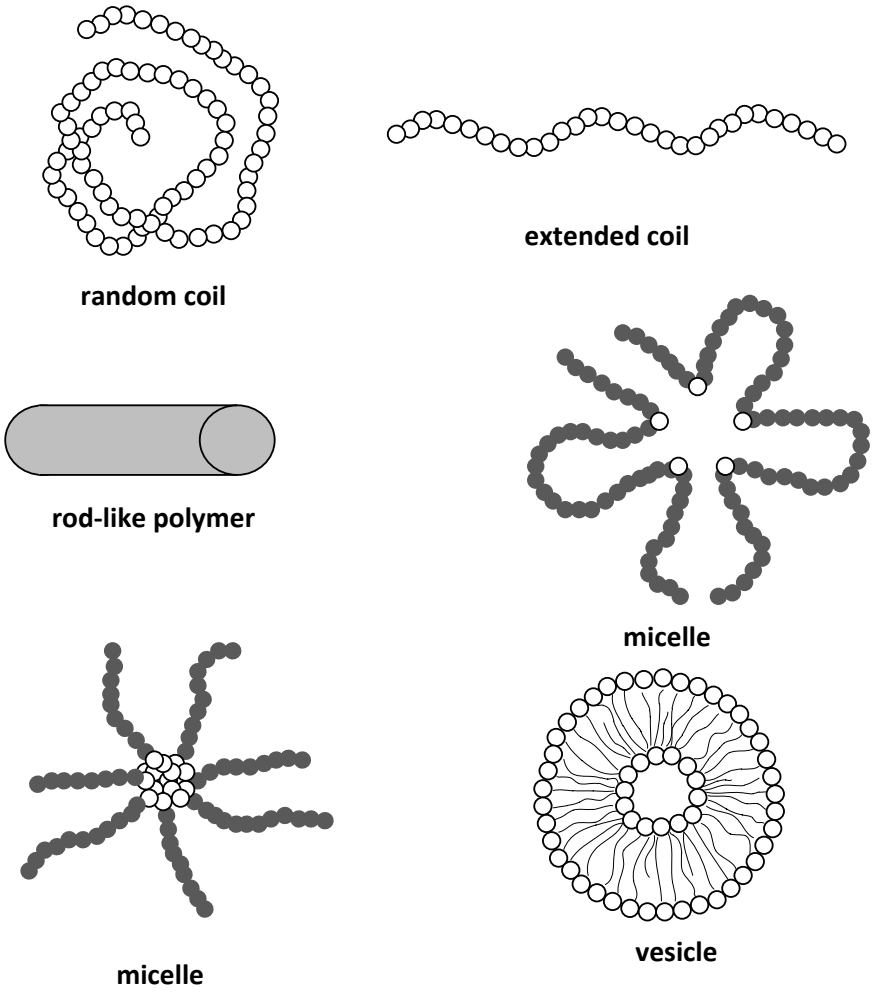

Figure 1.12 Possible polyelectrolyte morphology.

1.3. NATURAL POLYELECTROLYTES

In nature, biological materials with charges and complex architectures can achieve a variety of functional behaviors. These biopolymers, like polypeptides and proteins, polynucleotides and polysaccharides have attracted considerable scientific attention from both experimental and theoretical standpoints.

1.3.1. Polypeptides and Proteins

Most of the polypeptides and proteins are water-soluble. Chemically, protein chains are composed of combinations of the natural 20 amino acids (-NH-CHR-CO-) that are linearly linked together to form polypeptide chains. The R group makes the amino acids different from each other. The amino acids charged at neutral pH are shown in Figure 1.13.[1]

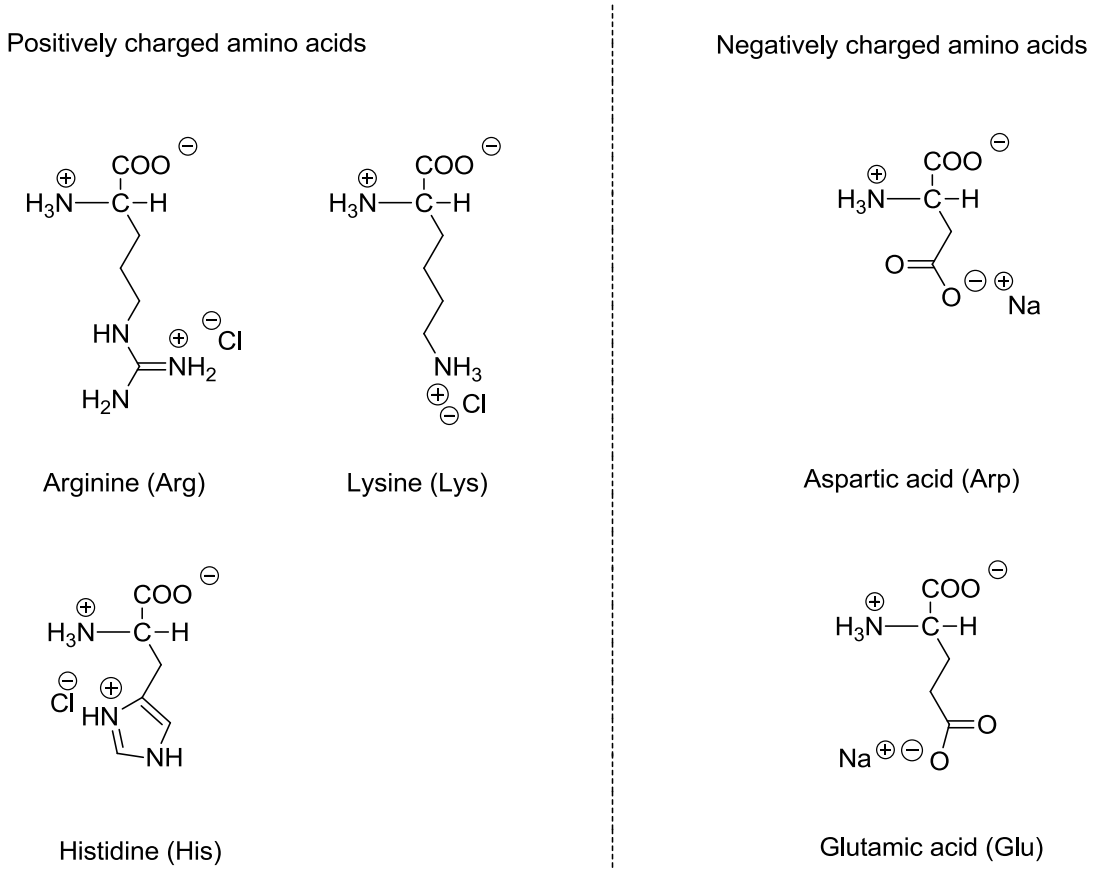

Figure 1.13 Structures of positively and negatively charged amino acids at neutral pH.

1.3.2. Polysacccharides

Polysaccharides, natural polyelectrolytes, can be directly extracted from natural renewable or semi-synthetic resources. They are abundant in nature, such as starch and gums from plant seeds, pectin from fruits, and algin and carrageenan from algae.[1] They are water-soluble polymers and are in cyclic-linear or branched conformations.

Polysaccharides can be prepared by enzyme-catalyzed condensation polymerization based on numerous activated sugar monomers. These activated sugar monomers carry hydroxyl groups that provide polysaccharides hydrophilic characteristics. The remaining monomers are generally hydrophobic. This balance between hydrophilicity and hydrophobicity makes polysaccharides water-soluble. Hydroxyl groups can be substituted either by hydrophobic chains to make the polymer chain more hydrophobic or by charged groups to make the polymer chain more hydrophilic.[126] A charged sugar monomer is shown in Figure 1.14.[1]

Polysaccharides have been widely employed in industry as emulsion stabilizers, flocculants, binders, lubricants and film-formers.[127-132] Natural charged polysaccharides including hyaluronic acid sodium salt, carrageenan, heparin, etc. (Figure 1.15) play an important role in complex biological systems and diverse industrial applications. For example, hyaluronic acid, found in most connective tissues, serves as a lubricant in the joints and participates in the wound-healing process.[133] It was reported that much hyaluronic acid is found to be produced at the wound area after an injury.[133] Carrageenan has been used in food production, like ice cream, chocolate milk, jellies, puddings, etc.[1] It also serves in pharmaceutical and industrial suspensions, such as toothpaste, shampoos, and emulsion polymerization.[1]

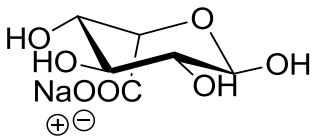

alpha-L-idopyranosyl-uronic acid sodium form

Figure 1.14 Example of charged monomer unit in natural polysaccharides.

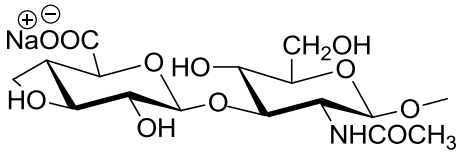

hyaluronic acid sodium salt

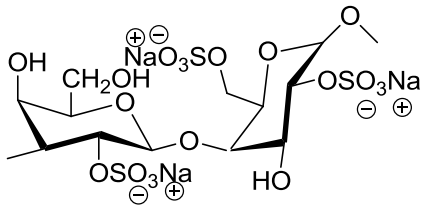

lambda-carrageenan

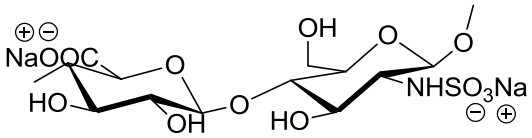

heparan sulfate

Figure 1.15 Representative charged polysaccharides.

1.3.3. Polynucleotides

Nucleic acids are the molecules that carry the information for synthesis of proteins and are considered as the "blue print" used in the design of living organisms. Nucleic acids are linear polymers mainly composed of three parts: nitrogenous bases, a pentose sugar and a negatively charged phosphate group, as shown in Figure 1.16.[134,135] The five principle nitrogenous bases are adenine (A), guanine (G), thymine (T), uracil (U) and cytosine (C), in Figure 1.16.

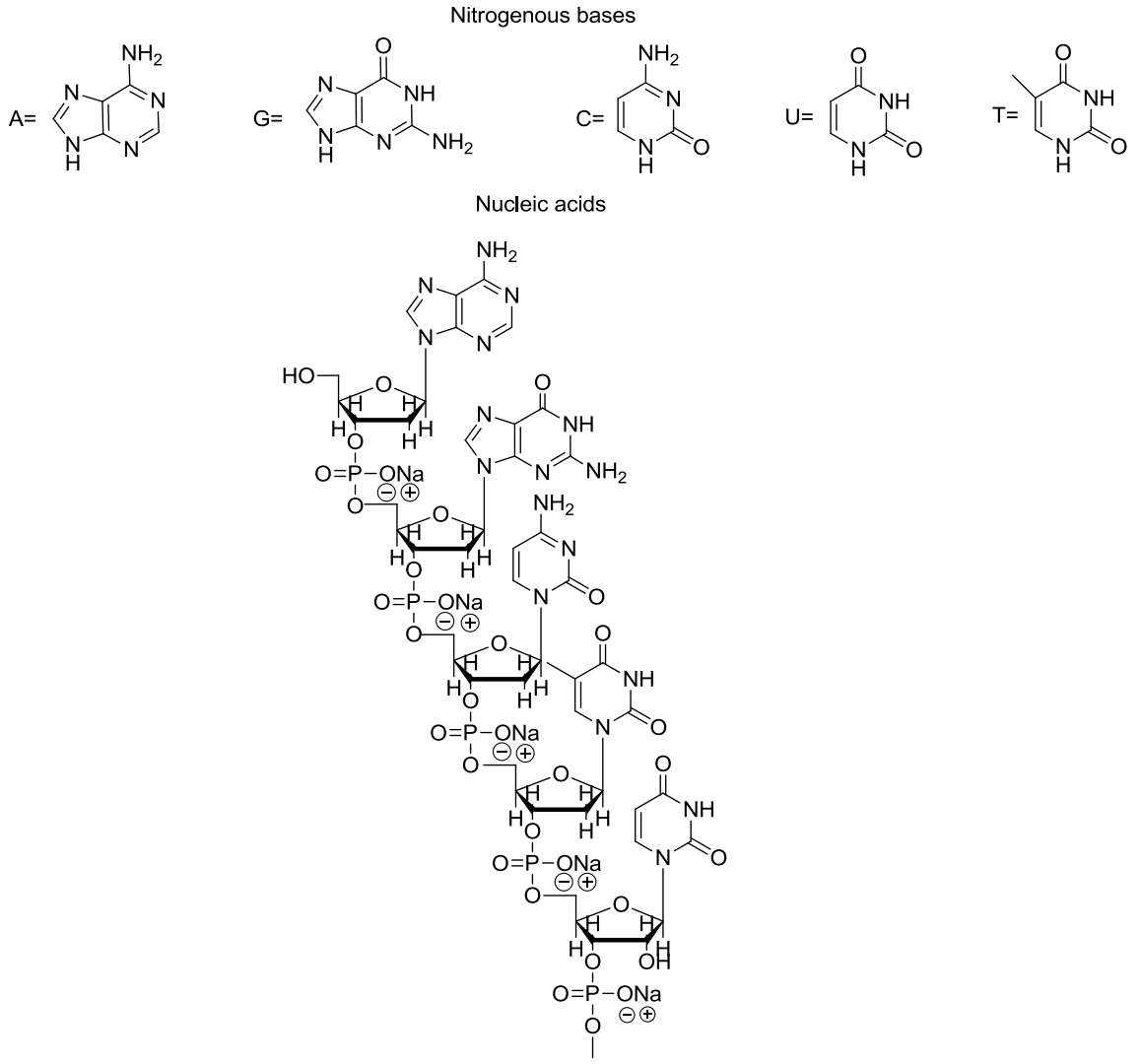

Figure 1.16 Chemical strucuture of nitrogenous bases and nucleic acids.

1.4. SYNTHETIC POLYELECTROLYTES

1.4.1. Anionic synthetic polyelectrolytes

Most synthetic polyanions are based on oxygen centered ionic sites, such as carboxylates, sulfates, sulfonates, phosphates and phosphonates. The typical synthetic anionic polyelectrolytes are sodium polyacrylate, sodium poly(styrene sulfonate), sodium polymethacrylate, and sodium poly(vinyl sulfonate). The common monomers employed in polyanion synthesis are shown in Figure 1.17.[1]

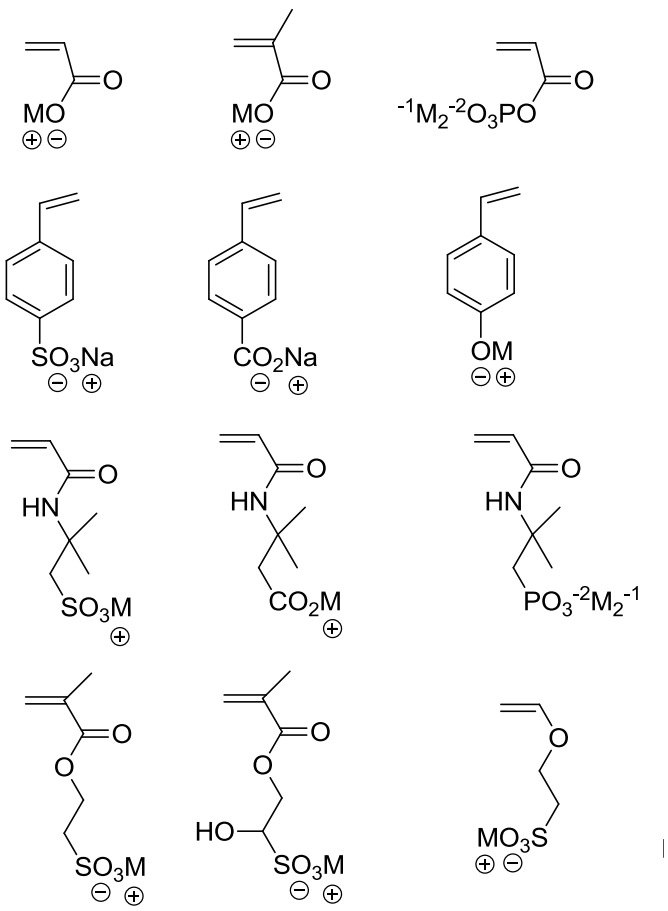

Figure 1.17 Examples of monomers for polyanion synthesis.[1]

Polymerizations of acrylic acids and their salts are usually conducted in aqueous solution by free radical initiation.[136] This direct polymerization is also used commercially and has the advantages of low-cost and environmental friendliness. An alternative strategy to prepare these polyelectrolytes is hydrolysis of polyelectrolyte precursors that are first synthesized in organic solvents. As shown in Figure 1.18,[137] poly(acrylic acid) (PAA) and its salt with controlled structures can be obtained by polymerizing its *tert*-butyl protected precursor using ATRP followed by hydrolysis in HCl solution. The glass transition temperature of dry sodium polyacrylate is almost two times as high as that of

PAA while that of sodium polyacrylate is about 251 ^{o}C and while that of PAA is only about 102 ^{o}C. This difference is due to strong intermolecular ionic interactions. The mechanical properties of PAA in salt form were reported to be higher than those in acid forms, such as rigidity, dynamic viscosity and moduli.[1,138] PAA can absorb many times its weight in water and thus is classified as a superabsorbent and used in products, like disposable diapers.[139,140]

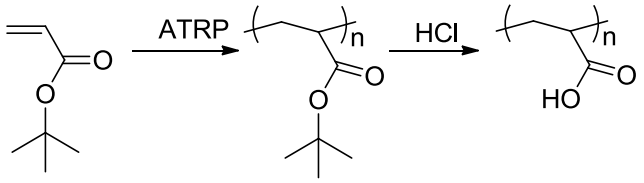

Figure 1.18 Synthesis of poly(acrylic acid) by precursor strategy.[137]

Poly(methacrylic acid) (PMAA) and its salt are common polyanions and have been widely studied. Polymerizations of methacrylic acids and their salts are similar to that of PAA: they can be synthesized by direct polymerization or by precursor strategy via anionic polymerization, as shown in Figure 1.19[141] In contrast to PAA, PMAA exhibits inverse solubility-temperature behavior in solution, i.e., a lower critical solution temperature (LCST). With this specific property, PMAA has been employed in interpenetrating polymeric networks (IPNs) with temperature sensitive poly(*N*-isopropylacrylamide) (PNIPAAm) for "smart" hydrogel materials.[142-149]

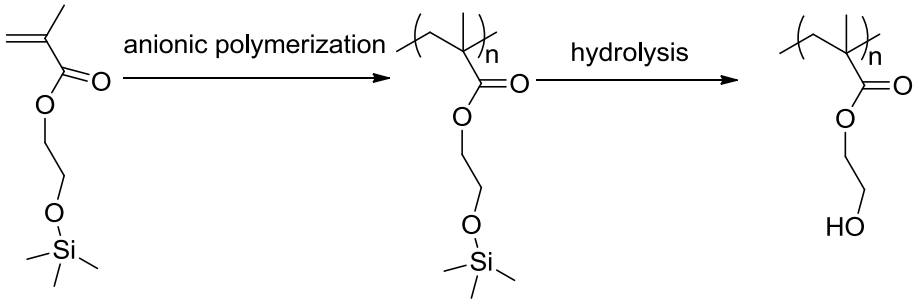

Figure 1.19 Synthesis of poly(hydroxyethyl methacrylate) by precursor strategy.[141]

Sodium poly(styrene sulfonate) (NaPSS) can be prepared by direct free radical polymerization in solution or by sulfonation of polystyrene.[150-154] The chemical structure of NaPSS is shown in Figure 1.20. NaPSS has been discovered as an effective antimicrobial agent for the prevention of HIV infection and sexually transmitted diseases.[155-161] Crosslinked NaPSS has also been employed in an ion-exchange resin and in heavy metal binding studies.[162]

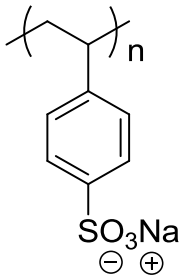

Figure 1.20 Structure of sodium poly(styrene sulfonate).

Maleic acid containing copolymers are a class of polyanions with unique structures and diverse applications in industry.[163] To prepare these anionic polymers, maleic anhydride (MAH) is often used to copolymerize with comonomer(s), since MAH does not homopolymerize.[163] It can be readily copolymerized with different vinylic or acrylic monomers, such as octadecene,[164] vinyl acetate,[165] alkyl vinyl ethers,[166] functionalized styrene[167-170] and stilbene monomers[171-175] to form alternating copolymers,[176] or acrylic acid, *n*-butyl methacrylate, and methyl methacrylate to form non-alternating copolymers.[177,178] In general MAH containing copolymers can be prepared in organic solvent via radical polymerization and are hydrolyzed in solutions to obtain maleic acid or maleate ion containing polyanions, as shown in Figure 1.21.

In contrast to PAA and PMAA, the dissociation behavior of the two carboxylic acids in maleic acid-containing copolymers involves a distinct two-step process. This indicates the two acid groups are in close proximity to exert influence on each other.[179] Amphiphilic maleic acid alternating copolymers show aggregation behavior in aqueous media, which is dependent on the hydrophobicity of comonomers.[180] Maleic acid-containing copolymers have been widely developed to be used in adhesives, binders, coating, paper additives, floor polishing agents, and emulsifiers for pigments.[163,179-181]

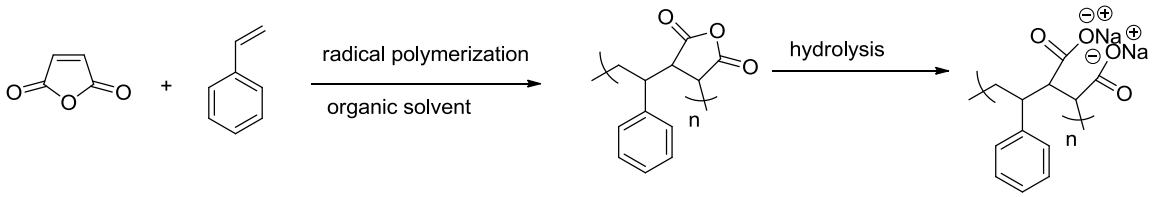

Figure 1.21 Representative synthesis of maleic anhydride containing copolymers and corresponding polyanions.

Besides these classical polyanions, much development work has been conducted on polyelectrolytes with less common anionic groups, like poly(vinylphosphonic acid) and its salt,[182-186] polymeric boronates for biosensor uses,[187,188] polymeric phosphonates,[189] arsonates,[190] polymeric sulfonylimides,[191] as shown in Figure 1.22.

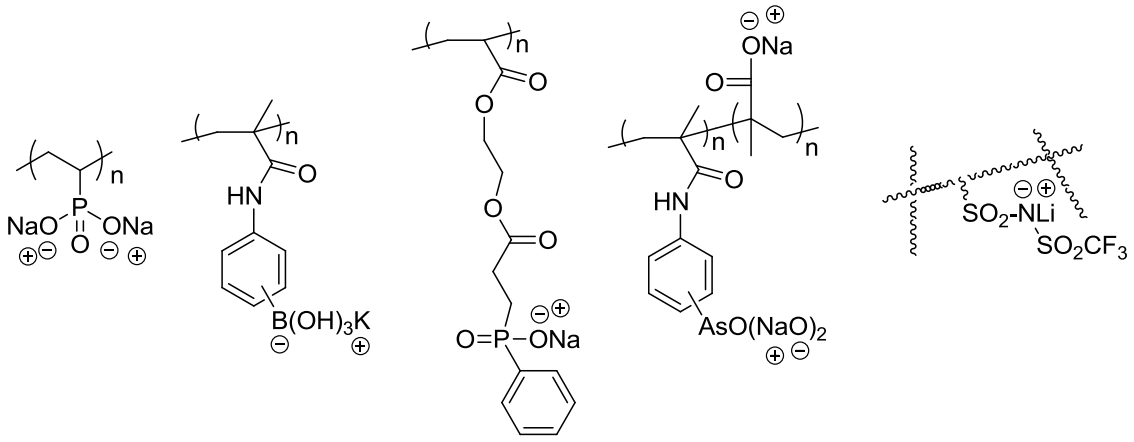

Figure 1.22 Examples of poly(vinylphosphonic acid) sodium salt, polymeric boronates, polymeric phosphonates,[189] arsonates[190] and polymeric sulfonylimides.[191,192]

A new class of anionic alternating polyelectrolytes based on substituted stilbenes and maleic anhydride/substituted *N*-phenyl maleimides has been reported by the Turner group,[171-175] as shown in Figure 1.23. The related monomer structures are shown in Figure 1.24. Precursors of most of these anionic polyelectrolytes were synthesized via free radical polymerization, followed by deprotection of *tert*-butyl groups along the backbone and then hydrolysis in basic solution to form anionic polyelectrolytes.

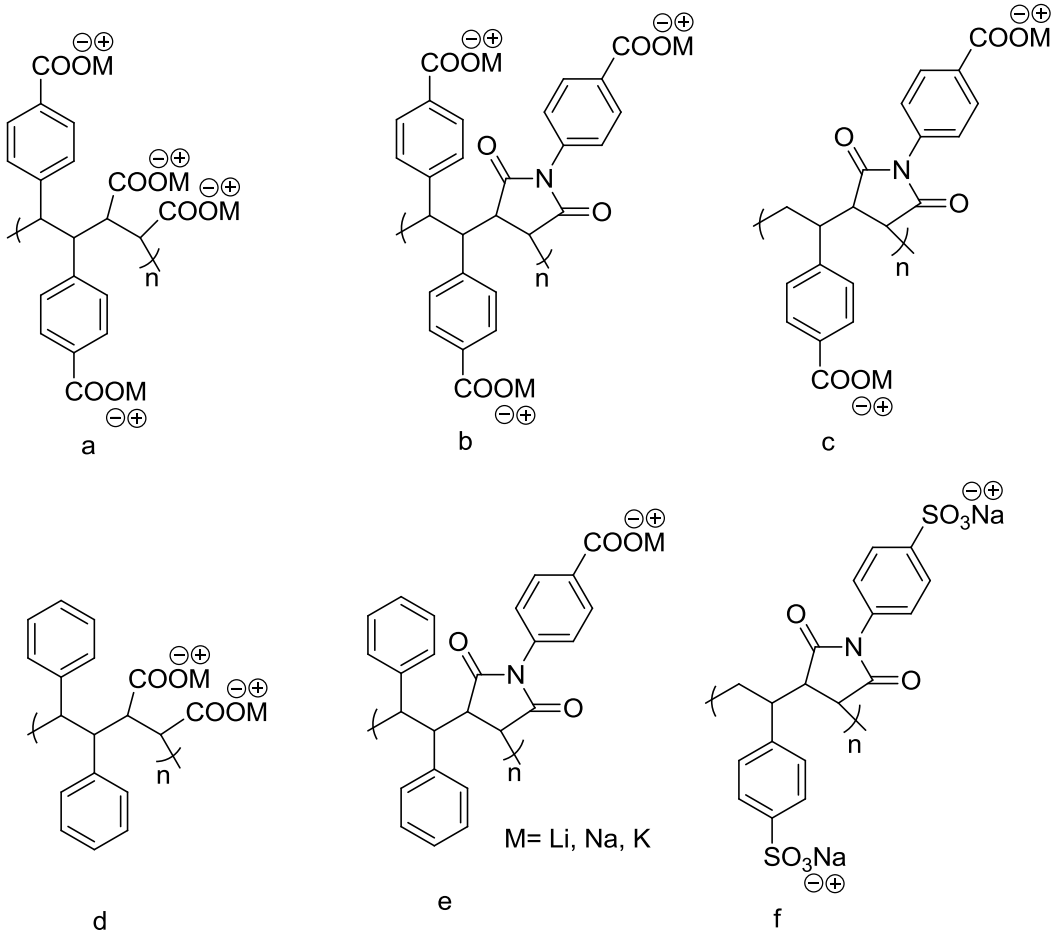

Figure 1.23 Examples of a new class of polyanions based on substituted stilbene monomers. Two styrene based polyanions (e, f) are also included.

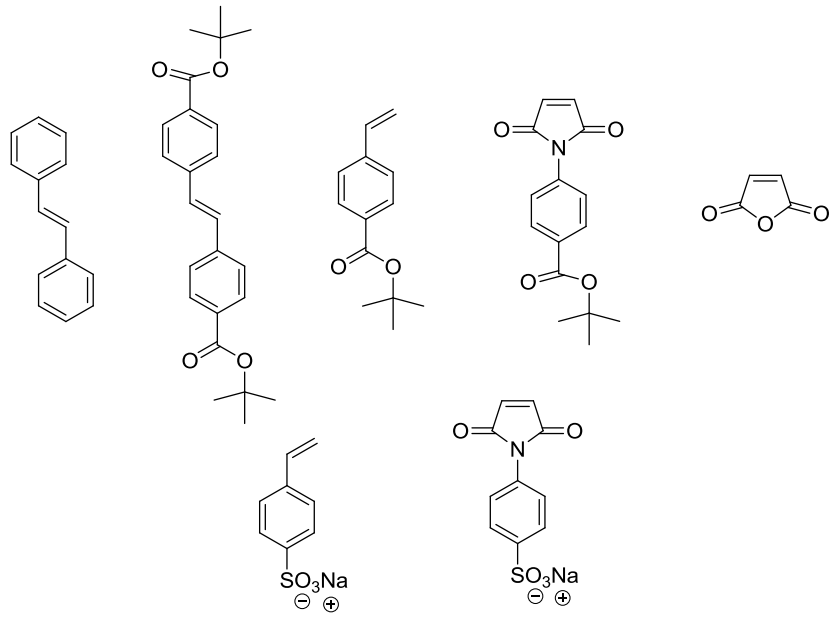

Figure 1.24 Monomer structures for the synthesis of a new class of polyanions.

1.4.2. Cationic synthetic polyelectrolytes

Synthetic polycations often are quaternary ammonium ions. The typical synthetic cationic polyelectrolytes are poly(dimethyldiallylammonium chloride), polyethyleneimine, polyvinylamine, polyacrylamides, etc. The corresponding monomers for the synthesis of polycations are listed in Figure 1.26.[1,193]

Poly(dimethyldiallylammonium chloride) Poly(DADMAC) is a very common polycation used in industry. It is cyclopolymerized from diallyl ammonium chloride monomers,[122,194] shown in Figure 1.25. The preferred structure of poly(DADMAC) is the five-membered ring shown in Figure 1.25, although a six-membered ring was originally postulated.[195] Poly(DADMAC) has been widely employed for applications in the paper industry and in water treatment.[196-199]

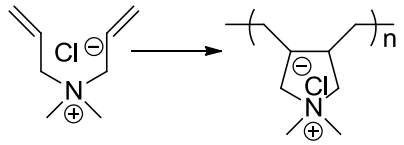

Figure 1.25 Synthesis of P(DADMAC) via cyclopolymerization.[195]

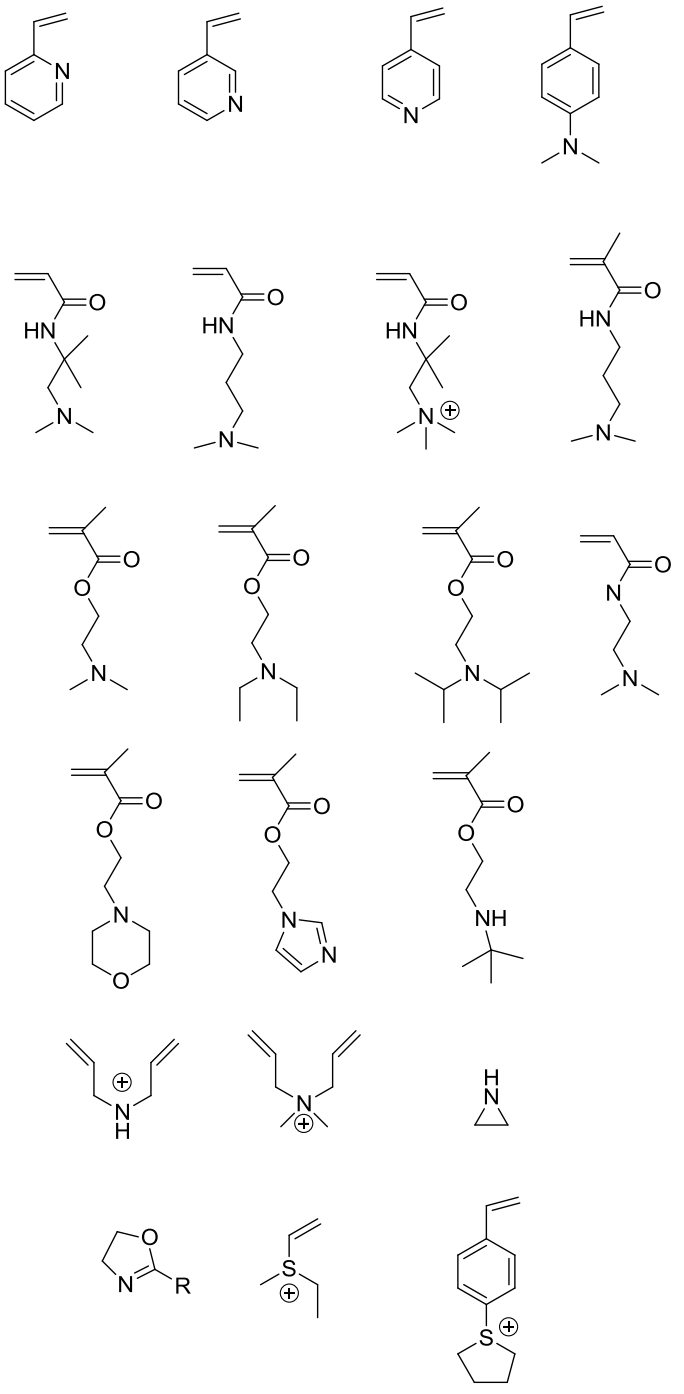

Figure 1.26 Examples of monomers for polycation and polycation precursor synthesis.[1,193]

Cationic polyethyleneimine (PEI) is widely used in applications in CO_2 capture,[200,201] attachment enhancement in cell culture and transfection reagents,[202-204] etc. It can be prepared by acid-catalyzed cationic polymerization with ethyleneimine. Ethyleneimine can be synthesized by reacting ethylene oxide with ammonia, as shown in Figure 1.27.[122] The monomer is relatively unstable and thus will undergo cationic polymerization very rapidly to result in a highly branched polymer structure due to chain transfer reactions.[122] Cationic PEI can be obtained under acidic conditions or by quaternization with reagents such as methyl chloride.

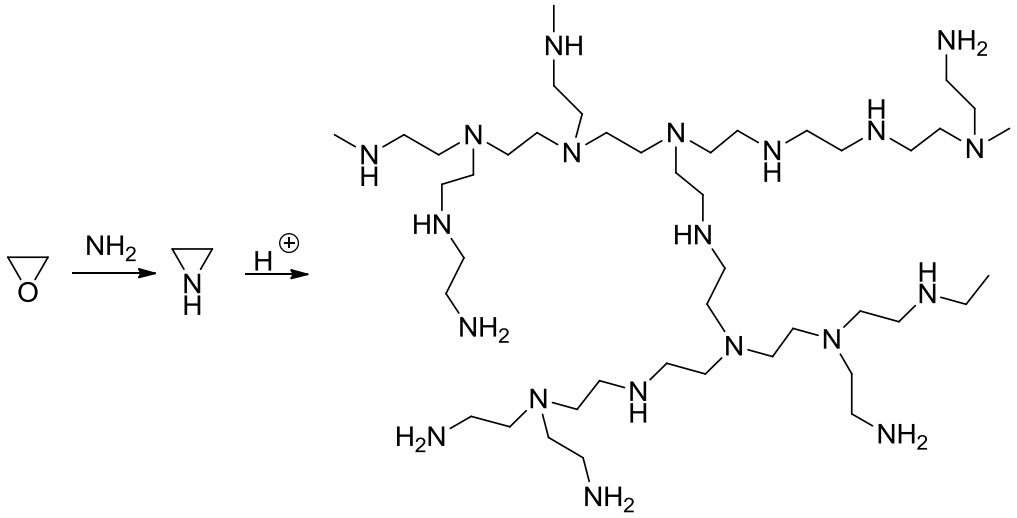

Figure 1.27 Preparation of cationic PEI precursors.[122]

Similar to the previous reported polyanions based on substituted stilbenes and maleic anhydride/substituted *N*-phenylmaleimides, a new class of cationic alternating polyelectrolytes based on substituted stilbenes and substituted *N*-phenylmaleimides has also been reported by the Turner group[171-175,205], shown in Figure 1.28. The related monomer structures are shown in Figure 1.29. These polycations paired with their anionic counterparts are good candidates for solution property studies because they have regular

placement and tunable density of anions and cations along the polymer chain. Thus, polymer architectures are well-understood and controlled.

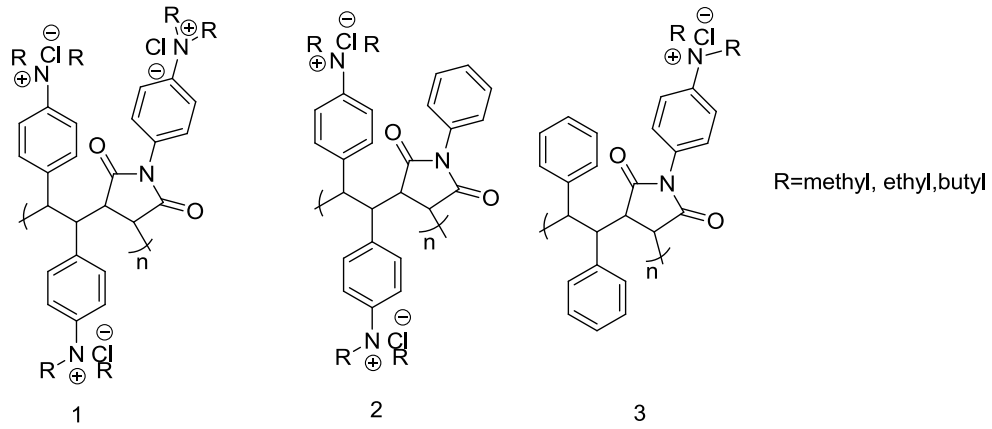

Figure 1.28 Examples of a new class of polycations based on substituted stilbene monomers.

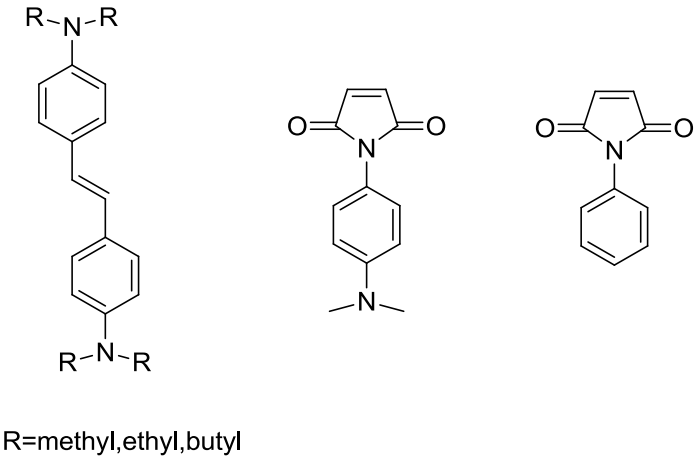

Figure 1.29 Monomer structures for the synthesis of a new class of polycations.

1.5. CHARACTERIZATION OF POLYELECTROLYTES

Polyelectrolyte precursors, when dissolved in organic solvents (e.g., polystyrene dissolved in tetrahydrofuran), can be characterized without the complication that complicates polyelectrolyte characterization efficiency, such as absorbance on column, aggregation, etc. Conventional SEC techniques can be used to obtain molecular weights and molecular weight distributions. Techniques such as osmometry, light scattering and

viscometry (intrinsic viscosity) can also be applied to determine molecular weights. Size of polyelectrolytes in solution can be obtained from dynamic light scattering (DLS). Also, intrinsic viscosity and Mark-Houwink constants of polyelectrolytes can be determined using solution viscosity measurements. Stiffness as determined by persistence length of polyelectrolyte backbones can be quantified by using size exclusion chromatography (SEC) and by small-angle X-ray scattering (SAXS).[206]

1.5.1. Solution properties of polyelectrolytes

In dilute organic solution, polyelectrolyte precursors with flexible chains adopt a "random coil" conformation (Figure 1.30a).[122] When these precursors are charged with anionic or cationic groups along the polymer backbone, flexible polymer chains will adopt more extended conformation from their original "random coils" due to the strong electrostatic repulsions, as shown in Figure 1.30b. The addition of enough electrolytes to the polyelectrolyte aqueous solutions, like NaCl, can cause chains to adopt a random coil conformation just as neutral polyelectrolyte precursors due to the charge screening effect, shown in Figure 1.30c. On the corresponding reduced viscosity vs concentration plot, the so-called "polyelectrolyte effect" can be observed (Figure 1.30d) as a rapid decrease of reduced viscosity of dilute polyelectrolyte solutions is exhibited as the ionic strength increases. Both anionic and cationic polyelectrolytes behave in a similar fashion. A more profound "polyelectrolyte effect" is observed when multivalent electrolytes, like e.g. Ca^{2+}, are added to the dilute solutions. This is because at the same concentration the ionic strength in the polymer solution with multivalent electrolytes is higher than the one with monovalent electrolytes (Figure 1.30d).

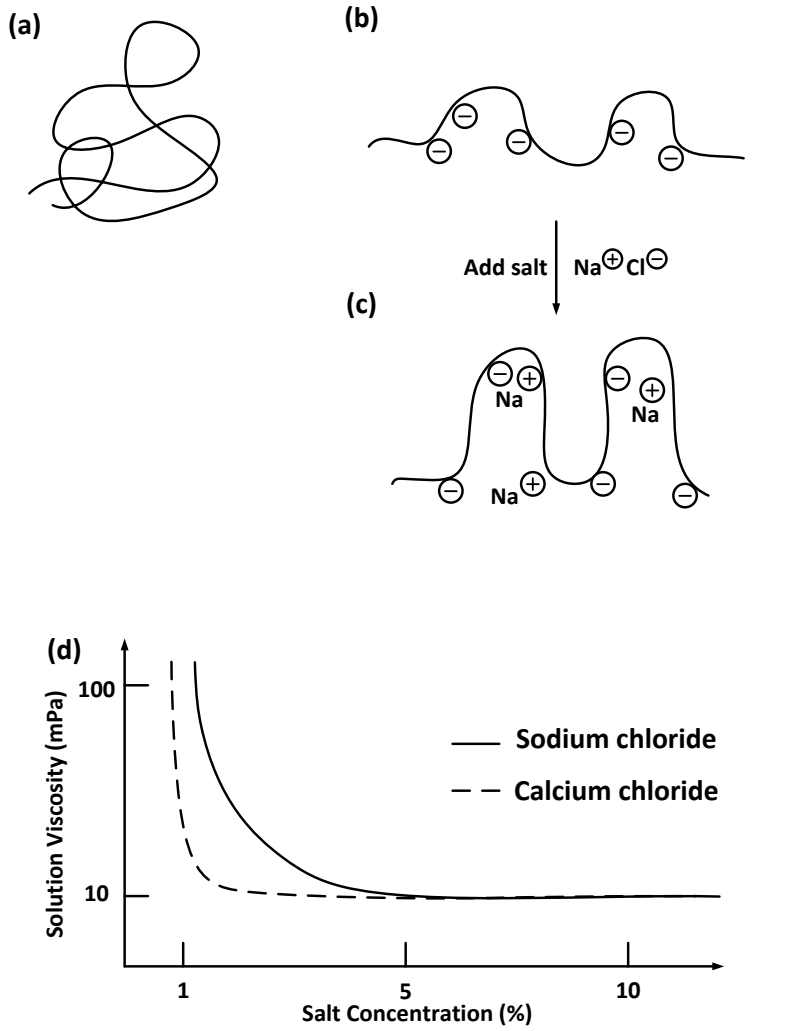

Figure 1.30 Schematic representation of polyelectrolyte behavior with added salt in dilute polymer solutions.[122]

For flexible polyelectrolytes, both intramolecular electrostatic interactions and intermolecular electrostatic interactions exist in the dilute solutions. The well-known "polyelectrolyte effect" observed in the Huggins plot (Figure 1.30d), i.e., reduced viscosity (η_{sp}/c_p) increases as polymer concentration (c_p) decreases or as ionic strength decreases in dilute solutions, which has been extensively discussed in the literature.[207-210] There are some statements that attribute the whole polyelectrolyte effect to conformational changes, i.e., increasing intramolecular coulomb repulsion due to coil

expansion at decreasing ionic strength. Meanwhile other concepts have been developed by Cohen, Priel and Rabin to better explain the effect:[211-215] it is assumed that the dilution of polyelectrolytes starts at a high ionic concentration. Hence, in the initial dilution steps, the Debye screening length, defined as the length over which charges are screened, increases much faster than the average distance between each macromolecule chain, shown in Figure 1.31[52] As a result, the intermolecular electrostatic repulsion increases, leading to the expansion of the macromolecule chains and thus the increase of η_{sp}/c_p upon the initial dilution of salt-free solutions.

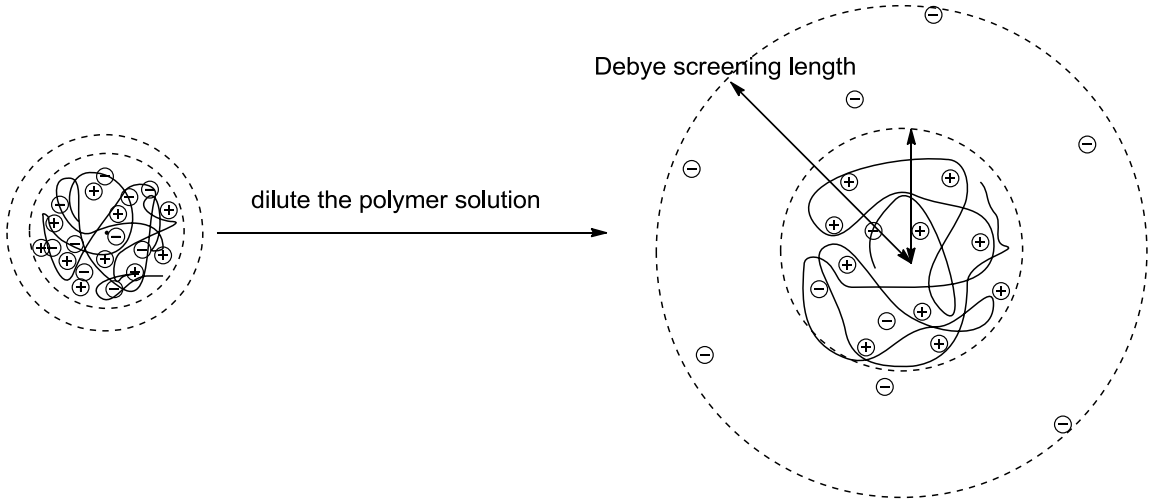

Figure 1.31 Presentation of changes of the Debye screening length (outer length) and the polyelectrolyte's chain conformation (inner circle) on decrease of ionic strength in salt-free solutions.

1.5.2. Chain stiffness of polyelectrolytes

Several analytical techniques can be used to probe the stiffness of a polymer chain. For relatively rigid polyelectrolyte chains, it may be qualitatively observed that in a solution ^{1}H NMR spectrum peaks of hydrogen atoms on the main chains are broadened and almost invisible and the peaks of the hydrogen atoms on the side chains are also very

broad.[171-175,205] This is in agreement with severely restricted mobility of the polymer backbone, indicating the rigidity of the polymer chains.

Another way to measure the stiffness of the polymer backbone is using multi-angle laser light scattering (MALLS).[216] Generally, the polymer conformation is related to the exponent v in the power dependence of the following equation[216] concerning z-average root-mean-square (RMS) radius ($R_{g,z}$) to the weight-average molecular weight (M_w).[217-219]

$$R_{g,z} \propto M_w^{\,v} \tag{1.1}$$

The theoretical value v for a rigid rod polymer is 1.[216] By comparing the experimental values v to the theoretical value v, the stiffness of the polymer backbone can be determined.

The most direct measurement of the rigidity of polyelectrolytes is to determine the persistence length. For stiff and semi-rigid macromolecules, Kratky and Porod proposed a chain model denoted as the "wormlike or Kratky-Porod chain model" which examines a real polymer chain in a simple way. Atoms on a polymer chain in the smallest length scale are recognized. As the length scale increases, a short sequence of monomeric units is exhibited, followed by a longer sequence of the polymer chain that resembles more or less a rigid-rod. The whole polymer chain is recognized as behaving like a Gaussian chain on an even larger length scale.[220,221] The persistence length, l_p, was introduced in this process by Kratky and Porod to reflect the stiffness of a polymer chain. The persistence length is defined as the distance over which the spatial orientations of monomers are not mutually independent, i.e., the orientation of monomer segments 'persist' from one monomer to the next.[222] Persistence length values can be estimated by both SEC and SAXS measurements. L_k is the Kuhn length, first developed by W. Kuhn in

1934 and defined as the distance one must travel along a polymer chain until the polymer has lost all memory of the starting direction.[223] $L_k = 2l_p$.

Persistence lengths can be estimated from a multi-detector SEC using intrinsic viscosity, $[\eta]$, molar mass, M, and $[\eta]$-M conformation plots or from the relationship between molar mass, and radius of gyration, R_g. Multi-detector SEC should be equipped with a UV-Visible absorption detector, a light scattering detector, a differential viscometry detector, and a differential refractive index detector. The lower measurable size is limited for the wavelength of incident light used in SEC light scattering detector because the light scattering detector is not very sensitive to small sized particles. This greatly restricts that range of accessible M-R_g data for the polymers. In comparison, intrinsic viscosity can be measured at lower molar masses and across a broader molar mass range than light scattering detection, making $[\eta]$-M conformation plots a desirable alternative to R_g-M plots.[222]

The persistence length can be estimated from the relationship between molar mass and root-mean-square radius of gyration. Both M and R_g can be readily measured by SEC with multi-angle laser light scattering (SEC-MALLS). The equation relating R_g, M and l_p is eq. (1.2):[222]

$$R_g^{\,2} = \frac{l_p M}{3M_L} - l_p^{\,2} + \frac{2l_p^{\,3}M_L}{3M} - \frac{2l_p^{\,4}M_L^{\,2}}{M^2}\left(1 - e^{-\frac{M}{l_p M_L}}\right) \qquad (1.2)$$

Where the persistence length and the molar mass per unit contour length M_L can be obtained by a least-squares non-linear regression fit of the data to eq. (1.2).[224-227] For example, to determine the persistence length of poly(*n*-hexyl isocyanate) (PHIC), the molar mass and root-mean-square radius of gyration were obtained from light scattering

detection by using SEC and plotted as R_g vs M in Figure 1.33 (a).[222] According to eq. (1.2), a least-squares non-linear regression fit of the data was applied. Persistence length from the fitting is 40 nm in THF. This result is in good agreement with previous studies (the general agreement on the persistence length of PHIC is in the range of 40 to 43 nm).[228-231]

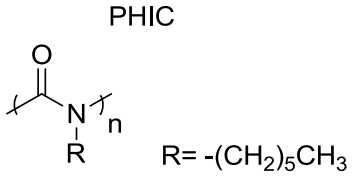

Figure 1.32 Structure of PHIC.

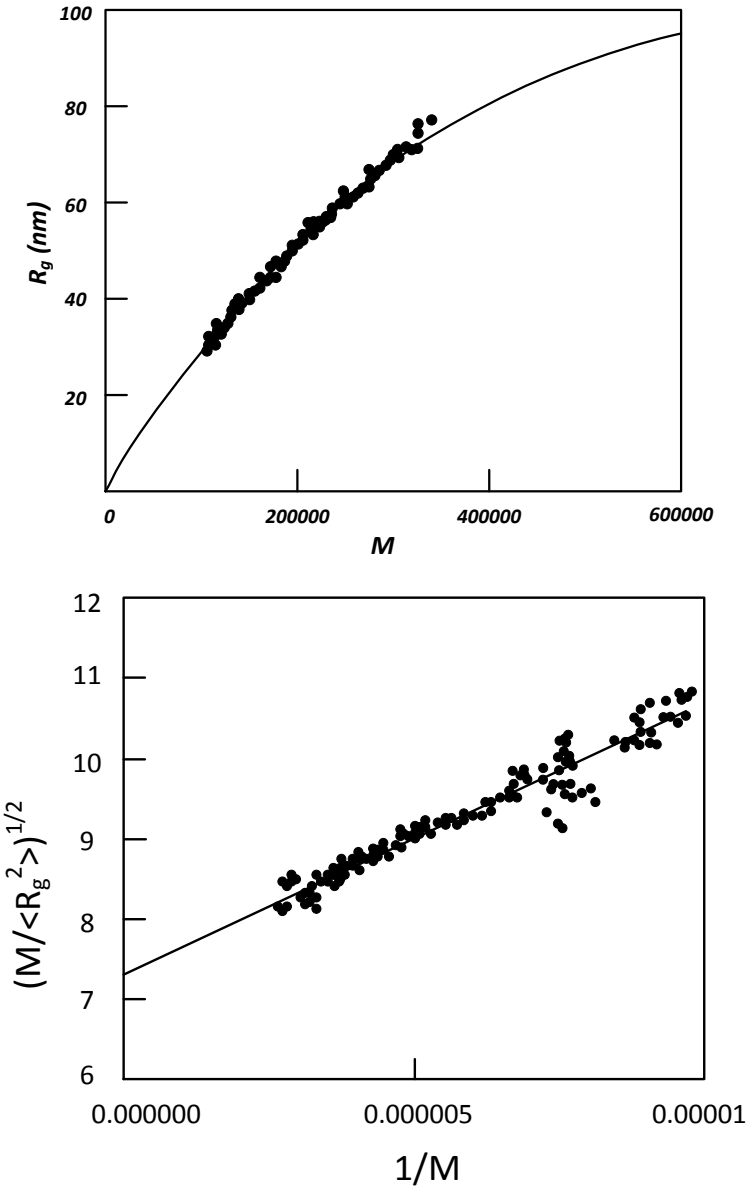

Figure 1.33 (a) R_g-M plot for PHIC in THF. (b) plot of $(M/\langle R_g^2\rangle)^{1/2}$ vs $1/M$ for PHIC in THF.[222]

As shown in eq. (1.3), a simpler method for obtaining the two adjustable parameters M_L and l_p, given by Murakami et al.,[232] is an approximation for eq. (1.2).

$$\left(\frac{M}{\left\langle R_g^{\,2}\right\rangle}\right)^{1/2} = \left(\frac{3M_L}{l_p}\right)^{1/2}\left[1+\frac{3l_pM_L}{2M}\right] \tag{1.3}$$

The two adjustable parameters M_L and l_p can be determined from the intercept and slope of this equation. The data displayed in Figure 1.33 (a) for PHIC in THF were plotted as $(M/\langle R_g^2\rangle)^{1/2}$ vs *1/M* (Figure 1.33 (b)).[222] According to eq. (1.3), a least-squares non-linear regression fit of the data was applied. A complementary estimate of l_p at 40 nm was obtained.

Synthetic vinyl polymers with persistence lengths over 1 nm are rarely reported.[233-237] Polymerization of sterically hindered multi-substituted ethylenes, like 1,2-disubstituted ethylenes, may result in sterically crowded polymer chains with larger persistence lengths, such as poly(*tert*-butyl crotonate) with l_p=5~6 nm.[234] To study this steric crowding effect, the persistence length of poly(diisopropyl fumarate) (poly(DiPF)) was studied by using SEC.[233] M and R_g measured by SEC were plotted as $(M/\langle R_g^2\rangle)^{1/2}$ vs *1/M* and a least-squares non-linear regression fit of the data was applied. l_p was determined to be 11 nm in THF. The structures of poly(*tert*-butyl crotonate) and poly(DiPF) are shown in Figure 1.34 and Figure 1.35, respectively.

Poly(*tert*-butyl crotonate)

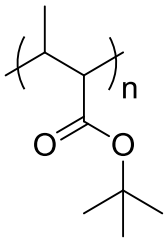

Figure 1.34 Structure of poly(*tert*-butyl crotonate).

Poly(DiPF)

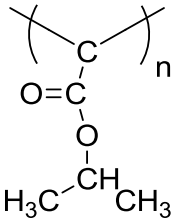

Figure 1.35 Structure of poly(DiPF).

The persistence length can also be estimated from the relationship between M and $[\eta]$. The relationship changes in the extreme case of rigid rod-like macromolecules from $[\eta]\sim M^{1.7}$ to $[\eta]\sim M^{1/2}$ for Gaussian coils at large M, without excluded volume.[222] If a polymer sample has broad enough molecular weight distribution, the transition from a higher to lower $[\eta]$ – M power law can be used to estimate the persistence length by applying a suitable hydrodynamic chain model.

A model proposed by Yamakawa, Fujii, and Yoshizaki (Y-F-Y) relates $[\eta]$ with M.[238] A popular method for obtaining the wormlike chain parameters of the Y-F-Y model is given by the Bohdanecký linear approximation.[239]

$$\left(\frac{M^2}{[\eta]}\right)^{1/3} = \mathrm{A}_\eta + \mathrm{B}_\eta M^{1/2} \tag{1.4}$$

where A_η and B_η are given as

$$A_\eta = \frac{A_0 M_L}{\phi_\infty^{1/3}} \tag{1.5}$$

$$B_\eta = \frac{B_0}{\phi_\infty^{1/3}}\left(\frac{2l_p}{M_L}\right)^{-1/2} \tag{1.6}$$

$\phi_\infty = 2.87\times10^{23}$,[222,239] and A_0 and B_0 are functions of $d/2l_p$,

$$A_0 = 0.46 - 0.53\log\left(d/2l_p\right) \tag{1.7}$$

$$B_0 = 1.00 - 0.0367 \log(d / 2l_p) \quad (1.8)$$

B_0 is nearly constant and replaced by its mean value, 1.05.[239] The persistence length l_p and wormlike chain hydrodynamic diameter d are obtained based on A_η, B_η and M_L values according to eq. (1.4), (1.4), (1.5) and (1.6). Mass per unit contour length, M_L, is not an easy parameter to determine but can be estimated from energy minimization using ChemBio3D Ultra. For example, M from light scattering detection and $[\eta]$ from the viscosity detection of poly(2,7-(9,9 di-*n*-hexylfluorene)) (PHF) were used to create a $(M^2/[\eta])^{1/3}$-M^2 plot as shown in Figure 1.36[222] A_η and B_η were determined from the slopes and intercepts of the Bohdanecký plots according to eq. (1.4). The persistence length l_p and wormlike chain hydrodynamic diameter d were obtained based on A_η, B_η and M_L values according to eq. (1.5), (1.6), (1.7) and (1.8), giving the values ~8.0 nm and ~0.90 nm, respectively. The structure of poly(2,7-(9,9 di-*n*-hexylfluorene)) (PHF) is shown in Figure 1.37.

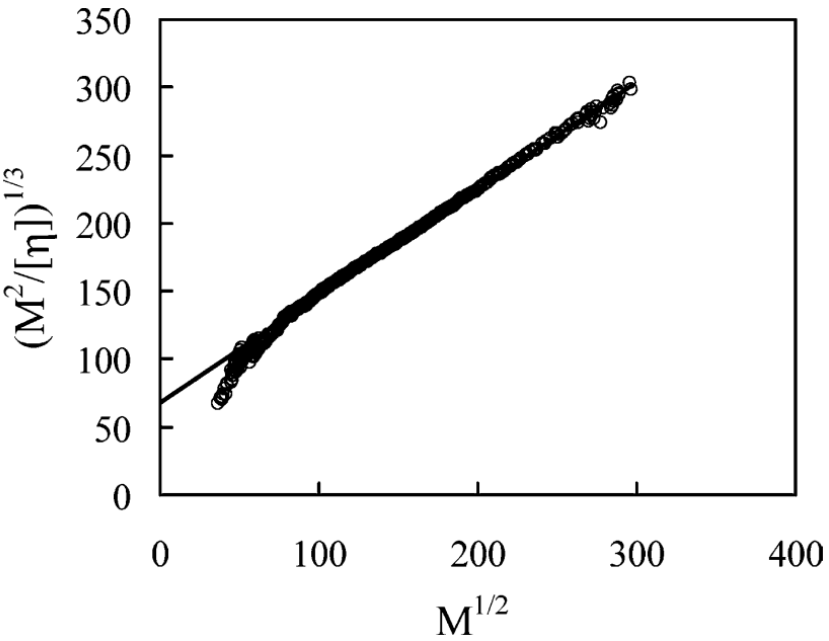

Figure 1.36 $(M^2/[\eta])^{1/3}$-M^2 plot of PHF.[222] (Copyright permission granted by Elsevier Limited).

PHF

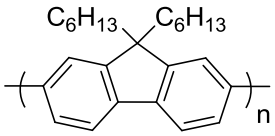

Figure 1.37 Structure of PHF.

The Y-F-Y model was also reported in the evaluation of the persistence length of poly(DiPF).[233] The mass per unit contour length, persistence length and wormlike chain hydrodynamic diameter were evaluated by a Bohdanecký plot according to eq. (3)-(6). l_p of PHF, evaluated by this method, was reported to be 11 nm in THF at 30 ^{o}C as well.[233]

It was concluded by Mourey et al. that light scattering detection and the Kratky-Porod wormlike chain model are more suitable for very stiff, high molar mass polymers, like PHIC, whereas for low molar mass polymers of moderate stiffness it's suggested to apply the Y-F-Y hydrodynamic cylindrical model to viscometry detection data.[222]

SAXS is the most direct and definite method to quantitatively evaluate the persistence length. The X-ray was first produced and detected by Wilhelm Conrad Roentgen in 1895 and the first solution X-ray scattering measurement was first performed in the late 1930s. The scope of small angle X-ray scattering with respects of spatial dimension covers a range of 1 nm to 1 μm. This makes SAXS a suitable measurement to probe both shapes and sizes in bio-polymeric and synthetic polymeric areas.

Physically, SAXS measures distances or structures by interference. As shown in Figure 1.38, the X-ray plane waves travel in phase before reaching two scattering particles. When reaching these two scattering particles, X-ray waves are scattered. When two scattered X-ray waves arrive at a detector pixel in phase, the constructive

interference makes them enhance each other. When they arrive at a detector pixel out of phase, the deconstructive interference makes them cancel each other. The interference pattern received on the detector contains information of the distances between these two scattering particles.

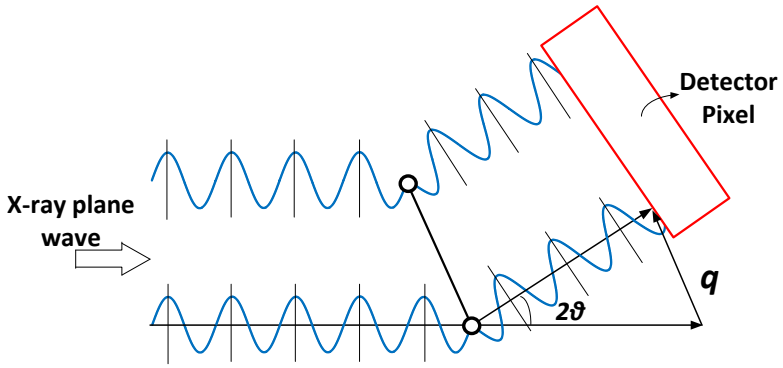

Figure 1.38 Interference pattern of X-ray waves. Retrieved from "Solution Small Angle X-ray Scattering: Basic Principles and Experimental Aspects" online.

Based on the interference pattern, Bragg's law illustrates a relationship between the particle distance *d*, and the constructive interference.[240-242]

$$\sin\theta = \frac{\lambda}{2d} \tag{1.9}$$

Where θ is the scattering angle, d is the distance between two scattering particles, and λ is the wavelength. As shown in Figure 1.39, s_0 is defined as the unit incident wave vector and s_1 is defined as the unit scattering wave vector. The wave vector change is $\vec{s} = \vec{s}_1 - \vec{s}_0$ and $|\vec{s}| = 2\sin\theta$. The scattering vector, q, is defined as $\vec{q} = (2\pi/\lambda)\vec{s}$. Therefore $|\vec{q}| = (4\pi/\lambda)\sin\theta$ and according to eq. (1.9)

$$q = 2\pi/d \tag{1.10}$$

where the reciprocity between q and d indicates that information on relatively large scale is obtained at a relatively small q.[243]

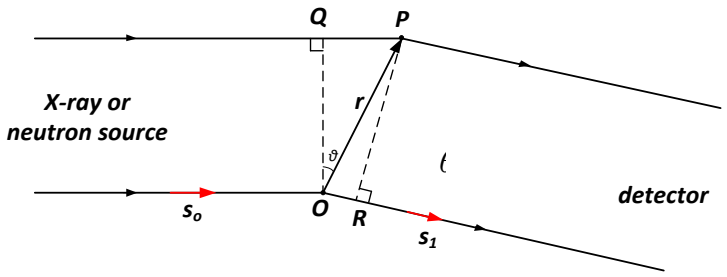

Figure 1.39 Geometry of X-ray scattering.

A scattering plot of $I(q)$ vs q, where $I(q)$ is the scattering intensity and q is the scattering vector, can be divided into different regions that probe various length scales associated with different dimensions of a polymer chain. Based on theoretical predictions for a sufficiently long chain (a Gaussian chain),[244] two characteristic regions may be observed. At small q, the scattering pattern reflects the random coil nature of a polymer chain, and is expressed by the Debye function, where $I(q) \sim q^{-2}$ is valid;[245] as q is increased, the scattering pattern is governed by the behavior of small sections of the polymer chain and exhibits $I(q) \sim q^{-1}$ characteristic of rigid rods, shown in Figure 1.40. The difference between these two scattering patterns is even more pronounced when plotting $I(q)q^2$ against q. This plot is so-called the "Kratky-Porod" plot. As shown in Figure 1.41, in a "Kratky-Porod" plot the horizontal line is representative of the Debye behavior while the q^{-1} region is represented by a sloped straight line that extrapolates back to the origin.[243] An intersection of these two regions defines the persistence length. To determine the persistence length, it is customary to use a log-log plot of $I(q)$-q where two regions are matched with lines having slopes of -2 and -1, respectively.[246,247] Alternatively, a "Kratky-Porod" plot can be used as well. An extrapolation of the intersection of these two linear regions at a value q^* is related to the persistence length by

$$l_p = A/q^* \tag{1.11}$$

where the constant A is derived from computations. Porod gave A=6/π=1.91 for Gaussian coils.[246,247] However this value 1.91 is limited to use in cases where the polymer chain is infinitely long or very large (usually over 100 times its persistence length).[248] For coils with finite sizes (non-Gaussian chains), A= 2.3 is calculated by the use of a Monte-Carlo technique that was suggested as a more accurate approximation.[249-251]

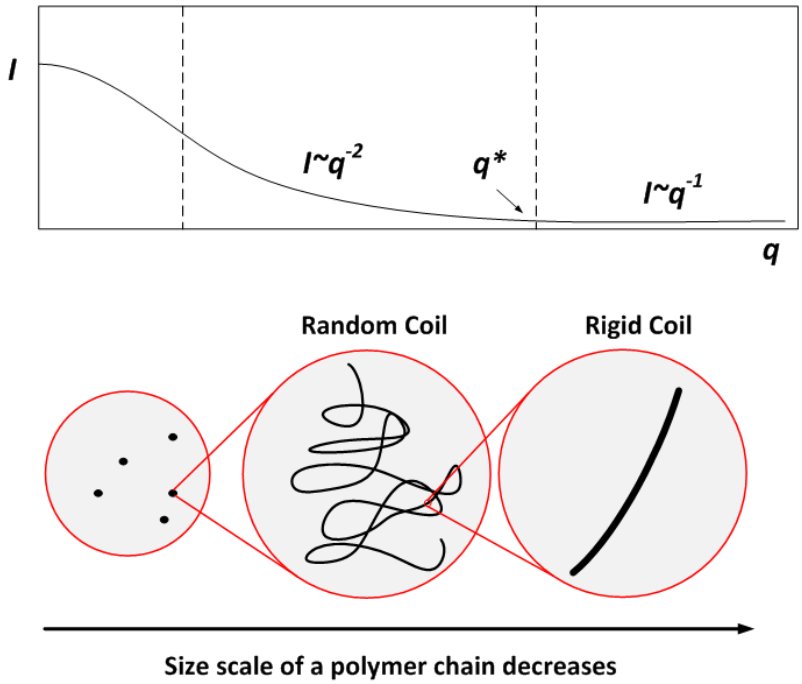

Figure 1.40 Schematic representation of X-ray scattering pattern. Retrieved from "SR summer school 2006" by Adam Squires at University of Reading.

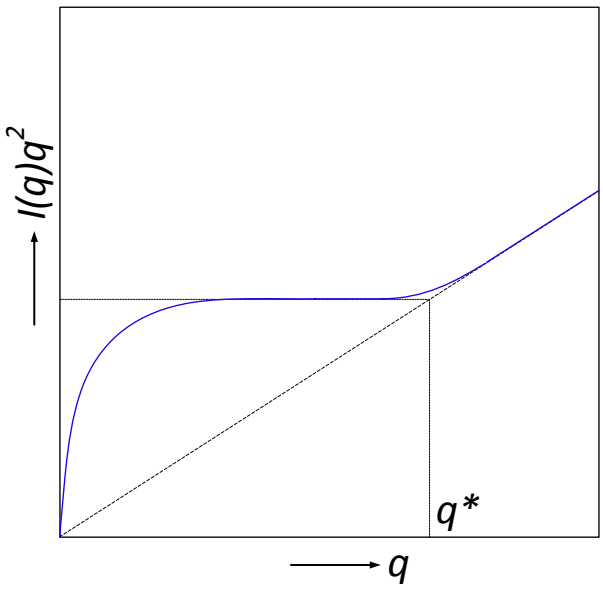

Figure 1.41 Kratky-Porod plot for persistence length determination.

For example, SAXS has been applied in determination of the persistence length of poly(acrylic acid) (PAA) in dioxane. Two characteristic regions were observed in a Kratky-Porod plot. The value of q^* was determined at the intersection of a horizontal line representative of the Debye behavior, and a sloped straight line that extrapolates back to the origin representative of the q^{-1} region. The persistence length was determined to be 1.4 nm by using $l_p = 2.3/q^*$, where q^* was 0.16 Å obtained from the Kratky-Porod plot.[237] The structure of PAA is shown in Figure 1.42.

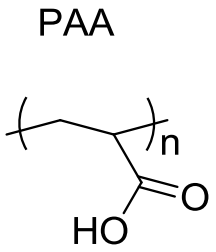

Figure 1.42 Structure of PAA.

For non-Gaussian coils, the ideal situation of two distinctly different linear regions having q^{-2} and q^{-1} scaling in the SAXS data is not often fulfilled. Various

authors[242,244,252-257] have reported that the ideal slope in the -2 region did not appear at a small q in scattering measurements; rather, the power law was generally less than -2 in the Debye region and a change in slopes of two characteristic regions was observed. This is similar to the theoretical curves described previously and the q^* at the slope change was used to define l_p. For example, the persistence length of hyaluronic acid (the structure shown in Figure 1.43) was estimated by SAXS in 0.05 M HNO_3 and in 0.2 M NaCl, respectively. The scattering pattern displayed a -2 Debye behavior and -1 rod behavior in 0.05 M HNO_3 with persistence lengths of 4 to 6 nm, but showed a non-horizontal line in the Debye region in 0.2 M NaCl. It was stated that the ionization of the polymer in NaCl solution might result in a stretching of the persistent elements. A change in slopes of two characteristic regions was observed and employed to define q^* with the persistence length of 4 nm by using $l_p=2.3/q^*$.[252]

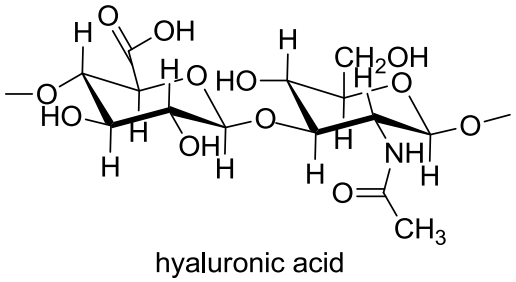

Figure 1.43 Structure of hyaluronic acid.

The persistence lengths of cellulose tricarbanilate (Figure 1.44) were determined in dioxane at different temperatures. Due to the finite molecular weights of cellulose tricarbanilate, the horizontal line in the -2 region was not observed in the Kratky-Porod plot. However, a change in two regions with different slopes was observed and used to estimate the persistence length. The persistence length at ambient temperature was found

to be 11.0 nm by using $l_p = 1.91/q^*$. The persistence length was reported to decrease with increasing temperature.[253]

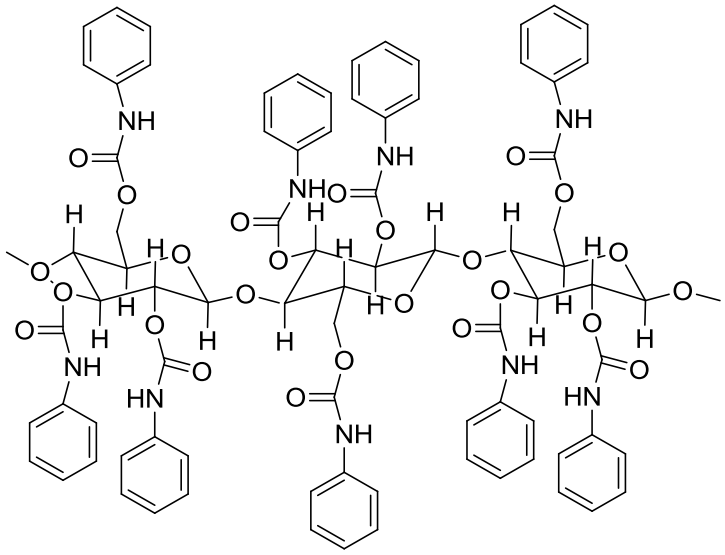

Figure 1.44 Representation of cellulose tricarbanilate.[258]

Poly(2-methoxy-5-(2'-ethylhexyloxy)-1,4-phenylenevinylene) (MEH-PPV) solution was studied by SAXS in xylene and THF, respectively.[256] From the Kratky-Porod plot of MEH-PPV in xylene, both ideal -2 and -1 regions were observed, while a slope of -1.3 in the Debye region was observed in THF. This was attributed to the interactions of MEH-PPV side groups with THF solvent, which facilitates the formation of compact coils. The persistence length was calculated by using l_p=1.91/q*. It was reported that the persistence lengths of MEH-PPV, determined to be in a range of 2.0 to 6.6 nm in xylene, are dependent on the extent of backbone conjugation.[256] The structure of MEH-PPV is shown in Figure 1.45.

MEH-PPV

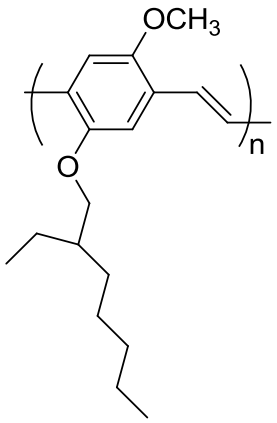

Figure 1.45 Structure of MEH-PPV.[256]

With all examples shown above, it is concluded that SAXS scattering pattern can be affected by various factors, such as solvents, molecular weights, ionic strength, etc. Also, most of the scattering curves exhibit a gradual transition between the two regions. These problems make the graphical determination of persistence lengths subject to some uncertainties.[244] To solve this problem, different analytical approaches were introduced to accurately determine the persistence length.[244,257,259,260] The most widely used methods are Sharp and Bloomfield function, corrected by Schmid[261], and a global scattering function.[262,263] An example is isotactic poly(hydroxybutyrate) (*i*-PHB). A gradual transition was observed in the log-log plot of $I(q)$-q where two regions were matched with lines having slopes of -2 and -1, respectively. This resulted in ambiguities in persistence length determination by the graphical approach. To solve this problem, the persistence length of *i*-PHB was also studied by the Sharp and Bloomfield function and a global scattering function. It was reported that the persistence length obtained using the global scattering function was in good agreement with the graphical approach. The Sharp and Bloomfield approach appeared to yield different values for the persistence length.

This was attributed to the limitation of SBF, which is adequate to be used as $q < 2/l_p$.[244] The structure of *i*-PHB is shown in Figure 1.46.

i-PHB

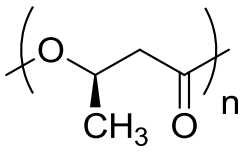

Figure 1.46 Structure of *i*-PHB.

The contour length $L << l_p$ appeared rigid. The contour length $L >> l_p$, on the other hand, appeared flexible. In the semi-flexible regime L is smaller than or comparable with l_p.[264,265] The semi-flexible regime is a broadly defined regime.

1.5.3. Polyelectrolyte complexes

In the polyelectrolyte area, there's a growing scientific and industrial interest in the field of complexes of cationic and anionic polyelectrolytes, which is reflected by an increasing number of published articles each year. Several reviews on polyelectrolyte complexes (PECs) have also been provided.[44,266-272] The process to form PECs is mainly entropy and electrostatic interaction driven. The strong electrostatic interactions between polyanions and polycations lead to interchain ionic condensation. Meanwhile, the liberation of the low molecular counterions results in an entropy gain because low molecular counterions are no longer restricted to the polymer chain. In addition, other interactions such as hydrogen bonding, van der Waals forces, hydrophobic and dipole interactions may also play an important part in the formation of PEC structures.

Studies on complexes between oppositely charged synthetic polyelectrolytes date back to 1961 by Michaels et al.[273] It was reported that high molecular weight

poly(vinylbenzyltrimethylammonium chloride) and sodium poly(styrene sulfonate) were mixed together in aqueous solution to form a water insoluble PEC which contained equivalent quantities of each polyelectrolyte. The formation of PEC can lead to various structures of complexes, depending on the structural features of the initial polyelectrolyte components and the external conditions, such as molecular weight of the polyelectrolytes, location of the charges, stoichiometry, etc. According to Kabanov et al.,[274] two main types of PEC structures need to be considered when mixing two oppositely charged polyelectrolytes with regard to their stoichiometric ratio. When weak ionic group charged polyelectrolytes with significantly different molecular weights were used and mixed together in a non-stoichiometric ratio, water-soluble PECs formed. Such complexes consist of a long host polymer chain sequentially coupled with a short oppositely charged polymer chain, as shown in Figure 1.47. Predominantly carboxylic groups containing polyanions were used to complex with various polycations.[44]

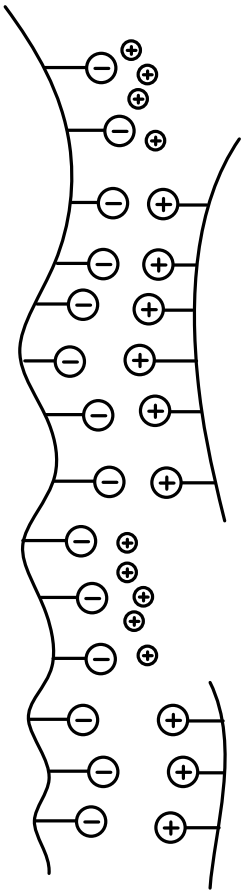

Figure 1.47 Schematic representation of PEC in a non-stoichiometric ratio.[275]

When strong ionic group charged polyelectrolytes with similar chain lengths were complexed together in a 1:1 stoichiometric ratio, the resulting structures of PEC are described by Kabanov et al. with two possible models, as shown in Figure 1.48. Model (a) reflects a more ordered structure, a "ladder" structure with fixed ionic crosslinks based on polymer chain conformational adaptation. Model (b) describes a less ordered situation where a "scrambled-egg" structure formation takes places due to a statistical charge compensation.[275]

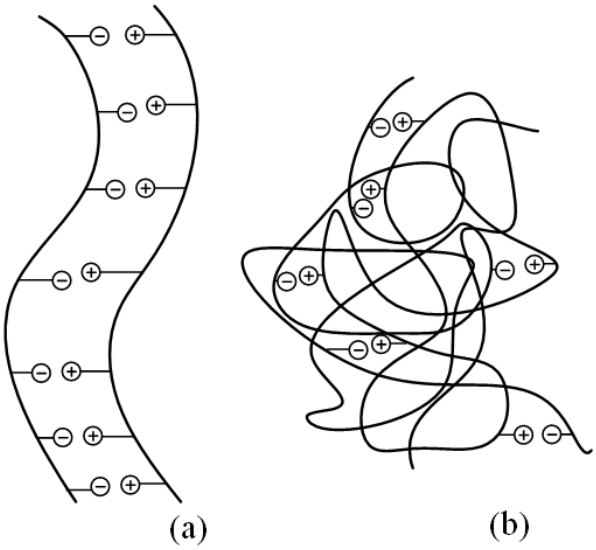

Figure 1.48 Formation of water-soluble PECs

Comprehensive and systematic studies on soluble PECs started with the pioneering work of the groups of Kabanov et al.[274,276] and Tsuchida et al.[277-279] The structure of water-soluble PECs is shown in Figure 1.47, where PECs consist of a long host polymer chain sequentially coupled with a short oppositely charged polymer chain. Such complexes are usually considered as block copolymers because they are composed of both hydrophilic single-stranded (uncomplexed segments) and hydrophobic double-stranded segments (complexed segments).[44] Water-soluble PECs have been widely investigated as potential drug carriers.[280-282] For example, polyelectrolyte complexes (PECs) between chitosan derivatives and insulin were prepared to inherit the nontoxic and biocompatible properties of chitosan by Kissel et al.[282] Parameters influencing complex formation were characterized by turbidimetric titration, dynamic light scattering (DLS) and laser doppler anemometry (LDA). It was found that the PEC formation was predominantly pH-dependent and the stability of PECs was influenced by polyelectrolyte chain lengths.

1.5.3.1. Effect of chain length

The PEC formation is dependent on many factors, including the polymer chain length, mixing ratios, the chemical structure of polymers, external stimuli, such as the ionic strength, temperature, etc. The stability of PECs is influenced by the polymer chain length. In the previous example, Kissel et al. reported that precipitation of PECs between chitosan derivatives and insulin was only avoided when the MW of the polymers was over 25 kDa. Also, an increase in the ionic strength of the solution accelerated complex dissociation.[282] It was stated by Karibyants et al. that poly(diallyldimethylammonium chloride) (PDADMAC) is preferably complexed with the shorter polystyrene sulfonates based on extensive studies on the complexation of polycations and polyanions with different molecular weights.[283]

1.5.3.2. Effect of mixing ratio

It was found that the mixing ratio of polyanions and polycations also plays a role in the formation of PECs. For example, Davison et al. prepared complexes between the polycationic quaternized poly(vinyl imidazole) and an excess of a higher molecular weight partially sulfonated dextran with different mixing ratios. It was found that an increasing polycation/polyanion ratio resulted in smaller, more compact complex aggregates.[284] PEC formation between components with strong ionic groups and high molecular weights were studied by static light scattering as a function of the mixing ratio by Dautzenberg et al.[285-287] Sodium poly(styrene sulfonate) and sodium poly(methacrylate) were used as polyanions and PDADMAC and its copolymer with acrylamide were used as polycations. It was concluded that in pure water there was a slight tendency of decreasing particle mass and size with increasing mixing ratio while at

higher salt contents an increase of the particle mass with rising mixing ratio was observed.[285]

1.5.3.3. Effect of neutral water-soluble chains

The stability of colloidal particles can be greatly improved by using polymers containing neutral water-soluble chains, like poly(ethylene oxide) (PEO) and poly(*N,N*-dimethylacrylamide) chains.[44,288-290] For example, complexes formed between the block copolymers containing anionic sodium poly(methacrylate) and PEO segments and cationic poly(*N*-ethyl-4-vinylpyridinium bromide) were investigated by Kabanov et al.[288] It was found that PECs were stable in a much broader pH range compared to the ones prepared from homopolymers. These PECs self-assembled to form the core of a micelle comprised of neutralized polyions, surrounded by the PEO corona. Dautzenberg et al. studied PECs between the cationic block copolymers of PDADMAC with PEG and the anionic block copolymers of poly(2-acrylamido-2-methyl-1-propanesulfonic acid) and PEG.[290] In pure water close to the 1:1 mixing ratio, the short PEG block (M = 2 kDa) is sufficient for the stabilization of the PECs. They also found the stability of complexes with short PEG blocks with regard to subsequent addition of salt was very low. When copolymers with long PEG blocks were used in PEC formation, high salt stability was observed.[290] Staikos et al.[291] studied the formation of PECs between the cationic PDADMAC and the anionic graft copolymers poly(sodium acrylate-*co*-sodium-2-acrylamido-2-methyl-1-propanesulphonate)-graft-poly(*N,N*-dimethylacrylamide) (PDMAM) (Figure 1.49) in aqueous solution in comparison with the PECs formed between PDADMAC and the poly(sodium acrylate-co-sodium-2-acrylamido-2-methyl-1-propanesulphonate) without the nonionic hydrophilic PDMAM side chains. A

combination of quasi-elastic light scattering measurements, turbidimetric study, conductivity and viscometry measurements were used to characterize PECs. It was observed that the water-insoluble PEC core was stabilized by a hydrophilic PDMAM corona.[291]

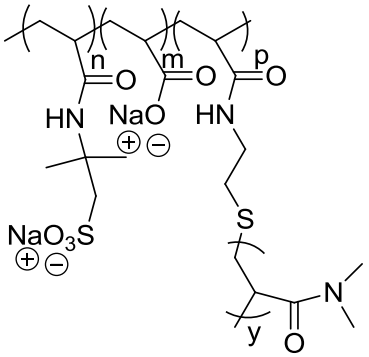

Graft copolymers poly(sodium acrylate-co-sodium-2-acrylamido-2-methyl-1-propanesulphonate)-graft-PDMAM

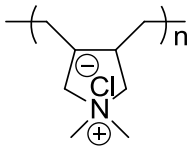

PDADMAC

Figure 1.49 Structure of PEC components.[291]

Salt plays a decisive role in PEC formation because it affects the electrostatic interactions and enables rearrangement processes.[44] Extensive research has been conducted in the field of salt impact on the PEC formation.[285,292-298] As shown in Figure 1.50, the level of aggregation for PECs between anionic sodium poly(styrene sulfonate)/sodium poly(methacrylate) and cationic PDADMAC and its copolymer with acrylamide dramatically decreased at the presence of a small amount of salt. At higher ionic strengths, the secondary aggregation and a strong increase in PEC masses and sizes took place because the surface charges of PECs were screened by additional salt. To keep

increasing the amount of salt eventually led to the macroscopic phase separation, such as flocculation.[285] Therefore, the amount of salt can tune the level of aggregation during complex formation.

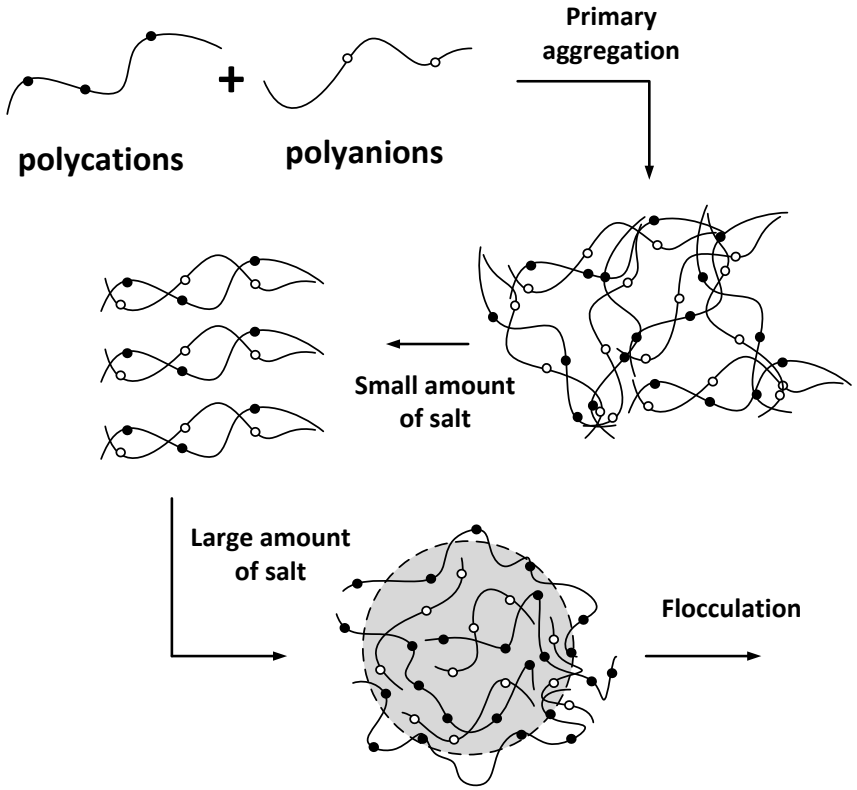

Figure 1.50 Schematic representation of salt influence on PEC formation.[44]

Poly(*N*-isopropylacrylamide) (PNIPAAm) is a classic thermally responsive polymer that has a lower critical solution temperature (LCST) around 32 ^{o}C. This means PNIPAAm is soluble in water at low temperatures, but becomes insoluble when the temperature is increased above 32 ^{o}C. This effect is due to the intermolecular and intramolecular hydrogen bonding switch in the small range of temperatures around its LCST, as shown in Figure 1.51. Recent studies on PEC formation between PNIPAAm with differing contents of anionic and cationic groups have shown a temperature controlled, reversible swelling-deswelling process at about 35 ^{o}C. The formation,

structure, and temperature behavior of these PECs were studied by viscometry and static and dynamic light scattering.[299]

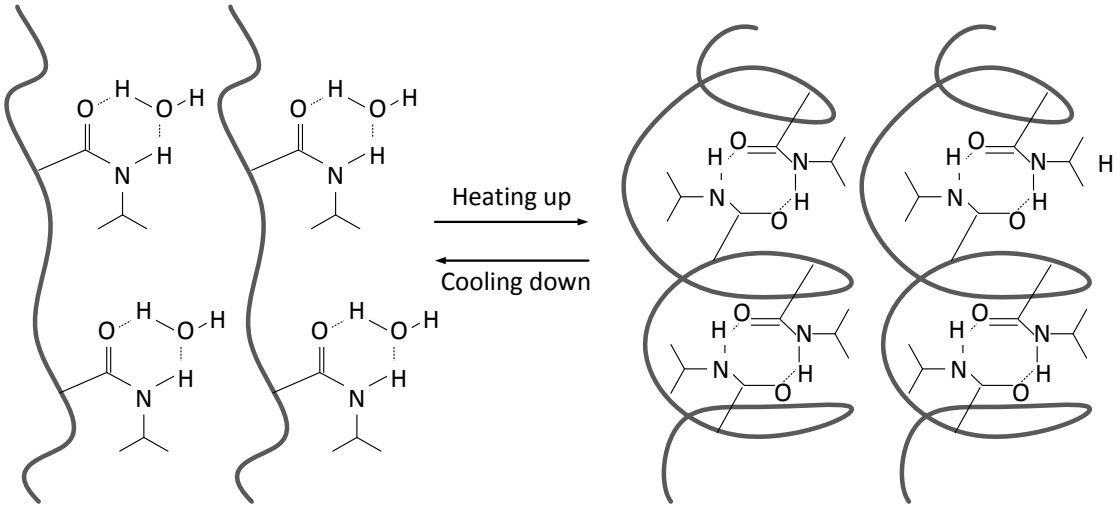

Figure 1.51 Schematic representation of the intermolecular and intramolecular hydrogen bonding switch for PNIPAAm.

The formation and stability of PECs can be influenced by chain stiffness also. For example, the effect of chain stiffness on the course of the complex formation between polyelectrolytes, such as hyaluronic acid (HA) and a copolymer of acrylamidomethylpropanesulfonate (AMPS) and acrylamide (AAm), with oppositely charged colloidal particles such as serum albumin was studied by Dubin et al.[300] It was found that binding was generally weaker for stiffer chains, like HA, relative to flexible chains like poly(AMPS-co-AAm). The increase of polymer stiffness promotes chain desorption on an oppositely charged sphere. Stoll et al. later investigated complex formation between a weak polyelectrolyte chain and an oppositely charged nano-particle using Monte Carlo simulations and concluded that chain stiffness promotes the polyelectrolyte expansion that penalizes the polyelectrolyte adsorption at the nano-particle surface.[301]

An interesting observation in a variety of systems, such as aggregation of DNA induced by multivalent counterions,[302] is the like-charge attraction between rod-like polyelectrolytes. A rod-like polyelectrolyte chain with condensed divalent counterions can be treated as a charged polyampholyte, and strong dipole-dipole attractions can overcome repulsions from the net charges on the rods.[303] It was observed that a block copolymer containing a polyampholyte based on TDAS-MAH comonomer and a poly(methoxy-capped oligo-(ethylene glycol)methacrylate) block exhibited PECs with unusual pH and salt responsive properties similar to like-charge attraction effects in rigid polyelectrolytes.[171]

1.5.3.4. Potential Applications

The size and structure of PECs can be tailor-made. External parameters such as the ionic strength, the pH of the medium or the temperature can be used to control the behavior of the PECs. Therefore, such complexes are of great interest with a variety of potential applications. It was reported by Rubner and coworkers[304] that a honeycomb-like polyelectrolyte surface layer-by-layer (LbL) assembled from poly(allylamine hydrochloride) and poly(acrylic acid) in a low-pH solution exhibited superhydrophobic behavior and created stable superhydrophobic coatings used as antifouling, self-cleaning and water resistant coatings.

Hammond et al.[305] reported that a polyelectrolyte film with an enhanced ionic conductivity was generated by LBL assembly of poly(2-(dimethylamino)ethylmethacrylate) star and poly(acrylic acid) star polymers. The thickness, porosity, and refractive index of this film were precisely tunable by pH conditions and thus charge density. This pH responsive film can be used in potential

applications such as vehicles for drug delivery, porous membranes, and pH-responsive surface engineering materials. Films consisting of anionic poly(sodium 3-(4-vinylbenzylsulfanyl)-propane-1-sulfonate)-co-poly(2-hydroxyethylvinylbenzyl sulfoxide) with different charge densities and cross-linkable cationic poly(4-methyl-1-(4-vinylbenzyl)-pyridinium chloride) were prepared by Laschewsk et al.[306] In this study it was found that film thicknesses increased with decreasing charge density. These films can be used for controlling wetting properties or interactions with biological systems.

REFERENCES

(1) McCormick, C. L.; Lowe, A. B.; Ayres, N. In *Encyclopedia of Polymer Science and Technology*; John Wiley & Sons, Inc.: 2002.

(2) Dai, Z.; Möhwald, H.; Tiersch, B.; Dähne, L. *Langmuir* **2002**, *18*, 9533.

(3) Bedard, M. F.; De Geest, B. G.; Mohwald, H.; Sukhorukov, G. B.; Skirtach, A. G. *Soft Matter* **2009**, *5*, 3927.

(4) Wattendorf, U.; Kreft, O.; Textor, M.; Sukhorukov, G. B.; Merkle, H. P. *Biomacromolecules* **2007**, *9*, 100.

(5) Brian A, B. *Prog. Polym. Sci.* **1995**, *20*, 987.

(6) Pasquier, N.; Keul, H.; Moeller, M. *Des. Monomers Polyms.***2005**, *8*, 679.

(7) Florjańczyk, Z.; Bzducha, W.; Wieczorek, W.; Zygadło-Monikowska, E.; Krawiec, W.; Chung, S. H. *J. Phys. Chem. B* **1998**, *102*, 8409.

(8) Schulz, C. R.; Okun, D. A.; Water; Project, S. f. H. *Surface Water Treatment for Communities in Developing Countries*; Wiley, 1984.

(9) Jahn, S. A. A. *J. Am. Water. Works. Assoc.* **1988**, *80*, 43.

(10) Babu, R.; Chaudhuri, M. *J. Water Health* **2005**, *3*, 27.

(11) Ndabigengesere, A.; Narasiah, K. S.; Talbot, B. G. *Water Res.* **1995**, *29*, 703.

(12) Tripathy, S. K.; Kumar, J.; Nalwa, H. S. *Handbook of Polyelectrolytes and Their Applications: Polyelectrolyte Multilayers, Self-Assemblies and Nanostructures*; American Scientific Publishers, 2003.

(13) Shahinpoor, M.; Bar-Cohen, Y.; Simpson, J. O.; Smith, J. *Smart Mater. Struct.* **1998**, *7*, R15.

(14) Hong, T.; Xiaopeng, Z.; Baoxiang, W.; Yan, Z. *Smart Mater. Struct.* **2006**, *15*, 86.

(15) Jaehwan, K.; Chun-Seok, S.; Sung-Ryul, Y. *Smart Mater. Struct.* **2006**, *15*, 719.

(16) Jaehwan, K.; Sang Yeol, Y.; Kyo, D. S.; Sean, J.; Sang, H. C. *Smart Mater. Struct.* **2006**, *15*, 809.

(17) Barbar, A.; Saila, N.; Donald, L. *Smart Mater. Struct.* **2007**, *16*, S256.

(18) Barbar, J. A.; Donald, J. L. *Smart Mater. Struct.* **2007**, *16*, 1348.

(19) Dibakar, B.; Bishakh, B.; Ashish, D. *Smart Mater. Struct.* **2007**, *16*, 617.

(20) Brufau-Penella, J.; Puig-Vidal, M.; Giannone, P.; Graziani, S.; Strazzeri, S. *Smart Mater. Struct.* **2008**, *17*, 015009.

(21) Brufau-Penella, J.; Tsiakmakis, K.; Laopoulos, T.; Puig-Vidal, M. *Smart Mater. Struct.* **2008**, *17*, 045020.

(22) Choonghee, J.; Hani, E. N.; Roy, H. K. *Smart Mater. Struct.* **2008**, *17*, 065022.

(23) Chi-An, D.; Chih-Chun, H.; Shih-Chun, W.; An-Cheng, K.; Chien-Pan, L.; Wei-Bor, T.; Wen-Shiang, C.; Wei-Ming, L.; Wen-Pin, S.; Chien-Ching, M. *Smart Mater. Struct.* **2009**, *18*, 085016.

(24) Kimiya, I.; Stephen, J.; Kazuo, Y.; Sachio, N. *Smart Mater. Struct.* **2009**, *18*, 095022.

(25) Sung-Ryul, Y.; Gyu Young, Y.; Jung Hwan, K.; Yi, C.; Jaehwan, K. *Smart Mater. Struct.* **2009**, *18*, 024001.

(26) Bonomo, C.; Bottino, M.; Brunetto, P.; Pasquale, G. D.; Fortuna, L.; Graziani, S.; Pollicino, A. *Smart Mater. Struct.* **2010**, *19*, 055002.

(27) Kyung Soo, L.; Byung Joo, J.; Sung Woon, C. *Smart Mater. Struct.* **2010**, *19*, 065029.

(28) Matteo, A.; Chekema, P.; Maurizio, P.; Sean, D. P. *Smart Mater. Struct.* **2010**, *19*, 015003.

(29) Colin, S.; Alex, V.; Keyur, J.; Yonas, T.; Shashank, P. *Smart Mater. Struct.* **2011**, *20*, 012001.

(30) Federico, C.; Roy, K.; Peter, S.-L.; Gursel, A. *Bioinspir. Biomim.* **2011**, *6*, 045006.

(31) Guo-Hua, F.; Jen-Wei, T. *Smart Mater. Struct.* **2011**, *20*, 015027.

(32) Scott, R. A.; Peppas, N. A. *Biomaterials* **1999**, *20*, 1371.

(33) Sudaxshina, M. *J. Controlled Release* **2003**, *92*, 1.

(34) Lloyd, C. H.; Scrimgeour, S. N.; Brown, D.; Clarke, R. L.; Curtis, R. V.; Hatton, P. V.; Ireland, A. J.; McCabe, J. F.; Nicholson, J. W.; Setcos, J. C.; Sherriff, M.; van Noort, R.; Watts, D. C.; Whitters, C. J.; Wood, D. *J. Dent.* **1997**, *25*, 173.

(35) Mendelsohn, J. D.; Barrett, C. J.; Chan, V. V.; Pal, A. J.; Mayes, A. M.; Rubner, M. F. *Langmuir* **2000**, *16*, 5017.

(36) Scranton, A.; Rangarajan, B.; Klier, J.; Peppas, N., Langer, R., Eds.; Springer Berlin / Heidelberg: 1995; Vol. 122, p 1.

(37) Peppas, N. A.; Bures, P.; Leobandung, W. *Eur. J. Pharm. Biopharm.* **2000**, *50*, 27.

(38) Nair, L.; Laurencin, C.; Lee, K., Kaplan, D., Eds.; Springer Berlin / Heidelberg: 2006; Vol. 102, p 47.

(39) Peppas, N. A.; Leobandung, W. *J. Biomater. Sci., Polym. Ed.* **2004**, *15*, 125.

(40) Krasemann, L.; Toutianoush, A.; Tieke, B. *J. Membr. Sci.* **2001**, *181*, 221.

(41) Krasemann, L.; Tieke, B. *Langmuir* **1999**, *16*, 287.

(42) Meier-Haack, J.; Lenk, W.; Lehmann, D.; Lunkwitz, K. *J. Membr. Sci.* **2001**, *184*, 233.

(43) Thünemann, A. F. *Prog. Polym. Sci.* **2002**, *27*, 1473.

(44) Thünemann, A. F.; Müller, M.; Dautzenberg, H.; Joanny, J.-F.; Löwen, H.; Schmidt, M., Ed.; Springer Berlin / Heidelberg: 2004; Vol. 166, p 19.

(45) Nizri, G. *Langmuir* **2004**, *20*, 4380.

(46) Valkama, S.; Lehtonen, O.; Lappalainen, K.; Kosonen, H.; Castro, P.; Repo, T.; Torkkeli, M.; Serimaa, R.; ten Brinke, G.; Leskelä, M.; Ikkala, O. *Macromol. Rapid Commun.* **2003**, *24*, 556.

(47) Severin, N.; Rabe, J. P.; Kurth, D. G. *J. Am. Chem. Soc.***2004**, *126*, 3696.

(48) de Kruif, C. G.; Weinbreck, F.; de Vries, R. *Curr. Opin. Colloid Interface Sci.* **2004**, *9*, 340.

(49) Imura, T.; Yanagishita, H.; Kitamoto, D. *J. Am. Chem. Soc.***2004**, *126*, 10804.

(50) Remuñán-López, C.; Bodmeier, R. *Int. J. Pharm.* **1996**, *135*, 63.

(51) Cohen Stuart, M. A.; Besseling, N. A. M.; Fokkink, R. G. *Langmuir* **1998**, *14*, 6846.

(52) Ballauff, M.; Blaul, J.; Guilleaume, B.; Rehahn, M.; Traser, S.; Wittemann, M.; Wittmeyer, P. *Macromol. Symp.* **2004**, *211*, 1.

(53) Laschewsky, A. *Curr. Opin. Colloid Interface Sci.* **2011**.

(54) Baśko, M.; Kubisa, P. *Macromolecules* **2002**, *35*, 8948.

(55) Ishizone, T.; Hirao, A.; Nakahama, S. *Macromolecules* **1989**, *22*, 2895.

(56) Macknight, W. J.; Demejo, L.; Vogl, O. *Acta polymerica* **1980**, *31*, 617.

(57) Braunecker, W. A. *Prog. Polym. Sci.* **2007**, *32*, 93.

(58) Ober, C. K.; Cheng, S. Z. D.; Hammond, P. T.; Muthukumar, M.; Reichmanis, E.; Wooley, K. L.; Lodge, T. P. *Macromolecules* **2008**, *42*, 465.

(59) Iovu, M. C.; Craley, C. R.; Jeffries-El, M.; Krankowski, A. B.; Zhang, R.; Kowalewski, T.; McCullough, R. D. *Macromolecules* **2007**, *40*, 4733.

(60) Moad, G.; Rizzardo, E.; Thang, S. H. *Acc. Chem. Res.* **2008**, *41*, 1133.

(61) Patten, T. E.; Matyjaszewski, K. *Adv. Mater.* **1998**, *10*, 901.

(62) Matyjaszewski, K. *Chem. Rev.* **2001**, *101*, 2921.

(63) Wang, J.-S.; Matyjaszewski, K. *Macromolecules* **1995**, *28*, 7901.

(64) Chiefari, J.; Chong, Y. K.; Ercole, F.; Krstina, J.; Jeffery, J.; Le, T. P. T.; Mayadunne, R. T. A.; Meijs, G. F.; Moad, C. L.; Moad, G.; Rizzardo, E.; Thang, S. H. *Macromolecules* **1998**, *31*, 5559.

(65) Mayadunne, R. T. A.; Rizzardo, E.; Chiefari, J.; Chong, Y. K.; Moad, G.; Thang, S. H. *Macromolecules* **1999**, *32*, 6977.

(66) Moad, G.; Chiefari, J.; Chong, Y. K.; Krstina, J.; Mayadunne, R. T. A.; Postma, A.; Rizzardo, E.; Thang, S. H. *Polym. Int.* **2000**, *49*, 993.

(67) Lowe, A. B.; McCormick, C. L. *Prog. Polym. Sci.* **2007**, *32*, 283.

(68) Yamago, S.; Iida, K.; Yoshida, J.-i. In *Advances in Controlled/Living Radical Polymerization*; American Chemical Society: 2003; Vol. 854, p 631.

(69) Yamago, S.; Ukai, Y.; Matsumoto, A.; Nakamura, Y. *J. Am. Chem. Soc.***2009**, *131*, 2100.

(70) Haddleton, D. M.; Jasieczek, C. B.; Hannon, M. J.; Shooter, A. J. *Macromolecules* **1997**, *30*, 2190.

(71) Heuts, J. P. A.; Roberts, G. E.; Biasutti, J. D. *ChemInform* **2003**, *34*, no.

(72) Bielawski, C. W.; Grubbs, R. H. *Prog. Polym. Sci.* **2007**, *32*, 1.

(73) Schrock, R. R. *Acc. Chem. Res.* **1990**, *23*, 158.

(74) Choi, T.-L.; Grubbs, R. H. *Angewandte Chemie* **2003**, *115*, 1785.

(75) Couvreur, L.; Lefay, C.; Belleney, J.; Charleux, B.; Guerret, O.; Magnet, S. *Macromolecules* **2003**, *36*, 8260.

(76) Lefay, C.; Belleney, J.; Charleux, B.; Guerret, O.; Magnet, S. *Macromol. Rapid Commun.* **2004**, *25*, 1215.

(77) Delaittre, G.; Charleux, B. *Macromolecules* **2008**, *41*, 2361.

(78) Georges, M. K.; Hamer, G. K.; Listigovers, N. A. *Macromolecules* **1998**, *31*, 9087.

(79) Lefay, C.; Charleux, B.; Save, M.; Chassenieux, C.; Guerret, O.; Magnet, S. *Polymer* **2006**, *47*, 1935.

(80) Nowakowska, M.; Zapotoczny, S.; Karewicz, A. *Macromolecules* **2000**, *33*, 7345.

(81) Okamura, H.; Takatori, Y.; Tsunooka, M.; Shirai, M. *Polymer* **2002**, *43*, 3155.

(82) Nowakowska, M.; Karewicz, A.; Kłos, M.; Zapotoczny, S. *Macromolecules* **2003**, *36*, 4134.

(83) Hawker, C. J.; Barclay, G. G.; Dao, J. *J. Am. Chem. Soc.***1996**, *118*, 11467.

(84) Phan, T. N. T.; Bertin, D. *Macromolecules* **2008**, *41*, 1886.

(85) Li, D.; Brittain, W. J. *Macromolecules* **1998**, *31*, 3852.

(86) Schierholz, K.; Givehchi, M.; Fabre, P.; Nallet, F.; Papon, E.; Guerret, O.; Gnanou, Y. *Macromolecules* **2003**, *36*, 5995.

(87) Götz, H.; Harth, E.; Schiller, S. M.; Frank, C. W.; Knoll, W.; Hawker, C. J. *J. Polym. Sci. Part A: Polym. Chem.* **2002**, *40*, 3379.

(88) Hawker, C. J.; Bosman, A. W.; Harth, E. *Chem. Rev.* **2001**, *101*, 3661.

(89) Sumerlin, B. S.; Donovan, M. S.; Mitsukami, Y.; Lowe, A. B.; McCormick, C. L. *Macromolecules* **2001**, *34*, 6561.

(90) McCormick, C. L.; Lowe, A. B. *Acc. Chem. Res.* **2004**, *37*, 312.

(91) Mitsukami, Y.; Donovan, M. S.; Lowe, A. B.; McCormick, C. L. *Macromolecules* **2001**, *34*, 2248.

(92) Donovan, M. S.; Sanford, T. A.; Lowe, A. B.; Sumerlin, B. S.; Mitsukami, Y.; McCormick, C. L. *Macromolecules* **2002**, *35*, 4570.

(93) Coessens, V.; Pintauer, T.; Matyjaszewski, K. *Prog. Polym. Sci.* **2001**, *26*, 337.

(94) Matyjaszewski, K.; Xia, J. *Chem. Rev.* **2001**, *101*, 2921.

(95) Lynn, D. M.; Mohr, B.; Grubbs, R. H. *J. Am. Chem. Soc.***1998**, *120*, 1627.

(96) Lynn, D. M.; Kanaoka, S.; Grubbs, R. H. *J. Am. Chem. Soc.***1996**, *118*, 784.

(97) Haddleton, D. M.; Depaquis, E.; Kelly, E. J.; Kukulj, D.; Morsley, S. R.; Bon, S. A. F.; Eason, M. D.; Steward, A. G. *J. Polym. Sci. Part A: Polym. Chem.* **2001**, *39*, 2378.

(98) Debuigne, A.; Warnant, J.; Jérôme, R.; Voets, I.; de Keizer, A.; Cohen Stuart, M. A.; Detrembleur, C. *Macromolecules* **2008**, *41*, 2353.

(99) Zhang, S.; Zhao, Y. *J. Am. Chem. Soc.***2010**, *132*, 10642.

(100) Koh, M. L.; Konkolewicz, D.; Perrier, S. b. *Macromolecules* **2011**, *44*, 2715.

(101) Dimitrov, I.; Jankova, K.; Hvilsted, S. *J. Polym. Sci. Part A: Polym. Chem.* **2010**, *48*, 2044.

(102) Sun, J.; Schlaad, H. *Macromolecules* **2010**, *43*, 4445.

(103) Sumerlin, B. S. *Macromolecules* **2001**, *34*, 6561.

(104) Davies, M. C.; Dawkins, J. V.; Hourston, D. J. *Polymer* **2005**, *46*, 1739.

(105) Chiefari, J.; Mayadunne, R. T. A.; Moad, C. L.; Moad, G.; Rizzardo, E.; Postma, A.; Thang, S. H. *Macromolecules* **2003**, *36*, 2273.

(106) Huang, F.; Hou, L.; Wu, H.; Wang, X.; Shen, H.; Cao, W.; Yang, W.; Cao, Y. *J. Am. Chem. Soc.***2004**, *126*, 9845.

(107) Walczak, R. M.; Brookins, R. N.; Savage, A. M.; van der Aa, E. M.; Reynolds, J. R. *Macromolecules* **2009**, *42*, 1445.

(108) Böhme, U.; Vogel, C.; Meier-Haack, J.; Scheler, U. *J. Phys. Chem. B* **2007**, *111*, 8344.

(109) Viale, S.; Best, A. S.; Mendes, E.; Picken, S. J. *Chem. Commun.* **2005**, 1528.

(110) Yamazaki, N.; Matsumoto, M.; Higashi, F. *J. Polym. Sci.: Polym. Chem. Ed.* **1975**, *13*, 1373.

(111) Frechet, J. *Science* **1994**, *263*, 1710.

(112) Turner, S. R.; Voit, B. I.; Mourey, T. H. *Macromolecules* **1993**, *26*, 4617.

(113) Turner, S. R.; Walter, F.; Voit, B. I.; Mourey, T. H. *Macromolecules* **1994**, *27*, 1611.

(114) Kainthan, R. K.; Gnanamani, M.; Ganguli, M.; Ghosh, T.; Brooks, D. E.; Maiti, S.; Kizhakkedathu, J. N. *Biomaterials* **2006**, *27*, 5377.

(115) Sukhorukov, G. B.; Donath, E.; Lichtenfeld, H.; Knippel, E.; Knippel, M.; Budde, A.; Möhwald, H. *Colloids and Surfaces A: Physicochem. Eng. Aspects* **1998**, *137*, 253.

(116) Kotov, N. A.; Dekany, I.; Fendler, J. H. *J. Phys. Chem.* **1995**, *99*, 13065.

(117) Decher, G.; Hong, J. D.; Schmitt, J. *Thin Solid Films* **1992**, *210–211, Part 2*, 831.

(118) Decher, G.; Hong, J. D. *Ber. Bunsen Ges. Phys. Chem.* **1991**, *95*, 1430.

(119) Hofer, R.; Bigorra, J. *Green Chemistry* **2007**, *9*, 203.

(120) Boris, D. C.; Colby, R. H. *Macromolecules* **1998**, *31*, 5746.

(121) Th.F, T. *Adv. Colloid Interface Sci.* **1993**, *46*, 1.

(122) Mortimer, D. A. *Polym. Int.* **1991**, *25*, 29.

(123) He, M.; Wang, Y.; Forssberg, E. *Powder Technol.* **2004**, *147*, 94.

(124) Bakshi, M. S.; Sachar, S. *Colloid Polym. Sci.* **2005**, *283*, 671.

(125) Zingg, A.; Winnefeld, F.; Holzer, L.; Pakusch, J.; Becker, S.; Gauckler, L. *J. Colloid Interface Sci.***2008**, *323*, 301.

(126) Caram-Lelham, N.; Sundelöf, L.-O. *Int. J. Pharm.* **1995**, *115*, 103.

(127) Baird, J. K.; Sandford, P. A.; Cottrell, I. W. *Nat. Biotech.* **1983**, *1*, 778.

(128) Couto, S. R.; Sanromán, M. Á. *J. Food Eng.* **2006**, *76*, 291.

(129) Donald, R. *Trends Biotechnol.* **1997**, *15*, 9.

(130) Guzey, D.; McClements, D. J. *Adv. Colloid Interface Sci.* **2006**, *128–130*, 227.

(131) Mathur, N. K.; Narang, C. K. *J. Chem. Educ.* **1990**, *67*, 938.

(132) Ian W, S. *Trends Biotechnol.* **1998**, *16*, 41.

(133) Baier Leach, J.; Bivens, K. A.; Patrick Jr, C. W.; Schmidt, C. E. *Biotechnol. Bioeng.* **2003**, *82*, 578.

(134) Wilkins, M. H. F.; Stokes, A. R.; Wilson, H. R. *Nature* **1953**, *171*, 738.

(135) Watson, J. D.; CRICK, F. H. C. *Nature (London)* **1953**, *171*, 737.

(136) Kabanov, V. A.; Topchiev, D. A.; Karaputadze, T. M. *J. Polym. Sci.: Polymer Symposia* **1973**, *42*, 173.

(137) Davis, K. A.; Matyjaszewski, K. *Macromolecules* **2000**, *33*, 4039.

(138) Konno, A.; Kaneko, M. *J. Makromol. Chem.* **1970**, *138*, 189.

(139) Zhang, J. P.; Li, A.; Wang, A. Q. *Polym. Adv. Technol.***2005**, *16*, 813.

(140) Kiatkamjornwong, S.; Phunchareon, P. *J. Appl. Polym. Sci.* **1999**, *72*, 1349.

(141) Hirao, A.; Kato, H.; Yamaguchi, K.; Nakahama, S. *Macromolecules* **1986**, *19*, 1294.

(142) Zhang, J.; Peppas, N. A. *Macromolecules* **1999**, *33*, 102.

(143) Díez-Peña, E.; Quijada-Garrido, I.; Barrales-Rienda, J. M. *Polymer* **2002**, *43*, 4341.

(144) Brazel, C. S.; Peppas, N. A. *Macromolecules* **1995**, *28*, 8016.

(145) Brazel, C. S.; Peppas, N. A. *J. Controlled Release* **1996**, *39*, 57.

(146) Lo, C.-L.; Lin, K.-M.; Hsiue, G.-H. *J. Controlled Release* **2005**, *104*, 477.

(147) Zhang, J.; Peppas, N. A. *J. Appl. Polym. Sci.* **2001**, *82*, 1077.

(148) Liu, S.; Liu, M. *J. Appl. Polym. Sci.* **2003**, *90*, 3563.

(149) Yang, C.; Cheng, Y.-L. *J. Appl. Polym. Sci.* **2006**, *102*, 1191.

(150) Gibson, H. W.; Bailey, F. C. *Macromolecules* **1980**, *13*, 34.

(151) Fernyhough, C. M.; Young, R. N.; Ryan, A. J.; Hutchings, L. R. *Polymer* **2006**, *47*, 3455.

(152) Hart, R.; Janssen, R. *J. Makromol. Chem.* **1961**, *43*, 242.

(153) Weiss, R. A.; Lundberg, R. D.; Turner, S. R. *J. Polym. Sci.: Polym. Chem. Ed.* **1985**, *23*, 549.

(154) Holboke, A. E.; Pinnell, R. P. *J. Chem. Educ.* **1989**, *66*, 613.

(155) Fang, W.; Cai, Y.; Chen, X.; Su, R.; Chen, T.; Xia, N.; Li, L.; Yang, Q.; Han, J.; Han, S. *Bioorg. Med. Chem. Lett.* **2009**, *19*, 1903.

(156) Sikkema, F. D.; Comellas-Aragones, M.; Fokkink, R. G.; Verduin, B. J. M.; Cornelissen, J. J. L. M.; Nolte, R. J. M. *Org. Biomol. Chem.* **2007**, *5*, 54.

(157) Zhu, M.-Q.; Wei, L.-H.; Li, M.; Jiang, L.; Du, F.-S.; Li, Z.-C.; Li, F.-M. *Chem. Commun.* **2001**, 365.

(158) Moulard, M.; Lortat-Jacob, H.; Mondor, I.; Roca, G.; Wyatt, R.; Sodroski, J.; Zhao, L.; Olson, W.; Kwong, P. D.; Sattentau, Q. J. *J. Virol.* **2000**, *74*, 1948.

(159) Garg, S.; Vermani, K.; Garg, A.; Anderson, R. A.; Rencher, W. B.; Zaneveld, L. J. D. *Pharm. Res.* **2005**, *22*, 584.

(160) Herold, B. C.; Bourne, N.; Marcellino, D.; Kirkpatrick, R.; Strauss, D. M.; Zaneveld, L. J. D.; Waller, D. P.; Anderson, R. A.; Chany, C. J.; Barham, B. J.; Stanberry, L. R.; Cooper, M. D. *J. Infect. Dis.***2000**, *181*, 770.

(161) Zaneveld, L. J. D.; Waller, D. P.; Anderson, R. A.; Chany, C.; Rencher, W. F.; Feathergill, K.; Diao, X.-H.; Doncel, G. F.; Herold, B.; Cooper, M. *Biol. Reprod.* **2002**, *66*, 886.

(162) Sen, A. K.; Roy, S.; Juvekar, V. A. *Polym. Int.* **2007**, *56*, 167.

(163) Trivedi, B. C.; Culbertson, B. M. *Maleic Anhydride*; Books on Demand, 1982.

(164) Schmidt, U.; Zschoche, S.; Werner, C. *J Appl Polym Sci* **2003**, *87*, 1255.

(165) Bumbu, G.-G.; Vasile, C.; Chitanu, G. C.; Staikos, G. *Macromol. Chem. Physic.* **2005**, *206*, 540.

(166) Dubin, P. L.; Strauss, U. P. *J. Phys. Chem.* **1970**, *74*, 2842.

(167) De Brouwer, H.; Schellekens, M. A. J.; Klumperman, B.; Monteiro, M. J.; German, A. L. *J. Polym. Sci. Part A: Polym. Chem.* **2000**, *38*, 3596.

(168) Majumdar, B.; Keskkula, H.; Paul, D. R. *Polymer* **1994**, *35*, 3164.

(169) Florjańczyk, Z.; Bzducha, W.; Langwald, N.; Dygas, J. R.; Krok, F.; Misztal-Faraj, B. *Electrochim. Acta* **2000**, *45*, 3563.

(170) Henry, S. M.; El-Sayed, M. E. H.; Pirie, C. M.; Hoffman, A. S.; Stayton, P. S. *Biomacromolecules* **2006**, *7*, 2407.

(171) Mao, M.; Turner, S. R. *J. Am. Chem. Soc.***2007**, *129*, 3832.

(172) Mao, M.; Turner, S. R. *Polymer* **2006**, *47*, 8101.
(173) Mao, M.; Kim, C.; Wi, S.; Turner, S. R. *Macromolecules* **2007**, *41*, 387.
(174) Mao, M.; England, J.; Turner, S. R. *Polymer* **2011**, *52*, 4498.
(175) Li, Y.; Turner, S. R. *Eur. Polym. J.* **2010**, *46*, 821.
(176) Park, E.-S.; Kim, M.-N.; Lee, I.-M.; Lee, H. S.; Yoon, J.-S. *J. Polym. Sci. Part A: Polym. Chem.* **2000**, *38*, 2239.
(177) Chitanu, G. C.; Rinaudo, M.; Desbrières, J.; Milas, M.; Carpov, A. *Langmuir* **1999**, *15*, 4150.
(178) Blockhaus, F.; Séquaris, J. M.; Narres, H. D.; Schwuger, M. J. *J. Colloid Interface Sci.***1997**, *186*, 234.
(179) Sauvage, E.; Amos, D. A.; Antalek, B.; Schroeder, K. M.; Tan, J. S.; Plucktaveesak, N.; Colby, R. H. *J. Polym. Sci. Part B: Polym. Phys.* **2004**, *42*, 3571.
(180) Sauvage, E.; Plucktaveesak, N.; Colby, R. H.; Amos, D. A.; Antalek, B.; Schroeder, K. M.; Tan, J. S. *J. Polym. Sci. Part B: Polym. Phys.* **2004**, *42*, 3584.
(181) Shao-Hai, F.; Kuan-Jun, F. *J. Appl. Polym. Sci.* **2007**, *105*, 317.
(182) Bingöl, B.; Strandberg, C.; Szabo, A.; Wegner, G. *Macromolecules* **2008**, *41*, 2785.
(183) Millaruelo, M.; Steinert, V.; Komber, H.; Klopsch, R.; Voit, B. *Macromol Chem Physic* **2008**, *209*, 366.
(184) Perrin, R.; Elomaa, M.; Jannasch, P. *Macromolecules* **2009**, *42*, 5146.
(185) Markova, D.; Kumar, A.; Klapper, M.; Müllen, K. *Polymer* **2009**, *50*, 3411.
(186) Rabe, G. W.; Komber, H.; Häussler, L.; Kreger, K.; Lattermann, G. n. *Macromolecules* **2010**, *43*, 1178.
(187) Chen, T.; Chang, D. P.; Liu, T.; Desikan, R.; Datar, R.; Thundat, T.; Berger, R.; Zauscher, S. *J. Mater. Chem.* **2010**, *20*, 3391.
(188) D'Hooge, F.; Rogalle, D.; Thatcher, M. J.; Perera, S. P.; van den Elsen, J. M. H.; Jenkins, A. T. A.; James, T. D.; Fossey, J. S. *Polymer* **2008**, *49*, 3362.
(189) Hua, D.; Tang, J.; Jiang, J.; Zhu, X. *Polymer* **2009**, *50*, 5701.
(190) Yáñez-Martínez, B. A.; Percino, J.; Chapela, V. M. *J. Appl. Polym. Sci.* **2010**, *118*, 2849.
(191) Matsumoto, K.; Endo, T. *J. Polym. Sci. Part A: Polym. Chem.* **2011**, *49*, 1874.
(192) Hong, S. W.; Jo, W. H. *Polymer* **2008**, *49*, 4180.
(193) Kanazawa, A.; Ikeda, T.; Endo, T. *J. Polym. Sci. Part A: Polym. Chem.* **1993**, *31*, 2873.
(194) Butler, G. B. *Cyclopolymerization and Cyclocopolymerization*; M. Dekker, 1992.
(195) Butler, G. B. *J. Polym. Sci.* **1960**, *48*, 279.
(196) Li, Y. *Macromolecules* **1995**, *28*, 8426.
(197) Zheng, L. *Polym. Adv. Technol.***2007**, *18*, 194.
(198) Wandrey, C. *Acta polymerica* **1985**, *36*, 100.
(199) Bolto, B. *Water Res. (Oxford)* **2007**, *41*, 2301.
(200) Son, W.-J.; Choi, J.-S.; Ahn, W.-S. *Microporous Mesoporous Mater.* **2008**, *113*, 31.
(201) Wang, Q.; Luo, J.; Zhong, Z.; Borgna, A. *Energy Env. Sci.* **2011**, *4*, 42.

(202) Manuel, W. S.; Zheng, J.; Hornsby, P. J. *J. Drug Target.* **2001**, *9*, 15.

(203) Zahn-Zabal, M.; Kobr, M.; Girod, P.-A.; Imhof, M.; Chatellard, P.; de Jesus, M.; Wurm, F.; Mermod, N. *J. Biotechnol.* **2001**, *87*, 29.

(204) Horbinski, C.; Stachowiak, M.; Higgins, D.; Finnegan, S. *BMC Neuroscience* **2001**, *2*, 2.

(205) Li, Y.; Mao, M.; Matolyak, L. E.; Turner, S. R. *ACS Macro Lett.* **2012**, *1*, 257.

(206) Glatter O, K. O. *Small Angle X-Ray Scattering* **1982**.

(207) Foerster, S.; Schmidt, M. *Adv. Polym. Sci.* **1995**, *120*, 51.

(208) Forster, S.; Schmidt, M.; Antonietti, M. *Polymer* **1990**, *31*, 781.

(209) Oppermann, W. *Makromolekulare Chemie* **1988**, *189*, 927.

(210) Yamanaka, J.; Matsuoka, H.; Kitano, H.; Hasegawa, M.; Ise, N. *J. Am. Chem. Soc.* **1990**, *112*, 587.

(211) Cohen, J.; Priel, Z. *Macromolecules* **1989**, *22*, 2356.

(212) Cohen, J.; Priel, Z. *Polymer Communications* **1989**, *30*, 223.

(213) Cohen, J.; Priel, Z. *J. Chem. Phys.* **1990**, *93*, 9062.

(214) Cohen, J.; Priel, Z.; Rabin, Y. *J. Chem. Phys.* **1988**, *88*, 7111.

(215) Mao, M.; Turner, S. R. *PMSE Preprints* **2007**, *96*, 562.

(216) Yoshida, M.; Fresco, Z. M.; Ohnishi, S.; Frechet, J. M. J. *Macromolecules* **2005**, *38*, 334.

(217) Ouali, N.; Mery, S.; Skoulios, A.; Noirez, L. *Macromolecules* **2000**, *33*, 6185.

(218) Percec, V.; Ahn, C. H.; Cho, W. D.; Jamieson, A. M.; Kim, J.; Leman, T.; Schmidt, M.; Gerle, M.; Moeller, M.; Prokhorova, S. A.; Sheiko, S. S.; Cheng, S. Z. D.; Zhang, A.; Ungar, G.; Yeardley, D. J. P. *J. Am. Chem. Soc.* **1998**, *120*, 8619.

(219) Zhang, A.; Zhang, B.; Waechtersbach, E.; Schmidt, M.; Schlueter, A. D. Chem. -*Eur. J.* **2003**, *9*, 6083.

(220) Kratky, O.; Porod, G. *Recl. Travaux Chim. Pays-Bas* **1949**, *68*, 1106.

(221) Porod, G. *Monatsh. Chem./Chem. Monthly* **1949**, *80*, 251.

(222) Mourey, T.; Le, K.; Bryan, T.; Zheng, S.; Bennett, G. *Polymer* **2005**, *46*, 9033.

(223) Kuhn, W. *Kolloid-Z* **1934**, *68*, 2.

(224) Schluter, A. D. *Top Curr. Chem*. **1998**, *197*, 165.

(225) Benoit, H.; Doty, P. *J. Phys. Chem.* **1953**, *57*, 958.

(226) Gettinger, C. L.; Heeger, A. J.; Drake, J. M.; Pine, D. J. *J. Phys. Chem.* **1994**, *101*, 1673.

(227) Cotts, P. M.; Swager, T. M.; Zhou, Q. *Macromolecules* **1996**, *29*, 7323.

(228) Fetters, L. J.; Yu, H. *Macromolecules* **1971**, *4*, 385.

(229) Itou, T.; Chikiri, H.; Teramoto, A.; Aharoni, S. M. *Polym. J.* **1988**, *20*, 143.

(230) Kuwata, M.; Murakami, H.; Norisuye, T.; Fujita, H. *Macromolecules* **1984**, *17*, 2731.

(231) Cook, R.; Johnson, R. D.; Wade, C. G.; O'Leary, D. J.; Munoz, B.; Green, M. M. *Macromolecules* **1990**, *23*, 3454.

(232) Murakami, H.; Norisuye, T.; Fujita, H. *Macromolecules* **1980**, *13*, 345.

(233) Matsumoto, A.; Nakagawa, E. *Eur. Polym. J.* **1999**, *35*, 2107.

(234) Noda, I.; Imai, T.; Kitano, T.; Nagasawa, M. *Macromolecules* **1981**, *14*, 1303.

(235) Hirao, T.; Teramoto, A.; Sato, T.; Norisuye, T.; Masuda, T.; Higashimura, T. *Polym. J.* **1991**, *23*, 925.

(236) Muroga, Y.; Sakuragi, I.; Noda, I.; Nagasawa, M. *Macromolecules* **1984**, *17*, 1844.

(237) Taylor, T. J.; Stivala, S. S. *Polymer* **1996**, *37*, 715.

(238) Yamakawa, H.; Fujii, M. *Macromolecules* **1974**, *7*, 128.

(239) Bohdanecky, M. *Macromolecules* **1983**, *16*, 1483.

(240) Gupta, A. *Carbon (New York)* **1994**, *32*, 953.

(241) Hsiao, B. S. *J. Synchrotron. Radiat.***1998**, *5*, 23.

(242) Brown, H. R.; Kramer, E. J. *J. Macromol. Sci. Part B* **1981**, *19*, 487.

(243) Roe, R. J. *Methods of X-ray and Neutron Scattering in Polymer Science*; Oxford University Press, 2000.

(244) *Small angle x-ray scattering / edited by O. Glatter and O. Kratky*; Academic Press: London ; New York :, 1982.

(245) Debye, P. *J. Phys. Colloid Chem.* **1947**, *51*, 18.

(246) Porod, G. *J. Polym. Sci.* **1953**, *10*, 157.

(247) Kratky, O. *Colloid Polym. Sci.* **1962**, *182*, 7.

(248) Glatter, O.; Kratky, O. *Small Angle X-ray Scattering*; Academic Press, 1982.

(249) Peterlin, A. *J. Polym. Sci.* **1960**, *47*, 403.

(250) Heine, V. S.; Kratky, O.; Roppert, J. *J. Makromol. Chem.* **1962**, *56*, 150.

(251) Kratky, O. *Pure Appl. Chem.* **1966**, *12*, 483.

(252) Cleland, R. L. *Arch. Biochem. Biophys.* **1977**, *180*, 57.

(253) Gupta, A. K.; Cotton, J. P.; Marchal, E.; Burchard, W.; Benoit, H. *Polymer* **1976**, *17*, 363.

(254) Muroga, Y.; Noda, I.; Nagasawa, M. *Macromolecules* **1985**, *18*, 1576.

(255) Yamazaki, S.; Muroga, Y.; Noda, I. *Langmuir* **1999**, *15*, 4147.

(256) Paramita Kar, C.; et al. *J. Phys.: Condens. Matter* **2009**, *21*, 195801.

(257) Beaucage, G.; Rane, S.; Sukumaran, S.; Satkowski, M. M.; Schechtman, L. A.; Doi, Y. *Macromolecules* **1997**, *30*, 4158.

(258) Siekmeyer, M.; Zugenmaier, P. *J. Makromol. Chem.* **1990**, *191*, 1177.

(259) Sharp, P.; Bloomfield, V. A. *Biopolymers* **1968**, *6*, 1201.

(260) Yamakawa, H.; Fujii, M. *Macromolecules* **1974**, *7*, 649.

(261) Schmid, C. W.; Rinehart, F. P.; Hearst, J. E. *Biopolymers* **1971**, *10*, 883.

(262) Beaucage, G. *J. Appl. Crystallogr.* **1995**, *28*, 717.

(263) Liquid, S. *J Non-Cryst Solids* **1995**, *186*, 159.

(264) Gutjahr, P.; Lipowsky, R.; Kierfeld, J. *EPL (Europhysics Letters)* **2006**, *76*, 994.

(265) Kierfeld, J.; Baczynski, K.; Gutjahr, P.; Lipowsky, R. *AIP Conf. Proc.* **2008**, *1002*, 151.

(266) Thunemann, A. F. *Prog. Polym. Sci.* **2002**, *27*, 1473.

(267) Kötz, J.; Kosmella, S.; Beitz, T. *Prog. Polym. Sci.* **2001**, *26*, 1199.

(268) Bertrand, P.; Jonas, A.; Laschewsky, A.; Legras, R. *Macromol. Rapid Commun.* **2000**, *21*, 319.

(269) Ober, C. K.; Wegner, G. *Adv. Mater.* **1997**, *9*, 17.
(270) Antonietti, M.; Burger, C.; Thunemann, A. *Trends Polym. Sci.* **1997**, *5*, 262.
(271) Antonietti, M.; Thünemann, A. *Curr. Opin. Colloid Interface Sci.* **1996**, *1*, 667.
(272) MacKnight, W. J.; Ponomarenko, E. A.; Tirrell, D. A. *Acc. Chem. Res.* **1998**, *31*, 781.
(273) Michaels, A. S.; Miekka, R. G. *J. Phys. Chem.* **1961**, *65*, 1765.
(274) Kabanov, V. A.; Zezin, A. B. *J. Makromol. Chem.* **1984**, *6*, 259.
(275) Koetz, J.; Kosmella, S.; Springer Berlin Heidelberg: **2007**, p 5.
(276) Dubin, P. *Macromolecular Complexes in Chemistry and Biology*; Springer-Verlag, **1994**.
(277) Tsuchida, E.; Abe, K.; Springer Berlin / Heidelberg: 1982; Vol. 45, p 1.
(278) Tsuchida, E.; Osada, Y.; Sanada, K. *J. Polym. Sci. Part A-1: Polymer Chemistry* **1972**, *10*, 3397.
(279) Tsuchida, E.; Osada, Y.; Ohno, H. *J. Macromol. Sci. Part B* **1980**, *17*, 683.
(280) Prabaharan, M.; Mano, J. F. *Drug Deliv.* **2004**, *12*, 41.
(281) Qiu, L. Y.; Bae, Y. H. *Biomaterials* **2007**, *28*, 4132.
(282) Mao, S.; Bakowsky, U.; Jintapattanakit, A.; Kissel, T. *J. Pharm. Sci.* **2006**, *95*, 1035.
(283) Karibyants, N.; Dautzenberg, H. *Langmuir* **1998**, *14*, 4427.
(284) Davison, C. J.; Smith, K. E.; Hutchinson, L. E. F.; O'Mullane, J. E.; Brookman, L.; Petrak, K.; Harding, S. E. *J. Bioact.Compat. Pol.***1990**, *5*, 267.
(285) Dautzenberg, H. *Macromolecules* **1997**, *30*, 7810.
(286) Karibyants, N.; Dautzenberg, H.; Cölfen, H. *Macromolecules* **1997**, *30*, 7803.
(287) Dautzenberg, H.; Hartmann, J.; Grunewald, S.; Brand, F. *Ber. Bunsen Ges. Phys. Chem.* **1996**, *100*, 1024.
(288) Kabanov, A. V.; Bronich, T. K.; Kabanov, V. A.; Yu, K.; Eisenberg, A. *Macromolecules* **1996**, *29*, 6797.
(289) Harada, A.; Kataoka, K. *J. Macromol. Sci., Part A* **1997**, *34*, 2119.
(290) Zintchenko, A.; Dautzenberg, H.; Tauer, K.; Khrenov, V. *Langmuir* **2002**, *18*, 1386.
(291) Sotiropoulou, M.; Cincu, C.; Bokias, G.; Staikos, G. *Polymer* **2004**, *45*, 1563.
(292) Buchhammer, H.-M.; Petzold, G.; Lunkwitz, K. *Langmuir* **1999**, *15*, 4306.
(293) Dautzenberg, H.; Jaeger, W. *Macromol. Chem. Physic.* **2002**, *203*, 2095.
(294) Dragan, S.; Cristea, M. *Eur. Polym. J.* **2001**, *37*, 1571.
(295) Liu, W. G.; De Yao, K.; Liu, Q. G. *J. Appl. Polym. Sci.* **2001**, *82*, 3391.
(296) Brand, F.; Dautzenberg, H. *Langmuir* **1997**, *13*, 2905.
(297) Huglin, M. B.; Webster, L.; Robb, I. D. *Polymer* **1996**, *37*, 1211.
(298) Webster, L.; Huglin, M. B.; Robb, I. D. *Polymer* **1997**, *38*, 1373.
(299) Dautzenberg, H.; Gao, Y.; Hahn, M. *Langmuir* **2000**, *16*, 9070.
(300) Kayitmazer, A. B.; Seyrek, E.; Dubin, P. L.; Staggemeier, B. A. *J. Phys. Chem. B* **2003**, *107*, 8158.
(301) Ulrich, S.; Laguecir, A.; Stoll, S. *Macromolecules* **2005**, *38*, 8939.

(302) Butler, J. C.; Angelini, T.; Tang, J. X.; Wong, G. C. L. *Phys. Rev. Lett.***2003**, *91*, 028301.

(303) Ha, B. Y.; Liu, A. J. *Phys. Rev. Lett.* **1997**, *79*, 1289.

(304) Zhai, L.; Cebeci, F. Ç.; Cohen, R. E.; Rubner, M. F. *Nano Lett.* **2004**, *4*, 1349.

(305) Kim, B.-S.; Gao, H.; Argun, A. A.; Matyjaszewski, K.; Hammond, P. T. *Macromolecules* **2008**, *42*, 368.

(306) Ott, P.; Gensel, J.; Roesler, S.; Trenkenschuh, K.; Andreeva, D.; Laschewsky, A.; Fery, A. *Chem. Mater.* **2010**, *22*, 3323.

Chapter 2. STERICALLY CROWDED ANIONIC POLYELECTROLYTES WITH TUNABLE CHARGE DENSITIES BASED ON STILBENE-CONTAINING COPOLYMERS

2.1. MANUSCRIPT PUBLISHED IN ACS MACRO LETTERS

(Published as: Li, Y.; Mao, M.; Matolyak, L. E.; Turner, S. R. *ACS Macro Lett.* **2012**, 257. Additional information added.)

Anionic polyelectrolytes with various charge densities and well defined chain architecture have great industrial and fundamental importance. In this article, we describe the synthesis and characterization of new sterically crowded conformationally constrained anionic polyelectrolytes with tunable charge densities based on highly functionalized stilbene-maleic anhydride/maleimide comonomers. Polyelectrolyte precursors with *tert*-butyl carboxylate protecting groups are first prepared by radical polymerization and readily characterized by ^{1}H NMR, SEC, TGA, and DSC without the complications normally arising with charged macromolecules. The precursors are converted into their corresponding deblocked forms by simply reacting with trifluoroacetic acid to deprotect the *tert*-butyl group and then neutralized in basic aqueous solutions to yield anionic polyelectrolytes.

Polyelectrolytes, a group of polymers containing a high level of ionizable groups, exhibit electrostatic interactions and find applications in industrial processes and daily life, such as drug delivery,[1,2,3] waste water purification,[4] surface modification for improved adhesion,[5] and ionic conducting materials.[6] Their properties depend on many

variables, such as the nature of functionalities on the polymer backbone, charge densities along the polymer chain, and the backbone's intrinsic properties such as stiffness. Bowman et al. studied complex formation between negatively charged polyelectrolytes and a net negatively charged polyampholyte due to the polarization-induced attraction.[7] They concluded that the greater charge density of negatively charged polyelectrolytes increased the complex stability in solutions. It was reported by Arys et al. that with an "appropriate polyanion" a lyotropic ionene could form structured coatings.[8-10] Later Koetse and coworkers studied cellulose sulfates as polyanions and found out the charge density of polyanions had a profound influence on coating properties, like the thickness and optical density.[11] A study of the impact of the charge density and hydrophobicity of polyanions on the stability of polyanion-protein complexes was carried out by Sedlak et al.[12] It was suggested that the charge density played a minor role on destabilization of the protein, while the hydrophobicity of polyanions was more responsible for perturbation of the protein structure. Poly(styrene-alt-maleic anhydride) derivatives were found by Fang et al. to be a 100 times more potent than conventional antiviral microbicides and were considered as a new class of polyanionic microbicides.[13] The study of negatively charged polyelectrolytes with tunable charge densities and well defined chain architecture continues to generate considerably fundamental and technological interest.

In this paper we report a simple and effective approach for synthesizing anionic polyelectrolytes with various charge densities via the design and synthesis of sterically crowded polymer backbones based on functionalized stilbenes and maleic anhydride/functionalized maleimides. Analogous styrenic copolymers, for direct comparison to the stilbene structures, have also been prepared. This approach permits the

preparation of new anionic polyelectrolytes with tunable charge densities and adds to the diversity of well-defined polyelectrolyte structures available for study, in Figure 2.1.

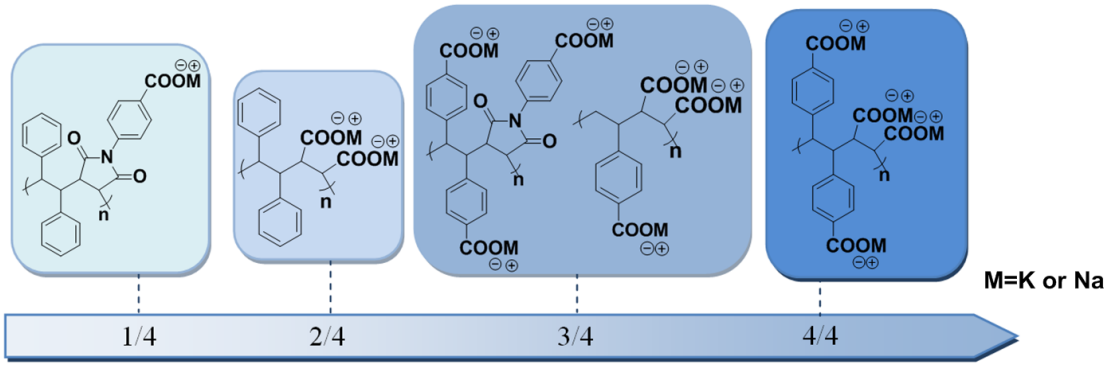

Figure 2.1 Polyelectrolytes with tunable charge densities.

Many reports on stilbene containing copolymers suggest that these copolymers have properties consistent with non-flexible backbones.[14-24] The pendant phenyl ring from the stilbene unit can add potential rigidity to the polymer backbone due to its steric hindrance effect. In addition the rich chemistry available for stilbenes makes the preparation of a variety of functional stilbene derivatives possible, which opens up interesting families of new polyelectrolytes for study. Our previous studies showed that from the solid-state NMR torsional angle measurement, the maleic anhydride units of *N,N,N',N'*-tetraethyl-4,4'-diaminostilbene (TDAS)-maleic anhydride (MAH) alternating copolymer were enchained in a predominately *cis* configuration, causing a highly contoured chain.[14] It was also observed that from DLS results the hydrodynamic radius (R_h) of this TDAS-MAH alternating copolymer did not change upon increasing temperature or introducing charges to the amino groups.[15] In addition we observed that a block copolymer containing a polyampholyte based on TDAS-MAH comonomer and a poly(methoxy-capped oligo-

(ethylene glycol)methacrylate) block exhibited polyion complexes with unusual pH and salt responsive properties similar to like-charge attraction effects in rigid polyelectrolytes.[16] It is our goal to take advantage of the rich stilbene chemistry and prepare and study new stilbene-based polyelectrolytes. To avoid the problems in direct characterization of polyelectrolytes as to the determination of molecular weight, molecular weight distributions, etc., a two-step blocked ionic group approach is taken as the synthetic strategy. Polyelectrolyte precursors are first prepared by radical polymerization due to its good tolerance to various functionalities.[25] The blocked polyelectrolyte precursors are then readily characterized by ^{1}H NMR, SEC, TGA, and DSC without the complications arising with charged macromolecules. The deprotection reactions are followed by neutralization in basic solution to obtain polyanions or in acid solution to yield polycations.[26] The advantage of this two-step blocked ionic group approach is that the charges of polyelectrolytes regularly positioned from carbon atoms of the polymer backbone are obtained by mild de-blocking reactions. The functional groups along the polymer chain are easily converted to their charged analogous polyelectrolytes with defined molecular weight and molecular weight distribution. The copolymers based on functionalized stilbenes were prepared at 110 ^{o}C with dicumyl peroxide (DCP) as initiator and chlorobenzene as solvent while the copolymers based on functionalized styrene were prepared at 60 ^{o}C with AIBN as initiator and THF as solvent. These copolymerizations are shown in Scheme 1. All of the copolymerization experiments employed an equimolar ratio of comonomers except for copolymerization of *tert*-butyl 4-vinylbenzoate (TBVB) with maleic anhydride (MAH) (TBVB: MAH=1:2 mol/mol) in order to optimize the formation of the alternating copolymer because of TBVB's

tendency to undergo homopolymerization. All of the copolymerizations were conducted for 24 h except for copolymerization of *tert*-butyl 4-vinylbenzoate (TBVB) with maleic anhydride (MAH), which was run for only 4 h to minimize any homopolymerization of TBVB. The initiator concentration was 1.0 wt % based on the monomers. The monomer concentration was 20 wt % based on the solution. The initiator and monomer concentrations may vary for different targeted molecular weight copolymers. For example, a mixture of (*E*)-di-*tert*-butyl 4,4'-stilbenedicarboxylate (DTBSC) (3.8 g 10 mmol), MAH (0.98 g, 10 mmol), chlorobenzene (17.2 mL, 20 wt %), DCP (0.0478 g, 1.0 wt %) was sealed in a 50 mL septum sealed glass bottle equipped with a magnetic stirrer and was degassed by purging with argon for 20 min and polymerized for 24 h. Copolymers were recovered by precipitating into hexanes twice and then Soxhlet extracted with hexanes to remove the residual monomers and dried under vacuum at 60 °C overnight before characterization. Two peaks associated with the anhydride groups of the copolymers (1847 cm^{-1} and 1777 cm^{-1}) were clearly observed in the IR spectrum (Figure 2.3). The 1:1 structures of the copolymers were confirmed by the elemental and TGA analyses. In TGA analysis, compositions of copolymers were identified by comparing mass loss of isobutylene caused by the cleavage of thermally unstable *tert*-butyl groups to the theoretical mass loss assuming the strictly alternating structure, shown in Figure 2.4. The elemental analysis and TGA analysis results are shown in Table 2.3 and in Table 2.1, respectively. For copolymer II, found nitrogen percentage in the elemental analysis is a little higher than the theoretical percentage, but within the experimental error ±0.30%. For copolymer III, calculated isobutylene elimination is about 18.6% which is a little less than the found mass loss of 19.6%. This indicates that

the styrene copolymer is not strictly alternating and its backbone may contain some TBVB-TBVB sequences.

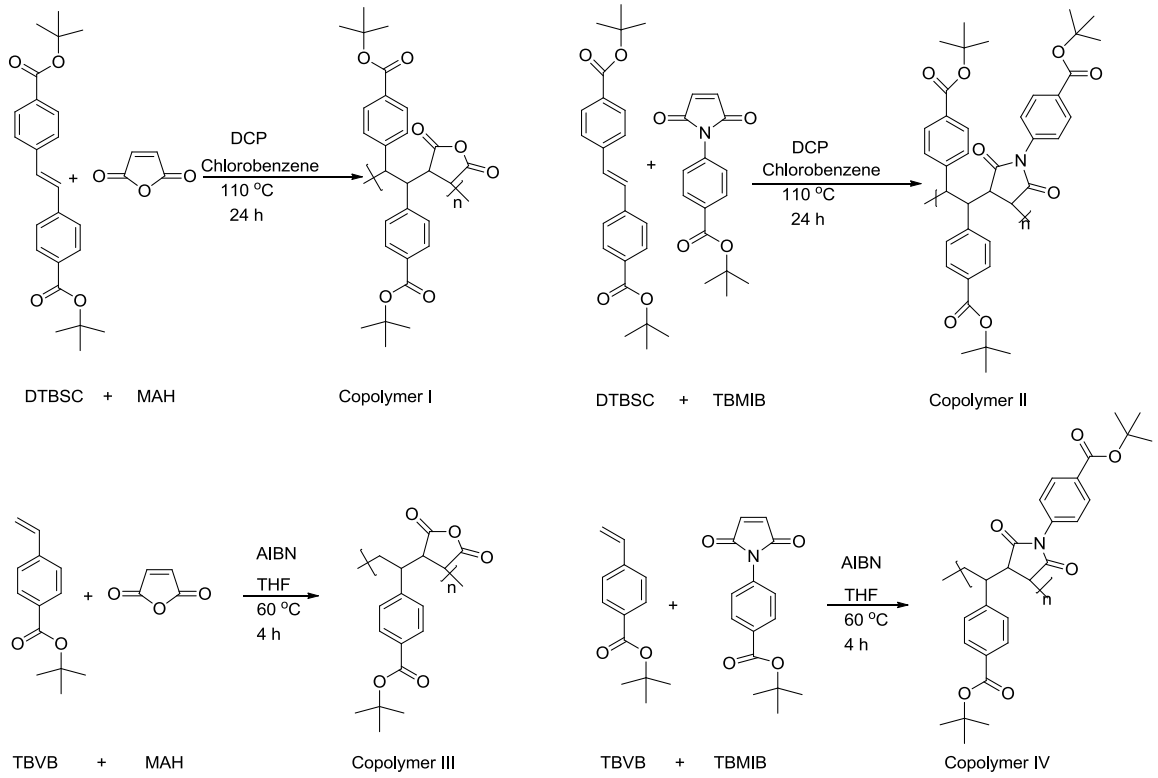

Scheme 2.1 Synthetic scheme for stilbene and styrene alternating copolymers.

Table 2.1 Calculated and found mass loss of copolymers I, II, III, and IV.

	Calculated isobutylene loss (%)	Found isobutylene loss (%)*
copolymer I	23.4	23.2
copolymer II	25.7	24.9
copolymer III	18.6	19.6
copolymer IV	23.4	22.0

*TGA balance precision is ±0.001%.

tert-Butyl carboxylate protecting groups were de-blocked from the copolymer backbones by reacting with trifluoroacetic acid (TFA) and then the resulting polymers with carboxylic acid groups and anhydride groups along the backbone were dissolved in

NaOH solutions to form polyanions, shown in Scheme 2.2. For example, copolymer I (0.80 g, 3.3 mmol of *tert*-butyl carboxylate group) was mixed with TFA (0.84 g, 7.4 mmol) and CH_2Cl_2 (0.45 ml, 7.4 mmol) for 12 h at room temperature. The excess of TFA and CH_2Cl_2 were stripped off in a stream of argon and the polymer was dried in vacuum oven for 24 h at 60 ^oC. The resulting copolymer (0.61 g) was then readily dissolved in stoichiometric NaOH aqueous solution (0.27 g of NaOH) with pH = 10. The polyanion solutions were frozen by immersion of sample vials in liquid nitrogen. The frozen samples were freeze-dried for 24 h on a Virtis lyophilizer. The conversion was confirmed by the IR shown in Figure 2.3. After the cleavage of the *tert*-butyl ester groups, the anhydride groups remained intact. The absorption peaks from the anhydride groups disappeared with the subsequent hydrolysis (Figure 2.3).

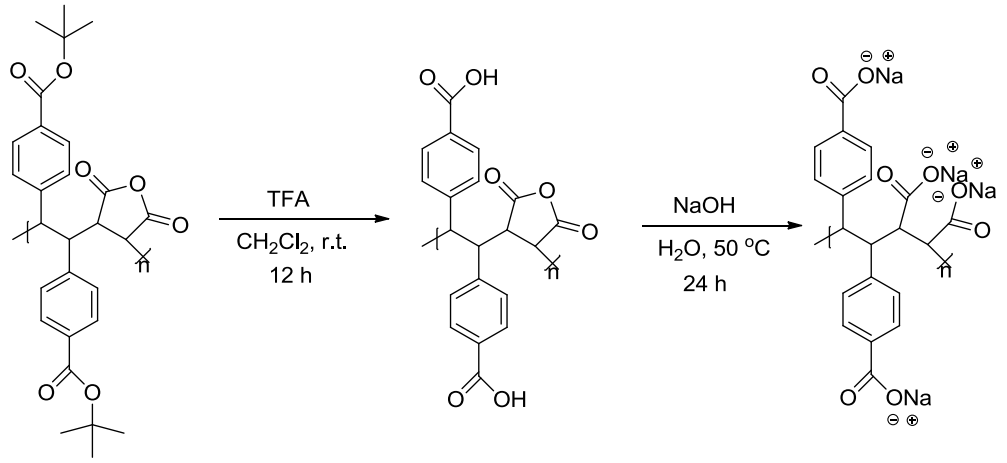

Scheme 2.2 Conversion of *tert*-butyl carboxylate protecting copolymer I into its corresponding polyanion.

.The influence of the copolymerization conditions (i.e., solvent, initiator, reaction temperature) on the rate of copolymerization and molecular weight of the copolymers was observed (Table 2.4). Under condition A (chlorobenzene-DCP-110 ^oC), all the copolymers had 2~3 times higher yields than under condition B (THF-AIBN-60 ^oC). This

may be partially due to DCP being more effective than AIBN as an initiator for the polymerization involving stilbene. This explanation is supported by Bevington et al. who found that stilbene is very reactive toward oxygen-centered radical such as the benzoyloxy radical from benzoyl peroxide (BPO); and it remained unreactive toward carbon-centered radicals like 1-cyano-1-methylethyl radical derived from AIBN.[27, 28] An analogous experiment was carried out to synthesize copolymer I with BPO as the initiator at 70 ^{o}C and resulted in a 60% yield which is consistent with Bevington's hypothesis. It was also observed that condition A resulted in higher molecular weights compared to the condition B for all three stilbene copolymers. This is probably because the steric hindrance in the transition state for cross propagation is overcome at higher temperature. It was concluded that condition A has a synergistic effect on stilbene copolymerization yields and the corresponding molecular weights and thus is used in stilbene copolymerization as an optimized condition. The typical yields and molecular weight information of copolymers I, II, III and IV are shown in Table 2.2.

Table 2.2 Typical yields and molecular weights of copolymers under optimized copolymerization conditions.

	Condition	Reaction duration (h)	Yield (%)	M_n (kg/mol)	M_w/M_n
copolymer I	A	24	85	28.6	1.87
copolymer II	A	24	77	7.00	1.68
copolymer III	B	4	65	17.7	1.54
copolymer IV	B	4	41	19.7	1.89

The aromatic hydrogen atoms and hydrogen atoms on the polymer backbone exhibited very broad peaks in the ^{1}H NMR spectrum, which is consistent with the lack of mobility

in the polymer chains (Figure 2.5). This observation is consistent with previously reported functionalized stilbene copolymers.[14-17] There was no glass transition temperature (T_g) or crystalline melting temperature (T_m) observed in DSC analysis for copolymers I, II, III and IV under their corresponding degradation temperatures (Figure 2.6). The cleavage of the *tert*-butyl groups occurs at around 200 ^{o}C as shown in Figure 2.2. After deprotection, the 5% weight loss degradation temperature was shifted to 400 ^{o}C. It is noted that T_g and T_m were still not observed under elevated degradation temperatures in the DSC curves after the cleavage, shown in Figure 2.6. This is indicative of a structure with restricted chain motion which is consistent with the extremely broad ^{1}H NMR results.

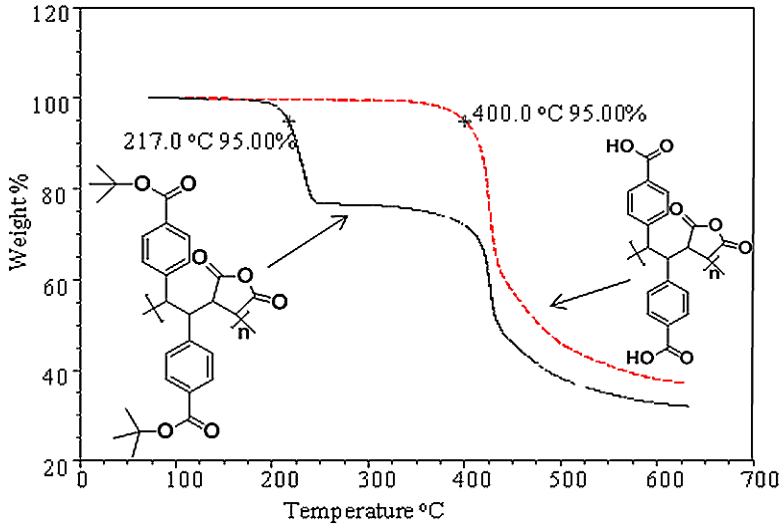

Figure 2.2 TGA curves for copolymer I. Solid line is for copolymer I; Dashed line is for copolymer I after deblocking the tert-butyl groups.

In summary, a new series of polyelectrolyte precursors with tunable charge densities were synthesized and characterized under optimized conditions with a two-step synthetic strategy. The steric crowding, arising from pendent phenyl groups along the polymer backbone, resulted in broad peaks in the ^{1}H NMR spectrum as well as the absence of

thermal transitions below the elevated degradation temperature at around 400 ^{o}C. Polyelectrolyte precursors were then readily converted into their corresponding anionic polyelectrolytes with new stilbene comonomers that have various types and amounts of ionic precursor groups. We are examining the steric crowding effect imparted to the chain by the stilbene comonomers by determination of persistence lengths and other solution measurements.[29] We anticipate that the synthetic versatility provided by this strategy will enable systematic variation of the type of ionic functionality with precisely placed charges with varying charge densities along the polymer backbone. These new polyelectrolytes could provide unique solution properties and other properties involved with polyion complexation.

Supporting Information Available: Experimental, IR, DSC and ^{1}H NMR spectra, additional tables. This material is available free of charge via the Internet at http://pubs.acs.org.

Acknowledgement

This work was supported by the donors of the American Chemical Society Petroleum Research Fund, the National Science Foundation under grant numbers DMR-0905-231 and the teaching assistantship from Department of Chemistry at Virginia Tech. We thank Professor Timothy Long's group, Professor Judy Riffle's group for the help on the SEC, TGA, DSC and rheological measurements.

REFERENCES

1. De Geest, B. G.; De Koker, S.; Sukhorukov, G. B.; Kreft, O.; Parak, W. J.; Skirtach, A. G.; Demeester, J.; De Smedt, S. C.; Hennink, W. E. *Soft Matter* **2009**, *5*, 282-291.
2. Wattendorf, U.; Kreft, O.; Textor, M.; Sukhorukov, G. B.; Merkle, H. P. *Biomacromolecules* **2008**, *9*, 100-108.
3. Dai, Z.; Möhwald, H.; Tiersch, B.; Dähne, L. *Langmuir* **2002**, *18*, 9533.
4. Bolto, B. A. *Prog. Polym. Sci.* **1995**, *20*, 987-1041.
5. Pasquier, N.; Keul, H.; Moeller, M. Des. Monomers and Polym. **2005**, *8*, 679-703.
6. Florjańczyk, Z.; Bzducha, W.; Wieczorek, W.; Zygadło-Monikowska, E.; Krawiec, W.; Chung, S. H. *J. Phys. Chem. B* **1998**, *102*, 8409.
7. Bowman, W. A.; Rubinstein, M.; Tan, J. S. *Macromolecules* **1997**, *30*, 3262.
8. Decher, G. *Science* **1997**, *277*, 1232.
9. Bertrand, P.; Jonas, A.; Laschewsky, A.; Legras, R. *Macromol. Rapid Commun.* **2000**, *21*, 319.
10. Arys, X.; Jonas, A. M.; Laguitton, B.; Legras, R.; Laschewsky, A.; Wischerhoff, E. *Prog Org Coat* **1997**, *34*, 108.
11. Koetse, M.; Laschewsky, A.; Jonas, A. M.; Wagenknecht, W. *Langmuir* **2002**, *18*, 1655.
12. Sedlák, E.; Fedunová, D.; Veselá, V. r.; Sedláková, D.; Antalík, M. n. *Biomacromolecules* **2009**, *10*, 2533.
13. Fang, W.; Cai, Y.; Chen, X.; Su, R.; Chen, T.; Xia, N.; Li, L.; Yang, Q.; Han, J.; Han, S. *Bioorg. Med. Chem. Lett.* **2009**, *19*, 1903.
14. Mao, M.; Kim, C.; Wi, S.; Turner, S. R. *Macromolecules **2007, 41,*** 387.
15. Mao, M.; Turner, S. R. *Polymer* **2006**, *47*, 8101-8105.
16. Mao, M.; Turner, S. R. J. Am. Chem. Soc.**2007**, 129, 3832.
17. Li, Y.; Turner, S. R. *Eur. Polym. J.* **2010**, *46*, 821.
18. Wagner-Jauregg, T. *Ber Dtsch Chem Ges (A and B Series)* **1930**, *63*, 3213-3224.
19. Lewis, F.M.; Mayo, F.R. *J. Am. Chem. Soc.***1948**, *70*, 1533-1536.
20. Hallensleben, M.L. *Eur Polym J* **1973**, *9*, 227-231.
21. Tanaka, T.; Vogl, O. *Polym. J. (Tokyo, Japan)* **1974**, *6*, 522-531.
22. Rzaev, Z. M.; Zeinalov, I. P.; Medyakova, L. V.; Babaev, A. I.; Agaev, M. M. *Vysokomol Soedin Ser A* **1981**, *23*, 614.
23. Ebdon, J. R.; Hunt, B. J.; Hussein, S. *Brit. Polym. J.* **1987**, *19*, 333-337.
24. McNeill, I.C.; Polishchuk, A.Y.; Zaikov, G.E. *Polym. Degrad. Stab.* **1995**, *47*, 319-329.
25. Braunecker, W. A.; Matyjaszewski, K. *Prog. Polym. Sci.* **2007**, *32*, 93.
26. Penelle, J.; Xie, T. *Macromolecules* **2001**, *34*, 5083.
27. Bevington, J. C.; Huckerby, T. N. *Macromolecules* **1985**, *18*, 176.
28. Bevington, J. C.; Breuer, S. W.; Huckerby, T. N. *Macromolecules* **1989**, *22*, 55.

29. Li, Y.; Zhang, M.; Mao, M.; Turner, S. R.; Moore, R. B.; Mourey, T. H.; Slater, L. A.; Hauenstein, J. R. *Macromolecules* **2012**, *45*, 1595.

2.2. SUPPORTING INFORMATION TO THE PAPER

2.2.1. Experimental Section

2.2.1.1. Materials

Maleic anhydride (MAH, Aldrich, ≥99.0%), potassium *tert*-butoxide solution 1.0 M in tetrahydrofuran (KO^tBu, Aldrich), *tert*-butanol (HO^tBu, Sigma-Aldrich, anhydrous, ≥99.5%), *N*-bromosuccinimide (NBS, Aldrich, 99%), *p*-toluic acid (Aldrich, 98%), formaldehyde (Aldrich, 37 wt. % in H_2O), triphenylphosphine (Sigma-Aldrich, 99%), thionyl chloride ($SOCl_2$, Fluka, ≥99.0%), acetic anhydride (Sigma-Aldrich, ≥98.0%), sodium acetate (Sigma-Aldrich, ≥99.0%), *4*-aminobenzoic acid (Sigma, ≥99.0%), *2,2*'-azobisisobutyronitrile (AIBN, Aldrich, 98%), dicumylperoxide (DCP, Aldrich, 98%), trifluoroacetic acid (TFA, Aldrich, 99%), sodium hydroxide (NaOH, Sigma-Aldrich, ≥98.0%) were used as received. (*E*)-Dimethyl-*4,4'*-stilbenedicarboxylate (DMSC) was received as a donation from Eastman Chemical Company. Tetrahydrofuran (Sigma-Aldrich, anhydrous, ≥99.9%), hexanes (Fisher, HPLC grade), methylene chloride (CH_2Cl_2, Fisher, HPLC grade), diethyl ether (Fisher, HPLC grade), toluene (Fisher, HPLC grade), chlorobenzene (Sigma-Aldrich, anhydrous, ≥99.8%), benzene (Sigma-Aldrich, anhydrous, ≥99.8%), and acetone (Fisher, HPLC grade) were used without further purification. Water was deionized before use.

2.2.1.2. Instrumental Characterization

^1H and ^{13}C NMR spectra were determined at 25 °C in deuterated solvents at 400/100 MHz with a Varian Unity spectrometer or 500/125 MHz with a Jeol Eclipse +500 spectrometer. Melting points of monomers were measured on a uncorrected BUCHI Melting Point B-540 instrument at a heating rate of 0.5 ^oC/min. IR spectra were

recorded with a MIDAC M2004 FT-IR spectrophotometer in the reflection mode. The elemental analysis was done by Atlantic Microlab, Inc. (Norcross, Georgia). Thermogravimetric analysis (TGA) was conducted under nitrogen, from 25 ^{o}C to 650 ^{o}C at a heating rate of 10 ^{o}C/min using a TA Instrument TGA Q5000. Differential scanning calorimetry (DSC) was carried out using a Perkin-Elmer Pyris 1 DSC at heating rate and cooling rate of 10 ^{o}C /min in a nitrogen atmosphere. Molecular weights of the polymers were determined using a size exclusion chromatograph equipped with a viscosity detector and a laser refractometer detector in chloroform at 30 ^{o}C. Data were analyzed utilizing a universal calibration made with polystyrene standards to obtain absolute molecular weights. A Virtis lyophilizer (Gardiner, NY) equipped with a drum manifold and a condenser was used at a pressure of <30 mTorr.

2.2.1.3. Monomer Synthesis

Synthesis of (E)-Di-tert-butyl 4,4'-stilbenedicarboxylate (DTBSC)

(*E*)-Di-*tert*-butyl 4,4'-stilbenedicarboxylate was prepared as shown in scheme 2.3: A suspension of DTBSC (2.3 g, 7.9 mmol) in toluene (45 mL) was refluxed at 110 ^{o}C, followed by addition of KO^{t}Bu (1.0 M in THF, 24 mL) dropwise. After adding KO^{t}Bu, the reaction mixture was cooled down to room temperature and stirred overnight. After the reaction was stirred overnight, the reaction solution was poured into aqueous concentrated NH_4Cl (100 mL) solution while stirring. The aqueous layer was then extracted (toluene, 2x25 mL) and the organic layer was dried over magnesium sulfate. After filtration the solution was concentrated with a rotary evaporator to give a yellow solid. The crude product was purified by silica column chromatography (hexanes/ethyl acetate 98:2 v/v). A white crystalline solid was obtained. Yield: 82%. ^{1}H NMR ($CDCl_3$,

500MHz) δ ppm: 7.99 (d, *J*=8.6 Hz, 4H), 7.56 (d, *J*=8.6 Hz, 4H), 7.21 (s, 2H), 1.61 (s, 18H). ^{13}C NMR ($CDCl_3$, 500MHz) δ ppm: 165.6, 140.9, 131.4, 130.0, 129.9, 126.5, 81.2, 28.3. Melting point: 168.6-169.1 ^{o}C. (Lit.:[1] 170 ^{o}C)

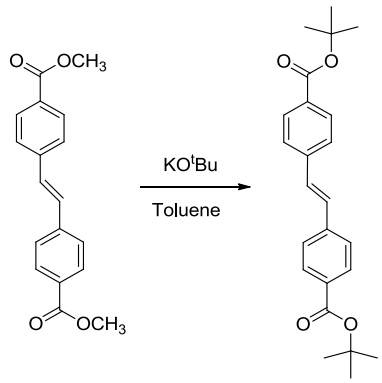

Scheme 2.3 Synthesis of (*E*)-di-*tert*-butyl 4,4'-stilbenedicarboxylate.

Synthesis of tert-Butyl 4-vinylbenzoate (TBVB)

tert-Butyl 4-vinylbenzoate was synthesized via a multistep process, Scheme 2.4: *p*-Carboxybenzyl bromide (A) was synthesized via radical halogenation.[2] *4*-Vinylbenzoic acid (C) was prepared with *p*-carboxybenzyltriphenylphosphonium bromide (B) and formaldehyde through a Wittig-reaction.[3] 4-Vinylbenzoyl chloride (D) was obtained by mixing the monomer C with thionyl chloride and then stripping off the excess of thionyl chloride in a stream of argon.[4] *tert*-Butyl 4-vinylbenzoate was prepared by adding the monomer D dropwise to a mixture of KO^{t}Bu and HO^{t}Bu in dry THF cooled in an ice bath. The mixture was reacted at room temperature overnight. Distillation gave a clear colorless liquid at 80 ^{o}C (0.2 mbar). Yield: 80%. ^{1}H NMR ($CDCl_3$, 500 MHz) δ ppm: 7.92 (d, *J*=8.4 Hz, 2H), 7.39 (d, *J*=8.4 Hz, 2H), 6.69 (dd, *J*=17.6, 10.9 Hz 1H), 5.80 (d, *J*=17.6 Hz, 1H), 5.31 (d, *J*=10.9 Hz, 1H), 1.56 (s, 9H). ^{13}C NMR ($CDCl_3$, 500MHz) δ ppm: 165.6, 141.4, 136.1, 131.2, 129.7, 125.9, 116.1, 80.9, 20.1.

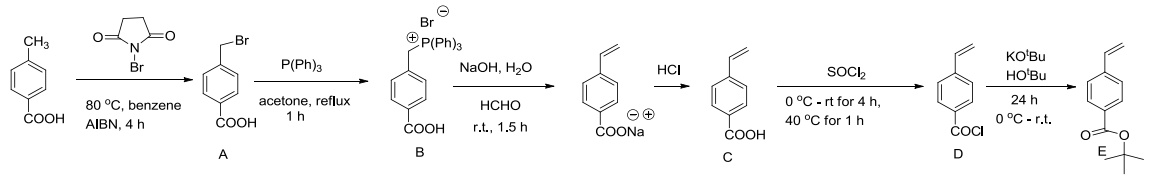

Scheme 2.4 Synthesis of *tert*-butyl 4-vinylbenzoate.

Synthesis of tert-Butyl 4-*maleimidobenzoate (TBMIB*)

tert-Butyl 4-maleimidobenzoate, a new maleimide, was prepared via a multistep process, Scheme 2.5: 4-Sulfinylaminobenzoyl chloride (B) was obtained by refluxing a solution of 4-aminobenzoic acid in thionyl chloride and then stripping off the excess of thionyl chloride in a stream of argon.[4] *tert*-Butyl 4-aminobenzoate (B) was prepared by portionwise addition of the monomer B to a mixture of KO^tBu and HO^tBu in dry THF cooled in an ice bath.[5] The crude yellow product was purified by Soxhlet extraction with hexanes for 48 h. *tert*-Butyl 4-maleimidobenzoate (D) was prepared as follows: A mixture of B (4.6 g, 24 mmol) and MAH (2.4 g, 24 mmol) in THF (40 ml, 0.6 M) was stirred at room temperature overnight. During the reaction the maleamic acid (C) precipitated as a white solid. C was filtered, washed with 100 mL diethyl ether and vacuum dried for 24 h. Yield: 75%. In the following step, a suspension of C (4.9 g, 17 mmol) and sodium acetate (0.7 g, 8 mmol), acetic anhydride (15.5 g, 151 mmol) was heated at 80 ^oC for 24 h. The solution was poured into ice water and extracted with CH_2Cl_2. The organic layer was dried with $MgSO_4$. A light yellow crude product was obtained and purified by silica column chromatography. A light yellow crystalline solid was obtained (hexanes: acetate=10:1). Yield: 70%. ^1H NMR ($CDCl_3$, 500 MHz) δ ppm: 8.08 (d, *J*=8.9 Hz, 2H), 7.45 (d, *J*=8.9 Hz, 2H), 6.87 (s, 2H), 1.59 (s, 9H). Elemental

Analysis: calculated C, 65.93; H, 5.49; N, 5.13; Found C, 65.88; H, 5.47; N, 5.07.

Melting point: 114.8-115.4 ^{o}C.

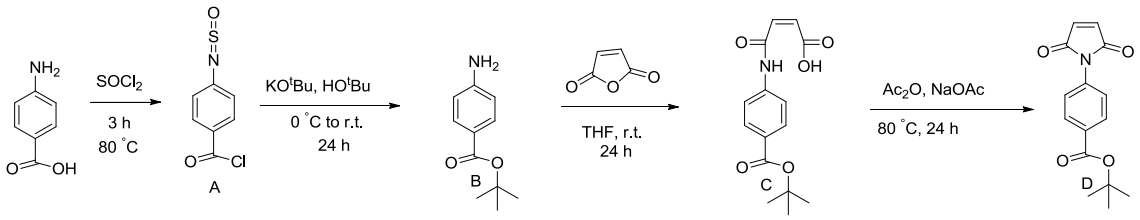

Scheme 2.5 Synthesis of *tert*-butyl 4-maleimidobenzoate.

REFERENCES

1. Mao, M. (2007). *Synthesis and characterization of highly functional substituted stilbene copolymers and semi-crystalline poly(aryl ether sulfone)s*. Blacksburg, Va, University Libraries, Virginia Polytechnic Institute and State University. http://scholar.lib.vt.edu/theses/available/etd-09192007-141158.
2. Rich, D. H.; Gurwara, S. K. *J. Am. Chem. Soc*. **1975**, *97*, 1575.
3. Rene Broos; Dirk Tavernier; Anteunis, M. *J. Chem. Educ.* **1978**, *55*, 813.
4. Ishizone, T.; Hirao, A.; Nakahama, S. *Macromolecules* **1989**, *22*, 2895.
5. Taylor, E. C.; Fletcher, S. R.; Sabb, A. L. *Synth. Commun.* **1984**, *14*, 921.

2.2.2. Figures and Tables

(1)

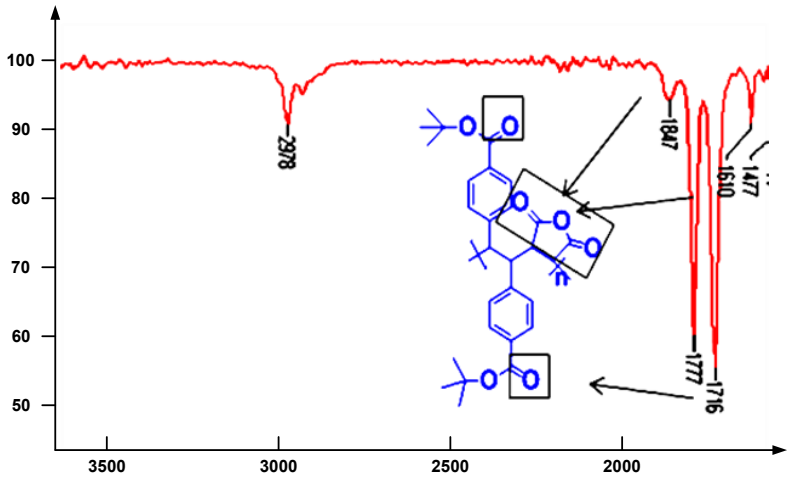

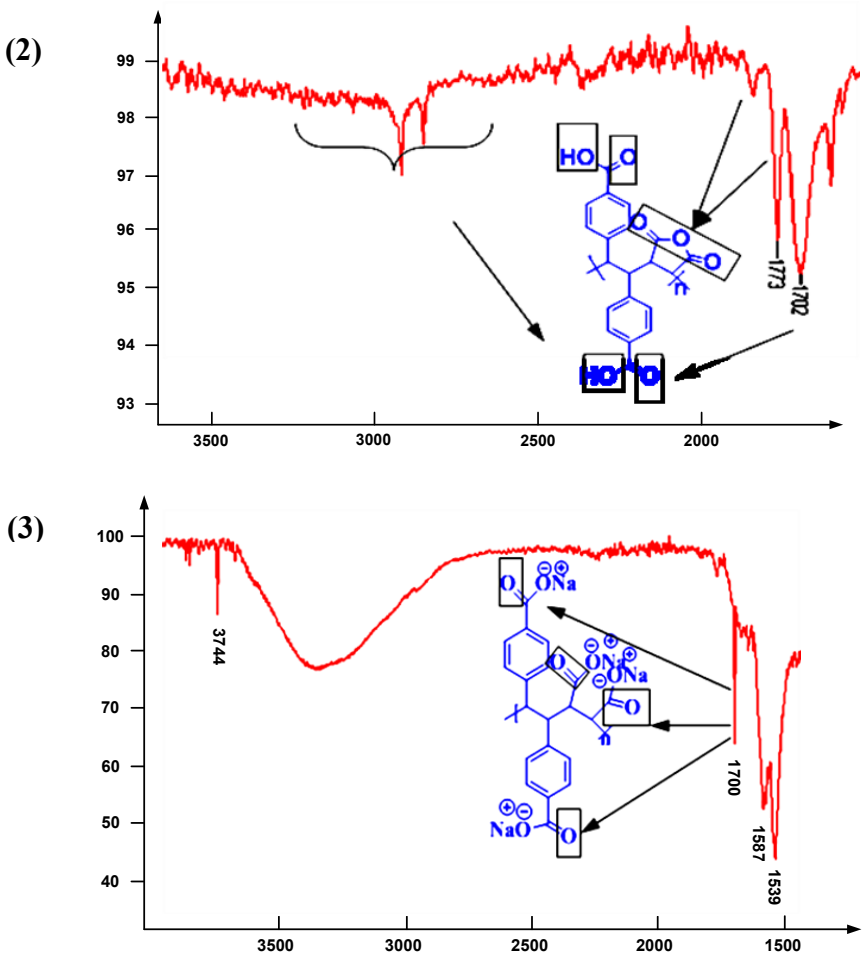

Figure 2.3 IR spectra of copolymer I (1), deprotected copolymer I (2) and its corresponding polyanion (3).

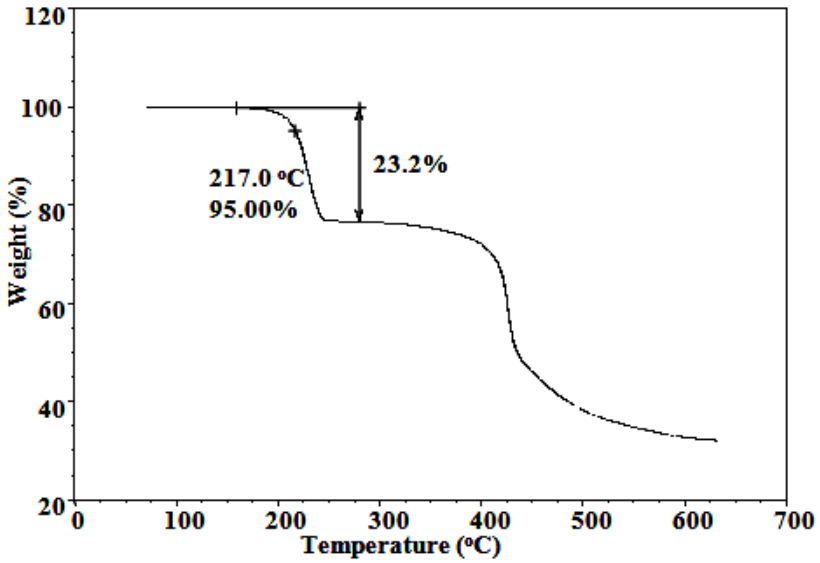

Figure 2.4 The TGA curve of polymer I.

Table 2.3 Elemental analysis results of copolymers I, II, III, and IV.

	Calculated C (%)	Calculated H (%)	Calculated N (%)	Found C (%)	Found H (%)	Found N (%)
copolymer I	70.15	6.26	N/A	69.98	6.30	N/A
copolymer II	71.56	6.57	2.14	70.84*	6.45	2.37
copolymer III	67.55	5.96	N/A	65.76*	6.06	N/A
copolymer IV	70.29	6.90	2.93	69.16	6.52	2.88

*Deviation from calculated values due to partial hydrolysis of MAH units

Table 2.4 Comparison of yields and molecular weights under condition A (chlorobenzene-DCP-110 °C) and condition B (THF-AIBN-60 °C).

	Yield (%)	M_n (kg/mol)	M_w/M_n
copolymer I-A	85	28.6	1.87
copolymer I-B	22	2.10	1.39
copolymer II-A	77	7.00	1.68
copolymer II-B	37	2.30	1.87

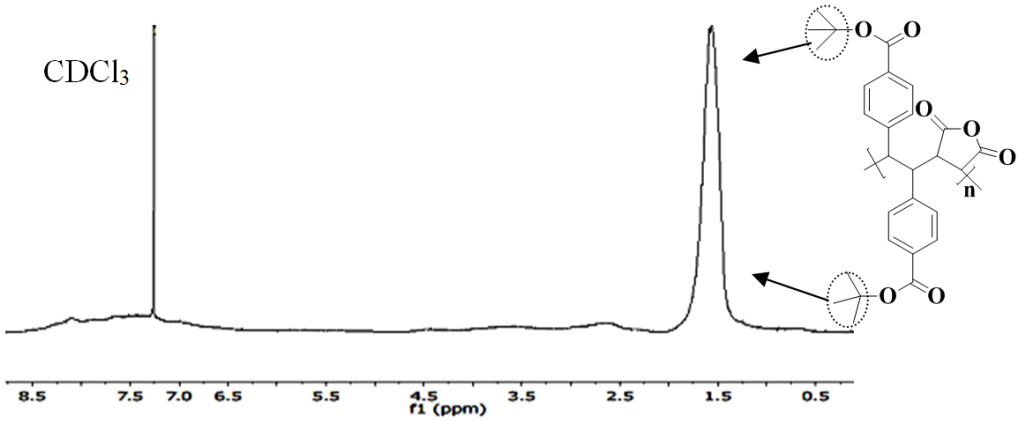

Figure 2.5 500/125 MHz ^{1}H NMR spectrum of copolymer I in $CDCl_3$.

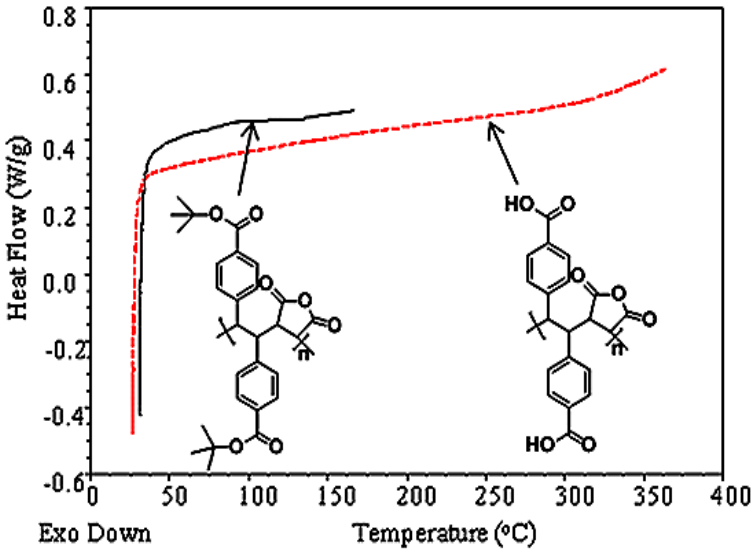

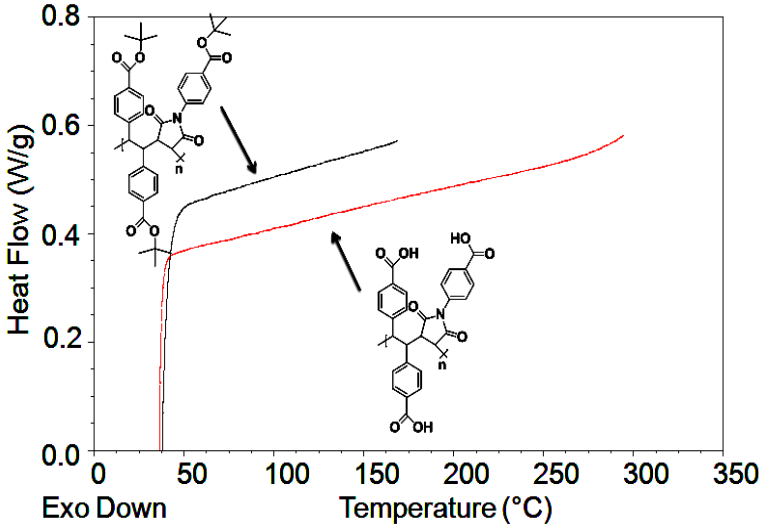
Heat Flow (W/g)
0.8
0.6
0.4
0.2
0.0
0
50
100
150
200
250
300
350
Exo Down
Temperature (°C)

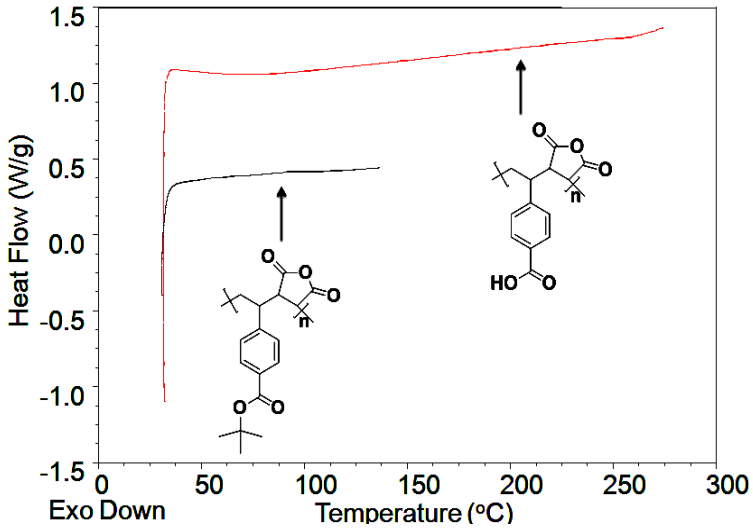
Heat Flow (W/g)
1.5
1.0
0.5
0.0
-0.5
-1.0
-1.5
0
50
100
150
200
250
300
Exo Down
Temperature (°C)

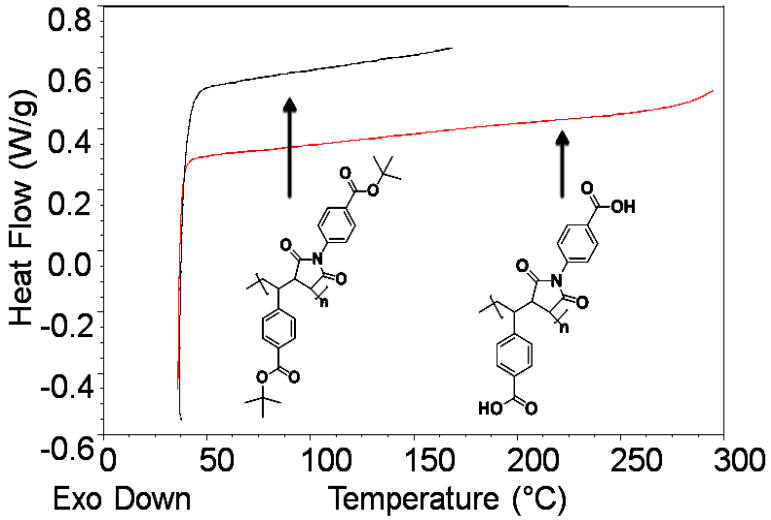

Figure 2.6 DSC curves for copolymers I, II, III, and IV and for their corresponding deprotected copolymers.

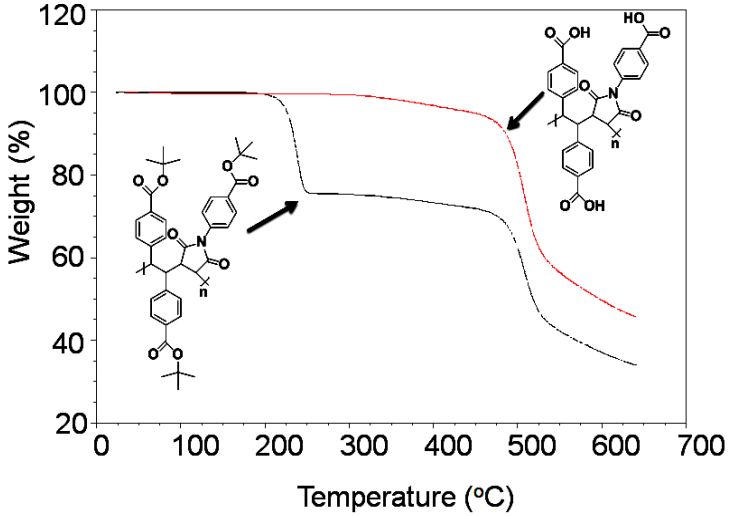

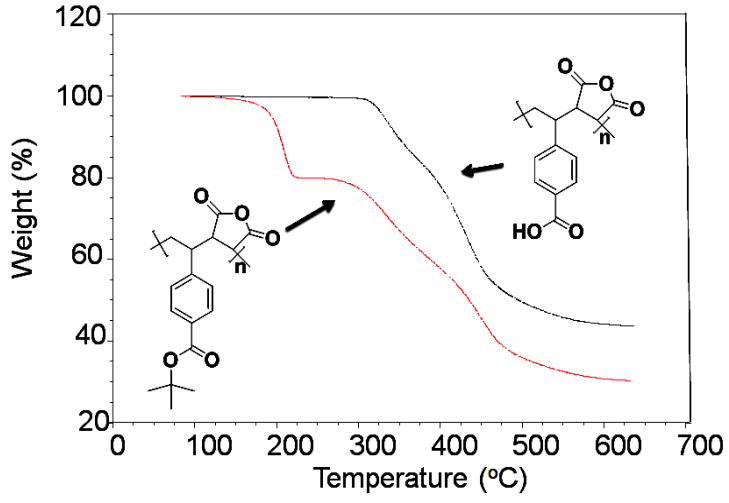

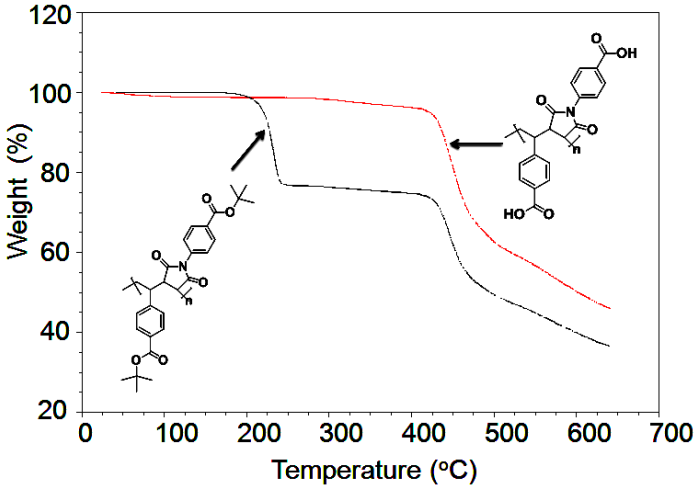

Figure 2.7 TGA curves for copolymer II, III, IV and for their corresponding deprotected copolymers.

2.3. APPENDIX TO CHAPTER 2

2.3.1. Monomer Synthesis with Details

Synthesis of (E)-Di-tert-butyl 4,4'-stilbenedicarboxylate (DTBSC)

Column chromatography was used to purify the crude product, (*E*)-di-*tert*-butyl 4,4'-stilbenedicarboxylate (DTBSC). In preparation for column chromatography, the solid is dissolved in a minimum amount of methylene chloride and preadsorbed on to silica which is then concentrated with a rotary evaporator. The solvent system used in column chromatography is 98 to 2 of hexanes to ethyl acetate. The preabsorbed silica was placed on a column (5 cm x 15 cm) of silica gel (20 g), which was packed in eluent (98:2 Hex:EtOAc). The eluent was pushed through the column using air pressure and 12–14 fractions (125 mL) were collected. The desired compound appeared in fractions 2–10. The fractions were combined in a round bottom flask and concentrated by rotary evaporation to give a white crystalline solid, which was dried overnight under high

vacuum at 60 °C. Yield: 1.89 g, 82 %. ^{1}H NMR spectrum of (*E*)-di-*tert*-butyl 4,4'-stilbenedicarboxylate in $CDCl_3$ is shown in Figure 2.8.

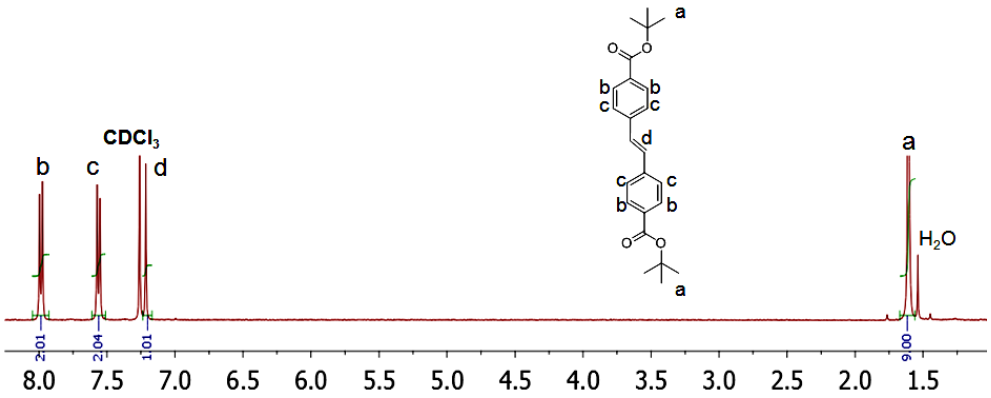

Figure 2.8 500/125 MHz ^{1}H NMR of (*E*)-di-*tert*-butyl 4,4'-stilbenedicarboxylate in $CDCl_3$.

Synthesis of tert-Butyl 4-vinylbenzoate (TBVB)

tert-Butyl-4-vinylbenzoate was synthesized via a multistep process. *p*-Carboxybenzyl bromide, *p*-carboxybenzyltriphenylphosphonium bromide, 4-vinylbenzoic acid, and 4-vinylbenzoyl chloride were prepared following a previously published procedure.

Step A. *p*-Carboxybenzyl bromide was synthesized via free radical halogenation mechanism.[1] To a mixture of p-toluic acid (4.03 g, 29.4 mmol) and *N*-bromosuccinimide (5.28 g, 29.7 mmol) was added AIBN (0.003 g). Dry benzene (27 mL) was added and the suspension was stirred for 4 h under refluxing temperature. After the reaction solution was cooled to room temperature, the precipitate was filtered out with suction, then extracted with hot water for 30 min to dissolve succinimide, the side product. The crude product was filtered and recrystallized from methanol as a white solid and vacuum dried. Yield: 72%, 4.55 g. ^{1}H NMR (CD_3COCD_3, 400MHz) δ ppm: 7.99 (d, *J*=8 Hz, 2H), 7.57 (d, *J*=8 Hz, 2H), 6.82 (s, 2H), 4.68 (s, 2H). Lit. Mp :[1] 224 – 226 ^{o}C.

Step B. 4-Vinylbenzoic acid was prepared with *p*-carboxybenzyltriphenylphosphonium bromide and formaldehyde. *p*-Carboxybenzyltriphenylphosphonium bromide was prepared following the previously published routes.[2] To a mixture of *p*-carboxybenzyltriphenylphosphonium bromide (36.20 g, 75.89 mmol) and 37% formaldehyde (150 mL) diluted with deionized water (78 mL), sodium hydroxide aqueous solution (0.20 g/mL, 100 mL) was added dropwise. The mixture was stirred at room temperature for 60 min. The precipitate was filtered and washed with deionized water. The filtrate was acidified with the diluted HCl solution to pH 1. 4-Vinylbenzoic acid was obtained as a white solid. Yield: 80%, 8.99 g. ^{1}H NMR (CD_3SOCD_3, 400MHz) δ ppm: 7.88 (d, *J*=8 Hz, 2H), 7.56 (d, *J*=8 Hz, 2H), 6.78 (dd, *J*=17.4, 10.9 Hz, 1H), 5.95 (d, *J*=17.4 Hz, 1H), 5.38 (d, *J*=10.9 Hz, 1H). Lit. Mp :[2] 144 ^{o}C.

Step C. *tert*-Butyl-4-vinylbenzoate was prepared as follows:[3] A solution of 4-vinylbenzoic acid (1.37 g, 9.26 mmol) and thionyl chloride (2.72 mL, 37.0 mmol) was stirred in an ice-water bath initially and heated at room temperature for 4 h. Then the solution was heated at 40 ^{o}C for another 1 h. Thionyl chloride in excess was stripped off by blowing argon and a clear light yellow liquid, 4-vinyl benzoyl chloride, was obtained. *tert*-Butyl-4-vinylbenzoate was prepared with 4-vinylbenzoyl chloride and potassium *tert*-butoxide following the previously published routes.[3] Distillation gave a clear light green-colored liquid at 80 ^{o}C (0.2 mbar). Yield: 45%, 0.85 g. ^{1}H NMR spectrum of *tert*-butyl 4-vinylbenzoate in $CDCl_3$ is shown in Figure 2.9.

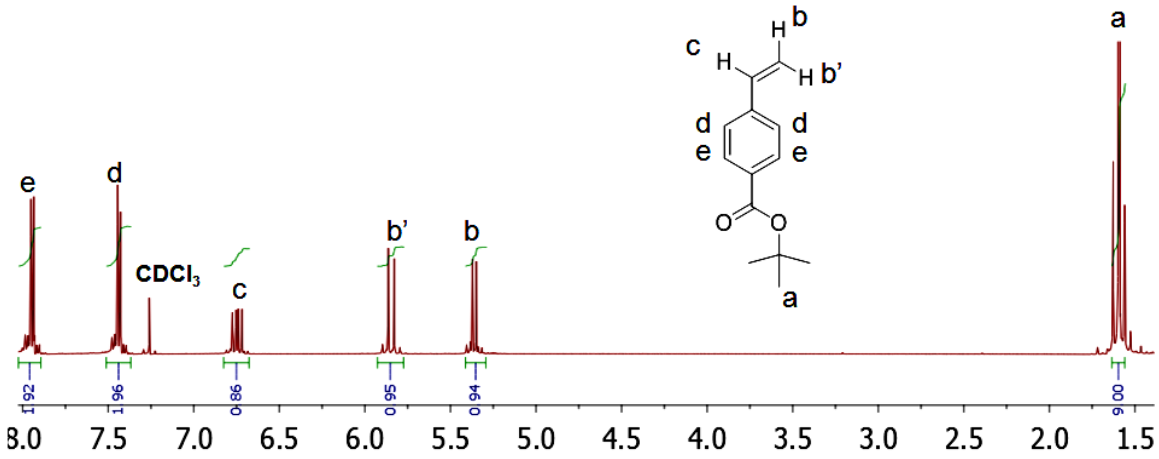

Figure 2.9 500/125 MHz ^{1}H NMR of *tert*-butyl 4-vinylbenzoate in $CDCl_3$.

Synthesis of tert-Butyl 4-*maleimidobenzoate (TBMIB*)

tert-Butyl 4-maleimidobenzoate, a new maleimide, was prepared via a 4-step process.[4] To purify the crude product, the solution was poured over sodium bicarbonate saturated solution and two layers appeared. The top layer was clear red and the bottom layer was clear yellow. The aqueous layer was then extracted with methylene chloride and discarded. The organic layer was dried with anhydrous $MgSO_4$. The mixture was filtered and the solvent was stripped off by a rotary evaporator; the crude yellow solid was dried overnight under vacuum at room temperature. The solid (15.8 g) from the second step was then purified through Soxhlet extraction with hexane (300 ml) for 48 h, obtaining a yellow crystalline product at 49.0% yield. Once the solid was purified, the third step was performed by combining the product (4.42 g, 46 mmol) and maleic anhydride (2.2 g, 46 mmol) in THF (40 mL, 0.6 M) in a one-to-one mole ratio, purging with argon for 10 min and allowing it to stir at room temperature overnight. During the reaction, maleamic acid precipitated as a white solid. The product was filtered and washed with diethyl ether, and then dried in a vacuum oven for 24 h at room temperature with a 70.6% yield. In the final

step, sodium acetate (0.78 g), acetic anhydride (16 mL, 18 mmol), and maleamic acid (5.4 g, 18 mmol) were heated at 80 °C for 12 h. The solution was poured into ice water after it is cooled to room temperature and the product was extracted with CH_2Cl_2 (2 x 150 mL). The organic layer was collected and dried with $MgSO_4$. The final crude product, *tert*-butyl 4-maleimidobenzoate, was a light yellow oil (5.9 g) that was preabsorbed onto silica (16.9g) in preparation for column chromatography. The solvent system used in column chromatography was 10 to 1 of hexanes to ethyl acetate. The preabsorbed silica was placed on a column (3" x14") of silica gel (410 g), which was packed with 1 L of eluent (10:1 Hex:EtOAc). The eluent was pushed through the column by using air pressure and 31 fractions (250-500 mL) were collected. The desired compound appeared in fractions 2–25. The fractions were combined in a round bottom flask and concentrated by rotary evaporation to give a light yellow crystalline solid, which was dried overnight under high vacuum at 25 °C. Yield: 56%, 3.32 g. ^{1}H NMR spectrum of *tert*-butyl 4-maleimidobenzoate in $(CD_3)_2CO$ is shown in Figure 2.10.

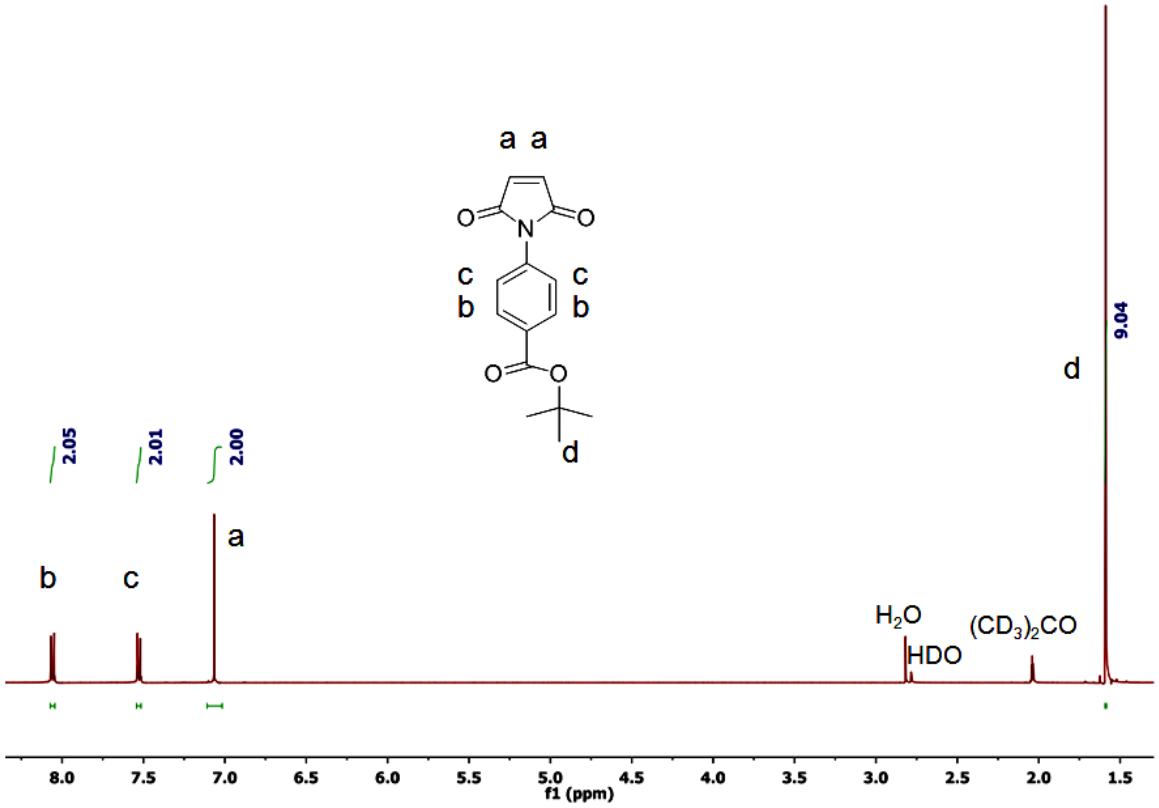

Figure 2.10 500/125 MHz ^{1}H NMR of *tert*-butyl 4-maleimidobenzoate in $(CD_3)_2CO$.

Synthesis of N-4-(N',N'-Dimethylaminophenyl)maleimide (DMAPM)

N-4-(*N',N'*-Dimethylaminophenyl)maleimide was prepared via a two-step reaction, Scheme 2.6:[5] The maleamic acid (a) was obtained by mixing MAH and *N-4*-amino-*N',N'*-dimethylaniline in toluene and heating at 80 ^{o}C for 4 h. The precipitate was filtered, washed with diethyl ether, and vacuum dried to yield a reddish powder. The maleimide (b) was formed by dehydration of the monomer (a) using acetic anhydride and sodium acetate. The solution was poured into ice water and the maleimide was filtered and purified by silica column chromatography (hexanes: ethyl acetate = 4:1). Orange crystals were obtained. Overall yield: 58%. ^{1}H NMR ($CDCl_3$, 500MHz) δ ppm: 7.13 (d, *J*=2.6 Hz, 2H), 6.81 (s, 2H), 6.76 (d, *J*=2.6 Hz, 2H), 2.97 (s, 6H), in Figure 2.11. ^{13}C NMR ($CDCl_3$,

500 MHz) δ ppm: 170.4, 150.4, 134.2, 127.4, 119.6, 112.6, 40.6. Melting point: 154-155 °C (lit.:[5] 153-154 °C).

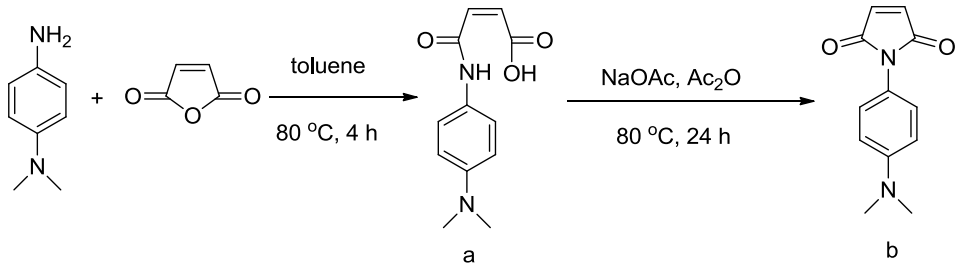

Scheme 2.6 Synthesis of *N-4-*(*N',N'*-dimethylaminophenyl)maleimide.

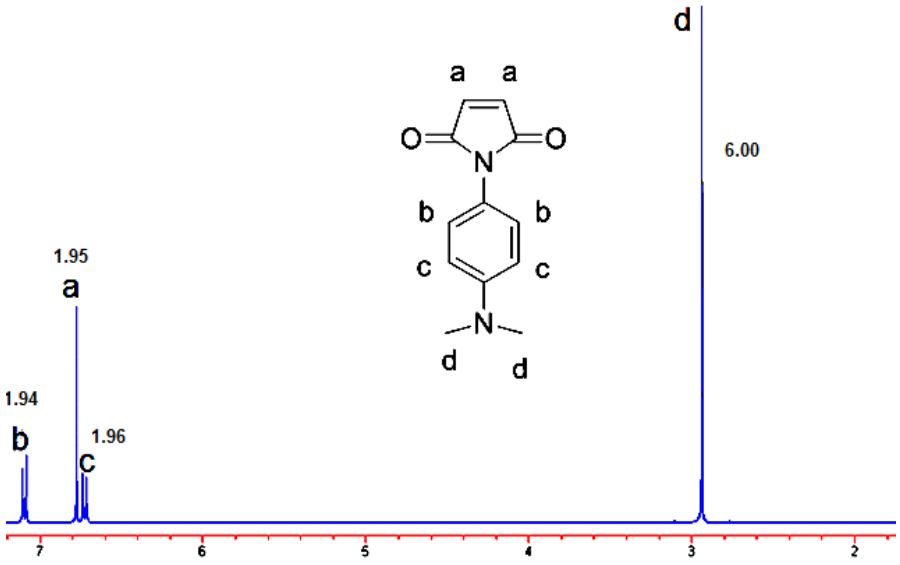

Figure 2.11 500/125 MHz ^{1}H NMR of *N-4-*(*N',N'*-dimethylaminophenyl)maleimide in $CDCl_3$.

2.3.2. Some routes for preparation of tert-Butyl 4-maleimidobenzoate (TBMIB)

A successful route but with low yield

tert-Butyl 4-maleimidobenzoate was synthesized via the multistep process shown in Scheme 2.7. 4-Maleimidobenzoic acid was prepared following a previously published procedure.[6] *N*-(4-(*t*-Butoxycarbonyl)phenyl)maleimide was synthesized as follows:[7] to a stirred suspension of anhydrous $MgSO_4$ (9.6 g, 80 mmol) and 60 mL CH_2Cl_2 was added

concentrated H_2SO_4 (1.1 mL, 20 mmol). The mixture was stirred for 15 min. A mixture of HO^tBu (7.4 g, 0.10 mol) and 4-maleimidobenzoic acid (4.31 g, 19.9 mmol) dissolved in 30 mL CH_2Cl_2 was then added. The reaction flask was connected with a dry ice-acetone condenser and the mixture was stirred at room temperature for 18 h. The reaction was terminated by adding 200 mL 15% sodium bicarbonate solution. The organic layer was extracted, washed with brine and dried with anhydrous $MgSO_4$. The crude product was obtained by evaporation of the solvent and purified by silica column chromatography (hexane/ethyl acetate changes gradually from 10:1 to 5:1). Yield: 25%, 1.36 g.

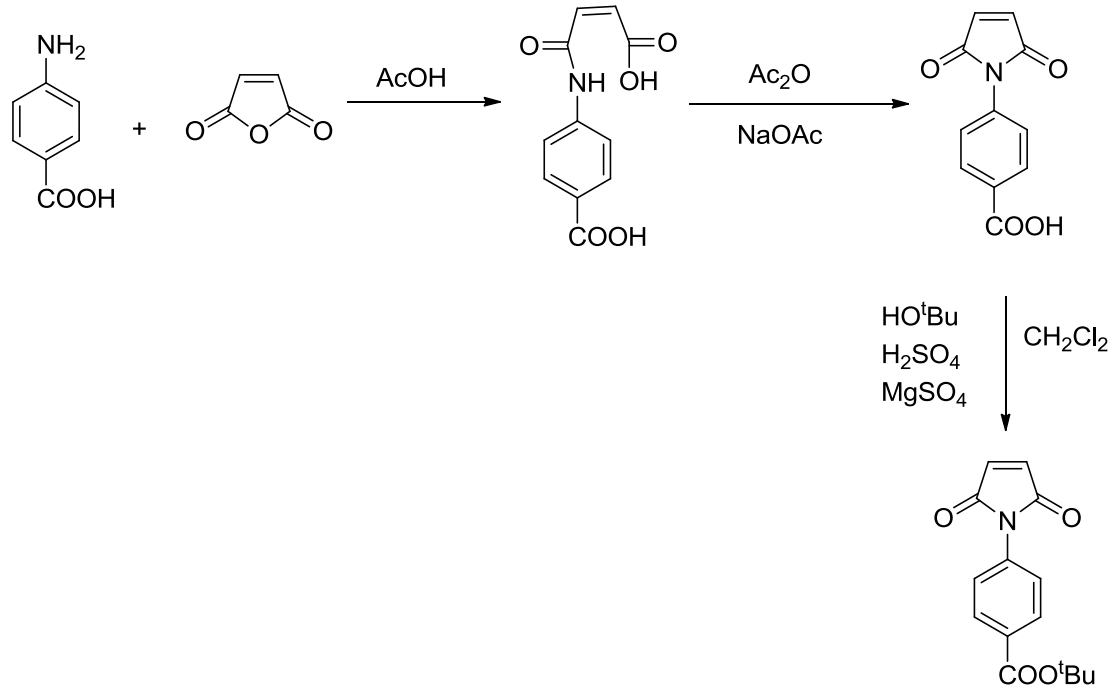

Scheme 2.7 Synthetic scheme of *tert*-Butyl 4-maleimidobenzoate with a low yield.

Unsuccessful routes

Route A

As shown in Scheme 2.8, 4-maleimidobenzoic acid (3.5 g, 16 mmol) was reacted with thionyl chloride (12 ml, 0.16 mol) at 40 ^oC for 6 h to afford 4-maleimidobenzoyl chloride.

The excess of thionyl chloride was stripped off by a stream of argon. Different reaction conditions were used, such as (a)-(d) in Scheme 2.8. In condition (a), to a round-bottomed flask equipped with a magnetic stirring bar and charged with 4-maleimidobenzoyl chloride (1.30 g; 5.5 mmol), a mixture of KO^tBu (6.6 mL, 6.6 mmol) in THF (8 mL) was added dropwise. After being reacted shortly at room temperature, the solution turned a dark color. After 24 h, the solution was washed with saturated $NaHCO_3$. THF was stripped off under vacuum and a dark oil was obtained. A messy ^1H NMR spectrum was observed for the crude product. The desired product could not be recognized or separated. In condition (b), to a round-bottomed flask equipped with a magnetic stirring bar and charged with 4-maleimidobenzoyl chloride (1.05 g; 4.5 mmol), a mixture of HO^tBu (0.5 mL, 5 mmol) and pyridine (0.9 mL, 0.11 mol) in CH_2Cl_2 (14 mL) was added dropwise. The solution turned a brownish color shortly. After 24 h, the solution was washed with saturated $NaHCO_3$. CH_2Cl_2 was stripped off under vacuum and dark oil was obtained. A very messy ^1H NMR spectrum was obtained. The desired product could not be recognized and separated. In condition (c), to a round-bottomed flask equipped with a magnetic stirring bar and charged with 4-maleimidobenzoyl chloride (1.05 g; 4.5 mmol), a mixture of HO^tBu (0.5 mL, 5 mmol) and proton sponge (2.3 g, 11 mmol) in CH_2Cl_2 (14 mL) was added dropwise. The solution turned a dark color shortly. The desired product could not be recognized from the ^1H NMR spectrum or separated. These unsuccessful reactions are probably due to the Michael addition of nucleophiles to the electron deficient double bond. As a result, the following strategies with protection of the double bond were attempted.

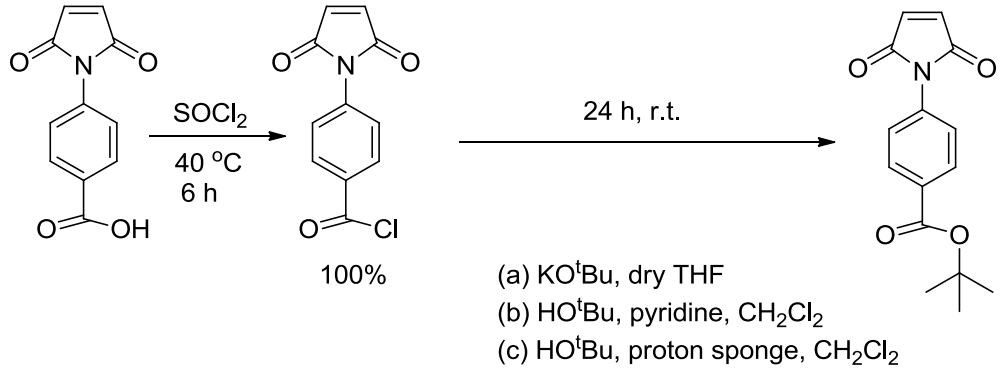

Scheme 2.8 Attempted synthetic schemes for *tert*-butyl 4-maleimidobenzoate.

Route B

The synthesis starts with Diels-Alder reaction of furan and 4-maleimidobenzoic acid to afford the adduct, Scheme 2.9.[8] To a round-bottomed flask equipped with a magnetic stirring bar and charged with a solution of 4-maleimidobenzoic acid (2.00 g; 9.2 mmol) in THF (7 mL), furan (5 mL) was added. After being reacted at room temperature for 24 h, the solution was concentrated under vacuum and precipitated in diethyl ether. The precipitate was collected and dried under vacuum for 24 h to yield a white solid. The ^{1}H NMR spectrum showed a mixture of the starting material 4-maleimidobenzoic acid and the desired adduct. Furan in larger excess was also tried to drive the reaction to completion. However, the starting material 4-maleimidobenzoic acid still showed up in the ^{1}H NMR spectrum.

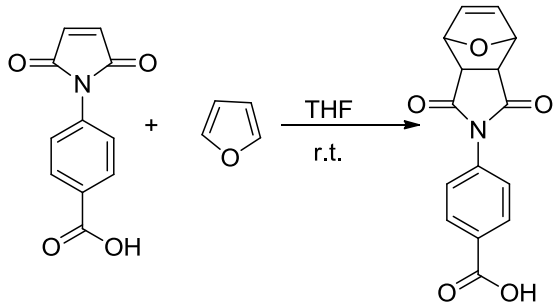

Scheme 2.9 Attempted synthetic scheme of protecting 4-maleimidobenzoic acid.

Route C

The synthesis starts with Diels-Alder reaction of furan and 4-maleimidobenzoyl chloride to afford the adduct, Scheme 2.10.[8] To a round-bottomed flask equipped with a magnetic stirring bar and charged with a solution of 4-maleimidobenzoyl chloride (2.00 g; 8.5 mmol) in dry toluene (7 mL), furan (5 mL) was added. After being reacted at room temperature for 24 h, the solution was concentrated under vacuum and dried in a vacuum oven for 24 h to yield a light yellow solid. Similar to the previous reactions, the ^{1}H NMR spectrum showed a mixture of the starting material 4-maleimidobenzoyl chloride and the desired adduct. Furan in larger excess was also tried to drive the reaction to complete. However the starting material 4-maleimidobenzoyl chloride still showed up in the ^{1}H NMR spectrum.

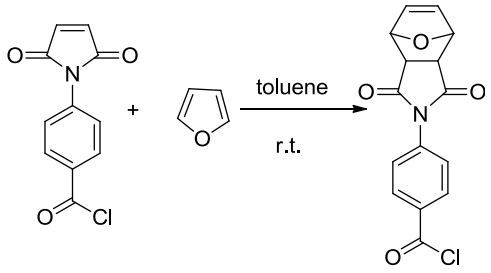

Scheme 2.10 Attempted synthetic scheme of protecting 4-maleimidobenzoyl chloride.

Route D

An alternative approach is to react the furan-maleic anhydride Diels-Alder adduct with 4-aminobenzoic acid, in Scheme 2.11.[8] 4-Aminobenzoic acid (1.64g, 12.0 mmol) was added to a solution of the furan-maleic anhydride Diels-Alder adduct (2.0 g, 12.0 mmol) in CH_3CN (8 mL). The solution was stirred at room temperature overnight to obtain a pure white powder, monomer (a). Monomer (a) was reacted acetic anhydride and sodium acetate at room temperature overnight. The solution was poured into water and extracted

with CH_2Cl_2 and concentrated under vacuum. No desire adduct monomer (b) was obtained. Most of the starting material monomer (a) remained unreacted.

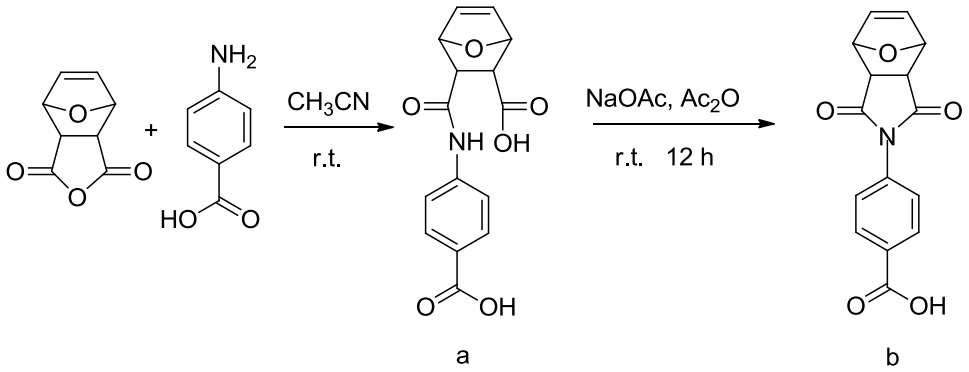

Scheme 2.11 Attempted synthetic scheme of protecting 4-maleimidobenzoic acid.

Route E

As shown in Scheme 2.12, 4-aminobenzoic acid (1.64g, 12.0 mmol) was added dropwise to a solution of the furan-maleic anhydride Diels-Alder adduct (2.0 g, 12.0 mmol) in THF (8 mL) under reflux. The solution was stirred under reflux overnight. The solution was concentrated under vacuum and washed with diethyl ether. The white product was dried under vacuum for 24 h. The ^1H NMR spectrum showed a mixture of the desired adduct and deprotected adduct.

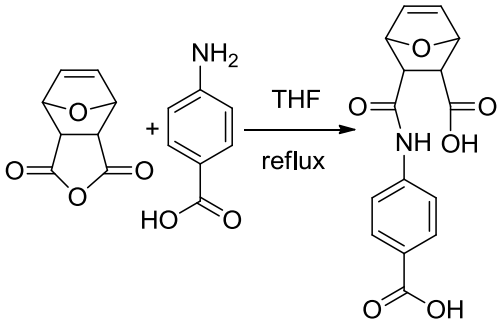

Scheme 2.12 Attempted synthetic scheme for protected 4-maleimidobenzoic acid.

2.3.3. Polymer Synthesis and Characterization

For copolymer III, the calculated isobutylene elimination is about 18.6% which is a little less than the found mass loss of 19.6%. This indicates that the styrene copolymer is not strictly alternating and its backbone may contain some TBVB-TBVB sequences. It is believed that the lower than calculated values of carbon percentage found by elemental analysis is due to the presence of some hydrolyzed enchained MAH units. If maleic anhydride units of copolymer III are all hydrolyzed, the calculated carbon percentage is 63.75. The found carbon percentage from elemental analysis is in between the hydrolyzed form and unhydrolyzed form of copolymer III (63.75 < 65.76 < 67.55), as shown in Table 2.5. This is consistent with part of copolymer III present in the hydrolyzed form. Our IR supports this by showing a low concentration of O-H stretch from hydrolyzed maleic anhydride units around 3400 nm^{-1}.

Table 2.5 Comparison of calculated carbon percentages for unhydrolyzed and hydrolyzed copolymer III with found values obtained by elemental analysis.

	Calculated C (%)	Found C (%)
unhydrolyzed copolymer III	67.55	N/A
Hydrolyzed copolymer III	63.75	N/A
elemental analysis	N/A	65.76

As shown in Scheme 2.13, to prepare copolymer V, a mixture of TEDAS (3.22 g 10.00 mmol), DMAPM (2.16 g, 10.0 mmol), chlorobenzene (18.4 mL, 20 wt %), DCP (0.0538 g, 1.0 wt %) were sealed in a 50-mL, septum sealed glass bottle equipped with a magnetic stirrer and was degassed by purging with argon for 20 min and polymerized for 24 h. Copolymers were recovered by precipitating into hexanes twice and then Soxhlet

extracted with hexanes to remove the residue monomers and dried under vacuum at 60 °C overnight before characterization.

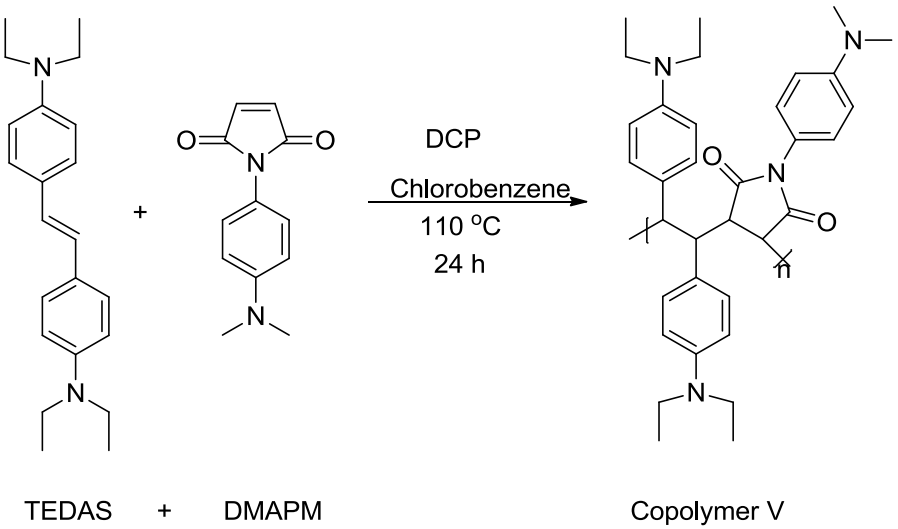

Scheme 2.13 Synthetic scheme for polycation precursors.

Amine functionalized copolymers can be easily dissolved into dilute hydrochloric acid-water solution and converted into polycations. The amine groups attached to the backbone can also be converted into quaternary ammonium groups by reacting with CH_3I (Scheme 2.14). For instance, copolymer V (0.60 g) was readily dissolved in dilute HCl solution (3.3 mL of 37% HCl). The polyanion was dried by freeze drying for 24 h on a Virtis lyophilizer.

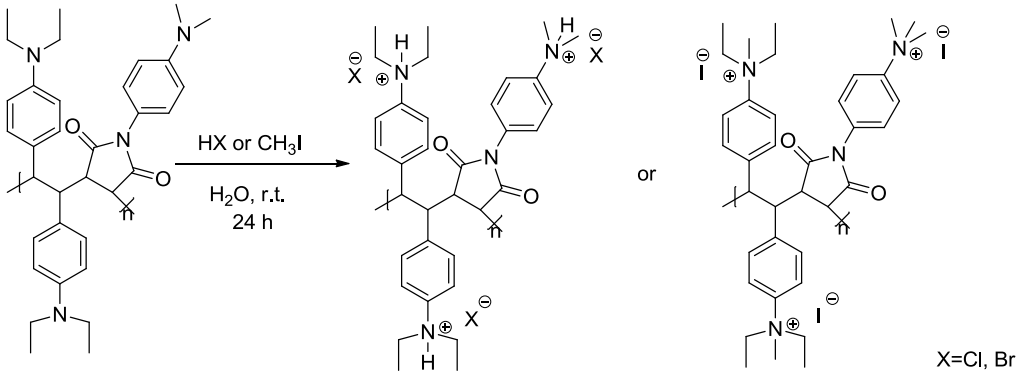

Scheme 2.14 Conversion of amine functionalized copolymer V into its corresponding polycation.

Table 2.6 Elemental analysis results for copolymer V-A.

	Calculated C (%)	Calculated H (%)	Calculated N (%)	Found C (%)	Found H (%)	Found N (%)
copolymer V	75.70	7.79	10.39	73.66	7.47	10.50

Table 2.7 Comparison of yields and molecular weights under condition A (chlorobenzene-DCP-110 ^{o}C) and condition B (THF-AIBN-60 ^{o}C).

	Yield (%)	M_n (kg/mol)	M_w/M_n
copolymer V-A	59	42.7	1.82
copolymer V-B	20	5.10	1.34

Table 2.8 Typical yields and molecular weights of copolymer V under optimized copolymerization conditions.

	Condition	Reaction duration (h)	Yield (%)	M_n (kg/mol)	M_w/M_n
copolymer V	A	24	59	42.7	1.82

Copolymers were precipitated in hexanes from THF, followed by a Soxhlet extraction to yield white powders. The ^{1}H NMR spectrum did not indicate any residual monomers after the extraction, as shown in Figure 2.12.

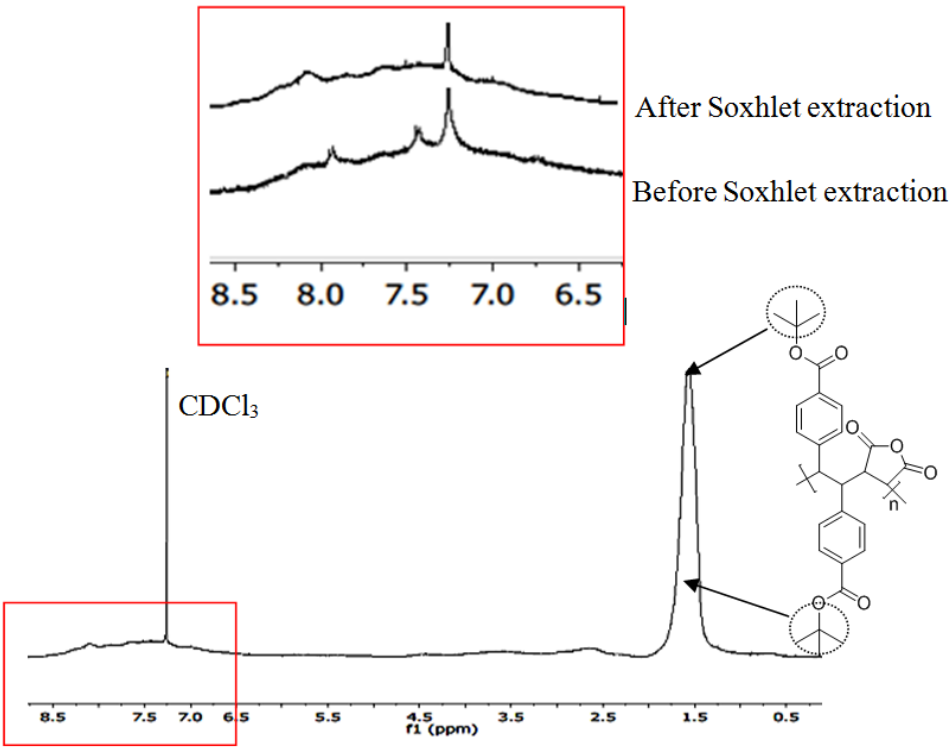

Figure 2.12 Comparison of ^{1}H NMR spectrum of copolymer I before and after Soxhlet extraction.

The initiator concentration can impact the polymerization rate as rate of polymerization is proportional to $[I]^{1/2}$

$$Rate \propto [I]^{1/2} \tag{2.1}$$

Where $[I]^{1/2} \propto$ (weight of initiator / molar mass of initiator)$^{1/2}$, as shown in eq. (2.2).

$$[I]^{1/2} \propto \left(\frac{Weight}{Molar\ Mass}\right)^{1/2} \tag{2.2}$$

Even though initiators are at the constant ratio of 1 wt % to monomers, molar masses of AIBN and DCP are 164 g/mol and 270 g/mol, respectively. With the same weight of initiators, the calculated $[I]^{1/2}$ of AIBN is 1.28 times of $[I]^{1/2}$ of DCP. Therefore, with the same monomer concentrations and the same initiator weights, the polymerization rate with AIBN is 1.28 times of the polymerization rate with DCP. It is believed that the

factor 1.28 is not the main reason for the large differences in yields as shown in Table 2.4.

As a result, other reasons were taken into account as stated previously.

REFERENCES

(1) Rich, D. H.; Gurwara, S. K. *J. Am. Chem. Soc.***1975**, *97*, 1575.
(2) Broos, R. *J. Chem. Educ.***1978**, *55*, 813.
(3) Ishizone, T.; Tsuchiya, J.; Hirao, A.; Nakahama, S. *Macromolecules* **1992**, *25*, 4840.
(4) Taylor, E. C.; Fletcher, S. R.; Sabb, A. L. *Synth. Commun.* **1984**, *14*, 921.
(5) Zhang, X.; Li, Z.-C.; Wang, Z.-M.; Sun, H.-L.; He, Z.; Li, K.-B.; Wei, L.-H.; Lin, S.; Du, F.-S.; Li, F.-M. *J. Polym. Sci. Part A: Polym. Chem.* **2006**, *44*, 304.
(6) Wright, S. W.; Hageman, D. L.; Wright, A. S.; McClure, L. D. *Tetrahedron Lett.* **1997**, *38*, 7345.
(7) Sauers, C. K. *J. Org. Chem.* **1969**, *34*, 2275.
(8) Wang, Z.; Olsen, P.; Ravikumar, V. T. *Nucleosides Nucleotides Nucleic Acids* **2007**, *26*, 259.

Chapter 3. CHAIN STIFFNESS OF STILBENE CONTAINING ALTERNATING COPOLYMERS BY SAXS AND SEC

(Li, Y.; Zhang, M. Q.; Mao, M.; Turner, S. R.; Moore, R. B.; Mourey, T.; Slater, L. A.; Hauenstein, J. R. *Macromolecules* **2012**, *45*, 1595. Additional information added)

3.1. ABSTRACT

Persistence lengths of stilbene- and styrene-containing alternating copolymers were measured using small-angle X-ray scattering (SAXS) and size-exclusion chromatography (SEC). For SAXS measurements, a graphical approach and the Sharp and Bloomfield methods were used to quantify the chain stiffness. For SEC measurements, the Bohdanecký linear approximation was applied to determine persistence lengths. The complementary results obtained from SAXS approaches as well as from SEC measurements characterized stilbene copolymers as a class of semi-rigid polymers with persistence lengths in a range of 2 to 6 nm. The stilbene copolymers are more rigid than their styrene analogs.

3.2. INTRODUCTION

Even though a large amount of research has been done to determine the structure-property relationships of polyelectrolytes, it is still hard to fully comprehend.[1-3] Rigid polymers are envisioned to simplify studies of polymer interactions because the conformational changes of a flexible polymer backbone are reduced or eliminated.[4-9] Sterically crowded polymeric structures arising from the use of substituted stilbene comonomers, enchained maleic anhydride or maleimide comonomers in an alternating

sequence, are anticipated to stiffen the backbone.[10-20] In addition the rich synthetic chemistry available for stilbenes makes the preparation of a variety of functional stilbene derivatives possible, which opens up interesting families of new polyelectrolytes and other functional copolymers for study. Our previous studies using the solid-state NMR torsional angle measurements of the maleic anhydride units in a *N, N, N', N'*-tetraethyl-4, 4'-diaminostilbene (TDAS)-maleic anhydride (MAH) alternating copolymer were enchained in a predominately *cis* configuration. This produced a highly contoured polymer chain.[12] We also observed that a block copolymer containing a TDAS-MAH polyampholyte block and a poly(methoxy-capped oligo-(ethylene glycol)methacrylate) block exhibited polyion complexes (PICs) with unusual pH and salt responsive properties similar to the "like-charge" attraction effects in rigid polyelectrolytes.[10] In addition films of the alternating copolymers of stilbene and *N*-(2-methylphenyl)maleimide were found to have a very strong negative birefringence and the corresponding alternating copolymers of styrene and *N*-(2-methylphenyl)maleimide did not show this effect. This significant difference is likely due to conformational constraints arising from the extra phenyl rings of enchained stilbene-maleic anhydride units.[21]

To confirm the steric crowding effect and quantify the chain stiffness of the alternating stilbene copolymers, a functionalized stilbene monomer with *tert*-butyl carboxylate groups on the 4,4'-position and an *N*-phenylmaleimide monomer functionalized with *tert*-butyl carboxylate on the 4-position have been prepared. Analogous styrenic copolymers have also been prepared for direct comparison to the stilbene structures. To obtain persistence lengths of the polymers, both SEC analysis and SAXS were performed. The

effect of the extra phenyl group along the backbone in the stilbene copolymers has on the chain stiffness was directly compared to the single phenyl ring (from styrene).

3.3. EXPERIMENTAL SECTION

3.3.1. Materials

Maleic anhydride (MAH, Aldrich, ≥99.0%), potassium *tert*-butoxide solution 1.0 M in tetrahydrofuran (KO^tBu, Aldrich), *tert*-butanol (HO^tBu, Sigma-Aldrich, anhydrous, ≥99.5%), *N*-bromosuccinimide (NBS, Aldrich, 99%), *p*-toluic acid (Aldrich, 98%), formaldehyde (Aldrich, 37 wt. % in H_2O), triphenylphosphine (Sigma-Aldrich, 99%), thionyl chloride ($SOCl_2$, Fluka, ≥99.0%), acetic anhydride (Sigma-Aldrich, ≥98.0%), sodium acetate (Sigma-Aldrich, ≥99.0%), *4*-aminobenzoic acid (Sigma, ≥99.0%), *2,2*'-azobisisobutyronitrile (AIBN, Aldrich, 98%), dicumylperoxide (DCP, Aldrich, 98%), sodium hydroxide (NaOH, Sigma-Aldrich, ≥98.0%) were used as received. (*E*)-Dimethyl *4,4'*-stilbenedicarboxylate (DMSC) was received as a donation from Eastman Chemical Company. Tetrahydrofuran (Sigma-Aldrich, anhydrous, ≥99.9%), hexanes (Fisher, HPLC grade), methylene chloride (CH_2Cl_2, Fisher, HPLC grade), diethyl ether (Fisher, HPLC grade), toluene (Fisher, HPLC grade), chlorobenzene (Sigma-Aldrich, anhydrous, ≥99.8%), benzene (Sigma-Aldrich, anhydrous, ≥99.8%), and acetone (Fisher, HPLC grade) were used without further purification. Water was deionized before use.

Stilbene and styrenic copolymers were synthesized via free radical polymerization.[22] Structures of copolymer I, II, III and IV are shown in Figure 3.1. Copolymer I was synthesized from *tert*-butyl 4-vinylbenzoate and maleic anhydride and copolymer III was composed of *tert*-butyl 4-vinylbenzoate and *tert*-butyl 4-maleimidobenzoate.[22] Copolymer II was synthesized from (*E*)-di-*tert*-butyl 4,4'-stilbenedicarboxylate and

maleic anhydride and copolymer IV was prepared from (*E*)-di-*tert*-butyl 4,4'-stilbenedicarboxylate and *tert*-butyl 4-maleimidobenzoate. The (*E*)-di-*tert*-butyl 4,4'-stilbenedicarboxylate was prepared from (*E*)-dimethyl 4,4'-stilbenedicarboxylate via a transesterification reaction;[22] maleic anhydride was purchased from Sigma-Aldrich; *tert*-butyl 4-maleimidobenzoate was synthesized from 4-aminobenzoic acid in 4 steps[22,23] and *tert*-butyl 4-vinylbenzoate was prepared from *p*-toluic acid in 6 steps.[24-27] Copolymers II and IV were synthesized at 110 ^{o}C for 24 h with dicumylperoxide as initiator and chlorobenzene as solvent.[24] Copolymers I and III were prepared at 60 ^{o}C for 4 h with AIBN as the initiator and tetrahydrofuran (THF) as the solvent.[24] For example, a mixture of (*E*)-di-*tert*-butyl 4,4'-stilbenedicarboxylate (3.80 g 10.0 mmol), *tert*-butyl 4-maleimidobenzoate (2.73 g, 10.0 mmol), chlorobenzene (23.5 mL, 20 wt %), DCP (0.0653 g, 1.0 wt %) was sealed in a 50-mL, septum sealed glass bottle equipped with a magnetic stirrer and was degassed by purging with argon for 20 min and polymerized for 24 h. All copolymers were recovered by precipitating into hexanes twice to remove the residual monomers and dried under vacuum at 60 °C overnight before characterization. The purity of samples was verified by ^{1}H NMR and proved to be sufficiently high for the present purpose. Molecular weights and their distributions for copolymers I and II (Table 3.1) were determined using *N, N*-dimethylformamide (DMF) containing 0.1 M lithium nitrate and 1% formic acid as eluent to avoid a small amount of maleic anhydride unit in acid form from interacting with the SEC columns. Molecular weights and their distributions of copolymers III and IV were determined using THF as eluent solvent. Absolute weight-average molecular weights are most accurately measured by light scattering detection, whereas absolute number-average molecular weights are normally

better measured by viscometry detection and a universal calibration curve because the viscometry detector is more sensitive in the low-molecular weight region of chromatograms than is the light scattering detector in Table 3.1.

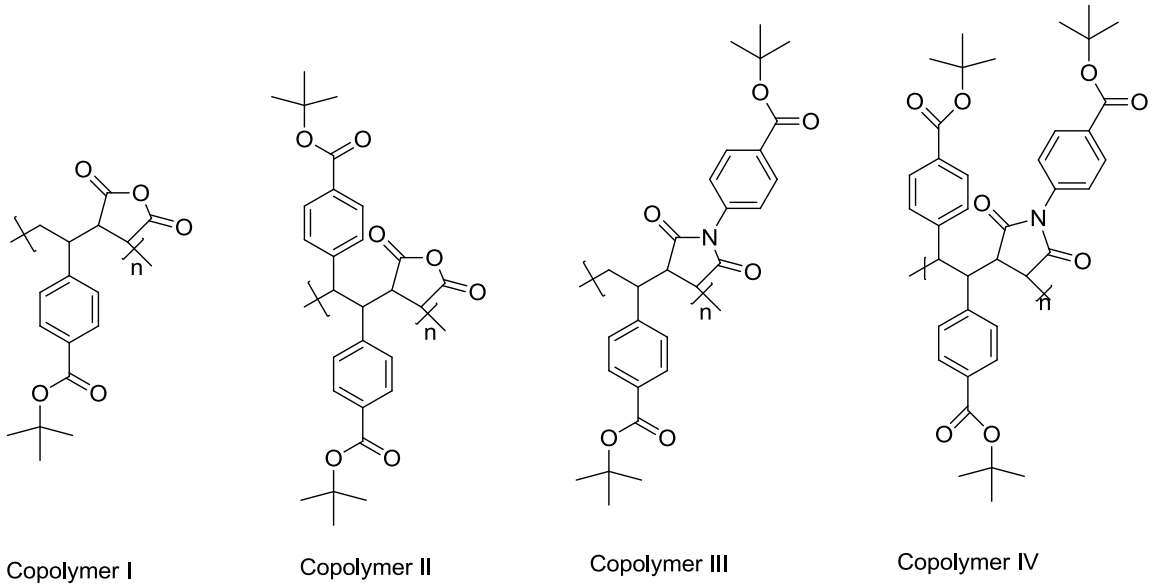

Figure 3.1 Chemical structures of copolymers I, II, III, and IV.

Table 3.1 Molecular characteristics of copolymers I, II, III, and IV.

	M_n (kg/mol)[c]	M_w (kg/mol)[d]
copolymer I[a]	41.1	64.6
copolymer II[a]	73.0	163
copolymer III[b]	60.3	154
copolymer IV[b]	97.2	225

[a.]SEC in DMF containing 0.1 M lithium nitrate and 1% formic acid; [b.]SEC in THF; [c.] Viscometry detection/universal calibration; [d.] Light scattering detection

3.3.2. Instrumentation

Small-*angle X-ray scattering*. SAXS experiments were performed using a Rigaku S-Max 3000 3 pinhole SAXS system, equipped with a copper rotating anode emitting X-rays with a wavelength of 0.154 nm (Cu K_α). Two-dimensional SAXS patterns were obtained using a fully integrated 2D gas-filled multiwire, proportional counting detector,

and with an exposure time of 1 hour. All SAXS data was analyzed using the SAXSGUI software package to obtain radically integrated SAXS intensity versus scattering vector q (SAXS), where $q=(4\pi/\lambda)\sin(\theta)$, θ is one half of the scattering angle and λ is the wavelength of X-rays. For all scattering experiments, the sample-to-detector distance was 1603 mm, and the q-range was calibrated using a silver behenate standard.

SAXS measurements were carried out on 1.0 wt % concentrations of polymer in DMF containing 0.1 M lithium nitrate and 1% formic acid for copolymers I, II, and in DMF for copolymers III, IV. Solution samples were measured in thin-walled capillary tubes with a diameter of 1.5 mm and wall thickness of 0.01 mm. The measured intensity was corrected for sample transmission, solvent scattering and background (capillary) scattering.

Size-exclusion chromatography. Copolymers I and II were examined at 35.0 °C using three 7.5 mm x 300 mm Plgel Olexis columns from Agilent Technologies. DMF containing 0.1M lithium nitrate and 1% formic acid was used as the eluent, and the column set was calibrated with narrow-molecular-weight distribution poly(methyl methacrylate) (PMMA) standards. Instrumentation consisted of an Agilent 1100 series isocratic pump, autosampler and UV-Visible absorption detector, Agilent PD2020 (formerly Precision Detectors) 15 and 90 degree elastic light scattering detector, Malvern 270 (formerly Viscotek) differential viscometry detector, and a Waters 410 differential refractive index detector plumbed in parallel with the differential viscometry detector. Uninhibited HPLC-grade THF was used as the SEC eluent for copolymers III and IV containing maleimide units. Three 7.5 mm x 300 mm Agilent PLgel mixed-C columns thermostated at 35.0 °C were calibrated with narrow-molecular-weight distribution

polystyrene standards. The solvent delivery and sample management system and UV-visible detector were Waters models 2695 and 2487, respectively. The light scattering, viscometry and refractive index detectors and their configuration were similar to those described above for the DMF system. Flow rates were nominally 1.0 mL/min and were corrected using the retention volume of acetone added to the sample solutions as a flow marker. All injection volumes were 0.1 mL and sample concentrations were between 1 and 2 mg/mL.

Persistence length can be estimated from the multi-detector SEC using intrinsic viscosity, $[\eta]$, and molar mass, M, conformation plots as well as from the relationship between molar mass, M, and radius of gyration, R_g. The lower measurable size limit for the 680 nm wavelength of incident light used in our SEC light scattering detector is $R_g \sim$ 10 nm, which greatly restricts that range of accessible M-R_g data for the polymers examined in this study. In comparison, intrinsic viscosity can be measured at lower molar masses and across a broader molar mass range than light scattering detection for these samples, making $[\eta]$-M conformation plots a desirable alternative to R_g-M plots.[28] Hence, for copolymers I, II, III, and IV intrinsic viscosity measured by the differential viscometry detector was combined with molar mass measured by light scattering detection at each data point along chromatograms to determine the persistence lengths.

3.4. Results and Discussion

3.4.1. Measurement of persistence length by SAXS

The SAXS measurement is typically used to probe polymer dimensions on the order of 10 Å or larger. Structural information on this order usually is contained in the intensity of the scattered X-rays at small angles (usually the scattering angle 2θ smaller than 2°). The

reciprocity between d and q, $q=2\pi/d$, indicates that a relatively large distance, d, on a particle can be examined at the scattering intensity $I(q)$ obtained at relatively small scattering vector q (q is directly related to the scattering angle θ).

It was found that a scattering pattern is shape dependent, i.e., a particle shape can determine the relationship between $I(q)$ and q. To study the shape effect, an independent scattering study was performed on particles with simple geometric shape, such as spheres (three dimensional), thin rods (one dimensional) and thin circular disks (two dimensional). It was found this shape effect at high q can be simplified to express by[29]

$$I(q) \sim q^{-\alpha} \tag{3.1}$$

where the exponent α is equal to 4 for spheres, 1 for thin rods and 2 for circular thin disks. The exponent α is used to reflect the dimensionality of the object. As for the dimensionality of a polymer chain in solution, a strongly self-attracting chain would pack itself into a ball and make into a sphere shape with a scattering pattern $I(q)\sim q^{-1}$; a strong self-repelling chain would stretch out into a completely extended rod with a scattering pattern $I(q)\sim q^{-1}$; a Gaussian chain behaves like a two-dimensional object and thus the corresponding scattering pattern exhibits $I(q)\sim q^{-2}$.[29]

For stiff and semi-rigid macromolecules, Kratky and Porod proposed a chain model denoted as the "wormlike or Kratky-Porod chain model", which examines a real polymer chain in a simple way: in the smallest scale, atoms on a polymer chain are recognized; as the scale increases, a short sequence of monomeric units are exhibited; as the scale increases further, a longer sequence of the polymer chain is recognized, which resembles more or less a rigid-rod; on an even larger length scale, the whole polymer chain is recognized as behaving like a Gaussian chain.[30,31] The persistence length, l_p, was

introduced in this process by Kratky and Porod to reflect the stiffness of a polymer chain. The persistence length, l_p, is defined as the distance at which the projection of the averaged end-to-end vector onto the first bond direction does not vanish but rather approaches a finite limit.[29] L_k is the Kuhn length, first developed by W. Kuhn in 1934.[32] In general, $2l_p=L_k$[33-35], where the persistence length, l_p, can be estimated in a SAXS experiment, as briefly discussed below. A scattering plot of $I(q)$ vs. q can be divided into different regions that probe various length scales associated with different dimensions of a polymer chain. Based on theoretical predictions for a sufficiently long chain (a Gaussian chain),[36] two characteristic regions may be observed: at small q, the scattering pattern reflects the random coil nature of a polymer chain, and is expressed by the Debye function, where $I(q)\sim q^{-2}$ is valid;[37] as q is increased, the scattering pattern is governed by the behavior of small sections of the polymer chain and exhibits $I(q)\sim q^{-1}$ characteristic of rigid rods. The difference between these two scattering patterns is even more pronounced when plotting $I(q)q^2$ against q. A "Kratky-Porod" plot of an ideal wormlike chain model is composed a horizontal line representative of the Debye behavior and a sloped straight line representative of the q^{-1} region.[29] Similar to of a $I(q)$ vs. q plot, an intersection of these two regions defines the persistence length. To determine the persistence length, it is customary to use a log-log plot of $I(q)$-q or to use a "Kratky-Porod" plot in which two regions are matched with lines having different slope values. An extrapolation of the intersection of these two linear regions at a value q^* is related to the persistence length by

$$l_p = A / q^* \tag{3.2}$$

where the constant A is derived from computations. Porod gave $A=6/\pi=1.91$ for Gaussian coils.[38,39] It is very common to use this value 1.91 in determination of

persistence lengths, as reported in several articles.[40-43] However, there is a limitation on this value 1.91. That is 1.91 usually fits the case where the polymer chain is infinite long or very large (usually over 100 times of its persistence length).[36] Since our copolymers are not infinite long or very large, it is not appropriate to use 1.91 as the constant A value to determine the persistence lengths of copolymers I, II, III, and IV. By use of a Monte-Carlo technique for coils with finite sizes (usually between 16~100 times of corresponding persistence lengths), A=2.3 was suggested as a more accurate approximation for the non-Gaussian chains.[44-46] In this work, the value of 2.3 has been used for determination of persistence lengths.

In fact, for non-Gaussian coils, the ideal situation of two distinctly different linear regions having q^{-2} and q^{-1} scaling in the SAXS data is not often fulfilled. Various authors[36,40,43,47-50] have reported that the ideal slope = -2 region did not appear at small q in scattering measurements; rather, the power law was generally less than -2 in the Debye region and a change in slope of two characteristic regions was observed.[36,40,43,47-50] Cleland in 1977 reported that the persistence length of hyaluronic acid estimated by SAXS in 0.05 M HNO_3 was 4 to 6 nm with two characteristic regions observed in the scattering plot. However, the scattering pattern obtained with 0.2 M NaCl showed a deviated form in low q region with no observation of $I \sim q^{-2}$.[47] It was stated that the ionization of the polymer with NaCl solution might result in a stretching of the persistent elements. It was reported by Gupta et al. that Kratky-Porod plots of cellulose tricarbanilate determined in dioxane and at different temperatures, did not exhibit the horizontal region (q^{-2} region) due to the finite molecular weights of cellulose tricarbanilate.[48] Instead there was a change in the two regions with different slopes and it

was used to estimate the persistence length.[48] Solutions of poly(2-methoxy-5-(2'-ethyl-hexyloxy)-1,4-phenylene vinylene) (MEH-PPV) were studied by Choudhury et al. using SAXS in different solvents. It was stated that the horizontal region (q^{-2} region) observed in xylene was not observed in THF, which was attributed to the interactions of MEH-PPV side groups with THF solvent.[40] Therefore, the scattering pattern generated by SAXS can be affected by many factors, like molecular weight, solvent, solution concentration, temperature, etc.

In order to determine the persistence lengths of copolymers I, II, III, and IV, different solvents were used in the SAXS measurements. As shown in Figure 3.2, THF was first used as solvent and there was only one region observed with a slope of about -1.2 and the scattering pattern absent of the two characteristic regions. Copolymers I, II, III, and IV have similar scattering patterns with THF as solvent. It is likely polymer chains are interacting with the THF solvent and this facilitates the formation of compact coils. When using DMF as solvent, as shown in Figure 3.3, the expected -1 region was obtained from the scattering data for copolymers I, II, III, and IV in the form of an $I(q)$-q plot. Due to the finite molecular weights of these samples, the -2 region corresponding to the Debye function was not observed. However, a change of slope in the two regions was observed. The deviation from -2 in the Debye region resulted in a non-horizontal line in the corresponding "Kratky-Porod" plot (Figure 3.4), which does not facilitate the determination of q^*. Only log-log plots of $I(q)$-q were used. The data in common ranges both in low q range (0.030-0.052) and in high q range (0.075-0.2) were used to determine the persistence lengths of copolymers. This allows the determination of persistence lengths by eq. (3.1), shown in Table 3.2.

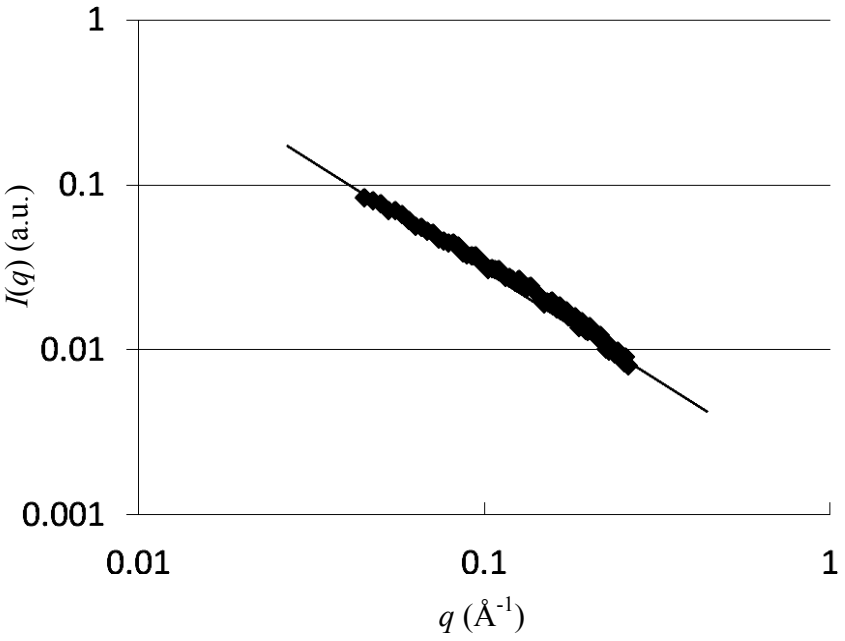

Figure 3.2 Representative scattering pattern of copolymer IV in THF.

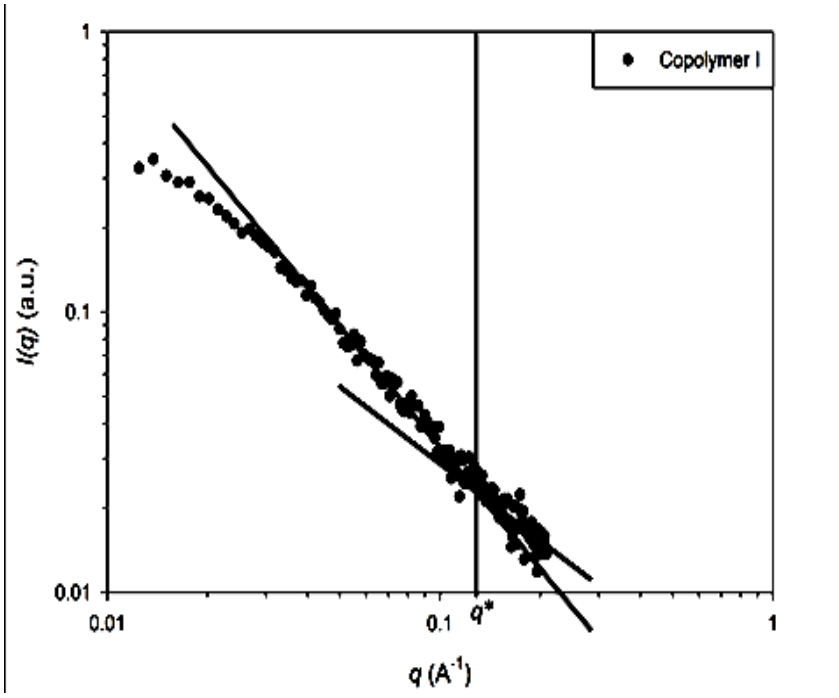

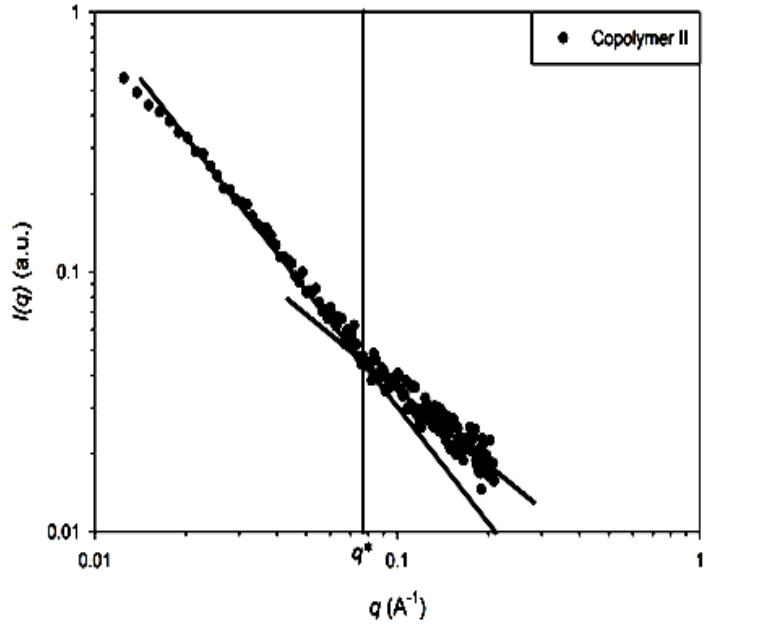
Copolymer II
I(q) (a.u.)
1
0.1
0.01
0.01
q*
0.1
1
q (A-1)

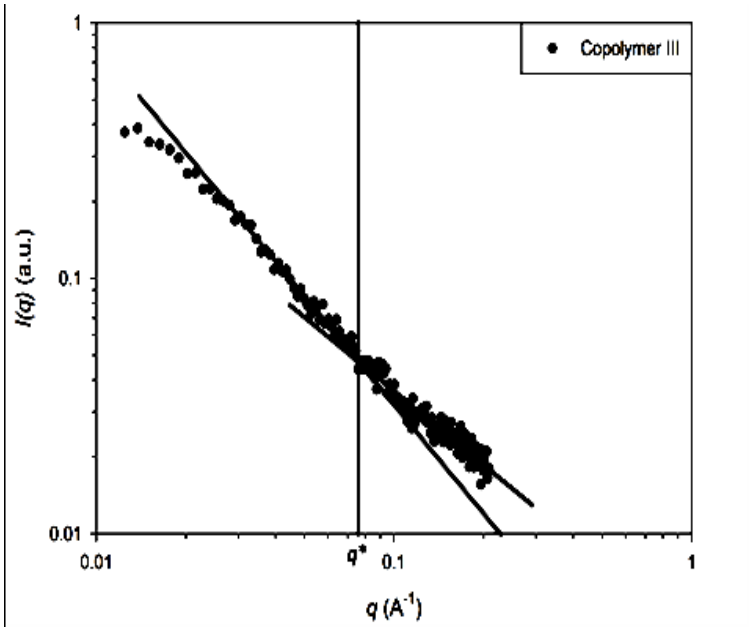
Copolymer III
I(q) (a.u.)
1
0.1
0.01
0.01
q*
0.1
1
q (A-1)

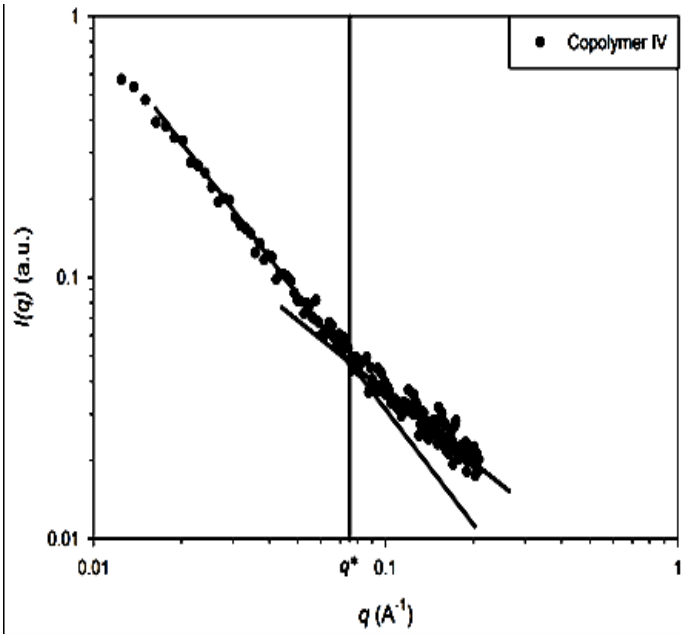

Figure 3.3 *I(q)* vs. *q* plots for copolymers I, II, III, and IV. The fit range includes all of the data points. Every fifth data point is selected to plot for clarity.

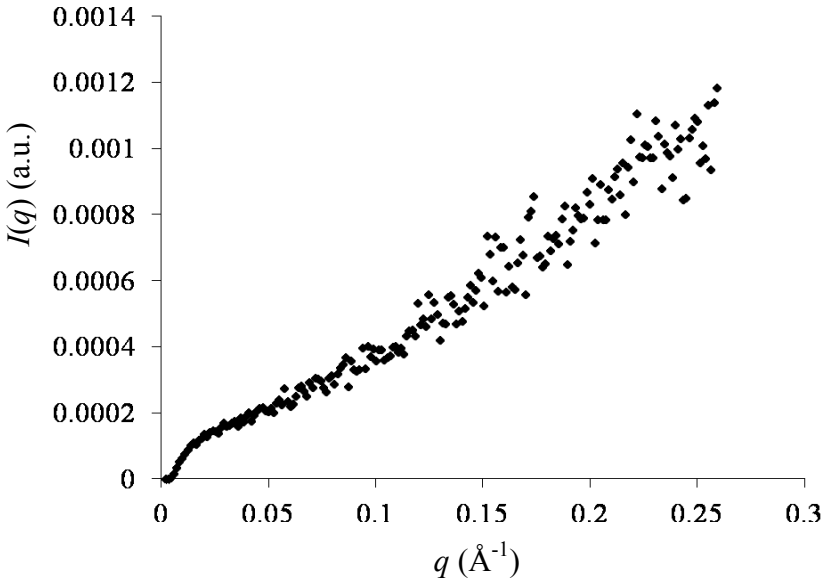

Figure 3.4 "Kratky-Porod" plot of copolymer IV.

Table 3.2 Results from SAXS measurements for copolymers I, II, III, and IV.

	q^* (Å^{-1})	l_p by eq. (1) (nm)
copolymer I	$10^{(-0.86\pm0.58)}$	$2.3*10^{(0.86\pm0.58)}$
copolymer II	$10^{(-1.11\pm0.11)}$	$2.3*10^{(1.11\pm0.11)}$
copolymer III	$10^{(-1.13\pm0.11)}$	$2.3*10^{(1.13\pm0.11)}$
copolymer IV	$10^{(-1.12\pm0.13)}$	$2.3*10^{(1.12\pm0.13)}$

The data in Table 3.2 confirms that copolymer I is less stiff than copolymer II. The rising trend of the chain stiffness from copolymer III to IV is not very obvious. This may be attributed to the uncertainties inherit in the graphical approach. Similar to the plots in Figure 3.3, most of the scattering curves exhibit a gradual transition between the two regions.[36,40,43,47-50] This makes the graphical determination of persistence lengths subject to some ambiguities.[36] To solve this problem, different analytical approaches were introduced to accurately determine the persistence length.[36,43,51,52] The most widely used method was developed by Sharp and Bloomfield[43,51] and corrected by Schmid[53]

$$I(q) = G_2\{g_D(x) + \frac{2l_p}{L}[\frac{4}{15} + \frac{7}{15x} - (\frac{11}{15} + \frac{7}{15x})e^{-x}]\} \tag{3.3}$$

with

$$g_D(x) = 2\frac{e^{-x} + x - 1}{x^2} \tag{3.4}$$

where $x=(Ll_pq^2)/3$, L is the contour length, $L=2l_pN_k$, N_k is the number of Kuhn segments per chain and G_2 in eq. (3.4) is the Debye prefactor. A least-squares fit of the data in the entire q range was performed using the Sharp and Bloomfield function (SBF). Since the scattering data were not corrected to absolute intensity values, the prefactor G_2' is treated as an undefined fitting constant and not reported here. The results of fitting variables l_p, N_k are listed in Table 3.3 and the fitting curves are shown in Figure 3.5.

Table 3.3 Parameters of Sharp and Bloomfield function for copolymers I, II, III, and IV.

	N_k	l_p (nm)
copolymer I	7.62±0.17	2.7±0.040
copolymer II	11.7±0.19	3.6±0.036
copolymer III	7.53±0.10	3.4±0.032
copolymer IV	11.2±0.15	4.0±0.034

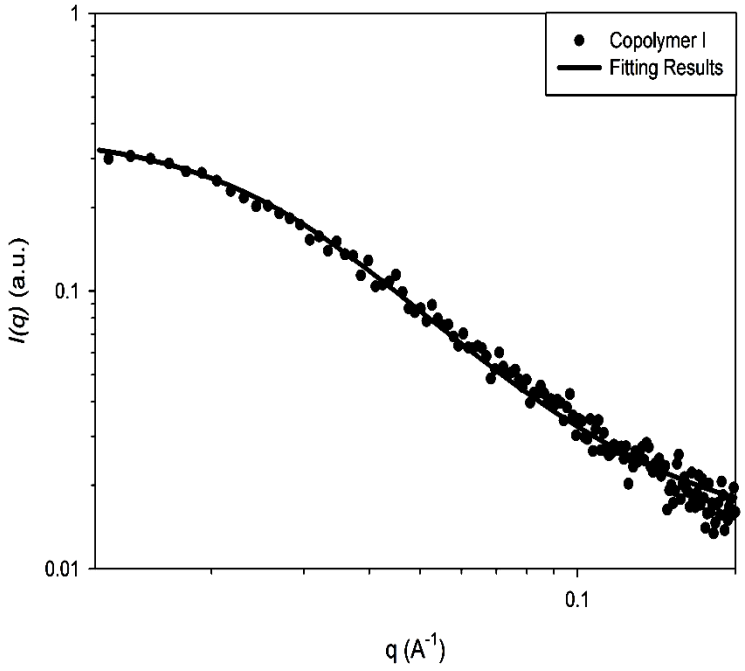

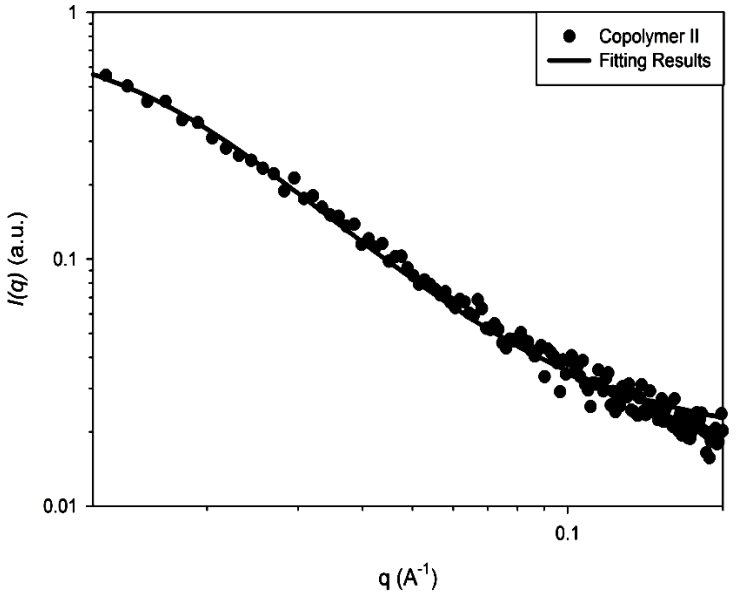

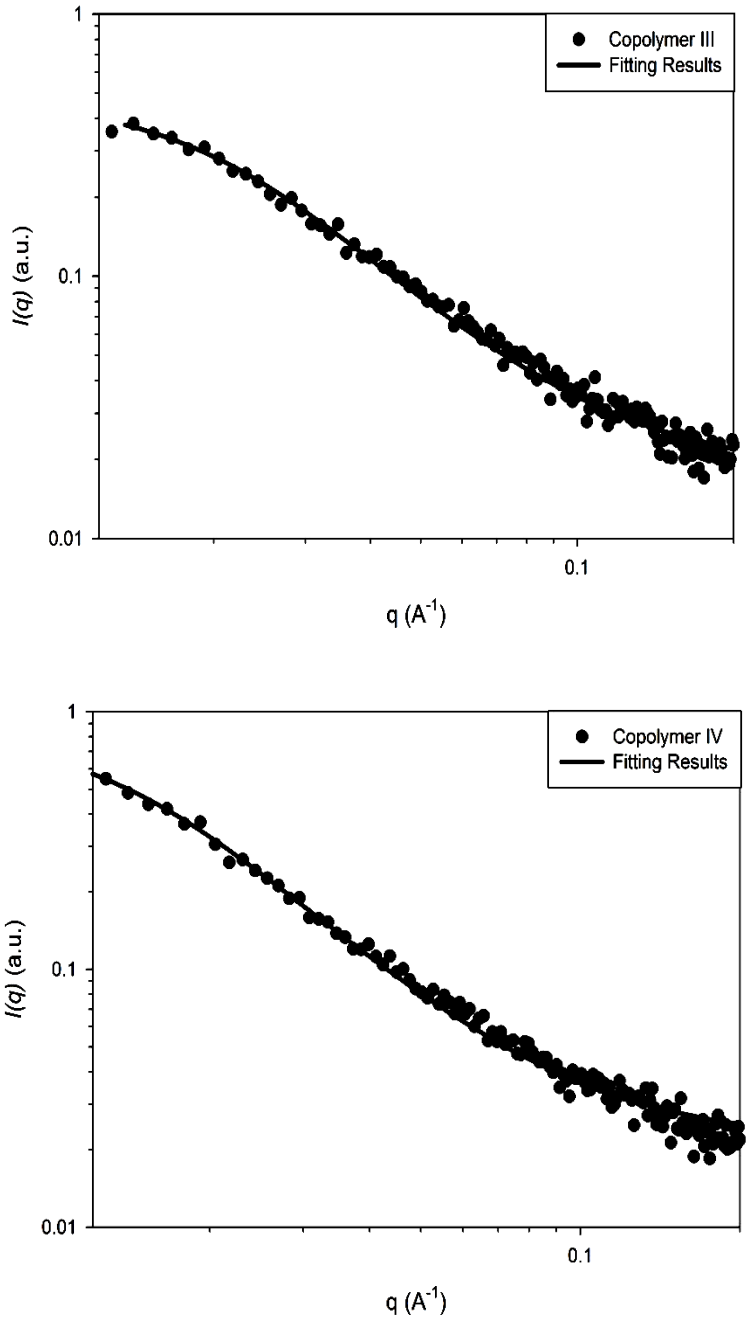

Figure 3.5 Sharp and Bloomfield fits to the data of Figure 3.3. The fit range includes all of the data points. Every fifth data point is selected to plot for clarity.

Another fitting approach used to determine the persistence length is the unified function.[43,54-56] Beaucage et al. stated that a major contribution of this approach is in

describing the transition between two scattering patterns.[43,54-56] This unified approach is given by[43]

$$I(q) = \{G_2 e^{-\left(q^2 R_{g2}{}^2\right)/3} + B_2 e^{-q^2 l_p{}^2/3}\left(q_2^*\right)^{-2}\} + \{G_1 e^{-\left(q^2 R_{g1}{}^2\right)/3} + B_1\left(q_1^*\right)^{-1}\} \tag{3.5}$$

where

$$q_i^* = [\frac{q}{\{erf(qkR_{gi}/\sqrt{6})\}^3}] \tag{3.6}$$

K ≈ 1.06.[43] In eq. (3.5), the term in the first bracket refers to the Debye region in a scattering pattern while the term in the second bracket represents the rod-like region. For a Gaussian chain

$$(R_{g2,Gaussian})^2 = \frac{N_k (2l_p)^2}{6} \tag{3.7}$$

for the non-Gaussian exponent α

$$R_{g2}{}^2 = \frac{N_k{}^{2/d_f} (2l_p)^2}{(1+2/\alpha)(2+2/\alpha)} \tag{3.8}$$

for a Gaussian chain

$$R_{2,Gaussian} = \frac{2G_2}{R_{g2}{}^2} \tag{3.9}$$

for the non-Gaussian exponent α

$$B_2 = \frac{G_2}{R_{g2}{}^\alpha}\Gamma(\alpha/2) \tag{3.10}$$

where G_2 is the Debye prefactor for the Debye behavior. R_{g2} is the coil's radius of gyration. G_1 in eq. (3.5) is G_2/N_K.[43] R_{g1} is defined as

$$R_{g1} = \frac{l_p}{\sqrt{3}} \tag{3.11}$$

B_1 is defined for a rod as

$$B_1 = \frac{\pi G_1}{2 l_p} \tag{3.12}$$

A least-squares fit of the data using the unified function can describe Gaussian chains in terms of three parameters: the Debye factor G_2, the persistence length l_P, and the number of Kuhn segments N_K. Additionally, non-Gaussian chains can be also described with the exponent α. The fitting results in terms of the persistence lengths of copolymers I, II, III, and IV obtained from the unified function are in a range of 4~7 nm. The persistence lengths are generally larger with higher deviations (±0.1~±0.3), when compared to those obtained from the SBG approach. The fitting curve for copolymer IV is shown below. For copolymers I, II, III, and IV, the SBG approach may be a more appropriate fitting approach.

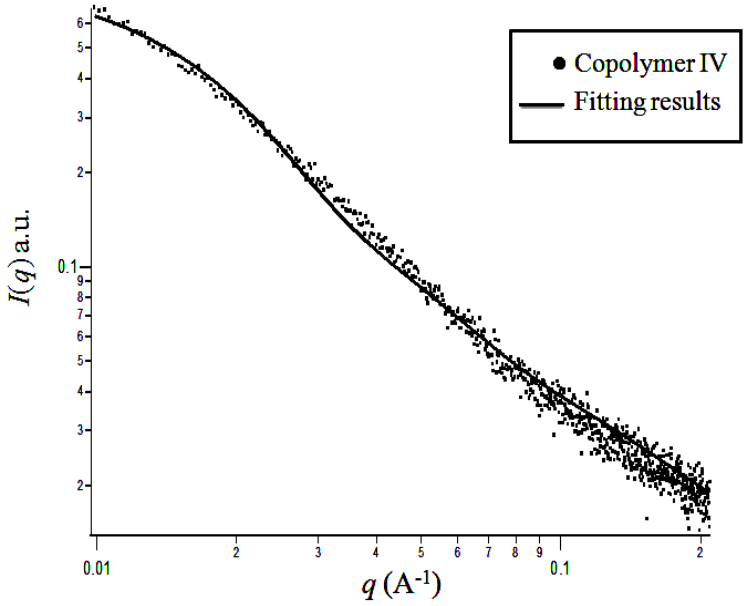

Figure 3.6 The unified function fits to the data of Figure 3.3. The fit range includes all of the data points.

Persistence lengths obtained from both the graphical approach and the SBF approach are summarized in Table 3.5. The rising trend of persistence lengths observed with these two approaches with the addition of bulky phenyl rings along the polymer chains are in

agreement with each other, i.e., stilbene containing copolymers have more stiff chains than their styrene analogies. However, because of the large errors inherent in the graphical approach, it is not surprising that the absolute values of persistence lengths obtained from the graphical approach are somewhat different than the values using the SBF method. Nevertheless, by comparing the persistence lengths of copolymer I to copolymer II or copolymer III to copolymer IV, the results illustrate that the stilbene containing alternating copolymers are always stiffer than the analogous styrene containing alternating copolymers. This trend is due to the addition of phenyl rings to the polymer backbone, which enhances steric conformational constraints, and decreases the polymer chain mobility and, thus, increases the chain stiffness in the stilbene copolymers.

3.4.2. Measurement of persistence length by SEC

SEC provides a complementary method for quantifying the stiffness of the copolymer. The persistence length can be estimated from the relationship between M and $[\eta]$. The relationship changes in the extreme case of rigid rod-like macromolecules from $[\eta] \sim M^{1.7}$ to $[\eta] \sim M^{1/2}$ for Gaussian coils at large M, without excluded volume.[28] If a polymer sample has broad enough molecular weight distribution, the transition from a higher to lower $[\eta] - M$ power law can be used to estimate the persistence length by applying a suitable hydrodynamic chain model.

For example, the two variables $[\eta]$ and M are related according to the wormlike chain model of Yamakawa, Fujii, and Yoshizaki (Y-F-Y model) equation.[57] A popular method for obtaining the wormlike chain parameters of the Y–F–Y model is given by the Bohdanecký linear approximation[58]

$$\left(\frac{M^2}{[\eta]}\right)^{1/3} = \mathrm{A}_\eta + \mathrm{B}_\eta M^{1/2} \tag{3.13}$$

where A_η and B_η are given as

$$A_\eta = \frac{A_0 M_L}{\phi_\infty^{1/3}} \tag{3.14}$$

$$B_\eta = \frac{B_0}{\phi_\infty^{1/3}}\left(\frac{2l_p}{M_L}\right)^{-1/2} \tag{3.15}$$

$\phi_\infty = 2.87\times10^{23}$, and A_0 and B_0 are functions of $d/2l_p$,

$$A_0 = 0.46 - 0.53\log\left(d/2l_p\right) \tag{3.16}$$

$$B_0 = 1.00 - 0.0367\log\left(d/2l_p\right) \tag{3.17}$$

where d is the chain hydrodynamic diameter. B_0 is nearly constant and replaced by its mean value, 1.05. Mass per unit contour length, M_L, was calculated from energy minimization in ChemBio3D Ultra. A segment of three repeating units of copolymer III was drawn. An MM2 energy minimization and an MMFF94 energy minimization were run on the segment, Figure 3.7. After two different energy minimizations, an average contour length of one repeating unit was obtained. Mass per unit contour length M_L was then calculated as the molar mass of one repeating unit divided by an average contour length of one repeating unit

$$M_L = M_0 / L_0 \tag{3.18}$$

where M_0 is molar mass of one repeating unit and L_0 is contour length of one repeating unit. The values of mass per unit contour length, M_L, are provided in Table 3.4. M from light scattering detection and $[\eta]$ from the viscosity detection were used to create the plots in Figure 3.8 for copolymers I, II, III, and IV. A_η and B_η were determined from the slopes and intercepts of the Bohdanecký plots according to eq. (3.13). The persistence length l_p was obtained from the intercept, B_η, $B_0 = 1.05$ and M_L values using eq. (3.15),

and are provided in Table 3.4. The theory underlying the linear approximation described by eq. (3.13) neglects the effects of excluded volume on molecular dimensions, and the viscosity expansion factor may not be negligible at high values of M. However, as explained by Bohdanecký in reference 57, the initial slope of the plot of $(M^{1/2}/[\eta])^{1/3}$ vs. $M^{1/2}$ will not be significantly affected by expansion and the copolymers in this study fall within the valid ranges of contour lengths provided in Table 1 of reference 57.

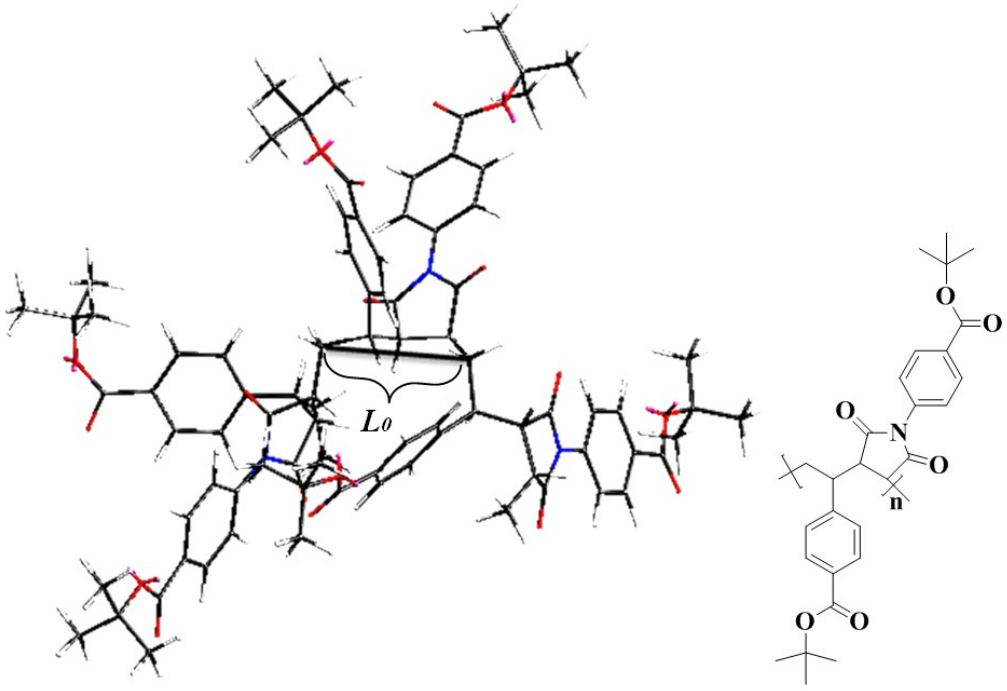

	M_0 (g/mol)	L_0	M_L (nm^{-1})
MM2 energy minimization	478	0.461	1037
MMFF94 energy minimization	478	0.466	1026
Average M_L			1032

Figure 3.7 Example of M_L calculation for copolymer III.

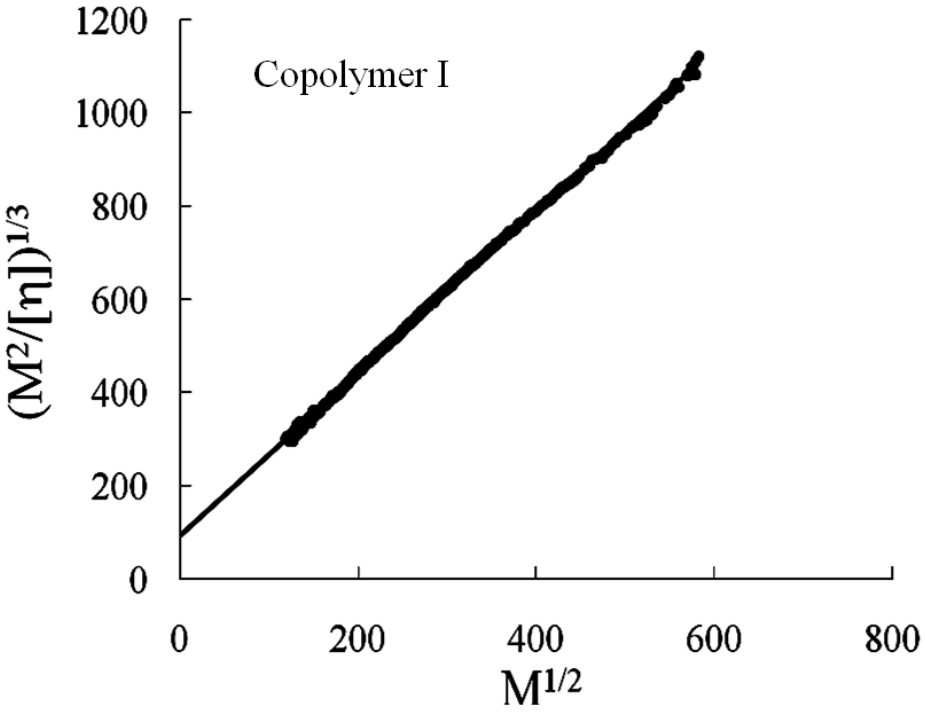
Copolymer I
1200
1000
800
600
400
200
0
0
200
400
600
800
$(M^2/[\eta])^{1/3}$
$M^{1/2}$

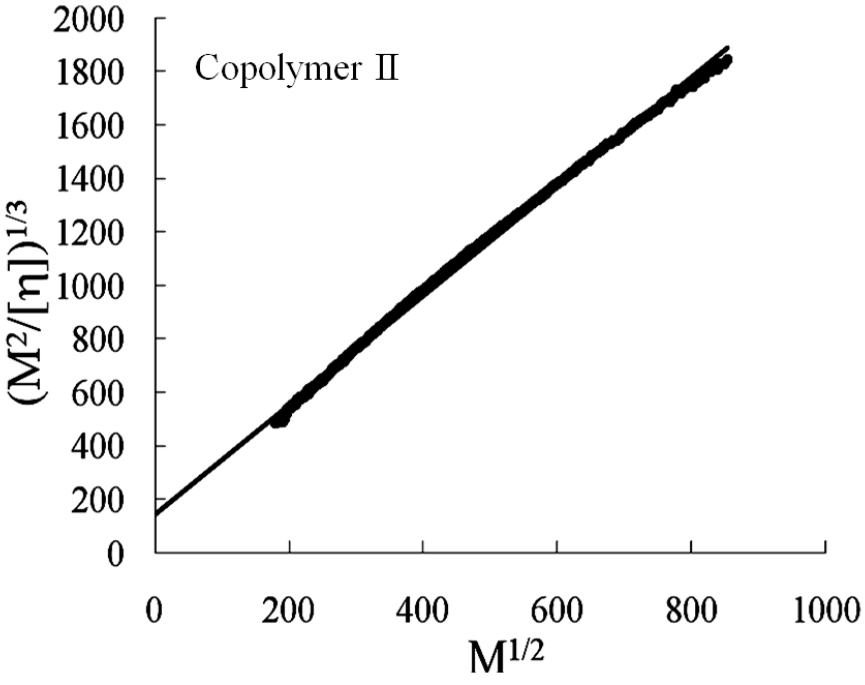
Copolymer II
2000
1800
1600
1400
1200
1000
800
600
400
200
0
0
200
400
600
800
1000
$(M^2/[\eta])^{1/3}$
$M^{1/2}$

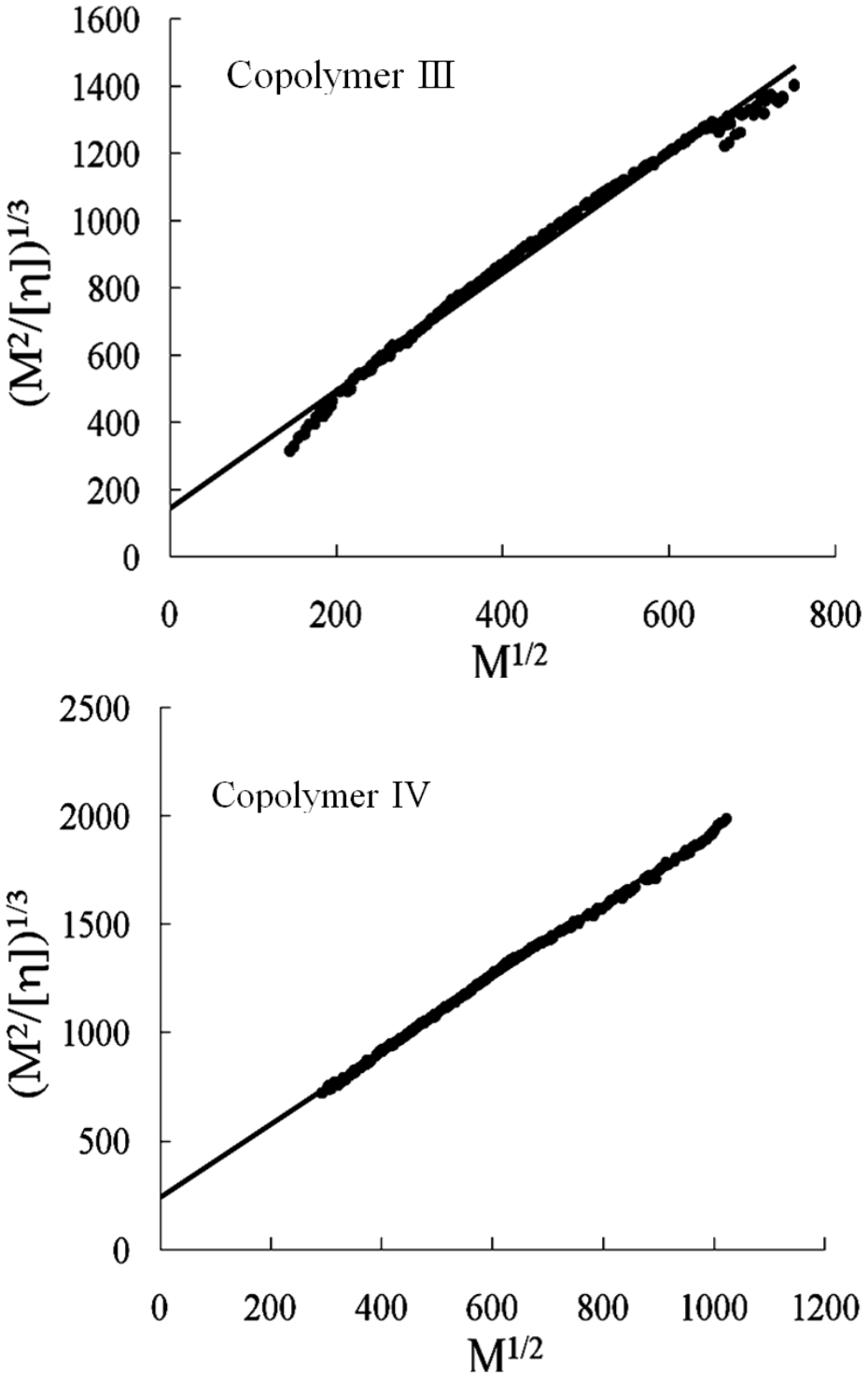

Figure 3.8 Bohdanecký plots of copolymers I, II, III, and IV.

Table 3.4 Parameters of Bohdanecký equation for copolymers I, II, III, and IV.

	A_η ($gmol^{-2/3}mL^{-1/3}$)	B_η ($g^{1/2}mol^{-1/6}mL^{-1/3}$)	M_L (nm^{-1})	l_p (nm)
copolymer I[a]	94.4±1.1	1.74±0.004	610	2.57±1
copolymer II[a]	145±2.7	2.04±0.006	1000	3.04±1
copolymer III[b]	145±4.3	1.75±0.10	1032	4.28±1
copolymer IV[b]	240±2.5	1.69±0.004	1369	6.08±1

[a.]SEC experiments were carried out in DMF containing 0.1 M lithium nitrate and 1% formic acid; [b.]SEC experiments were carried out in THF.

Table 3.5 Comparison of persistence lengths obtained from SAXS and SEC.

	l_p by SBF approach (nm)	l_p by Bohdanecký approximation (nm)
copolymer I	2.7±0.040	2.6±1
copolymer II	3.6±0.036	3.0±1
copolymer III	3.4±0.032	4.3*±1
copolymer IV	4.0±0.034	6.1*±1

l_p with * was determined in THF as the solvent, otherwise determined in DMF.

From Table 3.5 the Bohdanecký linear approximation applied to the SEC data, and the SBF approaches applied to the SAXS data provided similar trends. From both SEC and SAXS measurements, the addition of the phenyl rings to the polymer backbone increases the persistence length; however, the persistence length is considered a solvent-dependent quantity; hence the SEC values for Copolymers I and II in DMF/formic acid/$LiNO_3$ may not be directly comparable to those of Copolymers III and IV measured in THF. Additionally, the polymers with maleimide units are more rigid than the ones based on maleic anhydride units, by comparing persistence length values of copolymer I to its analog, copolymer III, or copolymer II to its analog copolymer IV. This is probably due to the steric hindrance caused by the bulky *tert*-butyl phenyl carboxylate functional group

located on maleimide unit. This is similar to the alternating copolymer of stilbene and *N*-(2-methylphenyl)maleimide) in which a strong negative birefringence was observed due to the steric hindrance caused by the methyl substituent.[21]

The results from SBF and Bohdanecký approaches showed that the added phenyl groups increase the rigidity of the polymer chains by about 30-50%. These persistence length values put these copolymers into a broadly defined "semi-rigid" category of polymers.

Table 3.6 Comparison of persistence lengths.

	l_p (nm)	Solvent	Reference
Schizophyllan	137	Water	58
DNA	50	Water	59
Poly(N-hexyl isocyanate)	40	THF	28,58
Cellulose trinitrate	15	Acetone	58
Poly(p-phenylene) backbone with sulfonate ester and dodecyl side chains	12.6	THF	60,61
Poly(2,7-(9,9 di-N-hexylfluorene))	8.0	THF	28
Poly(di-isopropyl fumarate)	11	THF	62
Poly(tert-butyl crotonate)	5.0~6.0	Ethyl acetate	63
Ladder-type poly(p-phenylene)	6.5	Toluene	64
Copolymer IV	6.1	THF	This work
Copolymer III	4.3	THF	This work
Poly(1-phenyl-1-propyne)	3.8	Cyclohexane	65
Copolymer II	3.0	DMF	This work
Copolymer I	2.6	DMF	This work
poly(tert-butyl methacrylate)	0.8~1.2	Toluene	66
Poly(acrylic acid)	1.4	Dioxane	41
Polystyrene	0.90	Melt	67
Poly(ethylene)	0.69	Melt	67
Poly(propylene)	0.56	Melt	67

Table 3.6 provides persistence length values of different types of polymers. In comparison to rigid rod polymers such as poly(*n*-hexyl isocyanate) (l_p=40 nm),[28,58] DNA (l_p=50 nm),[59] and schizophyllan (l_p=137 nm),[58] stilbene-containing alternating copolymers are a class of semi-rigid polymers, with chain stiffness similar to ladder-type poly(*p*-phenylene) (l_p=6.5 nm),[64] poly(*tert*-butyl crotonate) (l_p=5.0~6.0 nm),[63] and poly(1-phenyl-1-propyne) (l_p=3.8 nm).[65] Stilbene containing alternating copolymers

compared with the substituted polyethylenes are 4~10 times stiffer than most of the polymers with successive carbons in the main chain, such as poly(*tert*-butyl methacrylate) (l_p=0.8~1.2 nm),[66] polystyrene (l_p=0.90 nm),[67] and polypropylene (l_p= 0.56 nm).[67] In response to these observations we have worked to obtain dilute solution properties of the stilbene and styrene polyelectrolytes with steady-state solution shear rheology to assess the effect of steric crowding along the backbone from a different perspective.

3.5. SUMMARY

Using SAXS and SEC techniques, stilbene and styrenic alternating copolymers exhibited persistence lengths ranging from 2 to 6 nm, which characterizes these copolymers as semi-rigid. Based on the persistence length comparison between stilbene copolymers to their analogous styrene copolymers, the steric crowding effect of the second phenyl ring from enchainment of the stilbene units in the backbone increased the polymer chain stiffness by about 30-50%. It was also found the polymer backbones enchained with *tert*-butyl carboxylate functionalized *N*-phenyl maleimide units are more rigid than those containing maleic anhydride units. It is likely caused by the sterically hindered bulky *tert*-butyl phenyl carboxylate functional group located on the maleimide unit.

REFERENCES

(1) Förster, S.; Schmidt, M.; Springer Berlin / Heidelberg: 1995; Vol. 120, p 51.

(2) MacCallum, J. R.; Vincent, C. A. *Polymer electrolyte reviews*; Elsevier Applied Science, 1989.

(3) Schmitz, K. S. *Macroions in solution and colloidal suspension*; VCH, 1993.

(4) Bohrisch, J.; Eisenbach, C. D.; Jaeger, W.; Mori, H.; Müller, A. H. E.; Rehahn, M.; Schaller, C.; Traser, S.; Wittmeyer, P.; Schmidt, M., Ed.; Springer Berlin / Heidelberg: 2004; Vol. 165, p 277.

(5) Holm, C.; Rehahn, M.; Oppermann, W.; Ballauff, M.; Schmidt, M., Ed.; Springer Berlin / Heidelberg: 2004; Vol. 166, p 35.

(6) Cotts, P. M.; Berry, G. C. *J. Polym. Sci., Polym. Phys. Ed.* **1983**, *21*, 1255.

(7) Lee, C. C.; Chu, S. G.; Berry, G. C. *J. Polym. Sci., Polym. Phys. Ed.* **1983**, *21*, 1573.

(8) Roitman, D. B.; Wessling, R. A.; McAlister, J. *Macromolecules* **1993**, *26*, 5174.

(9) Roitman, D. B.; McAlister, J.; McAdon, M.; Wessling, R. A. *J. Polym. Sci. Part B: Polym. Phys.* **1994**, *32*, 1157.

(10) Mao, M.; Turner, S. R. *J. Am. Chem. Soc.***2007**, *129*, 3832.

(11) Mao, M.; Turner, S. R. *Polymer* **2006**, *47*, 8101.

(12) Mao, M.; Kim, C.; Wi, S.; Turner, S. R. *Macromolecules* **2007**, *41*, 387.

(13) Li, Y.; Turner, S. R. *Eur. Polym. J.* **2010**, *46*, 821.

(14) Wagner-Jauregg, T. *Ber. Dtsch. Chem. Ges. (A and B Ser.)* **1930**, *63*, 3213.

(15) Lewis, F. M.; Mayo, F. R. *J. Am. Chem. Soc.***1948**, *70*, 1533.

(16) Hallensleben, M. L. *Eur. Polym. J.* **1973**, *9*, 227.

(17) Tanaka, T.; Vogl, O. *Polym J* **1974**, *6*, 522.

(18) Rzaev, Z. M.; Zeinalov, I. P.; Medyakova, L. V.; Babaev, A. I.; Agaev, M. M. *Vysokomol Soedin Ser A* **1981**, *23*, 614.

(19) Ebdon, J. R.; Hunt, B. J.; Hussein, S. *Brit Polym J* **1987**, *19*, 333.

(20) Mcneill, I. C.; Polishchuk, A. Y.; Zaikov, G. E. *Polym Degrad Stabil* **1995**, *47*, 319.

(21) Mao, M.; England, J.; Turner, S. R. *Polymer* **2011**, *52*, 4498.

(22) Li, Y.; Mao, M.; Matolyak, L. E.; Turner, S. R. *ACS Macro Lett.* **2012**, *1*, 257.

(23) Taylor, E. C.; Fletcher, S. R.; Sabb, A. L. *Synth. Commun.* **1984**, *14*, 921.

(24) Li, Y.; Mao, M.; Matolyak, L. E.; Turner, S. R. *Submitted to ACS Macro Lett.*.

(25) Broos, R. *J. Chem. Educ.* **1978**, *55*, 813.

(26) Rich, D. H.; Gurwara, S. K. *J. Am. Chem. Soc.***1975**, *97*, 1575.

(27) Ishizone, T.; Hirao, A.; Nakahama, S. *Macromolecules* **1989**, *22*, 2895.

(28) Mourey, T.; Le, K.; Bryan, T.; Zheng, S.; Bennett, G. *Polymer* **2005**, *46*, 9033.

(29) Roe, R. J. *Methods of X-ray and neutron scattering in polymer science*; Oxford University Press, 2000.
(30) Kratky, O.; Porod, G. *Recl. Travaux Chim. Pays-Bas* **1949**, *68*, 1106.
(31) Porod, G. *Monatsh. Chem./Chem. Monthly* **1949**, *80*, 251.
(32) Kuhn, W. *Kolloid-Z* **1934**, *68*, 2.
(33) Benoit, H.; Doty, P. *J. Phys. Chem.* **1953**, *57*, 958.
(34) Doi, M.; Edwards, S. F. *The theory of polymer dynamics*; Clarendon Press, 1988.
(35) Gennes, P. G. *Scaling concepts in polymer physics*; Cornell University Press, 1979.
(36) Glatter, O.; Kratky, O. *Small angle x-ray scattering*; Academic Press, 1982.
(37) Debye, P. *J. Phys. Colloid Chem.* **1947**, *51*, 18.
(38) Porod, G. *J. Polym. Sci.* **1953**, *10*, 157.
(39) Kratky, O. *Colloid Polym. Sci.* **1962**, *182*, 7.
(40) Paramita Kar, C.; et al. *J. Phys.: Condens. Matter* **2009**, *21*, 195801.
(41) Taylor, T. J.; Stivala, S. S. *Polymer* **1996**, *37*, 715.
(42) Taylor, T. J.; Stivala, S. S. *J. Polym. Sci. Part B: Polym. Phys.* **2003**, *41*, 1263.
(43) Beaucage, G.; Rane, S.; Sukumaran, S.; Satkowski, M. M.; Schechtman, L. A.; Doi, Y. *Macromolecules* **1997**, *30*, 4158.
(44) Peterlin, A. *J. Polym. Sci.* **1960**, *47*, 403.
(45) Heine, V. S.; Kratky, O.; Roppert, J. *J. Makromol. Chem.* **1962**, *56*, 150.
(46) Kratky, O. *Pure Appl. Chem.* **1966**, *12*, 483.
(47) Cleland, R. L. *Arch. Biochem. Biophys.* **1977**, *180*, 57.
(48) Gupta, A. K.; Cotton, J. P.; Marchal, E.; Burchard, W.; Benoit, H. *Polymer* **1976**, *17*, 363.
(49) Muroga, Y.; Noda, I.; Nagasawa, M. *Macromolecules* **1985**, *18*, 1576.
(50) Yamazaki, S.; Muroga, Y.; Noda, I. *Langmuir* **1999**, *15*, 4147.
(51) Sharp, P.; Bloomfield, V. A. *Biopolymers* **1968**, *6*, 1201.
(52) Yamakawa, H.; Fujii, M. *Macromolecules* **1974**, *7*, 649.
(53) Schmid, C. W.; Rinehart, F. P.; Hearst, J. E. *Biopolymers* **1971**, *10*, 883.
(54) Beaucage, G. *J. Appl. Crystallogr.* **1995**, *28*, 717.
(55) Beaucage, G.; Schaefer, D. W. *J Non-Cryst Solids* **1994**, *172-174, Part 2*, 797.
(56) Schaefer, D. W.; Pekala, R.; Beaucage, G. *J Non-Cryst Solids* **1995**, *186*, 159.
(57) Yamakawa, H.; Fujii, M. *Macromolecules* **1974**, *7*, 128.
(58) Bohdanecky, M. *Macromolecules* **1983**, *16*, 1483.
(59) Wang, L.; Bloomfield, V. A. *Macromolecules* **1991**, *24*, 5791.
(60) Guilleaume, B.; Blaul, J.; Ballauff, M.; Wittemann, M.; Rehahn, M.; Goerigk, G. *Eur. Phys. J. E: Soft Matter Biol. Phys.* **2002**, *8*, 299.
(61) Vanhee, S.; Rulkens, R.; Lehmann, U.; Rosenauer, C.; Schulze, M.; Köhler, W.; Wegner, G. *Macromolecules* **1996**, *29*, 5136.
(62) Matsumoto, A.; Nakagawa, E. *Eur. Polym. J.* **1999**, *35*, 2107.

(63) Noda, I.; Imai, T.; Kitano, T.; Nagasawa, M. *Macromolecules* **1981**, *14*, 1303.

(64) Scherf, U.; Müllen, K. *J. Makromol. Chem., Rapid Commun.* **1991**, *12*, 489.

(65) Hirao, T.; Teramoto, A.; Sato, T.; Norisuye, T.; Masuda, T.; Higashimura, T. *Polym J* **1991**, *23*, 925.

(66) Muroga, Y.; Sakuragi, I.; Noda, I.; Nagasawa, M. *Macromolecules* **1984**, *17*, 1844.

(67) Fetters, L.; Lohse, D.; Colby, R. In *Physical Properties of Polymers Handbook*; Mark, J. E., Ed.; Springer New York: 2007, p 447.

Chapter 4. COPOLYMERIZATION OF METHYL SUBSTITUTED STILBENES WITH MALEIC ANHYDRIDE

4.1. ABSTRACT

Stilbene-maleic anhydride is a well-known donor-acceptor comonomer pair which undergoes free radical copolymerization to form an alternating copolymer. A series of methyl substituted stilbenes were synthesized and copolymerized with maleic anhydride. Size exclusion chromatography (SEC) measurements showed that the weight average molecular weights of these copolymers varied from 3.0 to over 1000 kg/mol. The SEC trace for poly((*E*)-4-methylstilbene-*alt*-maleic anhydride) exhibited bimodal peaks. Interchain aggregation observed in poly((*E*)-4-methylstilbene-*alt*-maleic anhydride) by dynamic light scattering (DLS) was responsible for SEC bimodal peaks.

4.2. INTRODUCTION

Nanotubes are hollow curved architectures with varying lengths and with diameters usually ranging in nanometers.[1] It was reported that poly(styrene-alt-maleic anhydride) (SMA) formed nanotubes of well-defined structures by self-assembly.[2,3] SMA derivatives, such as poly(styrene-*alt*-maleic acid) (SMA) and poly(styrene-*alt*-*N*-(dimethylamino)propylmaleimide) (SMI) had also been reported to form nanotubes by self-assembly. Garnier et al.[2] studied that the behavior of SMA in aqueous solution and at the air-water interface by static and dynamic light scattering, by surface tension measurements, and by transmission electron microscopy. It was revealed that SMA polymers associated in aqueous solution and a maximum size of the aggregates was

reached at pH 6.5. This pH value corresponded to the polymer salt in its monosodium form. An equilibrium reached between SMA in solution and at the air-water interface was observed. Whitehead et al.[3] later provided a conformational analysis of SMA at different pH values. A strong internal hydrogen bond formed at intermediate pH was found to induce a change in the conformation of the polymer chain to become linear. This linearity occurring only at intermediate pH is responsible for the maximum size of the aggregates observed by dynamic light scattering at intermediate pH. A further theoretical approach was used by Whitehead et al. to understand the conformational variations of SMA at different pH values.[4,5] At intermediate pH the most stable conformation is a linear chain, and chains associate with each other and stack to form a tubular structure. At higher or lower pH values (pH 3 or 12) a 90° angle between two repeating units was observed, leading to irregular helix conformation that hinders the chain aggregation.

The effect of different chiral sequences in alternating copolymers of styrene and maleimide was studied by Whitehead et al. using semi-empirical PM3 calculations.[6] It was found that only the racemo-diisotactic SMI polymer chains form a stable, minimum-energy nanotube structure because of the symmetrically distributed phenyl groups and maleimide monomers. The SMI polymer is isotactic with respect to the chiral site of the styrene monomers (R, S) and isotactic with respect to the chirality of the maleimide racemo (RR, SS), as shown in Figure 4.1. The racemo (SS or RR) chiral maleimide and the complementary S or R chirality in the styrene moiety form the repeating unit of racemo-diisotactic SMI. Ordered polymer self-assembly results from π-stacking of styrenes and van der Waals interactions between the maleimide chains.

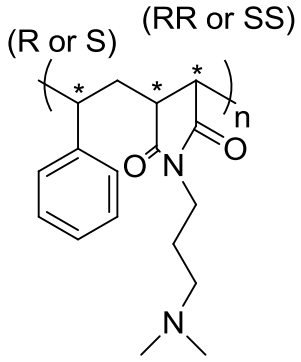

Figure 4.1 Representative a racemo-diisotactic SMI sequence.

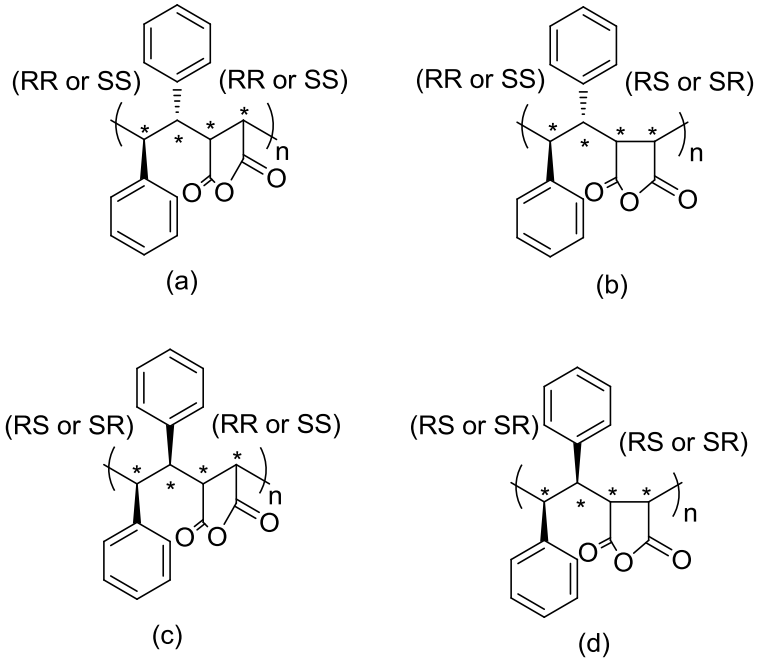

Figure 4.2 Possible stereo sequences of poly(stilbene-*alt*-maleic anhydride).

These special nanotube structures can be used as templates to linearly guide the growth of a secondary polymeric or inorganic material. For example, SMA was used as a template to chelate with zinc ion and to generate SMA-Zn with rigid-chain structure for the formulation of ZnO nanorods.[7] Linear silver cyanide nanowires were grown using this SMA template.[8]

Poly(stilbene-*alt*-maleic anhydride) is structurally similar to poly(styrene-*alt*-maleic anhydride) with one additional phenyl ring along the polymer backbone. We are interested in stilbene alternating copolymers because these structures are anticipated to exhibit more sterically crowded backbones, compared to their analogous styrene-containing copolymers.[9-13] In addition the solution association behavior of stilbene alternating copolymers may have some similarities to their analogous styrene-containing copolymers. According to the studies on poly(styrene-*alt*-maleic anhydride) aggregates,[1,6], poly(stilbene-*alt*-maleic anhydride) may possibly form aggregates with diisotacticity in respect to the chiral sites of the maleic anhydride monomers (RR, SS) and the complementary RR or SS chirality in the stilbene moiety, as shown in Figure 4.2 (a). However, we decided not to pursue NMR to detect stereoisomerism in stilbene copolymers. 1,2-Disubstituted ethylenes such as (*E*)-stilbene (*trans*-stilbene) and maleic anhydride usually exhibit very little or no tendency to undergo homopolymerization mainly due to kinetic considerations. The approach of the propagating radical to a monomer molecule is sterically hindered.[14] However, (*E*)-stilbene and maleic anhydride readily undergo free radical copolymerization to form an alternating copolymer because (*E*)-stilbene is a strong electron donor and maleic anhydride is an electron acceptor. The *(E)*-stilbene-maleic anhydride copolymer was first reported by Wagner-Jauregg in 1930 and appeared insoluble in xylene.[15] Lewis and Mayo investigated relative reactivities and stability of six pairs of *cis-trans* isomers and found *(E)*-stilbene was more reactive and more stable than *(Z)*-stilbene (*cis*-stilbene) towards the maleic anhydride radical and the yield for the copolymerization of (*E*)-stilbene with maleic anhydride was up to 60% in chloroform.[16] Later insoluble and crosslinked *(E)*-stilbene-maleic anhydride copolymer

was reported via free radical copolymerization by Hallensleben, who also obtained soluble *(E)*-stilbene-maleic anhydride copolymer upon U.V. irradiation in tetrahydrofuran or acetone.[17] Tanaka and Vogl, however, argued that high molecular weight led to insolubility, not crosslinking since the polymer became soluble in sodium hydroxide solution after hydrolysis of the anhydride units in the polymer chain.[18] More recently the copolymer has been studied by Rzayev et al.,[19] Edbon et al.,[20] and McNeill et al.[21] Rzayev et al. investigated the formation of a *(E)*-stilbene-maleic anhydride charge-transfer complex based on copolymerization in methyl ethyl ketone initiated with benzoyl peroxide at 80 ^{o}C.[19] *(E)*-Stilbene-maleic anhydride copolymer composition and molecular weight distribution have been investigated by Edbon et al. who obtained the copolymer from the free radical copolymerization in methyl ethyl ketone at 60 ^{o}C using 2, 2'-azo-bis(isobutyronitrile) as initiator. They found the copolymer composition rich in maleic anhydride with a broad molecular weight distribution and attributed these effects to phase separation during the copolymerization.[20] McNeill et al. have conducted an investigation of the alternating structure of (*E*)-stilbene-maleic anhydride copolymer and thermal degradation process and found no evidence for crosslinking based on TGA data or IR spectrum.[21]

In this work we prepared methyl substituted (*E*)-stilbene polymers and investigated their solution behaviors by dynamic light scattering. To the best of our knowledge, there has been no work on preparation of copolymers of methyl substituted (*E*)-stilbenes with maleic anhydride and characterization of the properties of these novel structures. These results have been published in References 23 and 24.

4.3. EXPERIMENTAL SECTION

4.3.1. Materials

(*E*)-Stilbene (EMS-I, Aldrich, 96%), maleic anhydride (MAH, Aldrich, ≥99.0%), 2-methylbenzyl chloride (Aldrich, 99%), 4-methylbenzyl chloride (Aldrich, 98%), *o*-tolualdehyde (Aldrich, 97%), benzaldehyde (Aldrich, ≥99%), potassium tert-butoxide solution 1.0 M in tetrahydrofuran (KO^{t}Bu, Aldrich), triethylphosphite (Aldrich, 98%), 2,2′-azobisisobutyronitrile (AIBN, Aldrich, 98%) were all purchased from Aldrich and used as received. Tetrahydrofuran (THF, Fisher, HPLC grade) and hexane (Fisher, HPLC grade) and methylene chloride (Fisher, HPLC grade) were used as received. Water was deionized before use.

4.3.2. Characterization

^{1}H NMR and ^{13}C NMR spectra of monomers were determined at 25 °C in $CDCl_3$ at 400/100 MHz with a Varian Inova spectrometer or 500/125 MHz with a Jeol Eclipse +500 spectrometer. Melting points of monomers were measured on BUCHI Melting Point B-540 instrument.

Molecular weights of the polymers were determined using a Waters size exclusion chromatograph equipped with a Waters 1515 isocratic HPLC pump, a Waters 2414 differential refractive index detector operating at 880 nm and 35 ^{o}C and a Waters 717 plus autosampler, a Wyatt miniDAWN multiangle laser light scattering (MALLS) detector operating a He-Ne laser at 690 nm. The d_n/d_c values were determined using the Wyatt Astra V software package. SEC measurements were performed at 35 °C in THF at a flow rate of 1.0 mL/min.

Dynamic light scattering (DLS) measurements were performed using a Malvern Zeta Sizer Nano Series Nano-ZS instrument (Malvern Instruments, Malvern, UK) using

Dispersion Technology Software (DTS) version 4.20 with a He-Ne laser (λ= 633 nm). The experiments were performed at of 25 °C. Samples were ultrasonicated for about 10 min if necessary and then syringed through 0.45 μm PTFE syringe filters directly into clean cuvettes. Data were obtained for the presence or absence of aggregation peaks based on particle diameter size.

4.3.3. Synthesis of methyl substituted (E)-stilbenes (EMSs)

The Wittig-Horner reaction of an aldehyde with a phosphorus ylide was employed to synthesize the EMSs (Scheme 1).[22-24]

A typical procedure to prepare ***(E)-2,2'-dimethylstilbene (EMS-II)*** is as follows: 2-methylbenzyl chloride (16.40 g, 117.0 mmol) was heated with excess triethylphosphite (78 g, 81 mL, 0.47 mol) at 160 ^{o}C for 24 h. The remaining triethylphosphite was then removed by vacuum distillation at 80 ^{o}C (0.2 mmHg) to afford 2-methylbenzyl diethylphosphonate. Yield: 95%, 26.90 g. To a solution of 2-methylbenzyl diethyl-phosphonate (27.47 g, 113.5 mmol) and *o*-tolualdehyde (13.62 g, 113.5 mmol) in dry THF (50 mL) cooled in an ice bath was added KO^{t}Bu (1.0 M in THF, 120 mL) dropwise over 20 min. The solution was stirred at room temperature for 24 h. Then the solution was poured into 500 mL of water. The product precipitated from the solution was collected by filtration and washed with water and vacuum dried overnight to yield a white crystalline solid. Yield: 80%, 18.89 g. There was no detectable Z isomer by ^{1}H NMR analysis. ^{1}H NMR ($CDCl_3$, 500 MHz) δ ppm: 7.63 (d, *J*=7.4 Hz, 2H), 7.20-7.25 (m, 8H), 2.43 (s, 6H). ^{13}C NMR ($CDCl_3$, 500 MHz) δ ppm: 136.9, 135.9, 130.5, 128.1, 127.7, 126.3, 125.7, 20.1. Mp: 82-84 ^{o}C (Lit.:[25] 83-84 ^{o}C).

(E)-2-Methylstilbene (EMS-III) was synthesized via condensation of 2-methylbenzyl diethylphosphonate (15.00 g, 61.98 mmol) and benzaldehyde (6.57 g, 61.98 mmol) under the same Wittig-Horner reaction conditions as EMS-II. After condensation, the solution was poured into water. The oily product was extracted twice with methylene chloride, and the solvent was evaporated under reduced pressure. The product was purified by silica column chromatography (hexane) yielded a clear oil. Yield: 87%, 9.70 g. There was no detectable Z isomer by ^{1}H NMR analysis. ^{1}H NMR ($CDCl_3$, 400 MHz) δ ppm: 7.59 (d, *J*=7.0 Hz, 1H), 7.52 (d, *J*=7.7 Hz, 2H), 7.29-7.40 (m, 3H), 7.27 (d, *J*=16.0 Hz, 1H), 7.15-7.25 (m, 3H), 7.00 (d, *J*=16.0 Hz, 1H), 2.42 (s, 3H). ^{13}C NMR ($CDCl_3$, 500 MHz) δ ppm: 137.8, 136.5, 135.9, 130.5, 130.1, 128.8, 127.72, 127.68, 126.68, 126.67, 126.3, 125.5, 20.0. Mp: 30-31 ^{o}C (Lit.:[26] 30 ^{o}C). Bp: 212 ^{o}C at atmospheric pressure.

(E)-4-Methylstilbene (EMS-IV) was synthesized via condensation of 4-methylbenzyl diethylphosphonate (12.00 g, 49.59 mmol) and benzaldehyde (5.26 g, 49.6 mmol) under the same Wittig-Horner reaction conditions as EMS-II, where 4-methylbenzyl diethyl-phosphonate was synthesized from 2-methylbenzyl chloride with excess triethylphosphite. After the condensation reaction, the solution was poured into water. The product precipitated from the solution was collected by filtration, and washed with water and vacuum dried overnight to yield a white solid. Yield: 86%, 7.68 g. There was no detectable Z isomer by ^{1}H NMR analysis. ^{1}H NMR ($CDCl_3$, 500 MHz) δ ppm: 7.03-7.60 (m, 11H), 2.37 (s, 3H). ^{13}C NMR ($CDCl_3$, 500 MHz) δ ppm: 137.6, 134.7, 129.5, 128.7, 127.8, 127.5, 126.54, 126.50, 21.4. Mp: 121-122 ^{o}C (Lit.:[27] 118-120 ^{o}C).

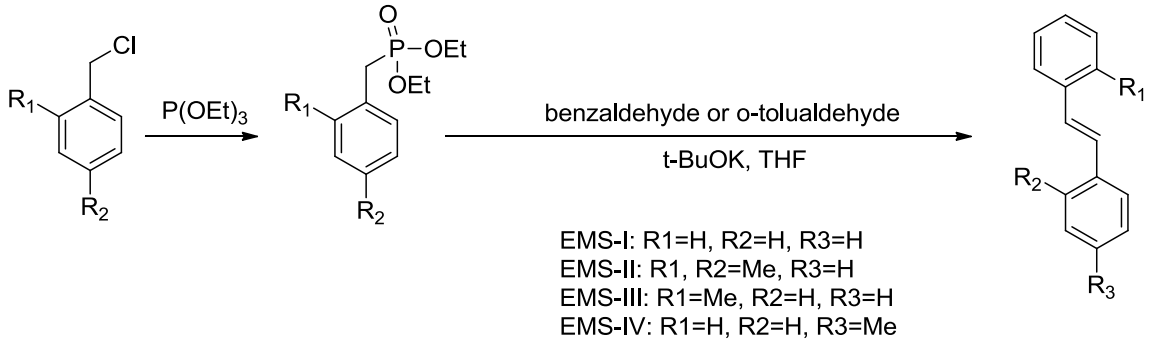

Scheme 4.1 Synthesis of (*E*)-methyl substituted stilbenes polymerization

The stilbenes (EMSs), maleic anhydride (MAH), and THF were mixed with the initiator, AIBN, in a 50-mL septum sealed glass bottle equipped with a magnetic stirrer. All of the copolymerization experiments used an equimolar ratio of EMSs and MAH except for the copolymer composition study. The initiator concentration was 1 wt % based on monomer in all polymerizations. For instance, EMS-II (2.08 g, 10.0 mmol), MAH (0.98 g, 10 mmol) and THF (13.75 mL) were mixed with AIBN (0.0306 g) in a 50-mL septum sealed glass bottle equipped with a magnetic stirrer. The mixture was degassed by purging with argon at room temperature for 10 min and polymerized at 60 °C (Scheme 2). The reaction duration was varied in the conversion versus time study and the copolymer composition study. Copolymers were recovered by precipitation into hexane in the conversion versus time study and purified by reprecipitation from THF into hexane in the copolymer composition study. All polymers were dried under vacuum at 60 °C overnight before characterization. Two peaks associated with the anhydride groups of the copolymers (1841 cm^{-1} and 1775 cm^{-1}) were clearly observed in the IR spectra. Copolymers VI and VII were soluble in THF, whereas copolymers V and VIII had poor solubility in THF.

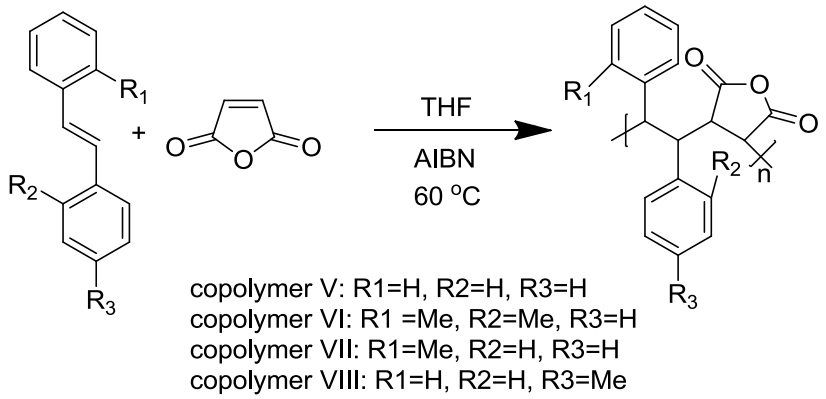

Scheme 4.2. Alternating copolymerization of methyl substituted (*E*)-stilbenes with maleic anhydride.

4.4. RESULTS AND DISCUSSION

The molecular weights of these EMSs-maleic anhydride copolymers were obtained from the SEC traces shown in Figure 4.3. These molecular weights were based on the use of both the light scattering (L.S.) detector which is more sensitive to relatively high molecular weights and refractive index (R.I.) detector. For copolymer VI and copolymer VII, SEC traces given by two detectors were unimodal, but not for copolymer VIII. As shown in Figure 3, the SEC trace given by R.I. detector on the bottom was bimodal and the higher molecular weight peak grew in height significantly and the lower molecular weight peak decreased in height relatively in the L.S. trace on the top. This significant change on height arises from the sensitivity difference of the two detectors. Both traces showed that the molecular weight distributions of the copolymers of EMS-IV with MAH were bimodal. The number-average molecular weight data and the weight-average molecular weight data of copolymer VI, copolymer VII and copolymer VIII are provided in Table 4.1, where the molecular weight for EMS-II-MAH copolymer was found to be below 5.0 kg/mol, and for EMS-III-MAH copolymer below 10.0 kg/mol. The low

molecular weights of these copolymers are most likely due to the steric effect of the ortho methyl substituent in the transition state which slows down the propagation step. The table also provides two sets of molecular weight information for the bimodal trace of copolymer VIII. The molecular weight for peak 1 was over 1000 kg/mol and for peak 2 was around 10.0 kg/mol which was still relatively high compared to the molecular weights of copolymer VI and copolymer VII. It is interesting to note that Edbon et al. also observed bimodal SEC traces and over 1000 kg/mol high molecular weights for copolymer V.[20] It was concluded that phase separation arising from crosslinking and gelation were probably the reasons for polymodality. However, Tanaka and Vogl[18] and McNeill[21] et al. stated that they found no evidence for crosslinking since the hydrolyzed copolymer all dissolved in aqueous solution. We observed that copolymer VIII had poor solubility in THF. And the polymerization solution got turbid quickly as copolymerization progressed. It is likely that high molecular weights and broad molecular weight distributions are due to the aggregation of the polymer chains in the THF solution.

Table 4.1 Molecular weights for EMSs-MAH copolymers.

	Mol fraction EMSs in feed		M_n kg/mol	M_w kg/mol	SEC Trace
copolymer VI	0.25		2.7	3.5	unimodal
	0.50		2.5	3.2	unimodal
	0.75		3.5	4.0	unimodal
copolymer VII	0.25		4.0	5.5	unimodal
	0.50		4.5	6.3	unimodal
	0.65		2.9	4.4	unimodal
	0.75		3.7	5.0	unimodal
copolymer VIII	0.25	peak 1 [a)]	7340	10900	bimodal
		peak 2 [b)]	6.8	9.9	
	0.35	peak 1	4860	5670	bimodal
		peak 2	18.0	23.2	
	0.50	peak 1	3.4	4440	bimodal
		peak 2	11.3	15.6	
	0.65	peak 1	2810	3880	bimodal
		peak 2	12.5	18.4	
	0.75	peak 1	3880	5500	bimodal
		peak 2	9.0	14.6	

[a)] Peak 1 in Figure 3. [b)] Peak 2 in Figure 3.

The aggregation was further corroborated by the DLS measurements. In Figure 4.4, polymodal peaks were observed. The particles with mean hydrodynamic diameter at 173 nm (peak 1 in the bottom curves) were close to 0% by volume, and at 47.9 nm (peak 2 in the bottom curves) the particles were close to 22.4% by volume, whereas the particles at 10.6 nm (peak 3 in the bottom curves) were up to 77.6% by volume. According to Table 4.2, however, it is observed that the size of the particles with mean hydrodynamic diameter at 47.9 nm decreased to 35.0 nm and the volume of the 47.9 nm-diameter particles decreased to 8.5% after treating in an ultrasonic bath for 10 min, which indicates that the particles are more likely aggregates and not free high molecular weight polymer chains. The samples that were treated in the ultrasonic bath exhibited a slow reaggregation which was observed by the increase of the volume and size of the aggregates by DLS over a one week period. In addition, even after hydrolyzing in dilute sodium hydroxide aqueous solution, aggregated samples were still observed by DLS. A combination of aggregation and phase separation during copolymerization could be responsible for the very high apparent molecular weights (peak 2) of copolymer VIII observed by SEC. As phase separation occurs, termination is depressed in the highly viscous phase, while monomer diffusion still occurs to the propagating chain. In this explanation, the interchain aggregation would enhance phase separation and thus promote the “gel effect” type polymerization. This aggregation phenomenon could originate from specific stereochemical sequences as observed in styrene/maleimide copolymers (Figure 4.1).[1,3-6,8]

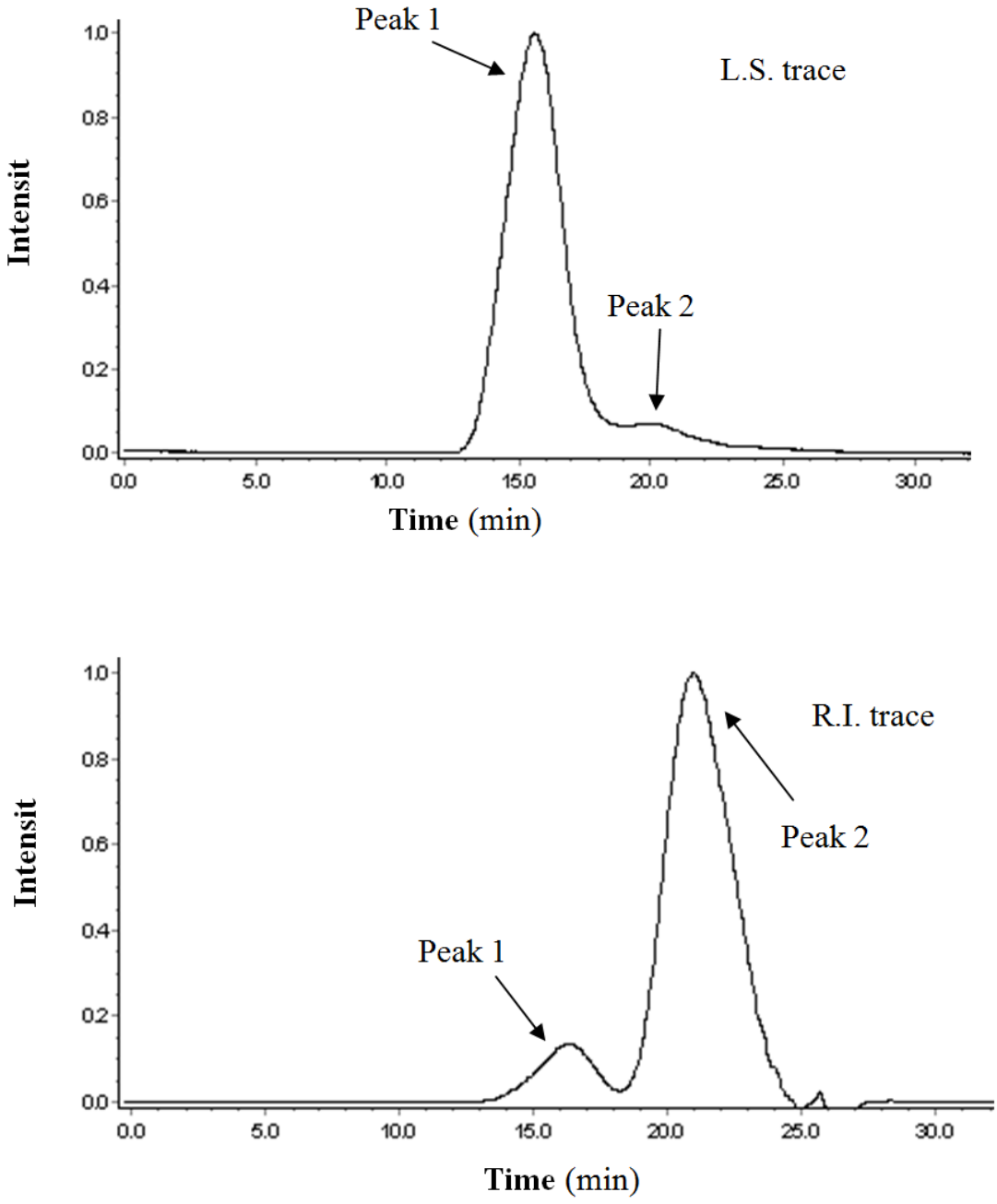

Figure 4.3 SEC traces of copolymer VIII obtained at 60 ^{o}C for 24 h. Trace on the top was obtained from L.S. detector, trace on the bottom was from R.I. detector.

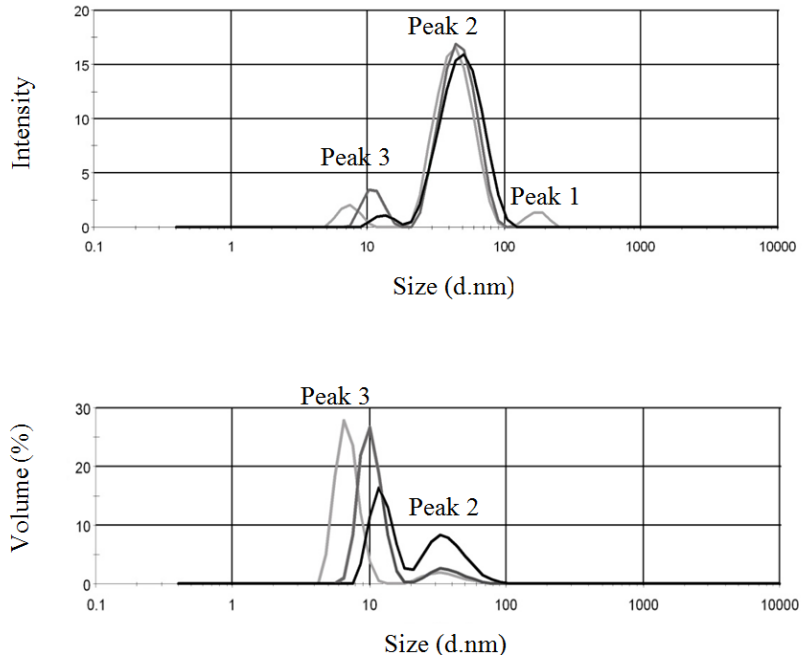

Figure 4.4 DLS plot of copolymer VIII in THF at a concentration of 1 mg/mL. Curves on the top are intensity vs size plot. Curves on the bottom are volume % vs size plot. (black, grey, and light grey curves were obtained from three measurements.)

Table 4.2 Volume change with applying ultrasonic bath and with the change of the concentration of the EMS-IV-MAH polymer solution.

polymer name-concentration	mean hydrodynamic diameter (nm) [a]	% peak 2 [b] by volume
copolymer VIII-1[c]	47.9±3.0	22.4
copolymer VIII-1-Ultrasonication[d]	35.0±2.5	8.5

[a] ± one standard deviation. [b] Peak 2 in Figure 4.4. [c] The concentration of the copolymer VIII solution was 1 mg/ml with no ultrasonic bath applied. [d] The concentration of the copolymer VIII solution was 1 mg/ml with ultrasonic bath applied.

4.5. CONCLUSIONS

A series of EMSs-MAH copolymers was synthesized and characterized. Copolymer VI and VII showed monomodal peaks in SEC measurements, while copolymer VIII had

bimodal peaks showing up in SEC with broad molecular weight distributions and high molecular weights. DLS study showed that both the size and volume of the higher molecular weight peak decreased after treating the polymer solution with an ultrasonic bath for 10 min prior the measurement. This indicated that the bimodal peak may be attributed to the interchain aggregation and "gel effect" during the course of the copolymerization.

REFERENCES

(1) Lazzara, T. D.; van de Ven, T. G. M.; Whitehead, M. A. *Macromolecules* **2008**, *41*, 6747.

(2) Garnier, G.; Duskova-Smrckova, M.; Vyhnalkova, R.; van de Ven, T. G. M.; Revol, J.-F. *Langmuir* **2000**, *16*, 3757.

(3) Malardier-Jugroot, C.; van de Ven, T. G. M.; Whitehead, M. A. *J. Phys. Chem. B* **2005**, *109*, 7022.

(4) Malardier-Jugroot, C.; van de Ven, T. G. M.; Cosgrove, T.; Richardson, R. M.; Whitehead, M. A. *Langmuir* **2005**, *21*, 10179.

(5) Malardier-Jugroot, C.; van de Ven, T. G. M.; Whitehead, M. A. *Mol Simulat* **2005**, *31*, 173.

(6) Lazzara, T. D.; Whitehead, M. A.; van de Ven, T. G. M. *J. Phys. Chem. B* **2008**, *112*, 4892.

(7) Lai, C.-T.; Hong, J.-L. *J. Phys. Chem. C* **2009**, *113*, 18578.

(8) Lazzara, T. D.; Whitehead, M. A.; van de Ven, T. G. M. *Eur. Polym. J.* **2009**, *45*, 1883.

(9) Mao, M.; Turner, S. R. *J. Am. Chem. Soc.***2007**, *129*, 3832.

(10) Mao, M.; Turner, S. R. *Polymer* **2006**, *47*, 8101.

(11) Mao, M.; Kim, C.; Wi, S.; Turner, S. R. *Macromolecules* **2007**, *41*, 387.

(12) Mao, M.; England, J.; Turner, S. R. *Polymer* **2011**, *52*, 4498.

(13) Li, Y.; Mao, M.; Matolyak, L. E.; Turner, S. R. *ACS Macro Lett.* **2012**, *1*, 257.

(14) Odian, G. G. *Principles of polymerization*; Wiley-Interscience, 2004.

(15) Wagner-Jauregg, T. *Ber. Dtsch. Chem. Ges. (A and B Ser.)* **1930**, *63*, 3213.

(16) Lewis, F. M.; Mayo, F. R. *J. Am. Chem. Soc.***1948**, *70*, 1533.

(17) Hallensleben, M. L. *Eur. Polym. J.* **1973**, *9*, 227.

(18) Tanaka, T.; Vogl, O. *Polym J* **1974**, *6*, 522.

(19) Rzayev, Z. M.; Zeinalov, I. P.; Medyakova, L. V.; Babayev, A. I.; Agayev, M. M. *Polym. Sci.U.S.S.R.* **1981**, *23*, 689.

(20) Ebdon, J. R.; Hunt, B. J.; Hussein, S. *Brit Polym J* **1987**, *19*, 333.

(21) Mcneill, I. C.; Polishchuk, A. Y.; Zaikov, G. E. *Polym Degrad Stabil* **1995**, *47*, 319.

(22) Wadsworth, W. S.; Emmons, W. D. *J. Am. Chem. Soc.***1961**, *83*, 1733.

(23) Li, Y.; Turner, S. R. *Eur. Polym. J.* **2010**, *46*, 821.

(24) Yi Li's Master Thesis.

(25) Buquet, A.; Couture, A.; Lablache-Combier, A. *J. Org. Chem.* **1979**, *44*, 2300.

(26) Cahiez, G. r.; Gager, O.; Lecomte, F. *Org. Lett.* **2008**, *10*, 5255.

(27) Sugihara, T.; Satoh, T.; Miura, M.; Nomura, M. *Angew. Chem. Int. Ed.* **2003**, *42*, 4672.

Chapter 5. CHARACTERIZATION OF STILBENE CONTAINING ALTERNATING POLYANIONS IN DILUTE SOLUTION

5.1. ABSTRACT

Stilbene-containing alternating polyanions were prepared via an indirect strategy of synthesizing "protected" monomers followed by deprotection and neutralization of the polyanion precursors. Dilute solution viscosity was studied by steady-state solution shear rheological experiments and a pronounced "polyelectrolyte effect" was observed. The dissociation behavior of polyanions was investigated by pH titration with HCl and multi-step dissociation behavior was observed. Solution behavior was studied by using DLS at varying ionic strengths. The aggregation process is sensitive to the ionic strength.

5.2. INTRODUCTION

The sterically crowded structures arising from the use of substituted stilbene comonomers, enchained in an alternating structure with maleic anhydride comonomer, are anticipated to rigidify the polymer chain. Stilbene-containing alternating copolymers open up an interesting family of new polyelectrolytes and other functional copolymers for study. Our previous studies showed the solid-state NMR torsional angle measurements of the maleic anhydride units in a *N,N,N',N'*-tetraethyl-4, 4'-diaminostilbene (TDAS)-maleic anhydride (MAH) alternating copolymer were enchained in a predominately *cis* configuration. This produced a highly contoured polymer chain.[1] SAXS and SEC measurements were conducted to quantify the chain stiffness by determining the persistence lengths of stilbene containing copolymers.[2] It was concluded that stilbene

containing copolymers are a new class of semi-rigid polymers. We also observed that a block copolymer containing a TDAS-MAH polyampholyte block and a poly(methoxy-capped oligo-(ethylene glycol)methacrylate) block exhibited polyion complexes (PICs) with unusual pH and salt responsive properties similar to the "like-charge" attraction effects in rigid polyelectrolytes.[3] In addition films of the alternating copolymers of stilbene and *N*-(2-methylphenyl)maleimide) were found to have a very strong negative birefringence and the corresponding alternating copolymers of styrene and *N*-(2-methylphenyl)maleimide did not show this effect. This significant difference is likely due to conformational constraints arising from the extra phenyl rings of enchained stilbene-maleic anhydride units.[4]

The "precursor" approach with organic soluble "blocked" functional group monomers that can be copolymerized and the non-charged copolymers characterized in normal organic solvents has been reported previously.[5] This avoids the well-known problems that are often encountered with characterizing the molecular weight and molecular weight distributions in charged macromolecules. Our approach enables us to prepare new polyelectrolytes with tunable charges and charge densities.[5] Analogous styrenic copolymers, for comparison to the stilbene structures, have also been prepared.

The research in this chapter is focused on the dilute solution characterization of stilbene- and styrene-containing alternating polyanions. The characterization of these polyanions includes viscosity measurements, a dissociation study and a salt responsive solution study.

5.3. EXPERIMENTAL

5.3.1. Materials

Synthesis of (*E*)-di-*tert*-butyl 4, 4'-stilbenedicarboxylate (DTBSC) and *tert*-butyl 4-vinylbenzoate (TBVB) monomers is described in Chapter 2.

Stilbene and styrenic copolymers were synthesized via free radical polymerization.[5] Copolymer I was synthesized from (*E*)-stilbene (STB) and maleic anhydride (MAH). Copolymer II was composed of (*E*)-di-*tert*-butyl 4,4'-stilbenedicarboxylate (DTBSC) and maleic anhydride (MAH). Copolymer III was based on *tert*-butyl 4-vinylbenzoate (TBVB) and maleic anhydride (MAH). Polymerization of (*E*)-stilbene (STB) and maleic anhydride (MAH) was limited to 5 h in order to avoid the increasing viscosity of the polymer solution observed in the course of 24 h polymerization. The specific procedures for preparing copolymers I, II, III are provided in Chapters 2 and 4. The structures of copolymers I, II, III are shown in Figure 5.1. Copolymer II used in the studies had M_n 40.0 kg/mol and M_w 47.2 kg/mol and M_n 21.6 kg/mol and M_w 31.7 kg/mol (for the polyelectrolyte effect study), determined by SEC in THF. Copolymer III used in the studies had M_n 41.1 kg/mol and M_w 64.6 kg/mol determined in DMF containing 0.1 M lithium nitrate and 1% formic acid as SEC eluent and had M_n 30.0 kg/mol and M_w 54.4 kg/mol for the polyelectrolyte effect study. Copolymer I was not soluble in organic solvents available for SEC measurement and its corresponding polyanion I formed aggregates in the solvents used for aqueous SEC. As a result, it was not possible to measure the molecular weight of copolymer I.

Conversion of polyelectrolyte precursors to their corresponding polyanions is reported in Chapter 2. Structures of the resulting polyanions are shown in Figure 5.2. After copolymers II and III were deblocked by TFA and neutralized in an excess of NaOH solution at 50 ^{o}C for 24 h, polyanions II and III were dialyzed in DI H_2O for 48 h to

remove the excess NaOH. Polyanion I was obtained by neutralization in an excess of NaOH solution at 50 ^{o}C for 24 h followed by dialysis in DI H_2O for 48 h. The polyanion solutions were frozen by immersion of sample vials in liquid nitrogen. The frozen samples were freeze-dried for 24 h on a Virtis lyophilizer to yield white fluffy solids.

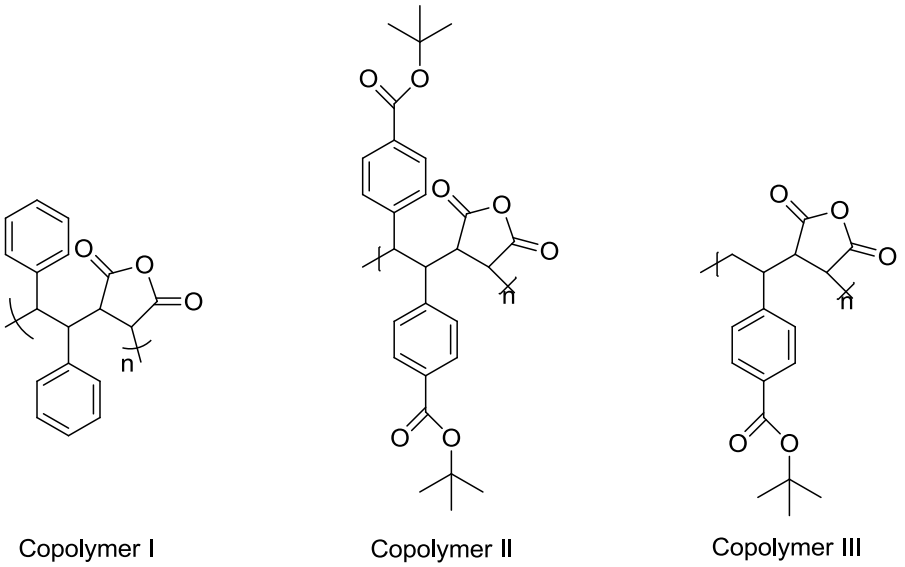

Figure 5.1 The structures of copolymers I, II and III.

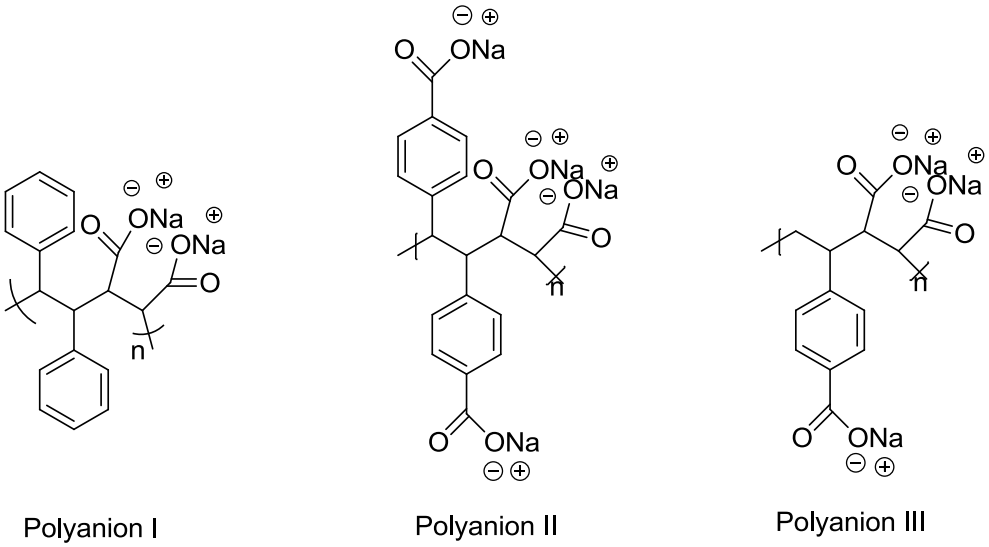

Figure 5.2 The structures of polyanions I, II and III.

5.3.2. Characterization

Molecular weights of the copolymers I, II, and III were determined using a Waters size exclusion chromatograph equipped with a Waters 1515 isocratic HPLC pump, a Viscotek 270 viscosity detector, and a Waters 2414 differential refractive index detector operating at 880 nm and 35 ^{o}C and a Waters 717 plus autosampler, a Wyatt miniDAWN multiangle laser light scattering (MALLS) detector operating a He-Ne laser at 690 nm. The d_n/d_c values were determined using the Wyatt Astra V software package. SEC measurements were performed at 35 °C in THF and DMF containing 0.1 M lithium nitrate and 1% formic acid at a flow rate of 1.0 mL/min. A Virtis lyophilizer (Gardiner, NY) equipped with a drum manifold and a condenser was used at a pressure of <30 mTorr.

Steady-state solution shear rheological experiments were performed with a TA Instruments AR-G2 rheometer at 25 ^{o}C using concentric cylinder geometry. Polyanion II and III in deionized water with NaCl as added salt were analyzed using shear rate sweeps from 0.01 to 1000 s^{-1}. Added NaCl concentrations were 0.l mg/g and 5.0 mg/g of the polymer solution. The lower torque limit was set at 0.01 microN.m.

All pH titrations were carried out with a pH glass electrode in conjunction with a pH meter at room temperature. For each titration of the polyanion ~25 mg was used with the concentration in a range of 1.1~1.4 mg/mL in $CaCl_2$ solution. The concentration of $CaCl_2$ solution used for each titration was 0.02 M. The aqueous HCl titrant (0.0075 M) was delivered into the stirred polymer solution from a 50 mL burette. The pH readings for the solution were stable and accurate to 0.01 pH unit. Dissociation behavior of polyanions I, II, III was studied by backward titration procedures. Titration was performed with HCl as the titrant for hydrolyzed samples that contain sodium carboxylate groups.

Dynamic light scattering (DLS) measurements were performed using a Malvern ALV/CGS-3 compact multi-angle light scattering spectrometer (Malvern Instruments Ltd, Malvern, UK) at a wavelength of 632.8 nm from a 22 mW, solid-state He-Ne laser at a scattering angle of 90°. The experiments were performed at a temperature of 25 °C. The temperature of the samples was equilibrated for at least 2 min before the measurements were taken. Typically, three measurements were acquired for each sample. Hydrodynamic radii R_h are volume averages of three measurements. The concentration of the polymer solution was 0.1 wt %. No filtration or ultrasonication of polymer solutions was applied prior to measurements. DI water was filtered by 0.2-μm filter before use.

5.4. RESULTS AND DISCUSSION

5.4.1. Polyelectrolyte effect

In Figure 5.3, the reduced viscosity (η_{sp}/C) vs. concentration of the polymer solution (C) plots, a strong polyelectrolyte effect was observed in deionized water for polyanions II (the stilbene copolymer) and was suppressed by adding NaCl.[6,7] The reduced viscosity was calculated by using the equation $\eta_{sp}/C = (\eta - \eta_0)/\eta_0 C$, where η is the viscosity at zero shear rate obtained from Figure 5.4. The increasing viscosity indicated that polyanions II backbone changed its conformation upon dilution with a classical polyelectrolyte effect and that this effect was suppressed in the presence of salt. A similar polyelectrolyte effect was also observed for polyanion III (the styrene control copolymers), Figure 5.3. These results are consistent for a polymer with a semi-rigid backbone characterized by previous persistence length measurement,[2] where chain collapse in the presence of added salt and chain expansion on dilution should be observed.

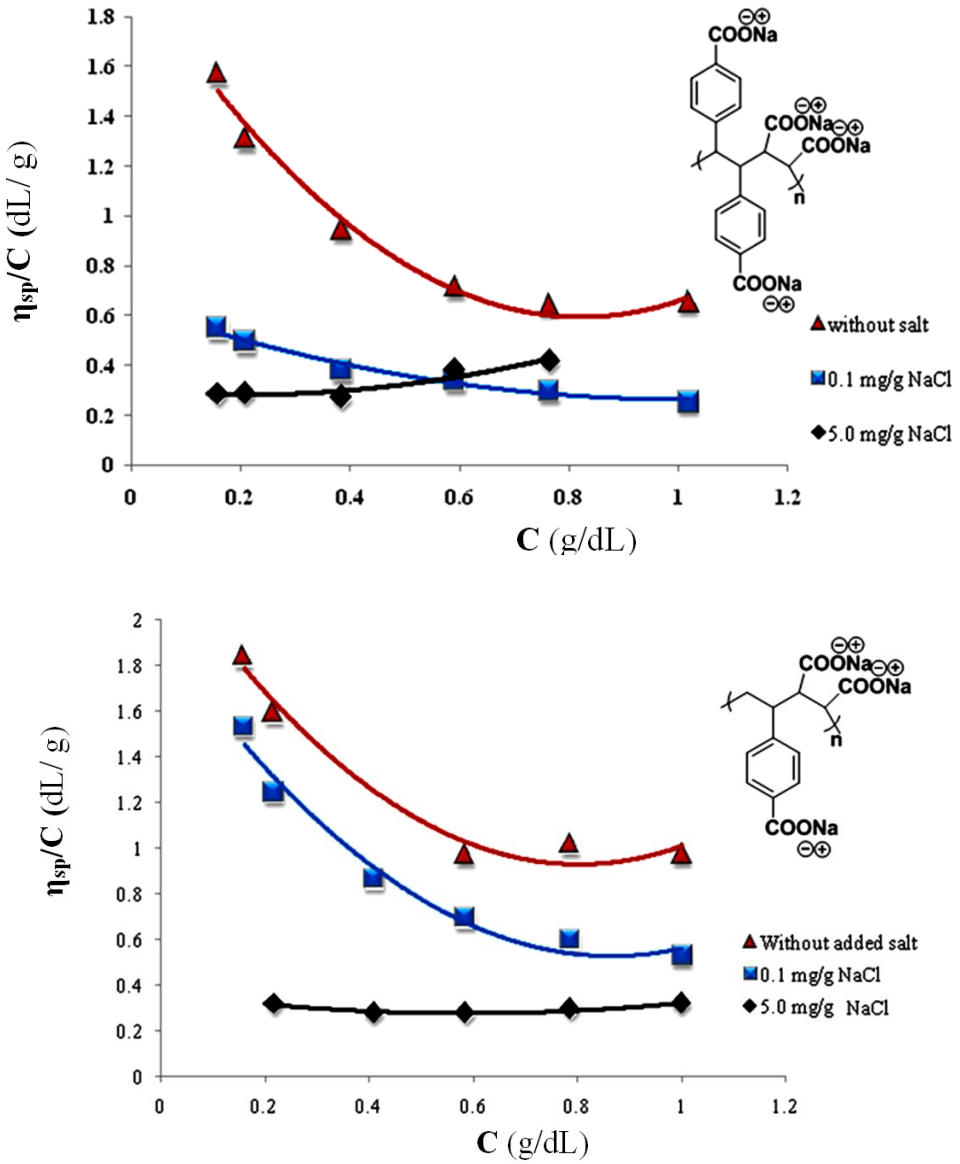

Figure 5.3 Plots of the reduced viscosity vs. concentration for polyanion II (the stilbene copolymer) and polyanion III (the styrene control copolymers).

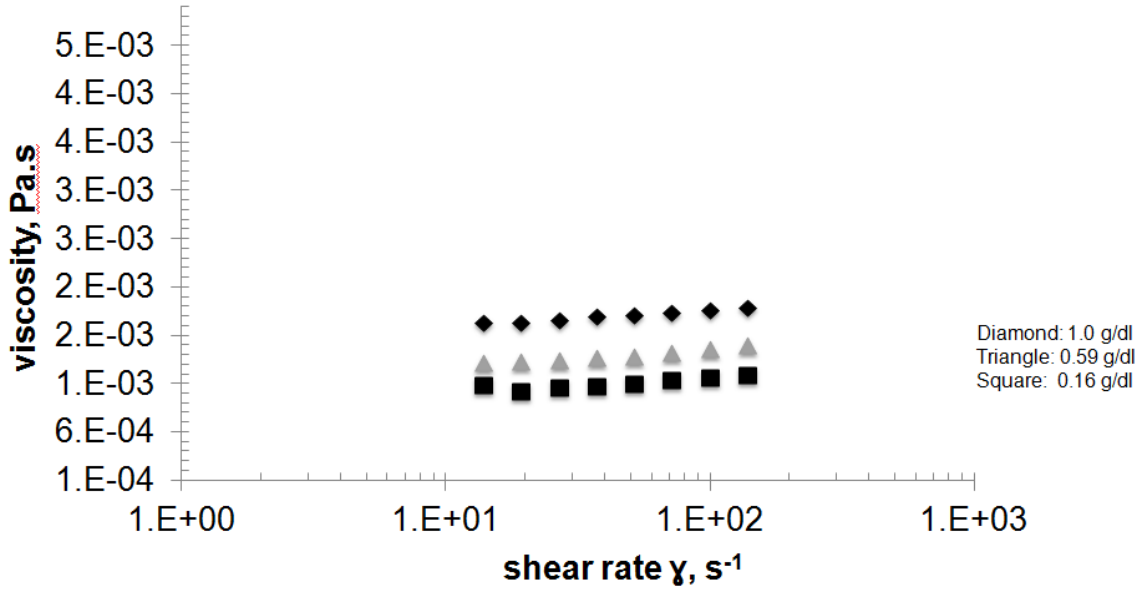

Figure 5.4 Dependence of viscosity on shear rate for polyanion III in deionized water at varying concentrations.

The pH titration curve for polyanions I from the dissociated to the acid form is shown in Figure 5.5. To convert freeze-dried polyanion I into the dissociated form, excess NaOH was added to adjust the solution pH to ~11 initially. In the presence of 0.02 M $CaCl_2$, two distinct inflection points for this sample can be identified in the curve, corresponding to the dissociation of the two carboxylic acid groups in the maleic acid comonomer.

A brief review of several model dicarboxylic acids may facilitate characterizing and evaluating the dissociation behavior of polyanions I, II and III. As shown in Table 5.1, model dicarboxylic acid compounds including succinic acid (4.16, 5.61), maleic acid (1.83, 6.07) and fumaric acid (3.03, 4.42) were studied using pH titration.[8] pK_1 and pK_2 values of maleic acid are far apart from each other, while those for fumaric acid and succinic acid are close to each other. On the corresponding titration curves maleic acid (*cis*-configuration) exhibited two-step dissociation behavior, while fumaric acid (*trans*-

configuration) only showed a single dissociation. It was stated by Colby et al. that the absence of the two-step titration curve is attributed to the closeness of two pKs, and is indicative of the absence of interference of the two acids.[8] Colby et al. also studied the dissociation behavior of a series of maleic acid containing copolymers.[8] In Figure 5.6, the pH titration in water for poly(isobutylene-*alt*-maleic acid) (IBMA) is shown as curve (1) with only one inflection point, but with two distinct inflection points in 0.02 M $CaCl_2$ solution in curve (2). This two step behavior corresponds to the dissociation of the two carboxylic acid groups in the maleic acid comonomer. The dissociation behavior of IBMA was sharpened by addition of $CaCl_2$ to the polymer solution.

In Figure 5.5, two distinct inflection points were observed, indicating that the two carboxylic acids from maleic acid comonomer are in close proximity and influence each other, i.e., the ionization of the first carboxylic acid can impose steric and electrostatic hindrance on the ionization of the second carboxylic acid.[8]

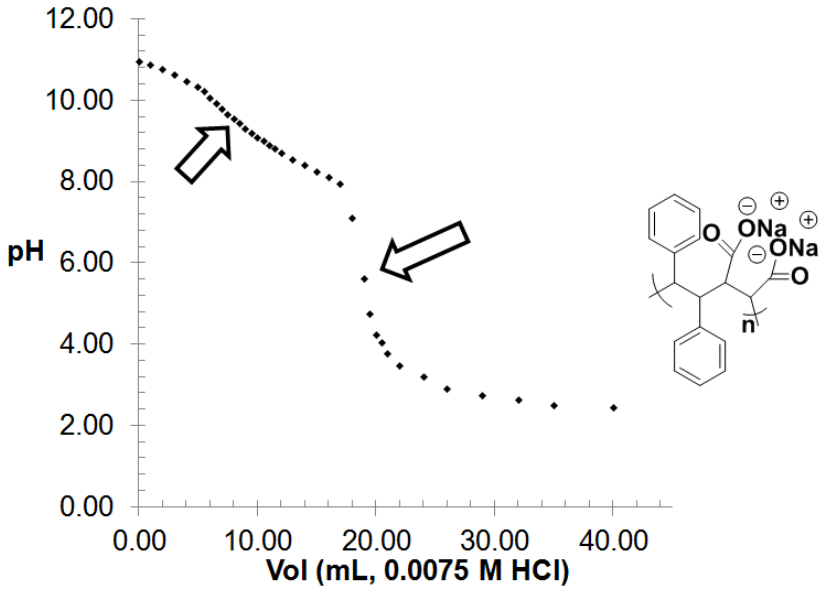

Figure 5.5 Titration curve of polyanion I (25.5 mg) in $CaCl_2$ solution (18 mL, 0.020 M) with excess NaOH (0.10 M, 1.1 mL).

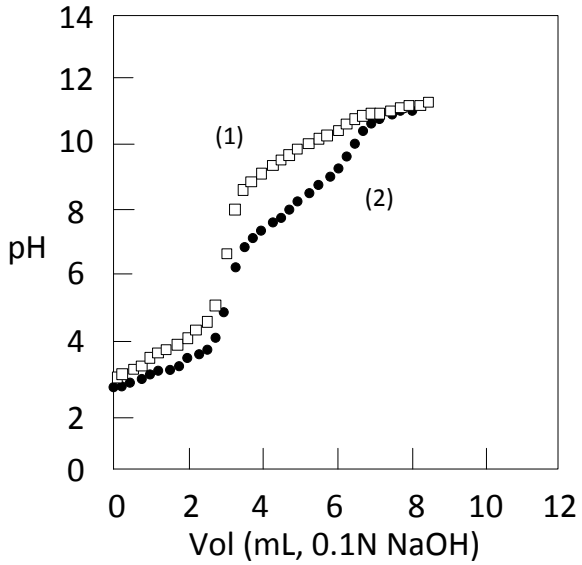

Figure 5.6 pH titrations for IBMA: curve (1) sample in water; curve (2) sample in 0.02 M $CaCl_2$.[3]

Table 5.1 pK_1 and pK_2 for dicarboxylic acids.

	(pK_1, pK_2)
succinic acid	(4.16, 5.61)
maleic acid	(1.83, 6.07)
fumaric acid	(3.03 4.42)

Similar two-step dissociation behavior of the two carboxylic acid groups in the maleic acid comonomer was also observed for polyanion II and polyanion III, Figures 5.7 and 5.8. A third inflection point was also observed for polyanions II and III, corresponding to the dissociation of benzoic acid groups.

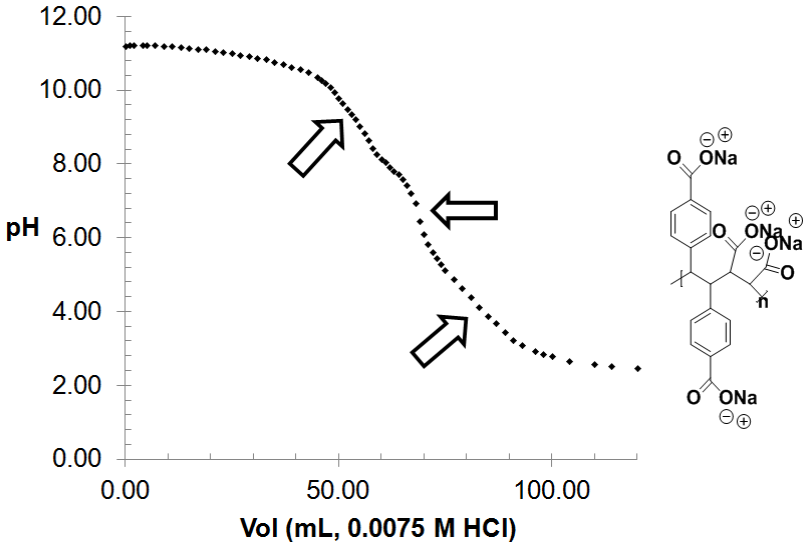

Figure 5.7 Titration curve of polyanion II (25.5 mg) in $CaCl_2$ solution (24 mL, 0.020 M) with excess NaOH (0.10 M, 6.8 mL).

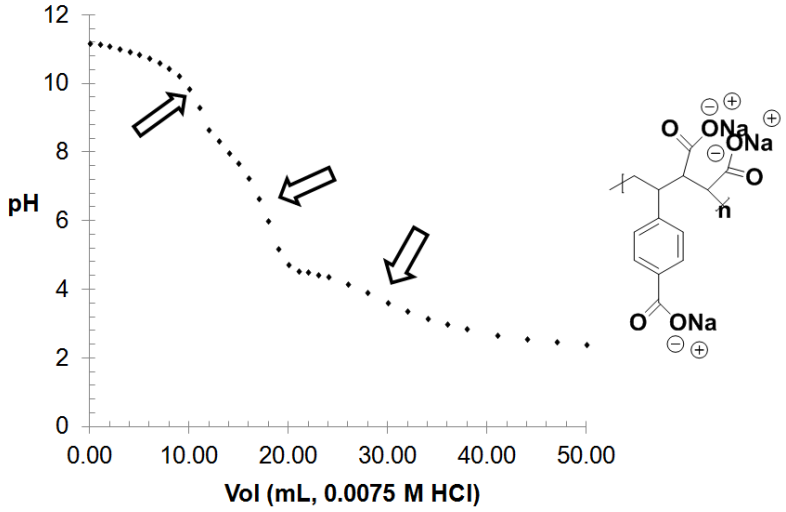

Figure 5.8 Titration curve of polyanion I (24.3 mg) in $CaCl_2$ solution (18 mL, 0.020 M) with excess NaOH (0.10 M, 1.3 mL).

5.4.2. Salt responsive polymer solution

From DLS measurements, up to ~100 nm R_h values were observed for polyanions I, II and III in deionized water without addition of salt, shown in Figure 5.9. Upon adding 0.05 M salt, the R_h values of the polyanions were lower than 10 nm. Upon increasing the salt concentration to 0.1 M, the R_h of the polyanions remained under 10 nm. With 1.0 M

salt added to polymer solutions, the R_h of polyanions II and III remained the same, while the R_h of polyanion I increased to ~1000 nm indicating that large aggregates formed in solution. As the salt concentration was increased to 2.0 M, the R_h of polyanions II and III also increased to ~1000 nm and the size of aggregates in polyanion I solution remained the same. In DLS study, NaOAc was used as additional salt because it is more hydrophobic than NaCl and facilitates the hydrophobic interactions of the polymer chains.

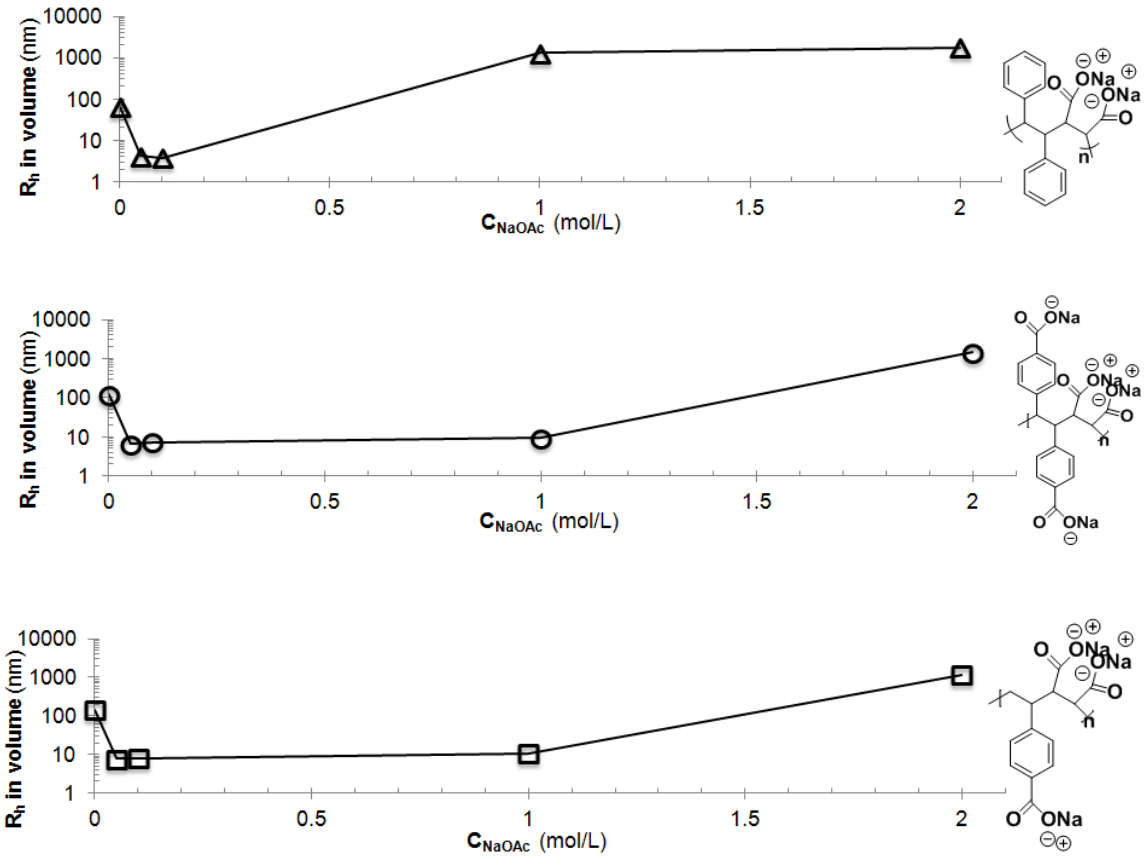

Figure 5.9 Dependence of R_h on concentration of salt, C_{NaOAc} for polyanions I, II and III.

These experimental results can be explained by polymer chain interactions, as depicted in Figure 5.10.[9-18] In aqueous media, stilbene-containing polyanions are highly expanded to behave like rigid rods due to electrostatic repulsion. The separation distance

is smaller than the debye length and therefore the polmer solution at 1 mg/mL is in concentrated regime. As the small amount of salt added to the polymer solution, some fraction of the charges along the polymer chain get screened by additional salt and the chain is prone to adopt a coil-like conformation with a more hydrophobic core formed inside and the more hydrophilic shell formed outside. The hydrophilic shell can help avoid aggregation due to electrostatic repulsion. Such a system, however, is very sensitive to the varying ionic strength. A rise in salt concentration suppresses the stabilizing effect of the hydrophilic shell because of the more effective screening of the anionic charges by small ions. As a result, the formation of high levels of aggregation is facilitated.

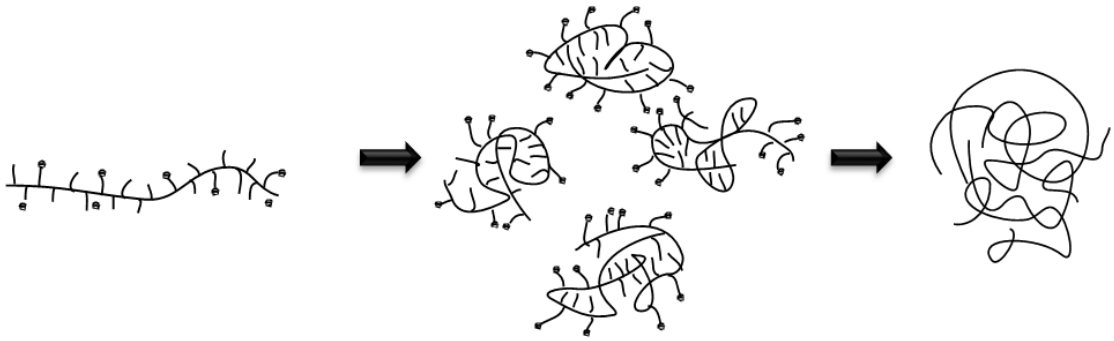

Figure 5.10 Representative polymer chains in solution at increasing salt concentrations.

The three curves in Figure 5.9 were superimposed on top of each other, as shown in Figure 5.11. It was observed that polyanion I is more prone to form aggregates at lower salt concentration compared to its analogs, polyanion II and III. This is probably due to the more hydrophobic nature of polyanion I.

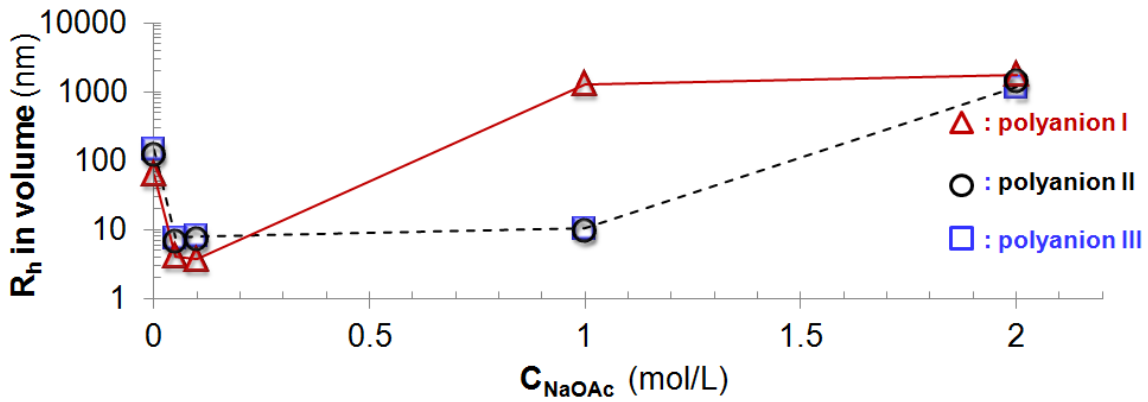

Figure 5.11 Superimposed R_h vs. C_{NaOAc} curves of polyanions I, II and III.

5.5. SUMMARY

Copolymers I, II and III were readily converted into their corresponding anionic polyelectrolytes via deprotection reactions. From dilute solution viscosity study, a pronounced "polyelectrolyte effect" was observed due to the chain collapse in the presence of added salt and chain expansion on dilution which is in a good agreement with the backbone of a flexible or semi-rigid polyelectrolyte. A two-step dissociation behavior was observed for the two carboxylic acids from maleic acid comonomer of polyanion I, II and III. This indicated that two acid groups are in close proximity to exert influence on each other. Salt responsive polymer solutions were investigated by using DLS at varying ionic strengths. It was found that the solutions of polyanion I, II and III are in concentrated regime at 1 m/mL. The addition of salt led to a decrease of R_h values and then facilitated the formation of a high level of aggregates at increasing the ionic strength.

REFERENCES

(1) Mao, M.; Kim, C.; Wi, S.; Turner, S. R. *Macromolecules* **2007**, *41*, 387.

(2) Li, Y.; Zhang, M. Q.; Mao, M.; Turner, S. R.; Moore, R. B.; Mourey, T.; Slater, L. A.; Hauenstein, J. R. *Accepted by Macromolecules*.

(3) Mao, M.; Turner, S. R. *J. Am. Chem. Soc.***2007**, *129*, 3832.

(4) Mao, M.; England, J.; Turner, S. R. *Polymer* **2011**, *52*, 4498.

(5) Li, Y.; Mao, M.; Matolyak, L. E.; Turner, S. R. *ACS Macro Lett.* **2012**, 257.

(6) Fernandes, A. L. P.; Martins, R. R.; da Trindade Neto, C. G.; Pereira, M. R.; Fonseca, J. L. C. *J Appl Polym Sci* **2003**, *89*, 191.

(7) Turner, S. R.; Wardle, R.; Thaler, W. A. *J. Polym. Sci.: Polym. Chem. Ed.* **1984**, *22*, 2281.

(8) Sauvage, E.; Amos, D. A.; Antalek, B.; Schroeder, K. M.; Tan, J. S.; Plucktaveesak, N.; Colby, R. H. *J. Polym. Sci. Part B: Polym. Phys.* **2004**, *42*, 3571.

(9) Dautzenberg, H.; Hartmann, J.; Grunewald, S.; Brand, F. *Ber. Bunsen Ges. Phys. Chem.* **1996**, *100*, 1024.

(10) Dautzenberg, H. *Macromolecules* **1997**, *30*, 7810.

(11) Dautzenberg, H.; Gao, Y.; Hahn, M. *Langmuir* **2000**, *16*, 9070.

(12) Dautzenberg, H.; Jaeger, W. *Macromol Chem Physic* **2002**, *203*, 2095.

(13) Izumrudov, V. A.; Gorshkova, M. Y.; Volkova, I. F. *Eur. Polym. J.* **2005**, *41*, 1251.

(14) Pergushov, D. V.; Buchhammer, H. M.; Lunkwitz, K. *Colloid Polym. Sci.* **1999**, *277*, 101.

(15) Nyström, R. S.; Rosenholm, J. B.; Nurmi, K. *Langmuir* **2003**, *19*, 3981.

(16) Ueda, M.; Hashidzume, A.; Sato, T. *Macromolecules* **2011**, *44*, 2970.

(17) Zhunuspayev, D. E.; Mun, G. A.; Hole, P.; Khutoryanskiy, V. V. *Langmuir* **2008**, *24*, 13742.

(18) Di Cola, E.; Plucktaveesak, N.; Waigh, T. A.; Colby, R. H.; Tan, J. S.; Pyckhout-Hintzen, W.; Heenan, R. K. *Macromolecules* **2004**, *37*, 8457.

Chapter 6. FUTURE WORK

6.1. INTRODUCTION

Human immunodeficiency virus (HIV) disease is a world-wide problem. Each year there are 4 million new HIV infections.[1] Women are physiologically and socially twice as likely to be infected with HIV as men. During the last decade significant advances have occurred in prevention of HIV infection. Noteworthy is the development of anti-HIV drugs acting through various ways, such as non-specific[1-7] and moderately specific microbicides active against several sexually transmitted pathogens or having a spermicidal effect,[8-29] and highly HIV-specific microbicides active only against HIV.[30-47] Most recently, much work has focused on anionic polymeric drugs inhibiting HIV entry, such as sulfate esters of polysaccharides (dextrin/dextran sulfates, cellulose sulfate, and carrageenans), aryl sulfonates (poly(styrene-4-sulfonate and poly(naphthalene sulfonate)/PRO 2000), and aliphatic (Carbomer 9748/BufferGel™) and aromatic carboxylates (cellulose acetate phthalate (CAP)), as shown in Figure 6.1.[48]

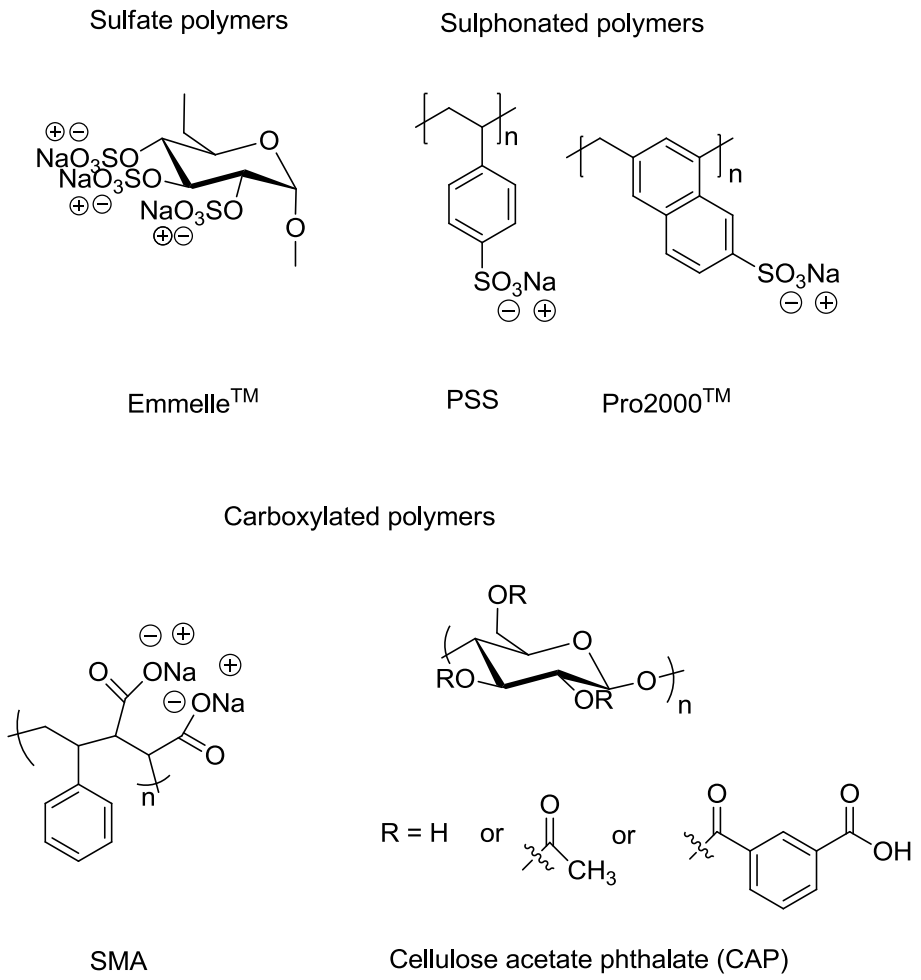

Figure 6.1 Structures of anionic polymeric drugs.

After sexual exposure to HIV, the virus attacks a particular type of white cells called CD4+. The virus uses the CD4+ cells to replicate themselves to infect more cells and the cells eventually die. The whole virus replication process, as shown in Figure 6.2, includes (1) viral entry into the host cell, and then (2) viral replication inside the host cell, followed by (3) viral assembly, and finishing with (4) budding and maturation of HIV virion.

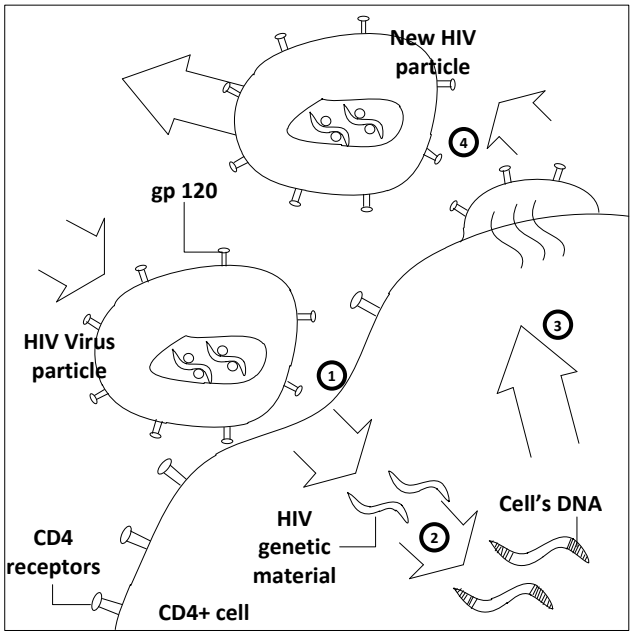

Figure 6.2 Schematic representation of HIV replication cycle in human cells. Retrieved from website: http://twin-science.blogspot.com/.

Anionic polymers with antimicrobial activities are designed to block the viral entry to inhibit the HIV infection. When HIV invades the normal human CD4+ cells, the viral envelope glycoprotein, gp120, binds to the host cell at a CD4 receptor site located outside the cell membrane. This causes a conformational change in gp120 to further expose the glycoprotein gp41, which facilitates HIV fusion into the host cell and thus to infect the cell (Figure 6.3). Glycoprotein gp120 of HIV is positively charged and charges are from the positively charged proteins, like arginine. The receptors on the host cell CD4 are negatively charged and charges are from the positively charged proteins, like glutamic acid. The electrostatic interactions between the positively charged virus and negatively charged host cell facilitate the HIV infection.[49] Before this binding occurs anionic polymer drugs can interact with the positively charged groups on the glycoprotein (gp120) through ionic interactions and therefore block the viral entry and inhibit the HIV infection, Figure 6.4.[50]

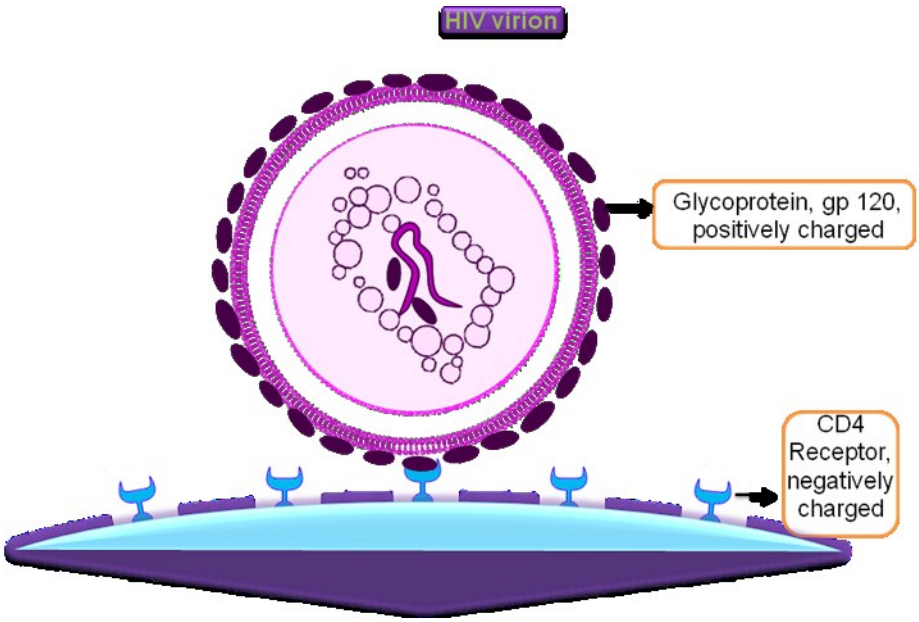

Figure 6.3 HIV infection mechanism.

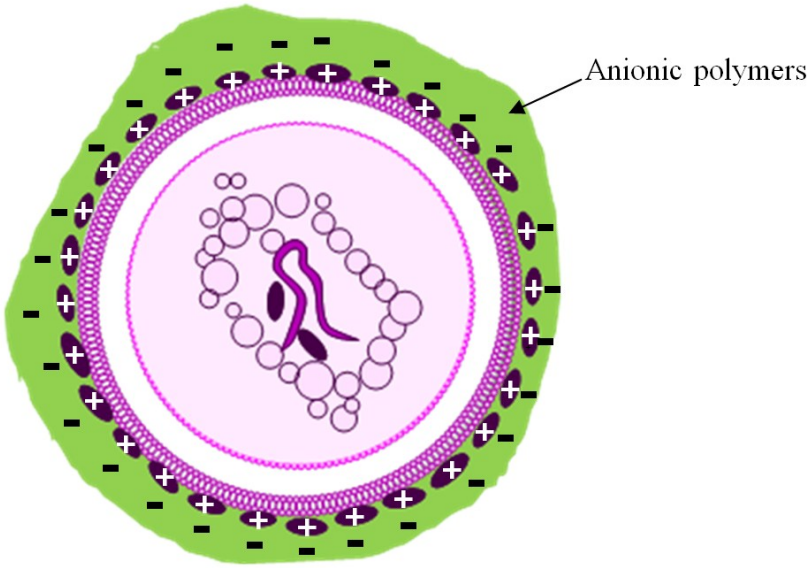

Figure 6.4 Schematic representation of interactions between HIV and anionic polymers.[50]

When the first report on the inhibitory effect of polyanionic materials on the replication of the herpes simplex virus and other viruses was published about five decades ago,[51] it received little interest because the antiviral action of the compounds was considered nonspecific.[51] Suramin, a polysulfonate salt, , was reported to exhibit potent

anti-HIV activity in 1984, Figure 6.5.[52] This result combined with the increasing number of AIDS diagnoses in the early 1980s generated great research interest on the study of anionic polymeric drugs with anti-microbial activities. Numerous synthetic and natural anionic polymers have been examined as potential microbicides candidates for prevention of HIV infection.

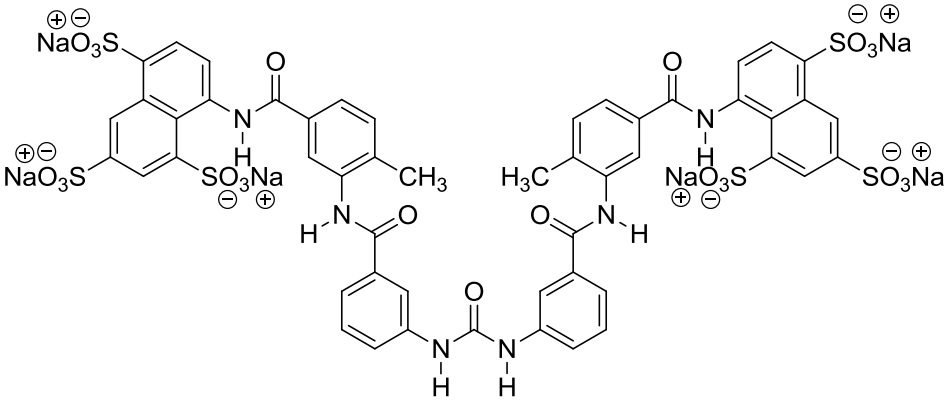

Figure 6.5 Chemical structure of Suramin.[52]

Despite the effective prevention on binding between the virus and its target human cell, generally high concentrations of these anionic substances need to be used to prevent the transmission of HIV from virus-infected human cells to uninfected normal cells.[8,9] Besides of possible toxic side effects, the use of anionic polymers has also been limited by their pharmacological properties (short plasma half-life, partial inactivation by plasma components, and a poor ability to penetrate infected tissues and cells), which result in a low bioavailability and hence poor antiviral activity *in vivo*.[53] Even with these disadvantages, anionic polymers have been actively pursued as anti-HIV microbicides.

Dextran sulfate, a sulfated polymer, was the first discovered polysaccharide with anti-HIV activity.[54,55] Currently sulfated polysaccharides are a class of well-established potent

inhibitors for HIV replication, including heparin, dextran sulfate, pentosan polysulfate, cellulose sulfate, and lentinan sulfate.[54-58]

The sulfate groups ($-OSO_3^-M^+$) can undergo hydrolysis to release SO_4^{2-} by sulphatases (enzymes) present in the vaginal ecosystem, leading to inactivation of the compounds.[13,59] It is possible the enzymatic activity of bacterial sulphatases greatly affects the antiviral activity of polymers containing sulfate groups during a limited time (a few hours). The antiviral activity of sulfated polymers is dependent on the density and distribution of the sulfate groups, molecular weight, and conformational factors related to the distribution and sequence of the substituents. In order to achieve high anti-HIV activity, a minimum molecular weight of 3,000 and an average of at least two sulfate groups per monosaccharide unit are necessary based on studies of different sulfated polysaccharides.[60] Sulfated polysaccharides have been shown effective at concentrations as low as 0.01 μg/mL and noncytotoxic up to 2.5 mg/mL.[51] An undesirable side effect of many sulfated polysaccharides is high blood anticoagulant activities.[53]

Synthetic anionic polysaccharide derivatives have been designed to possess the antiviral activity characteristic of natural polysaccharides, while minimizing the undesirable anticoagulant side effects. Derivatized dextrans with varying percentages of carboxymethyl, sulfonate, benzylamide, and benzylamide sulfonate substituents were synthesized and investigated for antiviral activity.[61] For example, dextrin 2-sulfate (D2S) (Emmelle™) exhibited potential topical microbial activity in Phase I and II clinical trials.[62] Other synthetic sulfated polysaccharide derivatives under investigation as anti-HIV microbicides are sodium cellulose sulfate (Ushercell™), carrageenans (Carraguard™),[63] sodium cellulose sulfate (NaCS), and sulfated derivatives of the

Escherichia coli K5 polysaccharide. Among these sulfated polysaccharide derivatives, more recently developed K5 polysaccharide exhibited low IC_{50} values (0.07~0.46 μM), low cytotoxicity and absence of anticoagulant activity. [277-279]

Sulfonated polymers have also proven highly effective as *in vitro* HIV inhibitors. Different than the sulfate groups, the sulfonate ($-SO_3^-M^+$) groups are linked to the polymers via a stable carbon-sulfur bond and are highly metabolically stable.[47] For example, sodium poly(styrene sulfonate) (PSS) exhibited broad-spectrum *in vitro* activity against HIV, human papillomavirus (HPV), HSV-1, HSV-2, Chlamydia trachomatis, and Neisseria gonorrhoeae.[64-66] The limitations on using PSS as microbicide are the high concentrations necessary to achieve anti-HIV activity in cultured cells, their well known property to bind serum proteins, and marked anticoagulating activity.[63] PRO 2000, a synthetic naphthalene sulfonic acid-formaldehyde copolymer, is also an effective anti-HIV microbicide.[67] PRO 2000™ Gel comprising a lactate buffer system, a carbomer, and a naphthalene sulfonate, was found to be safe and effective in Phase III clinical trials.[68]

Cellulose acetate phthalate (CAP), a polycarboxylate, has been investigated in advanced clinical trials as a potential microbicide[63] and has been shown to be virucidal against HIV and herpes viruses, and also inhibitory to pathogens of the genital tract.[47] CAP was considered safe for repeated use, showing no evidence of penetration into cells nor any adverse effect on affecting vaginal pH. More recently, a study of poly(styrene-*alt*-maleic anhydride) derivatives showed that these copolymer microbicides as the sodium salts are 100-times more potent than dextran sulfate based on an *in vitro* cellular assay (Figure 6.6).[69,70] Mpitso et al. synthesized poly(styrene-*alt*-

maleic anhydride) and its derivatives (Figure 6.7) for antiviral activity study.[71] However, they did not report any results related to the antiviral activity of these copolymers. Bellettini et al. studied the effect of molecular weight of the polymer on antiviral activity.[72] It was found that both sodium poly(styrene sulfonate) and sodium styrene sulfonate-maleic acid copolymer showed the highest antiviral activity when the molecular weight is approaching 4.6 kg/mol.

Besides polysulfate, polysulfonate and polycarboxylate, inorganic polyphosphates have been tested to possess antibacterial and anti-HIV activity.[73-78] Synthetic polynucleotides poly(A)-poly(U)[79] and poly(I)-poly(C)[80] represent a second class of polyphosphates exhibited anti-HIV activity[81].

Some dendrimers containing negatively charged groups have also been shown to interfere with HIV entry. They can also be considered as potential anti-HIV drug candidates.[82,83] An example is shown in Figure 6.8.

Many polyanion candidates, like PRO 2000™, CAP and Carraguard™, passed Phases I and II clinical trials but all failed in Phase III due to the low efficacy. Some scientists believed this signaled the end of polyanions as anti-HIV microbicides. However, it is believed that the study of existing polyanions will help understanding clinical failures and the difference between in *vitro* and in *vivo* results. In addition, the pursue of new polyanion microbicide candidates will further this understanding. Investigation of molecular structures and charge densities of polyanioin candidates is of great importance for microbicide applications.[84]

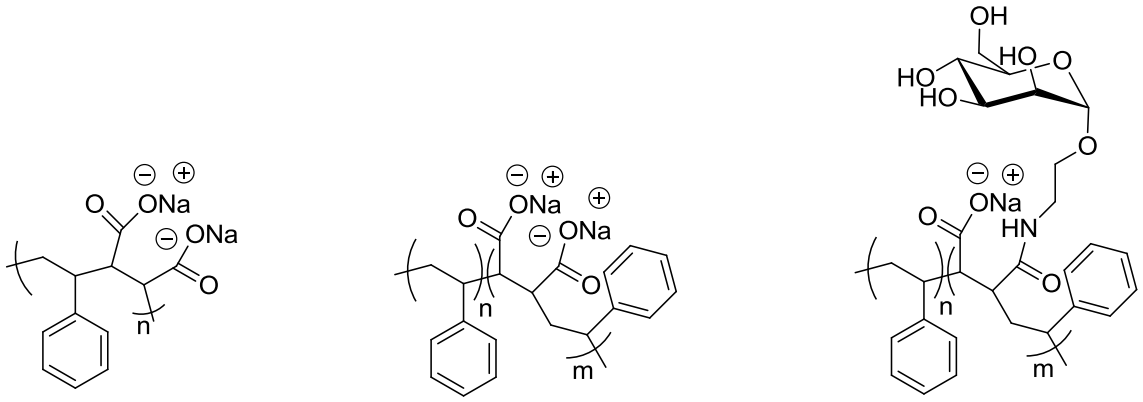

Figure 6.6 Examples of poly(styrene-*alt*-maleic anhydride) derivatives.[69,70]

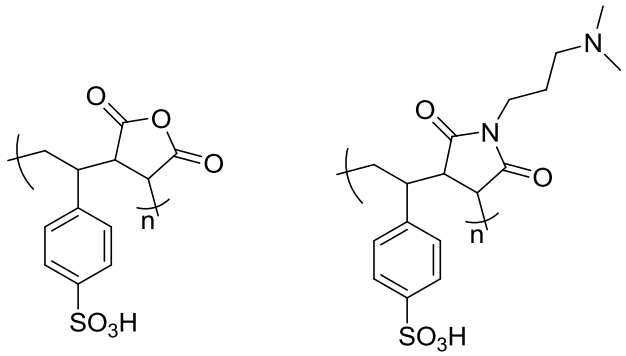

Figure 6.7 Poly(styrene-*alt*-maleic anhydride) derivatives synthesized by Mpitso et al..[71]

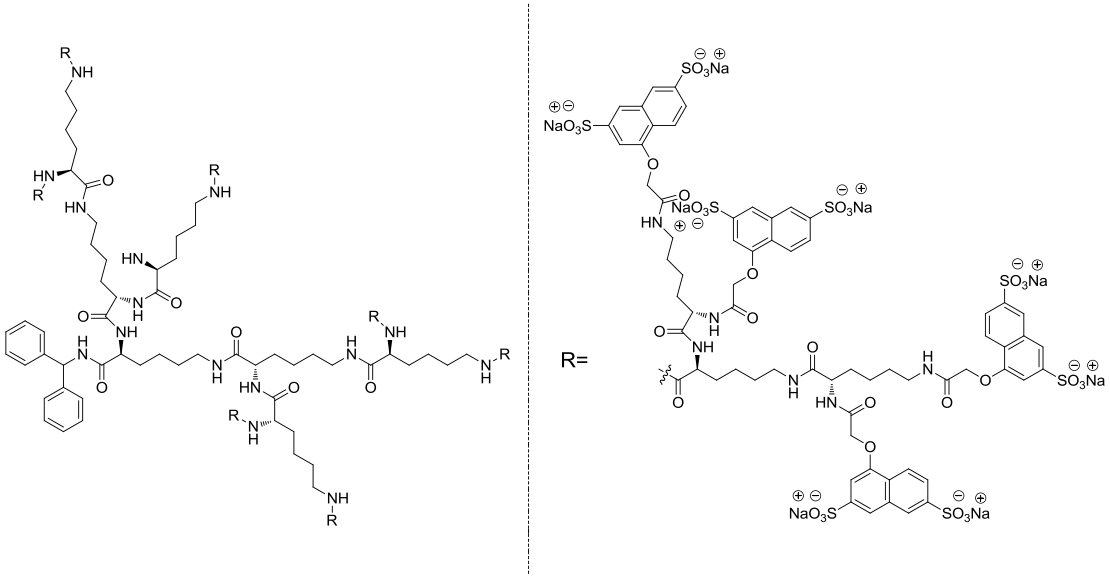

Figure 6.8 Example of antimicrobial dendrimers.[82,83]

Our research focuses on microbicides that are alternating copolymers with carboxylate groups or sulfonate groups that are negatively charged. The antimicrobial activity of the polyanion (Figure 6.9) based on sodium 4-styrenesulfonate and *N*-(4-sodium sulfopheny1)maleimide was found to be ~50 times higher than sodium poly(styrene sulfonate) (PSS). This result suggests that this alternating copolymer architecture, with the high density of ions and the chain stiffness features, may lead to the enhanced antimicrobial activity.

Since it is known that alternating polyanions of styrene and maleic acid exhibited the potent antimicrobial activity (Figure 6.6), we initiated a preliminary study of the antimicrobial activity of our carboxylated polyanion samples. We also attempted to synthesize methyl sulfonate ester-functionalized stilbene containing polyanion precursors, because these protected sulfonated polyanions dissolve in common organic solvents and can be characterized without complications caused by charged sulfonate groups.

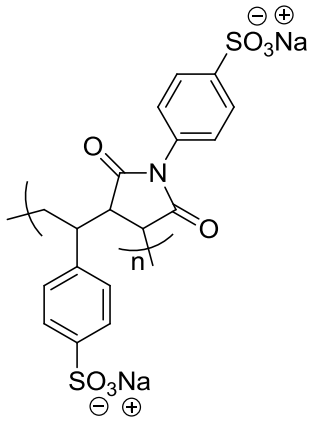

Figure 6.9 Representative sulfonated polyanion.

6.1.1. Materials

Maleic anhydride (MAH, Aldrich, ≥99.0%), potassium *tert*-butoxide solution 1.0 M in tetrahydrofuran (KO^{t}Bu, Aldrich), *tert*-butanol (HO^{t}Bu, Sigma-Aldrich, anhydrous,

≥99.5%), *N*-bromosuccinimide (NBS, Aldrich, 99%), *p*-toluic acid (Aldrich, 98%), formaldehyde (Aldrich, 37 wt. % in H_2O), triphenylphosphine (Sigma-Aldrich, 99%), thionyl chloride ($SOCl_2$, Fluka, ≥99.0%), acetic anhydride (Sigma-Aldrich, ≥98.0%), sodium acetate (Sigma-Aldrich, ≥99.0%), *4*-aminobenzoic acid (Sigma, ≥99.0%), *2,2*'-azobisisobutyronitrile (AIBN, Aldrich, 98%), dicumylperoxide (DCP, Aldrich, 98%), ammonium persulfate (APS, Aldrich), 2-cyano-2 propyl dodecyl trithiocarbonate (Aldrich), trifluoroacetic acid (TFA, Aldrich, 99%), sodium hydroxide (NaOH, Sigma-Aldrich, ≥98.0%) were used as received. (*E*)-Dimethyl-*4,4'*-stilbenedicarboxylate (DMSC) was received as a donation from Eastman Chemical Company. Tetrahydrofuran (Sigma-Aldrich, anhydrous, ≥99.9%), hexanes (Fisher, HPLC grade), methylene chloride (CH_2Cl_2, Fisher, HPLC grade), diethyl ether (Fisher, HPLC grade), toluene (Fisher, HPLC grade), chlorobenzene (Sigma-Aldrich, anhydrous, ≥99.8%), benzene (Sigma-Aldrich, anhydrous, ≥99.8%), and acetone (Fisher, HPLC grade) were used without further purification. Water was deionized before use.

6.1.2. Instrumental Characterization

^{1}H NMR spectra and ^{13}C NMR spectra were determined at 25 °C in deuterated solvents at 400 MHz with a Varian Unity spectrometer or 500 MHz with a Jeol Eclipse +500 spectrometer. Melting points of monomers were measured on uncorrected BUCHI Melting Point B-540 instrument at a heating rate of 0.5 ^{o}C/min. Molecular weights were determined using a size exclusion chromatograph equipped with a viscosity detector and a laser refractometer detector in chloroform at 30 ^{o}C. Data were analyzed utilizing a universal calibration made with polystyrene standards to obtain absolute molecular

weights. A Virtis lyophilizer (Gardiner, NY) equipped with a drum manifold and a condenser was used at a pressure of <30 mTorr.

6.1.3. Monomer Synthesis

Synthesis of (*E*)-di-*tert*-butyl 4,4'-stilbenedicarboxylate (DTBSC), *tert*-butyl 4-vinylbenzoate (TBVB), *tert*-butyl 4-maleimidobenzoate (TBMIB) is described in Chapter 2.

Synthesis of Sodium 4, 4'- distilbenesulfonate (SDSS)

Step 1 of Scheme 1: To prepare *p*-sulfocinnamic acid and its sodium salt, [85,86] finely ground cinnamic acid (5.0 g, 34 mmol) was slowly added to fuming sulfuric acid (18% anhydride, 15 mL) cooled in an ice bath. With vigorous stirring reaction temperature was kept less than 35 ^{o}C. After the addition was completed, the reaction mixture was stirred at room temperature for about 30 min. After this, the reaction solution was carefully poured into the ice water. The precipitate was filtered and recrystallized from 25% sulfuric acid solution. Yield is 45%, 3.5 g. The white crystalline product was dried room temperature for 24 h. The ^{1}H NMR was conducted in D_2O, shown in Figure 6.10. Lit. Mp: 82 ^{o}C.[86]

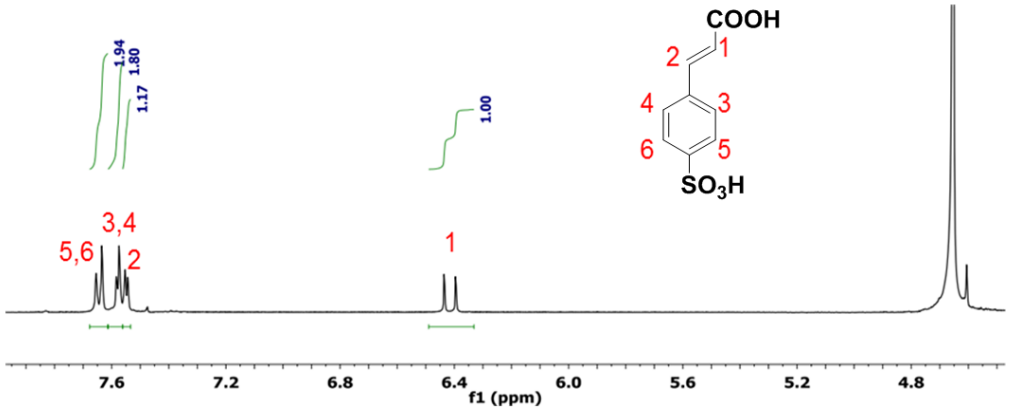

Figure 6.10 500/125 Hz ^{1}H NMR spectrum of *p*-sulfocinnamic acid in D_2O.

Step 2 of Scheme 1: To prepare the diazonium solution, a mixture of 4-aminobenzenesulfonic acid (0.82 g, 4.7 mmol), $NaNO_2$ (0.33 g, 4.72 mmol), Na_2CO_3 (0.25 g, 3.0 mmol), and H_2O (5.2 mL) was cooled in an ice bath for 15 min. 0.93 mL of concentrated HCl (37 wt %) was added dropwise to the vigorously stirred mixture to keep the temperature under 10 ^oC.[87] The diazonium solution was used in the following step right after the preparation without further characterization.

Step 3 of Scheme 1: To prepare sodium 4, 4'-distilbenesulfonate, the diazonium solution prepared in Step 2 was added slowly to a mixture of *p*-sulfocinnamic acid (1.08 g, 4.72 mmol), Na_2CO_3 (0.50 g, 4.7 mmol), NaOAc (2.71 g, 33.0 mmol) and H_2O (10.7 mL). After addition, a solution of $CuCl_2$ (0.25 g) in 2 mL of H_2O was added to the reaction solution and heated to boiling and saturated with NaCl. The reaction solution was cooled to room temperature and a brownish powder solid was precipitated and filtered. Yield is 45%, 0.82 g. ^1H NMR was conducted in D_2O, shown in Figure 6.11. Melting point of this compound was not reported in the related publication.[87]

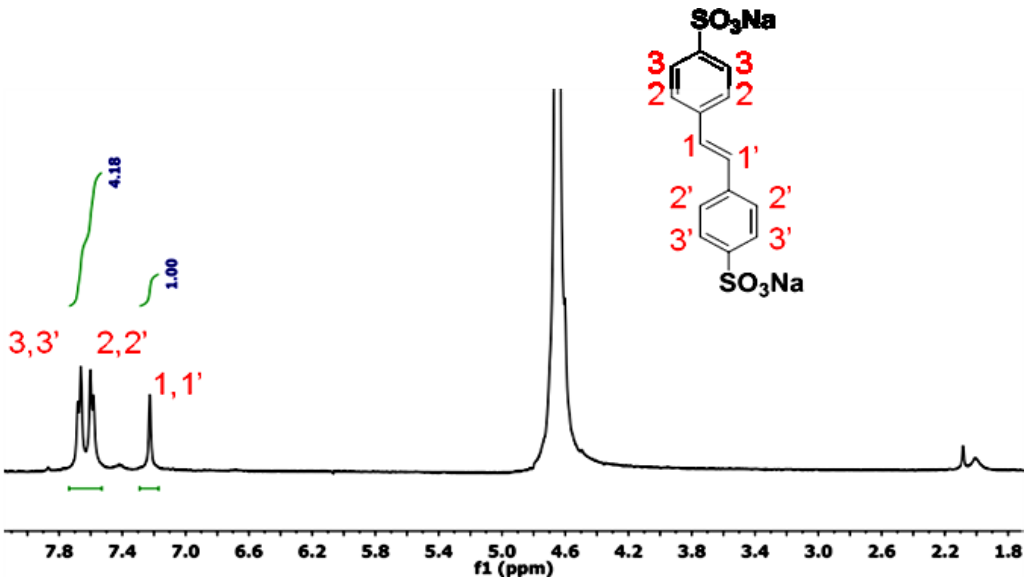

Figure 6.11 500/125 Hz ^1H NMR spectrum of sodium 4, 4'- distilbenesulfonate in D_2O.

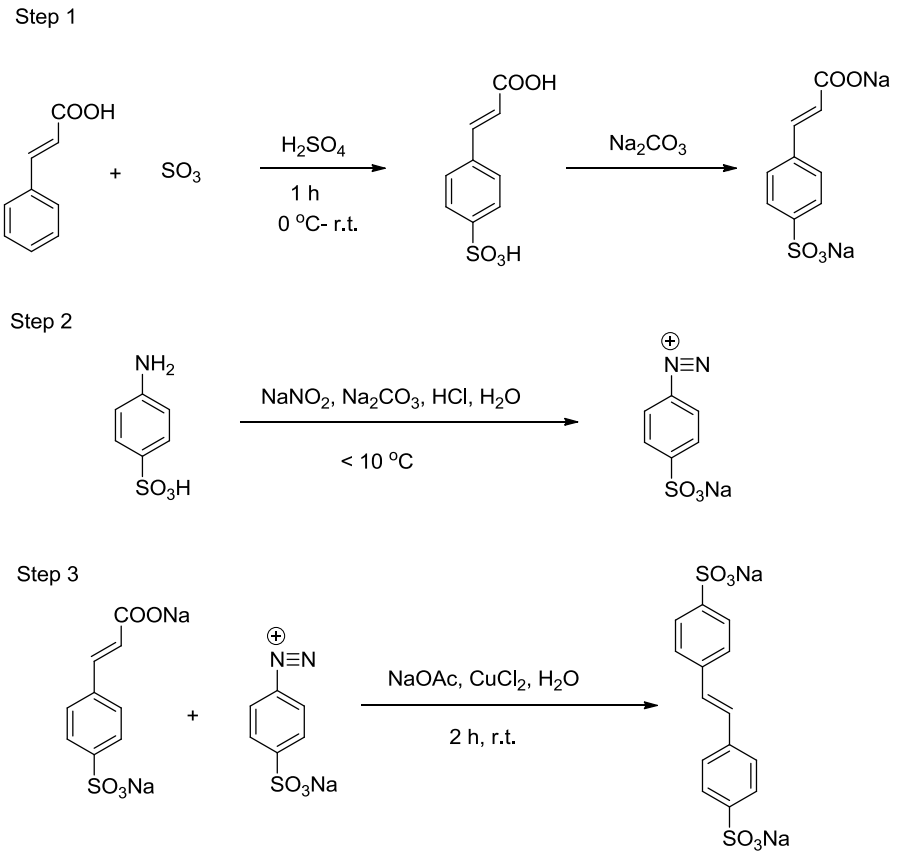

Scheme 6.1 Synthesis of sodium 4, 4'- distilbenesulfonate.

Synthesis of ethyl styrene-4-sulfonate

To prepare ethyl styrene-4-sulfonate,[88] a solution of sodium styrene sulfonate (2.06 g, 10 mmol), in water (15 mL) was cooled in an ice bath for 10 min. A solution of $AgNO_3$ (1.87 g, 11.0 mol) in water (5 mL) was added dropwise to the mixture. Considerable efforts were taken to exclude light from all further manipulations of the product. The mixture was stirred for 2 h and the precipitate was filtered off and washed with H_2O and with Et_2O. The solid was then re-dissolved in CH_3CN, and filtered. The solvent was stripped off under vacuum to yield a grey powder. The dry styrene sulfonate silver salt was then dissolved in CH_3CN (25 mL) and ethyl bromide was added (2 mL, 0.03 mol). The mixture was heated at 70 ^oC overnight. The mixture was filtered and evaporated

under vacuum. The resulting greenish oil was dissolved in toluene and filtered again. Yield: 1.2 g, 58%. ^{1}H NMR was conducted in $CDCl_3$, shown in Figure 6.12.

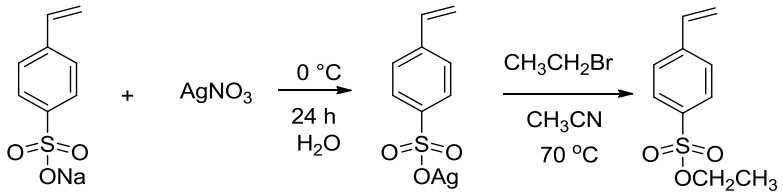

Scheme 6.2 Synthesis of ethyl styrene-4-sulfonate.

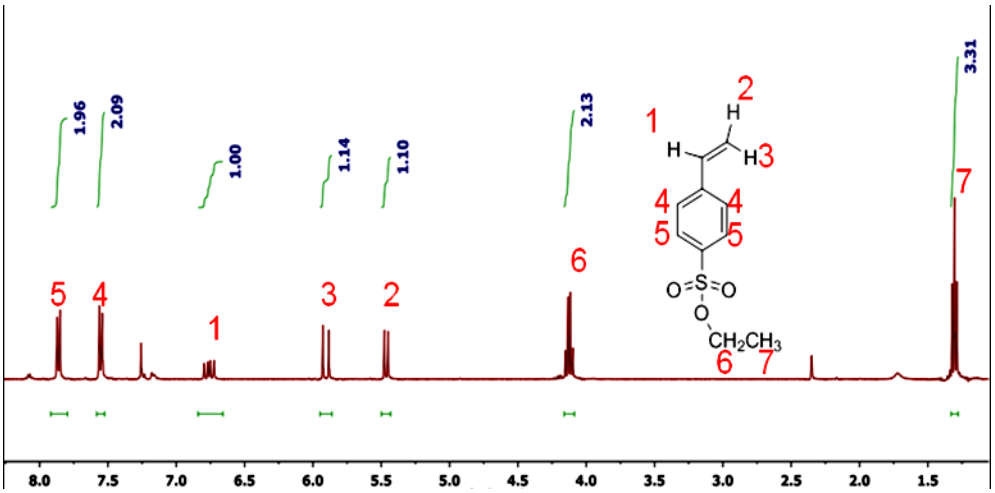

Figure 6.12 500/125 Hz ^{1}H NMR spectrum of methyl styrene-4-sulfonate in $CDCl_3$.

6.2. POLYMERIZATION

Radical polymerization

Procedures are provided in Chapter 2.

Controlled radical polymerization

Controlled radical copolymerization was used to provide copolymers with different molecular weights and narrow PDIs for examining the different anti-HIV properties. The solvent used was *m*-xylene (8.8 mL, 20 wt %). In order to obtain target molecular weights, the RAFT agent 2-cyano-2-propyl dodecyl trithiocarbonate was used in varying amounts. For example, when a targeted number average molecular weight polymer was 20 kg/mol,

0.58 mmol (0.199 g) of RAFT agent was used. The reaction was conducted at 70 °C and was purged with argon for 20 min to remove oxygen. The reaction was left for 24 h to stir. The copolymer was precipitated in hexanes and dried in the oven at 60 °C.

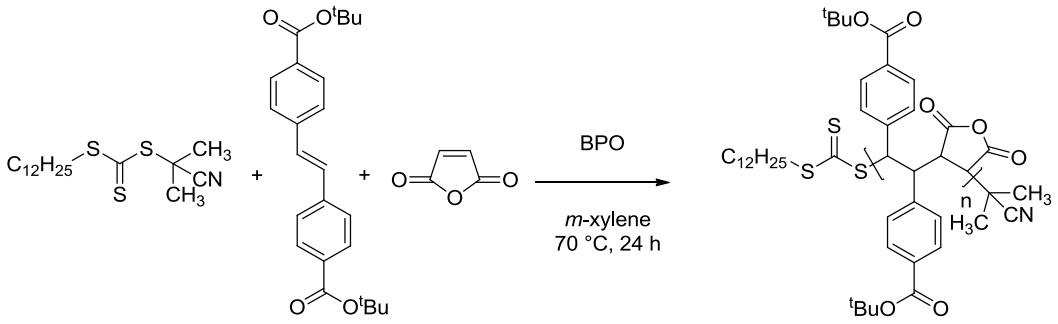

Scheme 6.3 Controlled radical polymerization.

As shown in Table 6.1, three different molecular weights were targeted at 5, 20, and 50 kg/mol. The percent yields were 8, 20, and 13%. All three copolymers had narrow PDIs, with an ideal PDI of 1.0 for living radical polymerization. However, the molecular weights for all three copolymerizations were lower than the targeted ones. This is probably because the assumed percent conversion was higher than the actual ones. In order to estimate how much RAFT agent was needed for each polymerization with a targeted molecular weight the following equation is used[89]

$$M_n = x(MW)\frac{[M]}{[RAFT]} \tag{6.1}$$

where [*M*] is the total monomer concentration, [*RAFT*] is the concentration of RAFT agent, *x* is the percent conversion, and *MW* is the average molar mass of the comonomers. In this case, *x* was assumed to be 61% for the first RAFT polymerization, where 61% was the percent yield of the corresponding radical copolymerization. As confirmed by the actual low percent yields in Table 6.1, the 61% yield was too high.

Table 6.1 Results of RAFT polymerization.

Polymer	Target MW (kg/mol)	RAFT (mmol)	BPO (mmol)	SEC M_n (kg/mol)	SEC M_w (kg/mol)	PDI	Percent Yield (%)
LY-154-5k	5	0.23	0.16	4.67	4.85	1.04	8
LY-154-20k	20	0.057	0.041	8.96	9.97	1.11	20
LY-154-50k	50	0.023	0.016	11.4	13.6	1.19	13

Conversion of polyanion precursors into polyanions

Once alternating copolymers were made, they were converted into the corresponding polyanions for anti-HIV study. Procedures are provided in Chapter 2.

Copolymerization of sodium 4,4'-distilbenesulfonate (SDSS) with sodium-N-(4-sulfophenyl)maleimide (SSPMI)

As shown in Table 6.2, four different sets of polymerization conditions were attempted to synthesize this copolymer (Figure 6.13). During the course of polymerizations, a homogeneous polymer solution was only formed under Condition 4. Polymer solutions remained cloudy under the other three conditions 1, 2, and 3. After 24 h, the copolymerization solution was added dropwise to acetone. However, no polymer precipitated under any polymerization conditions. This lack of copolymerization is probably due to the poor solubility of the stilbene monomer in H_2O. In addition, the strong electron withdrawing nature of SDSS may prevent cross-propagation that is necessary for the alternating copolymerization.

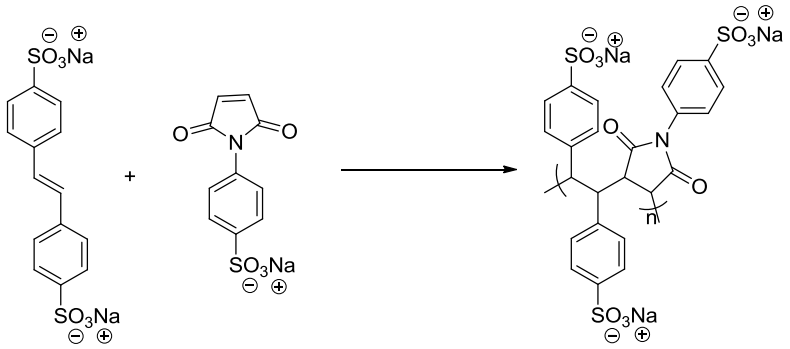

Figure 6.13 Attempted copolymerization of SDSS and SSPMI.

Table 6.2 Attempted copolymerization of SDSS with SSPMI.

Condition	Solvent	Initiator	Monomer Conc. (wt %)	Temp. (^{o}C)	Polymerization
1	H_2O	APS	20	80	N
2	DMF	DCP	20	110	N
3	H_2O (9): DMF (1)	APS	20	80	N
4	H_2O (9): DMF (1)	APS	10	80	N

6.3. CONCLUSIONS

Monomers DTBSC and TBMIB were prepared and copolymerized to alternating polyanion precursors. Alternating copolymers were made through conventional radical and RAFT polymerization. Copolymers with different molecular weights were synthesized via radical copolymerization. With RAFT copolymerization, copolymers were prepared with M_n values of 4.67-11.4 kg/mol and PDI values of 1.04-1.19 (Table 6.1). The corresponding polyanions were made (Figure 6.14) and eight polyanion samples were sent to the Eastern Virginia Medical School for anti-HIV testing. These eight samples are shown in Table 6.3. Results of the early antiviral study of these samples are shown in Table 6.4. It was found that these samples had lower cytotoxicity than the

positive control dextran sulfate. Antiviral acitivities of these samples are either greater or close to that of the positive control. From the sample DCSTB-MAH, it was found that the antiviral activity decreased as the molecular weight decreases. The results will be used to investigate (a) the antiviral activity of the stilbene and styrene containing carboxylated polyanions, (b) how the number of charges on a repeating unit affects the antiviral activity, (c) how the molecular weight of the polymer affects the antiviral activity, (d) how the distance of the charge from the polymer backbone affects the antiviral activity. In the future, the antiviral activity of sulfonated polyanions will be studied and compared to these carboxylated polyanions.

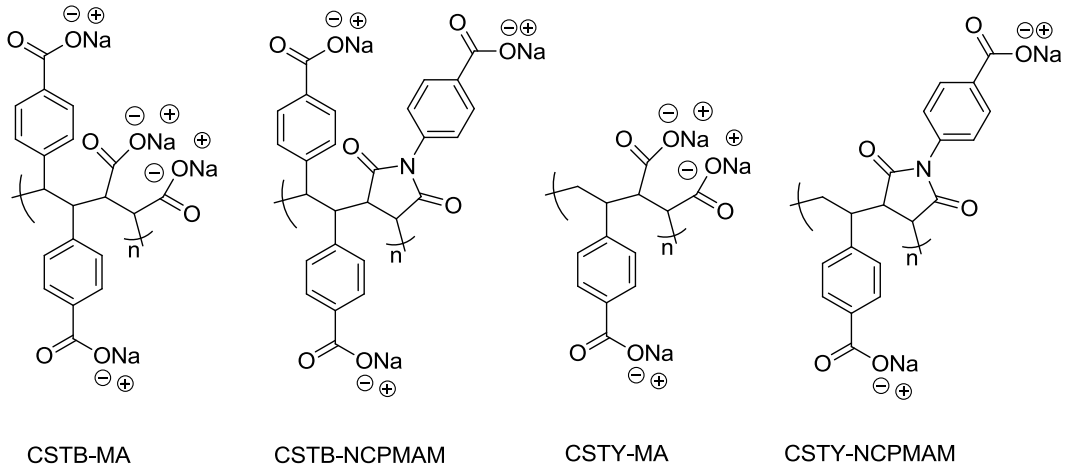

Figure 6.14 Structures of anionic polymer samples sent to Eastern Virginia Medical School.

Table 6.3 Polyanionic samples sent to Eastern Virginia Medical School.

Polymer	Code	M_n (kg/mol)	PDI	Weight (mg)	Solubility in H_2O (1mg/100 μL)	Solubility in saline (1 mg/100 μL)
DCSTB-MA						
1	LY-91	20.4	1.46	90	Y	Y
2	LY-90	111	1.53	100	Y	Y
3	LY149	40	1.18	230	Y	Y
4	LY-154	4.7	1.04	100	Y	Y
CSTY-MA						
5	LY-24	30	1.82	140	Y	Y
6	LY71	41.1	1.52	100	Y	Y
DCSTB-NCPMAM						
7	LY-32	80.4	1.79	40	Y	Y
CSTY-NCPMAM						
8	LY-103	93.8	1.89	100	Y	Y

Table 6.4. Anti-HIV evaluation - Single-round infection assay.

Polymer	Molecular weight (kg/mol)	Solvent stock solution	Diluent	Cytotoxicity EC(50) (μg/mL)	Antiviral activity EC(50) (μg/mL)		
					IIIb	BaL	CA*
DCSTB-MA							
LY-154	4.6	H_2O	R10	>100	0.099	0.3	
LY-91	20.4	H_2O	R10	>100	0.095	0.228	
LY-149	40	H_2O	R10	>100	0.2	1.6	
LY-90	111	H_2O	R10	>100	0.52	1.3	
CSTY-MA							
LY-24	30	H_2O	R10	>100	0.47	0.8	
LY71	41.1	H_2O	R10	>100	0.66	0.45	
DCSTB-NCPMAM							
LY-32	80.4	H_2O	R10	>100	0.76	1.2	
CSTY-NCPMAM							
LY-103	93.8	H_2O	R10	>100	0.23	1.01	
Positive control	N/A	H_2O	R10	>1000	0.36	1.6	

EC(50) = 50% effective concentration
MTS: cytoxicity assay
IIIB: HIV-1 X 4 strain
BaL: HIV-1 R5 strain
CA: cell-associated virus (IIIB)
R10=RPMI 1640 + 10% FBS
DMSO: concentrations expressed as solute equivalent concentrations
*Under evaluation
Error bars for EC(50) values: ±50%

REFERENCES

(1) Fichorova, R. N.; Tucker, L. D.; Anderson, D. J. *J. Infect. Dis.***2001**, *184*, 418.

(2) Van Damme, L.; Ramjee, G.; Alary, M.; Vuylsteke, B.; Chandeying, V.; Rees, H.; Sirivongrangson, P.; Tshibaka, L. M.; Ettiègne-Traoré, V.; Uaheowitchai, C.; Karim, S. S. A.; Mâsse, B.; Perriëns, J.; Laga, M. *Lancet* **2002**, *360*, 971.

(3) Hillier, S. L.; Moench, T.; Shattock, R.; Black, R.; Reichelderfer, P.; Veronese, F. *JAIDS J. Acquired Immune Defic. Syndromes* **2005**, *39*, 1.

(4) Roy, S.; Gourde, P.; Piret, J.; Désormeaux, A.; Lamontagne, J.; Haineault, C.; Omar, R. F.; Bergeron, M. G. *Antimicrob. Agents Chemother* **2001**, *45*, 1671.

(5) Bestman-Smith, J.; Piret, J.; Désormeaux, A.; Tremblay, M. J.; Omar, R. F.; Bergeron, M. G. *Antimicrob. Agents Chemother* **2001**, *45*, 2229.

(6) Ballagh, S. A.; Baker, J. M.; Henry, D. M.; Archer, D. F. *Contraception* **2002**, *66*, 369.

(7) Bax, R.; Douville, K.; McCormick, D.; Rosenberg, M.; Higgins, J.; Bowden, M. *Contraception* **2002**, *66*, 365.

(8) Baba, M.; Schols, D.; De Clercq, E.; Pauwels, R.; Nagy, M.; Györgyi-Edelényi, J.; Löw, M.; Görög, S. *Antimicrob. Agents Chemother* **1990**, *34*, 134.

(9) Pauwels, R.; De Clercq, E. *JAIDS J. Acquired Immune Defic. Syndromes* **1996**, *11*, 211.

(10) Moulard, M.; Lortat-Jacob, H.; Mondor, I.; Roca, G.; Wyatt, R.; Sodroski, J.; Zhao, L.; Olson, W.; Kwong, P. D.; Sattentau, Q. J. *J. Virol.* **2000**, *74*, 1948.

(11) Scordi-Bello, I. A.; Mosoian, A.; He, C.; Chen, Y.; Cheng, Y.; Jarvis, G. A.; Keller, M. J.; Hogarty, K.; Waller, D. P.; Profy, A. T.; Herold, B. C.; Klotman, M. E. *Antimicrob. Agents Chemother* **2005**, *49*, 3607.

(12) Lu, H.; Zhao, Q.; Wallace, G.; Liu, S.; He, Y.; Shattock, R.; Neurath, A. R.; Jiang, B. S. *AIDS Res Hum Retroviruses* **2006**, *22*, 411.

(13) Roberton, A. M.; Wiggins, R.; Horner, P. J.; Greenwood, R.; Crowley, T.; Fernandes, A.; Berry, M.; Corfield, A. P. *J. Clin. Microbiol.* **2005**, *43*, 5504.

(14) Christensen, N. D.; Reed, C. A.; Culp, T. D.; Hermonat, P. L.; Howett, M. K.; Anderson, R. A.; Zaneveld, L. J. D. *Antimicrob. Agents Chemother* **2001**, *45*, 3427.

(15) Simoes, J. A.; Citron, D. M.; Aroutcheva, A.; Anderson, R. A.; Chany II, C. J.; Waller, D. P.; Faro, S.; Zaneveld, L. J. D. *Antimicrob. Agents Chemother* **2002**, *46*, 2692.

(16) Malonza, I. M.; Mirembe, F.; Nakabiito, C.; Odusoga, L. O.; Osinupebi, O. A.; Hazari, K.; Chitlange, S.; Ali, M. M.; Callahan, M.; Van Damme, L. *AIDS* **2005**, *19*, 2157.

(17) Anderson, R. A.; Feathergill, K. A.; Diao, X.-H.; Cooper, M. D.; Kirkpatrick, R.; Herold, B. C.; Doncel, G. F.; Chany, C. J.; Waller, D. P.; Rencher, W. F.; Zaneveld, L. J. D. *J. Androl.* **2002**, *23*, 426.

(18) Mauck, C.; Weiner, D. H.; Ballagh, S.; Creinin, M.; Archer, D. F.; Schwartz, J.; Pymar, H.; Lai, J.-J.; Callahan, M. *Contraception* **2001**, *64*, 383.

(19) Jespers, V.; Buvé, A.; Van Damme, L. *Sex Transm. Dis.* **2007**, *34*, 519.

(20) Schaeffer, D. J.; Krylov, V. S. *Ecotox. Environ. Safe.***2000**, *45*, 208.

(21) Zacharopoulos, V. R.; Phillips, D. M. *Clin. Diagn. Lab. Immunol.* **1997**, *4*, 465.

(22) Perotti, M.-E.; Pirovano, A.; Phillips, D. M. *Biol. Reprod.* **2003**, *69*, 933.

(23) Elias, C. J.; Coggins, C.; Alvarez, F.; Brache, V.; Fraser, I. S.; Lacarra, M.; Lähteenmäkl, P.; Massai, R.; Mishell Jr, D. R.; Phillips, D. M.; Salvatierra, A. M. *Contraception* **1997**, *56*, 387.

(24) Keller, M. J.; Zerhouni-Layachi, B.; Cheshenko, N.; John, M.; Hogarty, K.; Kasowitz, A.; Goldberg, C. L.; Wallenstein, S.; Profy, A. T.; Klotman, M. E.; Herold, B. C. *J. Infect. Dis.***2006**, *193*, 27.

(25) Rusconi, S.; Moonis, M.; Merrill, D. P.; Pallai, P. V.; Neidhardt, E. A.; Singh, S. K.; Willis, K. J.; Osburne, M. S.; Profy, A. T.; Jenson, J. C.; Hirsch, M. S. *Antimicrob. Agents Chemother* **1996**, *40*, 234.

(26) Lacey, C. J.; Wright, A.; Weber, J. N.; Profy, A. T. *AIDS* **2006**, *20*, 1027.

(27) Mayer, K. H.; Karim, S. A.; Kelly, C.; Maslankowski, L.; Rees, H.; Profy, A. T.; Day, J.; Welch, J.; Rosenberg, Z.; Team, f. t. H. P. T. N. P. *AIDS* **2003**, *17*, 321.

(28) Boadi, T.; Schneider, E.; Chung, S.; Tsai, L.; Gettie, A.; Ratterree, M.; Blanchard, J.; Neurath, A. R.; Cheng-Mayer, C. *AIDS* **2005**, *19*, 1587.

(29) Otten, R. A.; Adams, D. R.; Kim, C. N.; Jackson, E.; Pullium, J. K.; Lee, K.; Grohskopf, L. A.; Monsour, M.; Butera, S.; Folks, T. M. *J. Infect. Dis.***2005**, *191*, 164.

(30) Reimann, K. A.; Khunkhun, R.; Lin, W.; Gordon, W.; Fung, M. *AIDS Res Hum Retroviruses* **2002**, *18*, 747.

(31) Vermeire, K.; Schols, D. *J. Antimicrob. Chemoth.* **2005**, *56*, 270.

(32) Trkola, A.; Ketas, T. J.; Nagashima, K. A.; Zhao, L.; Cilliers, T.; Morris, L.; Moore, J. P.; Maddon, P. J.; Olson, W. C. *J. Virol.* **2001**, *75*, 579.

(33) Kawamura, T.; Gulden, F. O.; Sugaya, M.; McNamara, D. T.; Borris, D. L.; Lederman, M. M.; Orenstein, J. M.; Zimmerman, P. A.; Blauvelt, A. *Proc. Nat. Acad. Sci.* **2003**, *100*, 8401.

(34) Torre, V. S.; Marozsan, A. J.; Albright, J. L.; Collins, K. R.; Hartley, O.; Offord, R. E.; Quiñones-Mateu, M. E.; Arts, E. J. *J. Virol.* **2000**, *74*, 4868.

(35) Pierson, T. C.; Doms, R. W. *Immunol. Lett.* **2003**, *85*, 113.

(36) Kazmierski, W.; Bifulco, N.; Yang, H.; Boone, L.; DeAnda, F.; Watson, C.; Kenakin, T. *Bioorg. Med. Chem.* **2003**, *11*, 2663.

(37) O'Hara, B. M.; Olson, W. C. *Curr. Opin. Pharmacol.* **2002**, *2*, 523.

(38) Princen, K.; Schols, D. *Cytokine Growth Factor Rev.* **2005**, *16*, 659.

(39) Schols, D.; Struyf, S.; Damme, J. V.; Esté, J. A.; Henson, G.; Clercq, E. D. *The J. Exp. Med.* **1997**, *186*, 1383.

(40) Rusconi, S.; La Seta Catamancio, S.; Citterio, P.; Bulgheroni, E.; Croce, F.; Herrmann, S. H.; Offord, R. E.; Galli, M.; Hirsch, M. S. *J. Virol.* **2000**, *74*, 9328.

(41) Hong, P. W.-P.; Flummerfelt, K. B.; de Parseval, A.; Gurney, K.; Elder, J. H.; Lee, B. *J. Virol.* **2002**, *76*, 12855.

(42) Lin, G.; Simmons, G.; Pöhlmann, S.; Baribaud, F.; Ni, H.; Leslie, G. J.; Haggarty, B. S.; Bates, P.; Weissman, D.; Hoxie, J. A.; Doms, R. W. *J. Virol.* **2003**, *77*, 1337.

(43) Poignard, P.; Saphire, E. O.; Parren, P. W.; Burton, D. R. *Annu. Rev. Immunol.* **2001**, *19*, 253.

(44) Zwick, M. B.; Wang, M.; Poignard, P.; Stiegler, G.; Katinger, H.; Burton, D. R.; Parren, P. W. H. I. *J. Virol.* **2001**, *75*, 12198.

(45) Wang, T.; Zhang, Z.; Wallace, O. B.; Deshpande, M.; Fang, H.; Yang, Z.; Zadjura, L. M.; Tweedie, D. L.; Huang, S.; Zhao, F.; Ranadive, S.; Robinson, B. S.; Gong, Y.-F.; Ricarrdi, K.; Spicer, T. P.; Deminie, C.; Rose, R.; Wang, H.-G. H.; Blair, W. S.; Shi, P.-Y.; Lin, P.-f.; Colonno, R. J.; Meanwell, N. A. *J. Med. Chem.* **2003**, *46*, 4236.

(46) Ho, H.-T.; Fan, L.; Nowicka-Sans, B.; McAuliffe, B.; Li, C.-B.; Yamanaka, G.; Zhou, N.; Fang, H.; Dicker, I.; Dalterio, R.; Gong, Y.-F.; Wang, T.; Yin, Z.; Ueda, Y.; Matiskella, J.; Kadow, J.; Clapham, P.; Robinson, J.; Colonno, R.; Lin, P.-F. *J. Virol.* **2006**, *80*, 4017.

(47) Jan, B. *Lancet Infect Dis.* **2005**, *5*, 726.

(48) D'Cruz, O. J. *Curr. Pharm. Des.* **2004**, *10*, 315.

(49) Trifonova, R. T.; Doncel, G. F.; Fichorova, R. N. *Antimicrob. Agents Chemother* **2009**, *53*, 1490.

(50) Du Toit, L. C. *Adv. Drug Deliv. Rev.* **2010**, *62*, 532.

(51) Witvrouw, M.; De Clercq, E. *Gen. Pharmacol.***1997**, *29*, 497.

(52) Mitsuya, H.; Popovic, M.; Yarchoan, R.; Matsushita, S.; Gallo, R. *Science* **1984**, *226*, 172.

(53) Flexner, C.; Barditch-Crovo, P.; Kornhauser, D.; Farzadegan, H.; Nerhood, L.; Chaisson, R.; Bell, K.; Lorentsen, K.; Hendrix, C.; Petty, B.; Lietman, P. *Antimicrob. Agents. Chemother.* **1991**, *35*, 2544.

(54) Ueno, R.; Kuno, S. *Lancet* **1987**, *1*, 1379.

(55) Mitsuya, H.; Looney, D. J.; Kuno, S.; Ueno, R.; Wong-Staal, F.; Broder, S. *Science* **1988**, *240*, 646.

(56) Ito, M.; Baba, M.; Pauwels, R.; De Clercq, E.; Shigeta, S. *Antivir. Res.* **1987**, *7*, 361.

(57) Baba, M.; Pauwels, R.; Balzarini, J.; Arnout, J.; Desmyter, J.; De Clercq, E. In *Proc. Natl. Acad. Sci.* USA, 1988; Vol. 85, p 6132.

(58) Yoshida, O.; Nakashimma, H.; Toshida, T.; Kanedo, Y.; Matsuzaki, K.; Uryu, T.; Yamamoto, N. *Biochem. Pharmacol.* **1988**, *37*, 2887.

(59) Fitzgerald, J. W. *Bacteriol. Rev.* **1976**, *40*, 698.

(60) Pauwels, R.; De Clercq, E. *J. Acquired Immune Defic. Syndromes Hum. Retrovirol.* **1996**, *11*, 211.

(61) Neyts, J.; Reymen, D.; Letourneur, D.; Jozefonvicz, J.; Schols, D.; Este, J.; Andrei, G.; McKenna, P.; Witvrouw, M.; Ikeda, S.; Clement, J.; De Clercq, E. *Biochem. Pharmacol.* **1995**, *50*, 743.

(62) Mitsuya, H.; Looney, D.; Kuno, S.; Ueno, R.; Wong-Staal, F.; Broder, S. *Science* **1988**, *240*, 646.

(63) D'Cruz, O. J.; Uckun, F. M. *Curr. Pharm. Des.* **2004**, *10*, 315.

(64) Zaneveld, L. J. D.; Waller, D. P.; Anderson, R. A.; Chany Ii, C.; Rencher, W. F.; Feathergill, K.; Diao, X.-H.; Doncel, G. F.; Herold, B.; Cooper, M. *Biol. Reprod.* **2002**, *66*, 886.

(65) Herold, B.; Bourne, N.; Marcellino, D.; Kirkpatrick, R.; Strauss, D.; Zaneveld, L.; Waller, D.; Anderson, R.; Chany, C.; Barham, B.; Stanberry, L.; Cooper, M. *J. Infect. Dis.* **2000**, *181*, 770.

(66) Christensen, N. D.; Reed, C. A.; Culp, T. D.; Hermonat, P. L.; Howett, M. K.; Anderson, R. A.; Zaneveld, L. J. D. *Antimicrob. Agents Chemother.* **2001**, *45*, 3427.

(67) Rusconi, S.; Moonis, M.; Merrill, D.; Pallai, P.; Neidhardt, E.; Singh, S. *Antimicrob. Agents Chemother.* **1996**, *40*, 234.

(68) Mayer, K. H. *AIDS (London)* **2003**, *17*, 321.

(69) Fang, W.; Cai, Y.; Chen, X.; Su, R.; Chen, T.; Xia, N.; Li, L.; Yang, Q.; Han, J.; Han, S. *Bioorg. Med. Chem. Lett.* **2009**, *19*, 1903.

(70) Zhu, M.-Q.; Wei, L.-H.; Li, M.; Jiang, L.; Du, F.-S.; Li, Z.-C.; Li, F.-M. *Chem. Commun.* **2001**, 365.

(71) Mpitso, K. *Master of Science Thesis* **2009**.

(72) Bellettini, A. G.; Bellettini, R. J. *US pat 6210653 2001*.

(73) Kornberg, A. *J. Bacteriol.* **1995**, *177*, 491.

(74) Kulaev, I. *The Biochemistry of Inorganic Polyphosphares*; John Wiley & Sons: New York, 1979.

(75) Wood, H.; Clark, J. *Annu. Rev. Biochem.* **1988**, *57*, 235.

(76) Matsuoka, A.; Tsutsumi, M.; Watanabe, T. *J. Food. Hyg. Soc. Jpn.* **1995**, *36*, 588.

(77) Palumbo, S.; Call, J.; Cooke, P.; Williams, A. *Food Safety* **1995**, *15*, 77.

(78) Lorenz, B.; Leuck, J.; Kohl, D.; Muller, W.; Schroder, H. *J. Acquired Immune Defic. Syndromes Hum. Retrovirol.* **1997**, *14*, 110.

(79) Krust, B.; Callebaut, C.; Honavessian, A. *AIDS Res. Hum. Retroviruses* **1993**, *9*, 1087.

(80) Montefiori, D.; Mitchell, W. *Proc. Nat. Acad. Sci. USA* **1987**, *84*, 2985.

(81) Luscher-Mattli, M. *Antivir. Chem. Chemoth.* **2000**, *11*, 249.

(82) Witvrouw, M.; Fikkert, V.; Pluymers, W.; Matthews, B.; Mardel, K.; Schols, D.; Raff, J.; Debyser, Z.; De Clercq, E.; Holan, G.; Pannecouque, C. *Mol. Pharmacol.* **2000**, *58*, 1100.

(83) McCarthy, T. D.; Karellas, P.; Henderson, S. A.; Giannis, M.; O'Keefe, D. F.; Heery, G.; Paull, J. R. A.; Matthews, B. R.; Holan, G. *Mol. Pharmaceutics* **2005**, *2*, 312.

(84) Pirrone, V.; Wigdahl, B.; Krebs, F. C. *Antivir. Res.* **2011**, *90*, 168.

(85) Moore, F. J.; Tucker, G. R. *J. Am. Chem. Soc.* **1927**, *49*, 258.

(86) Müller, C. E.; Sandoval-RamIrez, J.; Schobert, U.; Geis, U.; Frobenius, W.; Klotz, K.-N. *Bioorg. Med. Chem.* **1998**, *6*, 707.

(87) van Es, T.; Backeberg, O. G.; Morrison, I. *J. South Afr. Chem. Inst.* **1964**; Vol. 17, p 95.

(88) Sikkema, F. D.; Comellas-Aragones, M.; Fokkink, R. G.; Verduin, B. J. M.; Cornelissen, J. J. L. M.; Nolte, R. J. M. *Org. Biomol. Chem.* **2007**, *5*, 54.

(89) Davies, M. C.; Dawkins, J. V.; Hourston, D. J. *Polymer* **2005**, *46*, 1739.